Russian Academy of Sciences
Joint Institute for High Temperatures RAS
Institute of Problems of Chemical Physics RAS

Kabardino-Balkarian State University

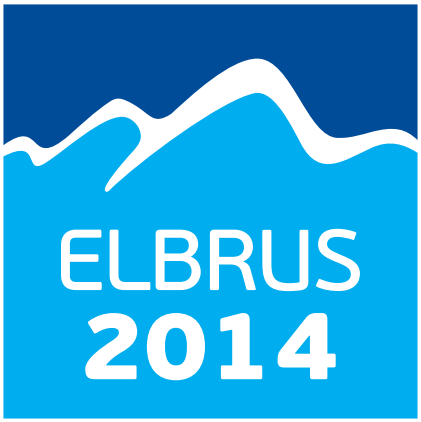

EOS

XXIX International Conference on

Equations of State for Matter

March 1–6, 2014, Elbrus, Russia

Book of Abstracts

Moscow & Chernogolovka & Nalchik
2014

Devoted to the centenary
of birth of academician

Yakov B. Zeldovich

(8.03.1914–2.12.1987)

The book consists of the abstracts of plenary, oral and poster contributions to the XXIX International Conference on Equations of State for Matter (March 1–6, 2014, Elbrus, Kabardino-Balkaria, Russia). The conference is devoted to the centenary of birth of academician Yakov Borisovich Zeldovich (March 8, 1914–December 2, 1987). The reports deal with the contemporary investigations in the field of physics of extreme states of matter. The following topics are covered: equations of state and constitutive equations for matter at high pressures and temperatures; shock waves, detonation and combustion physics; interaction of intense laser, x-ray and microwave radiation, powerful ion and electron beams with matter; techniques of intense energy fluxes generation; experimental methods of diagnostics of ultrafast processes; low-temperature plasma physics; issues of physics and power engineering, technology projects.

The conference is held under financial support of the Russian Academy of Sciences and the Russian Foundation for Basic Research (grant No. 13-02-06212).

The editorial board announces with deep regret the death of the colleagues and friends, Dr. Vladimir Vladimirovich Milyavskiy (July 22, 1969–June 12, 2013), who was the organizing and program committees member of the Conferences on Equations of State for Matter and Interaction of Intense Energy Fluxes with Matter, and Prof. Gennady Vasil'evich Sin'ko (February 7, 1950–September 8, 2013), who was a regular and active participant of these conferences starting with one of the first meeting.

ISBN 978-5-94691-621-9

CONTENTS

CHAPTER 1. EQUATIONS OF STATE FOR MATTER

CHAPTER 3. POWER INTERACTION WITH MATTER

BINODAL LAYER IN ISENTROPIC EXPANSION OF HIGH ENERGY DENSITY MATTER

Iosilevskiy I.L.,* Borovikov D.

JIHT RAS, Moscow, Russia

**iosilevskiy@gmail.com*

Yakob Zeldovich is one of the great scientists who laid significant part of foundation for thermo- and hydrodynamics of adiabatic transformations in high energy density matter, such as shock compression, isentropic and isenthalpic expansion etc. (see e.g. [1]). Features of isentropic expansion of warm dense matter (WDM) created by intense energy fluxes (strong shock compression or instant quasi-isochoric heating by laser or heavy ion beam) are under discussion in situation, when (i) thermodynamic trajectory of such expansion crosses phase boundary (binodal) of liquid–gas phase transition, (ii) the expansion within the two-phase region is going along equilibrium branch of two-phase mixture isentrope (not metastable one) and (iii) this two-phase mixture is highly dispersed to justify hydrodynamic description in frames of the "one-fluid" approximation and the local thermodynamic equilibrium concept (LTE). It is known for the plane geometry (see e.g. [2]) that because of sharp break of the expansion isentrope at the phase boundary of boiling liquid (in P–V plane) i.e. because of discontinuity in sound velocity at this point, there appears extended "plateau" (layer) of uniformity with constant thermodynamic and kinematic parameters in expanding material. The state of material at this layer corresponds just to the point on binodal. It is important that due to self-similarity of such expansion in plane case this layer contains ("freezes") finite and fixed part of whole material, which is involved in isentropic expansion. This remarkable property make it possible (at least formally) to discuss this type of isentropic WDM expansion as a tool for generation and diagnostics of uniform and extended state of warm dense matter exactly on liquid and gaseous binodal (and even in critical point) of unexplored phase transition in the case when its parameters are not known. It is natural to use the term "phase freeze-out" for this regime of expansion [3, 4]. It is analogous to similar terms "chemical freeze-out" and "kinetic freeze-out", which are widely used in interpretation of quark–hardon transformations during the expansion of products for relativistic ions collision in super-colliders. Remarkable features of binodal layer are discussed for the case of isentropic

expansion of slab or spherical samples ("fireball") through the boundary of ordinary (VdW-like) or non-standard ("entropic" [5]) phase transitions, or even for the case of exotic (quark–hadron) phase transition in ultra-high energy density nuclear matter [6].

1. Zeldovich Ya. B., Raizer Yu. P. Physics of Shock Waves and High-Temperature Hydrodynamic Phenomena. Moscow: Nauka, 1966; Fizmatlit, 2008.
2. Anisimov S. I., Inogamov N. A., Oparin A. M., Rethfeld B., Yabe T., Ogawa M., Fortov V. E. // Appl. Phys. A. 1999. V. 69. P. 617–620.
3. Iosilevskiy I. L. // Physics of Extreme States of Matter—2011 / Eds. Fortov V. E., et al. Chernogolovka: IPCP RAS, 2011. P. 99–102, arXiv:1401.5481.
4. Borovikov D. S., Iosilevskiy I. L. // Physics of Extreme States of Matter—2012 / Eds. Fortov V. E., et al. Chernogolovka: IPCP RAS, 2012. P. 12–15, arXiv:1209.0398; 2013. P. 140–144, arXiv:1306.2765.
5. Iosilevskiy I. L. // Physics of Extreme States of Matter—2013 / Eds. Fortov V. E., et al. Chernogolovka: IPCP RAS, 2013. P. 136–140.
6. Iosilevskiy I. Binodal layer in isentropically expanding high energy density matter // Int. Workshop on High Energy Density Physics, Hirschegg, Austria, 2014.

Ya. B. ZELDOVICH AND EOS PROBLEMS

Fortov V.E.,[1] ***Lomonosov I.V.****[2]

[1] *JIHT RAS, Moscow,* [2] *IPCP RAS, Chernogolovka, Russia*

**ivl143@yahoo.com*

In this report, we'll present an impact by Ya. B. Zeldovich on the problem of developing equation of state (EOS) of matter. In 1950th, Zeldovich proposed most fruitful ideas for experimental researches and theoretical models. Those are: measuring of shock adiabats for porous matter, studing of adiabatically expanded shocked materials and developing thermodynamically complete EOS.

STRUCTURAL SIMPLICITY AND COMPLEXITY OF COMPRESSED CALCIUM: ELECTRONIC ORIGIN

Degtyareva V.F.

ISSP RAS, Chernogolovka, Russia

degtyar@issp.ac.ru

Simple cubic structure with one atom in the unit cell found in compressed calcium above 32 GPa [1] is counterintuitive with regards to traditional view on tendency of transition to densely packed structures on the increase of pressure. To understand this unusual transformation it is necessary to assume electron transfer from outer core to the valence band and increase of valence electron number for calcium from 2 to ∼3.5. This assumption is supported by the model of the Fermi sphere—Brillouin zone interaction [2] that increases under compression. Recently found structure of Ca-VII above 210 GPa [3] with a commensurate host-guest structure based on a tetragonal cell containing 32 atoms ($tI32$) is similar to the known ambient pressure intermetallic compound In_5Bi_3 with 3.75 valence electrons per atom. The temperature of superconductivity in Ca-VII riches 29 K—the highest value among elements known at present. Structural relations are analyzed in regard to a resemblance of the electronic structure. Correlations of structure and physical properties of Ca under high pressure are discussed.

1. Olyjnik, H., Holzapfel, W.B. // Phys. Lett. A, 1984. V. 100. P. 191.
2. Degtyareva V.F., // Physics-Uspekhi. 2006. V. 49. P. 369.
3. Fujihisa, H., Nakamoto, Y., Sakata, M. et al. // Phys. Rev. Lett. 2013. V. 110. P. 235501.

THERMODYNAMICS OF ELECTRONS IN CRYSTALLINE METALS: COMPARISON OF DIFFERENT APPROACHES

Sin'ko G.V.,[1] ***Smirnov N.A.***,[1] ***Ovechkin A.A.***,[1]
Levashov P.R.,*[2] ***Khishchenko K.V.***[2]

[1]*RFNC–VNIITF, Snezhinsk,* [2]*JIHT RAS, Moscow, Russia*

**pasha@ihed.ras.ru*

We present electronic heat capacities and thermal pressures calculated for aluminum and tungsten at densities $\rho_0 \leq \rho \leq 2\rho_0$ in the case when the temperature of electrons is finite (a few electronvolts) and nuclei are cold. Calculations were done with the all-electron full-potential linear muffin-tin orbital method (FP-LMTO) [1] and compared with data obtained by the

Thomas–Fermi model with different corrections [2], Liberman's average–atom model and the Vienna Ab-initio Simulation Package (VASP) pseudopotential code [3, 4]. We analyze contribution of different effects, in particular, exchange and correlation and investigate their influence on the results. It is shown that different approaches qualitatively agree within the ranges of electron temperatures and densities under consideration; mean atom and DFT models are in quantitative correspondence within 10% in most cases.

1. Savrasov S.Y. // Phys. Rev. B. 1996. V. 54. P. 16470.
2. Kirzhnits D.A., Lozovik Yu.E., Shpatakovskaya G.V. Physics-Uspekhi. 1975. V. 18. P. 649–672.
3. Kresse G., Hafner J. // Phys. Rev. B. 1993. V. 47. P. 558.
4. Kresse G., Hafner J. // Phys. Rev. B. 1994. V. 49. P. 14251.

INCLUSION OF SHELL EFFECTS IN THE STATISTICAL MODEL OF PLASMA

Shpatakovskaya G.V.,[*1] ***Karpov V.Ya.***[2]

[1]*KIAM RAS,* [2]*INEUM, Moscow, Russia*

[*]*shpagalya@yandex.ru*

The characteristics of plasma have been studied with a semiclassical method, based on the Thomas-Fermi statistical model. A generalized method is proposed to include of the discretness of the electronic spectrum of bound electrons in atomic systems (atom, ion, atomic cell of matter), in other words, the shell effects.

The effects have been successfully taken into account (see reviews [1], [2]) to calculate the equation of state (EOS) of a hot plasma by statistical model. The used semiclassical method has been previously based on the assumption that the shell effects smoothly change physical quantities. However, this assumption is invalid for low temperatures. At zero temperature the shell effects are manifested in sharp dependences, e.g. a casplike atomic volume curve [3] or a sawtooth dependence of ion ionization potentials on the ion charge. In paper [4] we proposed the method that removes the indicated restriction for free positive ions. In this report we generalize the method [4] for the plasma properties calculation.

This work was supported in part by the Russian Foundation for Basic Research (project no. 14–01–00828).

1. G.V.Shpatakovskaya, Phys. Usp. 55, 429 (2012).

2. Galina Shpatakovskaya, *Quasiclassical Method in Quantum Physics Problems* (LAP LAMBERT Academic Publishing GmbH, 2012) , ISBN 978–3–8465–2681–1.
3. D.A.Kirzhnits, Yu.E.Lozovik and G.V.Shpatakovskaya, Sov. Phys. Usp. 18, 587 (1975).
4. V.Ya. Karpov and G.V.Shpatakovskaya, JETP Letters, V. 98, No. 6, P. 348 (2013).

METHODS FOR CALCULATING THE SHELL CORRECTION IN THE THOMAS–FERMI MODEL

Dyachkov S.A.,* Levashov P.R.

JIHT RAS, Moscow, Russia

**serj.dyachkov@gmail.com*

The Thomas–Fermi model at finite temperatures [1] is a good approximation for the calculation of thermodynamic functions of electrons in wide range of parameters. Despite the fact that the model is simple to implement, taking into account the quantum, exchange [2] and shell effects [3], one can bring the accuracy to the more difficult models of average atom [4] and density functional theory. Moreover, the thermal contribution to the Thomas-Fermi model shows good precision for matter in normal conditions [5].

The method for calculating the shell correction, which was firstly proposed by G. V. Shpatakovskaya [6], has been essentially modified by the authors. Multiplicity of assumptions used in [3], [6] was too difficult to check numerically earlier. Modern numerical algorithms applied at powerful computers allowed us to eliminate these disadvantages.

In this work we have compared methods for calculating the shell correction at every step of modification and checked correspondence with more accurate models.

---

1. Feynman R. P., Metropolis N., Teller E. Equations of state of elements based on the generalized Fermi-Thomas theory // Phys. Rev. 1949. V. 75. No. 10. P. 1561–1573.
2. Kirzhnits D. A. Quantum corrections to the Thomas–Fermi equation // JETP. 1958. V. 32. No 1. P. 115–123.
3. Kirzhnits D. A., Shpatakovskaya G. V. Wide-range EOS on the basis of Refined Statistical Model. Preprint No 33. M.: Lebedev Physical Institute of RAS, 1998.
4. Nikiforov A. F., Novikov V. G., Uvarov V. B. Quantum statistical models of hot dense matter and methods for computation opacity and EOS. M.: Fiz-

matlit, 2000.
5. Dyachkov S. A., Levashov P. R. Region of validity of Thomas–Fermi model and its thermal part // Physics of Extreme States of Matter—2012. Chernogolovka: IPCP RAS, 2012. P. 14–17.
6. Shpatakovskaya G. V. Shell effects in the thermodynamics of nondegenerate plasma. Preprint No 8. M.: Keldysh Institute of Applied Mathematics, 1984.

EQUATION-OF-STATE CALCULATIONS FOR A MIXTURE OF ELEMENTS BASED ON HARTREE–FOCK–SLATER MODEL

Kadatskiy M.A.,* Khishchenko K.V.

JIHT RAS, Moscow, Russia

**makkad@yandex.ru*

The modified Hartree–Fock–Slater (HFS) model is successfully applied to calculate the equation of state (EOS) of matter over wide range of temperatures and densities [1]. An important separate task is calculating the EOS of a mixture of different chemical elements (compounds, alloys and other mixtures). Previously, for mixture of simple substances, a methodology was established for determining the self-consistent potentials [2]. In the present work, this technique is implemented for practical calculations. It has great practical importance because, for example, alloys and compounds are widely used as materials for various purposes.

Calculation is given in the approximation of the average ion without relativistic effects and band structure of the electron spectrum. As other quantum-statistical approaches for comparison, the approximation of constant density of electrons and the Thomas–Fermi (TF) model were selected. In this connection, the main qualitative dependences of thermodynamic properties of mixture are obtained for models HFS and TF. At high temperatures ($T > 5$ keV) partial density ceases to depend on T, and both models agree with a model of constant density of electrons. While at low temperatures ($T < 10$ eV), there is a sharp disagreement that shows the non-applicability of TF model or of both models in this temperature range. For the model HFS in the range of low temperatures ($T < 10$ eV), it is worth noting sharp increase of concentration of impurity and simultaneous decrease in the concentration of the main substance of the mixture; the relative change in the partial density of impurity is great.

---

1. Nikiforov A. F., Novikov V. G., Uvarov V. B. Quantum-Statistical Models of

Hot Dense Matter. Methods for Computation Opacity and Equation of State. M., 2000. P. 223–318.
2. Orlov N. Y. // Zh. Vych. Mat. Mat. Fiz. 1986. V. 26. N. 8. P. 1215–1233.

ENERGY SPECTRUM CALCULATION FOR SYSTEMS IN WIGNER'S REPRESENTATION OF QUANTUM MECHANICS

Larkin A.S., Filinov V.S.*

JIHT RAS, Moscow, Russia

**alexanderlarkin@rambler.ru*

In our report we propose a method to obtain an energy spectrum of quantum system through computer simulation. A central point is that spectrum of quantum time correlation function $C_{xx}(t) =< \Psi|\hat{x}e^{i\hat{H}t/\hbar}\hat{x}e^{-i\hat{H}t/\hbar}|\Psi >$ ($\hat{x}$ is a position operator) conforms to all allowed transitions between energy levels: $\omega_{ij} = (E_j - E_i)/\hbar$ [1]. Correlation function can be calculated in Wigner's representation of quantum mechanics through using quasi-probability distribution function in double phase space. Time evolution of such function is described by equation, which is similar to Wigner-Liouville equation for Wigner function. This equation can be solved with both Monte-Carlo and molecular dynamics methods.

We have shown this method on two simple models. The first one is one-dimension anharmonic oscillator with ax^4 - anharmonism; obtained results agree with perturbation theory. The second one is semi-relativistic harmonic oscillator with hamiltonian $\hat{H} = \sqrt{p^2c^2 + m^2c^4}$, which was introduced in [2]. In both cases energy transition spectra were obtained.

Besides calculations in quantum mechanics, this method can be used for correlation functions of thermodynamic system.

---

1. D. N. Zubarev, Non-equilibrium statistical thermodynamics, Nauka, (1971)
2. A.S. Larkin, V.S. Filinov // Phys. Lett. A. V. 377 (2013).
3. V. S. Filinov, Yu. B. Ivanov, M. Bonitz, V. E. Fortov, P. R. Levashov, Phys. Rev. C, 87, 035207 (2013).

EQUATION OF STATE AND PHASE TRANSFORMATIONS OF WATER AT HIGH PRESSURES AND TEMPERATURES

Khishchenko K.V.

JIHT RAS, Moscow, Russia

konst@ihed.ras.ru

A new semiempirical equation of state for H_2O is proposed with taking into account polymorphic transformations, melting, and evaporation effects. Calculations of thermodynamic characteristics of different crystal modifications of ice as well as liquid and vapor phases over a wide range of pressures and temperatures are carried out. Comparison of calculated results with available experimental data and theoretical predictions at high energy densities is presented. Obtained multiphase equation of state of water can be used effectively in numerical modeling of processes under conditions of intense pulsed influences on condensed matter.

VAPOR–LIQUID CRITICAL POINT FOR CUT-OFF COULOMB NON-IDEAL PLASMA MODEL

Butlitsky M.A.,* Zelener B.V., Zelener B.B.

JIHT RAS, Moscow, Russia

**aristofun@yandex.ru*

A Monte Carlo study has been made of "cut-off Coulomb" model of non-ideal plasma of electrons and protons. Thermodynamic proterties and pair distribution functions were obtained for a wide range of electron densities and temperatures.

Phase diagrams and gas-liquid critical point were calculated using NVT ensemble MC simulations. Possibility of observing a gas-liquid phase transition in real plasmas was evaluated based on the results of model calculations.

"Cut-off Coulomb" plasma model was initially developed and successfully used for analysis of nonideal plasmas properties in Zelener B. V, Norman G. E., Filinov V. S. TVT, 10, 6, 1972.

The idea of the model is based on calculating the electron-proton configuration integral using pair-state interaction approximation (3- and more particles quantum states are ignored) and describing the interaction between electrons and protons as the model pseudo-potential function. While ordinary Coulomb potentials are used for electron-electron and proton-proton interaction.

There are two dimensionless parameters in the model: gamma (non-ideality parameter) and epsilon (depth of coulomb potential cut-off).

Gas-liquid critical point near the gamma = 1.6 and epsilon = 13 has been found in this work.

The equilibrium electron and ion densities as well as ionization potential values of real atoms (H, Xe and Cs) were compared with cut-off Coulomb model critical point parameters. And rather interesting conclusion has been evaluated. The conclusion is that it is hardly possible to see the actual gas-liquid phase transition in real experiments with equilibrium plasmas, due to extremely high densities required, where pair-state interaction approximation and the described model cannot be applied.

This work was supported by the MK-4092.2014.2, the RFBR 14–02–00828, the Presidium of the RAS (Basic Research Program "Investigation of Matter in Extreme States" headed by V.E. Fortov), and the Ministry of Education and Science of the Russian Federation federal program No: 8679, 8513, and 8364.

CALCULATION OF BINODAL AND CRITICAL PARAMETERS OF VAPOR–LIQUID TRANSTION IN METAL VAPORS

Shumikhin A.S.,* Khomkin A.L.

JIHT RAS, Moscow, Russia

**shum_ac@mail.ru*

We suggested the new method for binodal and critical parameters of metal vapors calculation using the cohesion energy and embedding energy calculations available in literature. This data are available in functional form of scaling dependence on expansion ratio of metals. As a rule, they are multiparametric and referred to one of solid phase characteristic: sublimation energy, normal density, compressibility factor, bulk modulus etc. The basis of model is the hypothesis that cohesion exists not only in solid and liquid phases of metals, but in small vicinity (gas) of critical point (gaseous metal of Likalter is exist). The attractive energy in equation of state is the cohesion that extrapolated in gas-liquid region. We assumed the existence of phase transition with respective critical point as in the case of alkali metals [1]. The calculation of critical point parameters (density, temperature, pressure) is made and compared with known experimental data for alkali metals. The comparison with estimated critical parameters for other groups of metals is made also. This approach may be used in addition to existence method that used extrapolation of liquid and gaseous

branches of binodal.

1. Khomkin A. L., Shumikhin A. S. // JETP. 2014. V. 145. No. 1. P. 84.

EQUATION OF SPECIFIC THERMAL HEAT CAPACITY OF GAS CONDENSATES AND THEIR FRACTIONS IN LIQUID PHASE ON PSEUDO-CRITICAL ISOBAR

Bukhovich Y.V.,* Maltsev R.G., Magomadov A.S.

KubSTU, Krasnodar, Russia

**evapo@br.ru*

We are studying specific isobaric thermal heat capacity of gas condensates and their fractions in liquid phase on pseudo-critical isobar. The range of temperatures was from 233.15 K till 523.15 K. The mathematical treatment of the results is carried out in strange coordinates. The common equation expressing specific isobaric thermal heat capacity as the function of temperature has been obtained. The method of investigating specific isobaric thermal heat capacity of liquids as the function of temperature with the mean relative error unexceeded 1% has been worked out.

1. Bernal, J. D. Structure and Properties of Liquids / J. D. Bernal. London: Elsevier, 1965. P. 25.
2. Chen, Z. Y., Abbaci, A., Tang S., Sengers, J. V. Global thermodynamic behavior of fluids in the critical region / Z. Y. Chen, A. Abbaci, S. Tang, J. V. Sengers. // Phys. Rev. 1990. A. 42. P. 4470.

ABOUT THERMODYNAMIC SIMILARITY AND TWO ONE-PARAMETER FAMILIES OF EQUATIONS OF STATE BASED ON THE MODEL OF INTERACTING POINT CENTERS

Petrik G.G.

IGR DSC RAS, Makhachkala, Russia

galina_petrik@mail.ru

The equation of state (EOS) of van der Waals (VDW) is 140. Hundreds of little-parametric equations offered during this time as its independent empirical modifications. Currently (and not for the first time), there is a tendency of refusal from such EOS in favor of complex many-constant (up to 100 and more parameters) equations. The little now can mean and 10

and 15 parameters. But simple increasing the number of fitting parameters does not lead to the clarification of questions arising in the analysis even of two-parametrical EOS and does not result in a new fundamental knowledge. At the same time one can prove that the possibilities of simple equations far from exhausting, and get new information based on a system approach to the modeling. Its realization has led us to a new three-parametrical equation of state on the basis of a simple molecular model of interacting point centers (IPC). The fact that all the parameters of EOS are not fitting, but have the physical sense, revealed the control parameter of the model, defined as the ratio between the manifestation of the acting forces that puts it into a one-parameter family of EOS. The paper presents some new results. It is shown that depending on the structure of the control parameter, two boundary one-parametrical family of EOS can be obtained. The first includes the equations, for which the forces of attraction are weak, as expected in the VDW EOS, but forces of repulsion are mitigated (like EOS by Carnachan and Starling). EOS of the second family reflect the hard nature of the forces of repulsion, but optimized one for the forces of attraction. For EOS parameters the expressions were obtained in the form of analytical functions of the control parameters in the models. The second family until studied more, because it includes many EOS with realistic values of the critical compressibility factor (0.25–0.30), and since it was the confirmation of the one-parametric law of corresponding states that makes it possible to put the control parameter of the model in one row with such crucial criteria of thermodynamic similarity as acentric factor by Pitcer and the Riedel and L.P.Philippov criteria. It is important that after a certain reformulation many EOS of vdW-type can also be included in the model IPC that allows to consider them not formal structures but physically based models associated with each other. Some of the results obtained with the support of RFBR (grant 09-08–96521).

SOME ANALYTICAL AND COMPUTATIONAL CAPABILITIES OF THE MODEL OF SPHERICAL SHELLS AS THE BASIS OF THE EQUATION OF STATE

Petrik G.G.,* Gadjieva Z.R.

IGR DSC RAS, Makhachkala, Russia

**galina_petrik@mail.ru*

The paper presents new results obtained in the framework of the molecular model of spherical shells and showing its analytical and computational capacities. The molecularly substantiated equation of state (EOS) is the

goal of many researchers. At first glance, the result should be EOS, the parameters of which are connected with parameters of the model potential (MP), most adequately describing the interaction of objects substituting real molecules. At the same time, as a rule, the parameters of EOS and MP are considered as ajustable ones that complicates the identification of such communication. We believe that to define the parameters of EOS and MP, the formulas must be obtained as functions of their control parameters. And it is required to find the relation of these two parameters. It is obvious that for such an approach the choice of a model of the molecule as well the most common its characteristic is very important. This characteristic should be evident in the properties (first) of interaction of the pair of molecules, and then in the properties of the substance formed by such model objects, being thus the control (defining) parameter at the molecular and thermodynamic level. We have obtained EOS based on of the simplest molecular model of interacting point centers (IPC) (most popular central MP–family of Mi(n-m)), that has allowed to acquire a new information. The main was that we managed to find the control parameter of the model and link it with the manifestation of the acting force in terms of size. However, since the object is a material point, it was only the effective its size. Primitiveness of the object results in restrictions of the new EOS IPC, that makes moving to a more realistic model of the object. It seems the most reasonable, the choice of the model of spherical shells and the spherical shells potential to describe interactions. New results we obtained for it quarter century ago. Identification of the most common characteristic of the model object, which we called the hardness of the shell, became fundamental. It is shown that namely its value generates interaction potential of two shells, i.e. determines the values of the parameters (for them the formuls have been obtained) and the shape of the curve (the technique of choice of MP-analogues in Mi(n-m)-families has been suggested). It was identified as a control parameter of the model. The latter is the more justified that were able to establish that the found characteristic reflects an universal fact of electron-nuclear structure of molecules.

A GENERALIZED EQUATION OF STATE OF THE VAN DER WAALS–BERTHELOT

Sobko A.A.

AES, Moscow, Russia

ainrf@mail.ru

Full calculation of vaporization curve is made for equations of state of van der Waals

$$P^\star = \frac{8T^\star}{3V^\star - 1} - \frac{3}{V^{\star 2}}$$

and Berthelot

$$P^\star = \frac{8T^\star}{3V^\star - 1} - \frac{3}{V^{\star 2}T^\star},$$

where $P^\star = P/P_c$, $T^\star = T/T_c$, $V^\star = V/V_c$.

It is shown that the vaporization curves of real gases are situated between the same curves of van der Waals and Berthelot gases. A generalized equation of state of van der Waals–Berthelot gas is proposed:

$$P^\star = \frac{8T^\star}{3V^\star - 1} - \frac{3}{V^{\star 2}T^{\star \alpha}},$$

where a good agreement with the vaporization curves of real gases may be obtained by varying the parameter α. Using obtained values of α, it is shown that the generalized van der Waals–Berthelot equation well describes not only qualitatively but also quantitatively also other characteristics of real gases, such as the temperature dependence of the volume of the gas and liquid phases at vaporization of krypton $V_G^\star = f(T^\star)$, $V_L^\star = f(T^\star)$ [1].

---

1. Vargaftik N. B. Reference Thermophysical Properties of Gases and Liquids. M.: Nauka, 1972.

SINGLE STATE EQUATION OF MOLECULAR SYSTEMS WITH CENTRAL INTERACTION

Narkevich I.I, Farafontova E.V.*

BSTU, Minsk, Belarus

**inarkevich@mail.ru*

Using the method of correlative functions of Bogolyubov–Born–Green–Kirkwood–Yvon and the method of conditional distributions of Rott a single two-parameter equation of state for the crystal, liquid and gas have been received:

$$p = -\frac{\theta}{\omega}\ln\left(1-\frac{\omega}{\upsilon}\right) - \frac{A\omega}{2\upsilon^2} - \frac{\omega^2}{2\upsilon^3}\left(\frac{\partial A}{\partial n}\right)_{\theta,\omega}.$$

Here $\theta = kT$, $\upsilon = V/N$ is a molecular volume, $\omega = f_1(\theta, \upsilon)$ is a microcell volume, $A = f_2(\theta, \omega, n)$ is an energy-entropy parameter of model, $n = N/M$ is a concentration of molecules in the volume V of system which is divided into M microcells, $M = V/\omega$ is the number of microcells with a volume ω. Parameters ω and A depend on the thermodynamic parameters and are calculated with the help of statistic-variational method.

THE FUNDAMENTAL EQUATION OF STATE THAT TAKES INTO ACCOUNT THE ASYMMETRY OF THE FLUID RELATIVE TO THE CRITICAL ISOCHORE

Rykov S.V.

SPbSU ITMO, Saint-Petersburg, Russia

togg1@yandex.ru

Based on the method pseudocritical points, in which singularly component of the isochoric heat capacity is:

$$C_v(\rho, T) = A \cdot \tau_p^{-\alpha}(\tilde{x} + x_1)^{-\alpha}, \tag{1}$$

and the next representation of a scale hypothesis:

$$\Delta S \cdot (C_v)^{\frac{1-\alpha}{\alpha}} = \sum_{n=0}^{3} a_n \cdot C_v^{-\Delta_n/\alpha} \cdot \varphi_n(\tau_p^{1/\beta} \cdot C_v^{\beta/\alpha}), \tag{2}$$

calculated fundamental equation of state of argon, taking into account the asymmetry of the fluid relative to critical isochore:

$$\frac{\rho}{p_c}F(\rho,T) = f(\rho)\sum_{n=0}^{3}|\tau_p|^{2-\alpha+\Delta_n}a_n(\tilde{x}) + \frac{\rho}{p_c}F_r(\rho,T). \quad (3)$$

Here $a_n(\tilde{x})$ — scale functions of free energy $F(\rho,T)$

$$a_n(\tilde{x}) = A_n^*(\tilde{x}+x_1)^{2-\alpha+\Delta_n} + B_n^*(\tilde{x}+x_1)^{\beta\delta+\Delta_n} + D_n^*(\tilde{x}+x_1)^{\gamma+\Delta_n} + C_n; \quad (4)$$

$\Delta S = \rho T_c/p_c \cdot (s(\rho,T) - s_0(\rho,T))$; s — entropy; p_c — critical pressure; $\Delta_0 = 0$; α, β, δ, γ, Δ_1, Δ_2 and Δ_3 — critical indexes; $f(\rho)$ — crossover function; $s_0(\rho,T)$, $F_r(\rho,T)$ — regular functions of temperature T and density ρ; $\tilde{x} = \tau_p/\tau$ — generalized scale variable, $\tilde{x} = -x_1$ — equation of the pseudocritical points line.

The fundamental equation of state (3) with scale functions developed on the basis (4) was tested on the description of the thermodynamic surface of argon. Calculated tables of equilibrium properties of argon in a wide range of state parameters: density from 0 to $3.35\rho_c$, temperature from threefold point to 1200 K. Also calculated detailed thermodynamic tables for critical and metastable parts of thermodynamic surface. It is shown that the accuracy of the description of the isochoric heat capacity in the critical region of suggested equation of state is significantly higher than crossover equation Rizi A. and Abbaci A. (2012) and accuracy description of the density and sound speed in the metastable region corresponds to the experimental.

THE SCALE NON-PARAMETRIC EQUATION BASED ON THE PHENOMENOLOGICAL THEORY OF CRITICAL PHENOMENA

Rykov S.V., Kudryavtseva I.V., Rykov V.A.*

SPbSU ITMO, Saint-Petersburg, Russia

**rykov-vladimir@rambler.ru*

Considered one of the variants of the phenomenological Migdal's theory in the form:

$$\Delta S \cdot X^{\frac{1-\alpha}{\chi}} = \varphi_0 + \varphi_2 \cdot (\Delta\rho)^2 \cdot X^{\frac{2\beta}{\chi}}. \quad (1)$$

Here $\Delta S = \rho T_c/p_c(s(\rho,T) - s_0(T))$; s — entropy; $s_0(T)$ — regular function of temperature; p_c — critical pressure; α, β, χ — critical indexes; $\Delta\rho = \rho/\rho_c - 1$; φ_0 and φ_2 — constant coefficients; X — thermodynamic

function (for example, isochoric C_v or isobaric C_p heat capacity, coefficient of isothermal compressibility K_T), which behavior in the asymptotic neighborhood of critical point is described in accordance with the Benedek's hypothesis.

$$X(\rho, T) = A|\Delta\rho|^{-\frac{\chi}{\beta}}(x + x_1)^{-\chi}. \quad (2)$$

On the basis of (1) and (2) the scale equation in physical variables is calculated:

$$\Delta S = |\Delta\rho|^{(1-\alpha)/\beta}(\varphi_0 A^{\frac{\alpha-1}{\chi}}(x + x_1)^{1-\alpha} + \varphi_0 A^{\frac{1-\gamma}{\chi}}(x + x_1)^{\gamma-1}). \quad (3)$$

On the basis of the offered approach also authors have proved a method of several pseudospinodal curves (Rykov, 1985) and have calculated scale function of entropy:

$$a_s(x) = A_s((x + x_1)^{1-\alpha} - x_1/x_2 \cdot (x + x_2)^{1-\alpha}) + B_s(x + x_3)^{\gamma-1}). \quad (4)$$

It is shown that the scaling equation of state, calculated on the basis of (4) in its calculation characteristics substantially exceeds nonparametric equation Bezverkhy-Martynets-Matizen (2009), in particular, does not contain integrals of differential binomials, and is not inferior to the equation Scofield-Litstera-Ho. Deviation between the scale functions Helmholtz free energy, entropy, isochoric heat capacity, isothermal compressibility coefficient calculated from (4) and scale functions of a linear model in the range of state parameters from the critical isochore to the saturation line do not exceed 1.1%.

ABOUT USE OF THE WIDE-RANGE EQUATIONS OF STATE IN HYDROCODES

Ostrik A. V.

IPCP RAS, Chernogolovka, Russia

ostrik@ficp.ac.ru

The wide range equations of a state (EOS) are necessary part of modern numerical hydrodynamics codes [1, 2]. However EOS employment leads to a set of difficulties having in widely used and known numerical codes (for example, [3]).

Some of these difficulties and ways of their overcoming are considered in the present work. The basic requirements to which have to satisfy

modern wide range EOS are formulated. EOS use specialties that arise at numerical modeling of non-stationary processes taking place in physics of high energy density are discussed.

The main difficulties when using tabular EOS are caused by a choice of the interpolation method [4] and processing of cases when independent variables go beyond tabulation area. Basic moment defining success of numerical modeling is the method of numerical EOS realization in areas of two-phase states. Refusal from interpolation of available tabular data and return to an initial curve P(T) of two phases balance are offered [5] for this realization.

Difficulties arise in areas of two-phase states and at realization of metastable states when we use caloric EOS. Methods of overcoming of these difficulties are considered in work [6].

Creation of the defining equations is required for heterogeneous materials when EOS of its components are known. The method of an elementary cell is widely used for calculation of defining equations [7].

---

1. Bushman A.V., Fortov V.E. //Usp. Fiz. Nauk. 1983. V. 140. No. 6. P. 177–232.
2. Kuropatenko V.F. //The digest of scientific works Extreme Conditions of Substance under editor V. E. Fortov. M.: IVTAN. 1991. P. 3–38.
3. sites: www.ansys.com; www.cadfem-cis.ru/products/ls-dyna
4. Prokopov G.P. //Preprint, Inst. Appl. Math., the Russian Academy of Science, 2004.
5. Ostrik A.V., Romadinova E.A. //Book of Abstracts XX International Conference on Interaction of Intense Energy Fluxes with Matter, Elbrus, Russia, 2005, P. 111–112.
6. Ostrik A.V., Romadinova E.A. //J. Constructions from composite materials, 2004. Num. 2. P. 42–49.
7. Ostrik A.V., Romadinova E.A. //J. Chemical physics, 2001. V. 20. No. 8. P. 90–93.

THE EQUATIONS OF STATE OF HIGH-POROSITY SUBSTANCES

Belkheeva R.K.

NSU, Novosibirsk, Russia

rumia@post.nsu.ru

To describe the material subjected to shock-wave action, the equation of state in the form of Mie-Grüneisen is used. If the shock wave is of low intensity, then the Grüneisen coefficient γ is assumed to be constant and equal to the Grüneisen coefficient under standard conditions γ_0.

A method of constructing the equation of state in the form of Mie-Grüneisen for porous substances and mixtures is proposed in [1]. The parameters of this equation are expressed via the corresponding parameters and mass fractions of the species.

If the porosity of the substance is such that $\frac{\rho_{c0}}{\rho} < h$, $h = \frac{2}{\gamma} + 1$, the equations of state, in which the Grüneisen coefficient is described by the formula $\gamma = \gamma_0 \left(\frac{\rho_0}{\rho}\right)^l$, (1) where ρ is the substance density, ρ_0 is the density under standard conditions, describes well the porous material under shock wave impact. But if the porosity is such that $\frac{\rho_{c0}}{\rho} > h$ behavior of the shock adiabat becomes abnormal: with increasing pressure the density of matter decreases. Here ρ_{c0} is the initial density of condensed substances. In this case, the more porous the material, the more the shock adiabat, calculated using the equation of state in which the Grüneisen coefficient is described by (1), deviates from the experimental adiabat. The data presented in the literature on shock-wave loading substances indicate that the Grüneisen coefficient decreases with increasing pressure loading. In the case of large porosities in the abnormal behavior of the shock adiabat Grüneisen coefficient given by the formula (1) will increase with increasing pressure. In this paper for describing the Grüneisen coefficient at high porosity we propose to use the following relation $\gamma = \gamma_0 \left(\frac{\rho_0}{\rho}\right)^{-l}$, wherein l has the same meaning as in the case (1). Hugoniots substances with high porosity (as an example, the Hugoniots copper), calculated using the equation of state in which the Grüneisen coefficient is given by (2), are in good agreement with the experimental data.

---

1. Belkheeva R. K. // J. of Appl. Mech. and Tech. Phys. 2012. V. 53. No. 4. P. 3–15.

BEHAVIOR OF COMPOSITES AT PULSED LOADING

Efremov V.P.,[*1] ***Gins S.M.,***[2] ***Degtyar V.G.,***[2] ***Demidov B.A.,***[3] ***Kalashnikov S.T.,***[2] ***Khishchenko K.V.,***[1] ***Khlybov V.I.,***[2] ***Potapenko A.I.,***[4] ***Utkin A.V.***[5]

[1]*JIHT RAS, Moscow,* [2]*OAO "Makeyev GRTs", Miass,*
[3]*NRC KI, Moscow,* [4]*12CSRI MOD RF, Sergiev Posad,*
[5]*IPCP RAS, Chernogolovka, Russia*

**dr.efremov@gmail.com*

Modern composites materials are designed for work under conditions of pulsed mechanical and thermal loadings. The source of the loadings may be impact or intense irradiation pulse. Generally the behavior of composite constructions at pulsed loading is predicted by 3D numerical simulations. Accuracy of this modeling is determined by adequate describing of all involved physical process including valid model of equation of state (EOS). By turn the model of EOS construction is based on data from shock-wave and thermophysical measurements. For necessary data obtaining, we had carried out shock-wave and irradiation tests with a material in question. Shock loadings are created by impact of plane fliers accelerated by high explosives. Irradiation loadings are created by pulse electron beam. Used experimental techniques and diagnostics are described elsewhere [1, 2]. EOS model is taken from [3].

---

1. Efremov V.P., Potapenko A.I. // Teplofiz. Vys. Temp. 2010. V. 48. P. 924–930.
2. Efremov V.P., Potapenko A.I., Skripov P.V., Fortov V.E. Thermal-Mechanical Processes in Heterogeneous Materials under the Action of Volumetric-Absorbent Intense Energy Fluxes. Sergiev Posad: 12CSRI MOD RF, 2013.
3. Lomonosov I.V., Fortov V.E., Khishchenko K.V. // Chem. Phys. Rep. 1995. V. 14. P. 51–57.

ATOMISTIC MODELING OF GRAPHITE MELTING

Orekhov N.D.,* Stegailov V.V.

JIHT RAS, Moscow, Russia

**nikita.orekhov@gmail.com*

For many years the graphite melting curve has been the object of essential debates due to large discrepancies in experimental data. We report here the two-phase molecular dynamic simulations of graphite melting with the semiempirical bond-order potential AIREBO. In the pressure range up

to 14 GPa the graphite melting line is obtained and properties of liquid carbon are investigated. For the superheated graphite the melting front velocity dependencies on temperature are calculated to verify the melting temperatures values. The influence of the defect formation in superheated crystal on melting process is considered. Different melting regimes are revealed. The results provide a possible way to resolve the long-standing question for the reasons of large discrepancies in experimental data.

MOLECULAR DYNAMICS SIMULATION OF Fe–H WITH EAM POTENTIAL: TESTING AND DETALIZATION RESULTS

Emelin D.A.,* Mirzoev A.A.

SUSU, Chelyabinsk, Russia

**emelin_d_a@mail.ru*

Of all elements hydrogen has the smallest radius of the atom. It is the main feature affecting its diffusion characteristics. And therefore hydrogen is considered one of the main types of impurities affecting the mechanical properties of materials, and often causing hydrogen embrittlement (HE). It is a defect of the most kinds of steel.

There are a lot of HE models existing nowadays [1–3].The most widely used method to determine the mechanism of HE in metals is the method of molecular dynamics using EAM potentials. The main problem of the method is to find an appropriate interaction potential. In particular, for the MD simulation system FeH a number of EAM potentials exist, such as Ruda, Wen, Carter potentials and Lee MEAM potential (references in article [4]). In this article Carter has proved that at present time her EAM potential is the most suitable one.

The Carters potential was tested in the system of bcc Fe with embedded H by means of MD simulations. According to the MD simulation results the potential reproduces dissolution energy of hydrogen,formation energy of vacancy and the diffusivity of hydrogen.These data are consistent with other experiments, results of MD simulations and ab initio simulations (references in article [5]) . Moreover, the dependency of H-H binding energy and the dependency of H-V binding energy were further detailed.

It is interesting that at a hydrogen concentration of 5% and upwards the “swelling” effect of the sample was observed.

---

1. Beachem C. B. // Metall trans A. 1972. V. 3. No. 1. P. 437–451.
2. Lynch S. P.: Mechanism of hydrogen-assisted cracking. 1979.

3. Shih D. S.,Robertson I. M.,Birnbaum H. K. // Acta Metallurgica. 1972. V. 36. No. 1. P. 111–124.
4. Ramasubramaniam A., Carter E. A., Itakura M. //Physical Review B. 2009. V. 79. No. 17. P. 174101–174101.
5. Kimizuka H., Mori H., Ogata S. //Physical Review B. 2011. V. 83. No. 9. P. 0941101.

SOME MATHEMATICAL MODELS OF FRACTIONAL BROWNIAN MOTION

Nakhushev A.M.,* Nakhusheva V.A.

RIAMA KBRC RAS, Nalchik, Russia

**niipma@mail333.com*

As it was noted by Zel'dovich Ya.B. and Sokolov D.D. [1] "physical applications of fractals in a sense, were mentioned by Einstein and Smolukhowski on Brownian motion at the very beginning of the century"; "fear of singularities in general relativity, is essentially, is an echo of the inapplicability of undifferentiated representation of objects". Classical Brownian motion is based on the Fourier diffusion equation: $\rho_t = \varkappa\rho_{xx}$, where $\rho = \rho(x,t)$ is the particle density at the point $x \in [0,\infty[$ at time t. It is an exceptional case of fractal diffusion equation [2]:

$$D^{\alpha}_{0y}\rho(x,\eta) = a_{\alpha}\rho_{xx}(x,t), \quad y \equiv t > 0, \tag{1}$$

Here D^{α}_{0y} is the Riemann-Liouville fractional partial differentiation operator with respect to y of order α, $\alpha \in]0,1]$, $a_{\alpha} = \text{const}$ is fractal diffusion coefficient. The fundamental $\Gamma_{\alpha}(x,y;\xi,\eta)$ of equation (1) is defined by

$$\Gamma_{\alpha}(x,y;\xi,\eta) = \frac{1}{2\sqrt{a_{\alpha}}}(y-\eta)^{\beta-1}\Phi_{\alpha}\left(-\frac{|x-\xi|}{\sqrt{a_{\alpha}(y-\eta)^{\alpha}}}\right), \quad y > \eta, \tag{2}$$

where $\beta = \alpha/2$, $\Phi_{\alpha}(z) = \phi(-\beta,\beta;z)$ is the Wright function.

We justify that function (2) can be effectively used to determine the generalized Brownian motion as a non-Markovian stochastic process with transition density that is the fundamental solution of equation (1). This approach allows us to introduce concept of fractional Brownian motion as a random process with transition density which is a solution of the loaded differential equation of fractal diffusion (1). Fractional Brownian motion investigated by Mandelbrot and Van Ness has no this property: transition density which is corresponding to transition function, is a solution of equation $\rho_t = h\sigma^2(t-\eta)^{2h-1}\rho_{xx}$, whehe $0 < h = \text{const} < 1$, $\sigma = \text{const} > 0$.

This equation can simply be reduced to Fourier equation by time variable replacement.

1. Zel'dovich Ya. B., Sokolov D. D. Fractals, similarity, intermediate asymptotic// Soviet Physics Uspekhi, 1985. V. 28, No. 7. P. 608–616.
2. Nakhusheva V. A. On Some Fractal Differential Equations of Mathematical Models of Catastrophic Situations// Differential Equations. 2013. V. 49, No. 1. P. 487–494.

THE EQUATION OF STATE OF A SOLID WITH A FRACTIONAL DERIVATIVE OF RIEMANN–LIOUVILLE

Mamchuev M.O.

RIAMA KBRC RAS, Nalchik, Russia

mamchuevmo@yandex.ru

Currently urgent task is to obtain the equation of state in a wide range of pressures and temperatures. The most widely used are electronic and molecular statistical methods [1, 2], numerical simulation Monte Carlo and molecular dynamics, quantum methods based on consideration of the thermal vibrations of atoms, taking into account features of the interatomic potential. For all of these methods, there are characteristic assumptions, rationality of which in each case requires justification. For this reason, the development of the universal equation of state, essentially expanding the class of systems described, is the actual problem. We obtain the equation of state of a solid with a fractional derivative of Riemann–Liouville [3], expression for the free energy, the bulk modulus, and the relationship between the ratio of the fractional derivative and the fractal dimension of the crystal. The resulting equation of state can be applied to crystals with fractal structure [4].

1. Ukhov V. F., Kobeleva R. M., Dedkov G. B., Temrokov A. I. Electronic and Statistical Theory of Metals and Ionic Crystals. Moscow: Nauka, 1982.
2. Mamchuev M. O. // Inzhenernaia Fizika. 2009. V. 7, No. P. 8.
3. Nakhushev A. M. Fractional Calculus and Its Application. Moscow: Fizmatlit, 2003. 272 p.
4. Kronover R. Fractals and Chaos in Dynamical System. Moscow: Tekhnosfera, 2006. 488 p.

CALCULATION OF THE THERMOPHYSICAL PARAMETERS OF THE COMPLEX MATTER ON A BASE OF FRACTAL STATE EQUATION

Meilanov R.P., Magomedov R.A.*

IGR DSC RAS, Makhachkala, Russia

**lanten50@mail.ru*

The generalization of thermodynamics in formalism of fractional derivatives is given. The Boltzmann-Gibbs thermodynamics results are obtained for particular case, when the rate of derivative of fractional order is equal to one. The one-parametric fractal state equation with second virial coefficient is obtained. It is shown that transition from standard derivatives to derivatives of fractional order represents the technique of accounting of the local nonequilibrium concept, when the thermodynamic process is affected by fluctuations of the thermodynamic parameters. The conditions of application of the traditional Boltzmann-Gibbs thermodynamics are violated, namely the principle of the molecular chaos. Using fractal state equation the thermodynamic parameters of R 404A, R 409B (freon) refrigerants are calculated.The compressibility factor, entropy, enthalpy are calculated. Obtained results satisfactorily coincide with the experimentally measured data. The opportunity of application of the fractal state equation for the extremal state research is discussed.

ON DETERMINATION OF THE TRUE TEMPERATURE OF OPAQUE MATERIALS BY WIEN'S DISPLACEMENT LAW

Rusin S.P.

JIHT RAS, Moscow, Russia

sprusin@yandex.ru

It is known that according to Wien's displacement law to determine the thermodynamic temperature of a black body is enough to know the wavelength of its thermal radiation maximum (peak-wavelength). However, for real materials, this law does not hold.For opaque materials the equation connecting the directional spectral emissivity at the peak-wavelength, the peak-wavelength value and the thermodynamic (true) temperature of the opaque heated body was obtained in [1]. For black and gray bodies, this equation gives the same result as Wien's displacement law.

In this report the problem of determining the true temperature of the opaque material is suggested to solve in two stages. In the first stage with the relative spectral emissivity is allocated the spectral interval that is most

comfortable for the approximation of the surface emissivity [1, 2]. Then, value of true temperature is determined using the least squares technique. In the second stage using the equation obtained in [1] the true temperature is determined again. The dimensionless parameter that relates the radiative properties of the material with the peak-wavelength value is found. If the absolute value of the parameter is small, the value of true temperature obtained in the first stage may be refined in the second stage. For real material deviation from Wien's displacement law is analyzed. This approach is illustrated by the experimental data obtained in comparison temperature lamps radiances [3].

1. Rusin S. P. // Thermophysics and Aeromechanics. 2013. V. 20. No. 5. P. 643.
2. Rusin S. P. // Thermophysics and Aeromechanics. 2011. V. 18. No. 4. P. 603.
3. Khlevnoy B. B. Supplementary comparison // Final Report: Spectral Radiance 220 to 2500 nm, 24 July 2008. Metrologia. 2008. V. 45.

EVALUATION OF THERMAL CONDUCTIVITY OF METALS IN THE FIELD OF CENTRIFUGAL ACCELERATIONS AND FORCES

Lepeshkin A.R.,* Bychkov N.G.

CIAM, Moscow, Russia

**lepeshkin.ar@gmail.com*

The turbine blades operate at extreme centrifugal accelerations of $40000 \ldots 100000$ m/s^2 ($4000 \ldots 10000$ g) and we can expect significant thermoconductivity change in these conditions. In addition to acceleration the tension centrifugal force acts on rotary parts. When the pressure (compressive force) rises to $250 \ldots 350$ MPa the thermoconductivity GaSb increased by $15 \ldots 20\%$ [2]. The investigations of the thermoconductivity of materials at tension have not been conducted. The russian scientists Mandelstam L.I. and Papaleksi N.D. established electron phenomenon by experimentally in 1913 [3]. This experiment has been enhanced in 1916 by the American scientist Tolman R.C. These experiments confirmed that the acceleration effect on the electron phenomena (electron transport) in metals under braking. The developed method of evaluation of thermal conductivity of materials in the field of centrifugal acceleration and forces has been used [1]. A device with a heat conductor (metal sample) to determine the thermophysics characteristics of materials on the spin rig using the vacuum chamber in conditions of centrifugal accelerations and forces has been developed [1]. From the analysis of the results of exper-

imental investigations it may be stated that the thermal conductivity of the heat-conductor increases significantly with an increase of a rotation frequency compared to the steady state without rotation. In the studied phenomenon of thermal conductivity the two components are present: the action of the centrifugal acceleration and centrifugal tensile load. The second component is a small value (10–20%). Thus, this increase of the thermal conductivity significantly associated with an increase of an electronic conductivity (electron transport) under the influence of centrifugal accelerations. The obtained results are of practical importance for the assessment of the thermal state of the rotating parts of aircraft engines.

1. Lepeshkin A. R., Bychkov N. G., Method and device for determining the thermofysical properties of solid materials in the field of centrifugal forces. Patent 2235982 RF. 2011. Bull. 11.
2. Emirov S. N., Bulaeva N. The effect of pressure on the thermal conductivity gallium antimonide. Proc. 12 RKTS. Nauka. 2008. P. 306.
3. Ginzburg V. L. Memory Andronov A. A. Academy of Sciences USSR. 1955. 622 p.

AB INITIO CALCULATIONS OF TRANSPORT AND OPTICAL PROPERTIES OF ALUMINUM AND THEIR THEORETICAL INTERPRETATION

Knyazev D.V.,* Levashov P.R.

JIHT RAS, Moscow, Russia

**d.v.knyazev@yandex.ru*

The information on the transport and optical properties of matter is necessary for the different applications of the physics of high energy densities. In this work at first transport and optical properties of aluminum are calculated *ab initio*. The calculation is based on the quantum molecular dynamics, density functional theory and the Kubo-Greenwood formula. The details of the calculation method are available in our previous paper [1].

The calculations are performed for liquid aluminum at normal density $\rho = 2.70$ g/cm^3. The electron and ion temperatures are varied within the range 3 kK $\leq T_i \leq T_e \leq$ 20 kK. The frequency range for the calculation of optical properties is $\omega \leq$10 eV.

The obtained results on the transport and optical properties are ap-

proximated by the simple semiempirical expressions:

$$\sigma_{1_{\rm DC}}(T_i,T_e)=\frac{A}{T_i^{0.25}},\quad L_{22}(T_i,T_e)=B\frac{T_e}{T_i^{0.25}},\quad \tau(T_i,T_e)=\frac{C}{T_i^{0.25}},\qquad(1)$$

$$\sigma_1(T_i,T_e,\omega)=\frac{\sigma_{1_{\rm DC}}(T_i,T_e)}{1+\left(\tau(T_i,T_e)\right)^2\omega^2}.\qquad(2)$$

The error of the approximation is not larger than 13%.

Then it was figured out that the results of *ab initio* calculation are well described by the Drude expressions if (1) is used as the relaxation time τ.

The comparison with other models of static electrical and thermal conductivities [2–4] is performed. The models mentioned all may be reduced to the Drude model in the low-temperature limit.

The models [2, 4] are reduced to the Drude model with the relaxation time $\tau\propto T_i^{-1}$. This is not supported by our results, implying the slower decrease of the relaxation time (1). The similar slow decrease of the relaxation time is presented in the paper [3].

1. Knyazev D. V., Levashov P. R. // Comput. Mater. Sci. 2013. V. 79. P. 817–829.
2. Anisimov S. I., Rethfeld B. // Proc. SPIE. 1997. V. 3093. P. 192–203.
3. Inogamov N. A., Petrov Yu. V. // JETP. 2010. V. 110, no. 3. P. 446–468.
4. Lee Y. T., More R. M. // Phys. Fluids. 1984. V. 27, no. 5. P. 1273–1286.

ABOUT LIQUID CARBON PROPERTIES IN THE Mbar REGIME

Batani D.,[1] ***Paleari S.,***[2] ***Benocci R.,***[2] ***Dezulian R.,***[2] ***Aliverdiev A.****[3]

[1]*CELIA, Talence, France,* [2]*UMB, Milano, Italy,*
[3]*IGR DSC RAS, Makhachkala, Russia*

**aliverdi@mail.ru*

Carbon properties at high pressures and temperatures are a subject of interest for many branches of science, including astrophysics and planetology, material science, applied engineering, inertial confinement fusion, etc. A number of solid forms of carbon are known. Except the best-known forms, graphite and diamond, very different from each other, there are pyrolytic graphite, fullerite, amorphous carbon, glassy carbons, etc. At higher temperatures, liquid phases are predicted, going from non-metallic at low pressures to semi-metallic and metallic at high ones. Nowadays, the

most accepted phase diagram of carbon by Grumbach and Martin sets the structural changes in liquid carbon at pressures of 4 and 10 Mbar. This suggests that laser-driven shocks should reach a liquid metallic phase.

We present the results of our resent works, concerning: (i) investigation of the reflectivity changes of high-pressures and high-temperatures carbon, compressed by means of laser-induced shocks, as a possible signature of phase transition, in particular the metallization in liquid phase [1], [2]; (ii) impedance mismatch analysis of equation-of-state of carbon at high pressure [3]. Numerical simulations (required to optimize target parameters and to clarify shock dynamics) are presented.

The authors would like to thank LGM (Universita degli Studi di Milano), LNF (Frascati, Italy), ITA (Trapani), ILE (Osaka University, Japan), PALS (Czech Republic) and LULI (France) for the fruitful collaboration in considered experiments. The work was supported by CNISM (Consorzio Nazionale Interuniversitario per le Scienze Fisiche della Materia). A.A. is also grateful to ESF (program SILMI), COST (Action MP1208) and RFBR (12–01–96500, 12–01–96501).

---

1. Paleari S. et al. // Eur. Phys. J. D 2013, V. 67. P. 136.
2. Paleari S. et al. // Physica Scripta (accepted) 2014.
3. Aliverdiev A. et al. // HPLaser. 2013. V. 1(2), P. 102.

PHASE TRANSITION OF Lu-MONOPNICTIDES: A HIGH PRESSURE STUDY

Bhat I.H.,* Pandey M.K., Gupta D.C.

CMTG SSP JU, Gwalior, India

**idu.idris@gmail.com*

The structural and mechanical properties of lutatium-pnictides (LuN, LuP, LuAs, LuSb, and LuBi) have been analyzed by using full-potential linearized augmented plane wave within generalized gradient approximation in the stable Fm-3m and high-pressure Pm-3m phase. Under compression, these materials undergo first-order structural transitions from B1 to B2 phases at 241, 98, 56.82, 25.2 and 32.3 GPa, respectively. The structural properties viz, equilibrium lattice constant, bulk modulus and its pressure derivative, transition pressure, equation of state and volume collapse show good agreement with available data.

EQUATION OF STATE FOR 1,3,5-TRIAMINO-2,4,6-TRINITROBENZOL BASED ON THE RESULTS OF STATIC EXPERIMENTS

Badretdinova L.Kh.,[*1] ***Kostitsyn O.V.,***[2] ***Smirnov E.B.,***[2] ***Stankevich A.V.,***[2] ***Ten K.A.,***[3] ***Tolochko B.P.,***[4] ***Shakirov I.Kh.***[2]

[1]*KNRTU, Kazan,* [2]*RFNC–VNIITF, Snezhinsk,*
[3]*LIH SB RAS, Novosibirsk,* [4]*ISSCM SB RAS, Novosibirsk, Russia*

[*]*salamandra_1985@mail.ru*

A simple model of the Mie–Grüneisen equation of state is proposed to describe thermodynamic properties of HE without the regard for phase transitions. The equation of state (EOS) was constructed proceeding from the determination of $F(V,T)$ Helmholtz free energy that is in the most simple way related to the matter structure model in the assumption that pressure and energy can be presented as thermal and potential (elastic) components. The form of the potential component depends on the solid body type. The thermal component depends on the oscillating motion of molecules found in a crystal and is described by the Debye approximation. As the area of static experiments does not go beyond low and moderate temperatures (up to 1000 K), this paper is focused on a phonon component of the thermal pressure energy. The Landau–Slater approximation describes the $\gamma(V)$ Grüneisen coefficient versus specific volume relationship being a connective element between thermal and potential components of the equation of state. The semi-empirical equation of state is obtained for 1,3,5-triamino-2,4,6-trinitrobenzol (TATB) being of interest due to its uniquely low sensitivity to the external thermal and mechanical stimuli. High stability, as compared to most known explosive materials, expands the range of varying thermodynamic parameters (pressure, temperature, etc.) in experimental investigations necessary for EOS construction. Moreover, TATB is extremely attractive for scientific research due to its complicated crystalline structure. Having the triclinic system, TATB crystals are characterized by high anisotropy and low symmetry that poses serious difficulties for the X-ray diffraction analysis. EOS parameters were determined in the X-ray diffraction study of TATB under isothermal and isobaric conditions. Good description of experiments on shock compression, thermal expansion, and thermal capacity, which were attained for the macrostructural pressed TATB members, confirms EOS correctness. The proposed EOS is expected to improve accuracy in describing thermodynamic parameters of unreacted TATB in numerical simulation of shock-wave and detonation processes.

STUDY OF CARBON MODIFICATIONS IN THE ULTRAFINE MATERIAL PRODUCED FROM GRAPHITE–CATALYST MIXTURE UNDER EXTREME ENERGY ACTION

Melnikova N.V.,[*1] ***Alikin D.O.,***[1] ***Dolgikh E.A.,***[1]
Grigorov I.G.,[2] ***Chaikovsky S.A.,***[3] ***Labetskaya N.A.,***[3]
Datsko I.M.,[3] ***Oreshkin V.I.,***[3] ***Khishchenko K.V.***[4]

[1] *UrFU, Ekaterinburg,* [2] *ISSC UB RAS, Ekaterinburg,*
[3] *IHCE SB RAS, Tomsk,* [4] *JIHT RAS, Moscow, Russia*

[*] *nvm.melnikova@gmail.com*

The goal of this work is to study carbon forms in the ultrafine material produced under conditions of extreme energy effects on the mixture of graphite and catalysts. Experiments on the electrical explosion of the copper tubes filled with a mixture of industrial graphite and Ni–Mn catalyst were performed under conditions described previously [1]. The samples were obtained by precipitation of the electrical explosion products on glass substrates [1]. Those samples were studied using X-ray diffraction and phase analysis, optical microscopy, Scanning Electron Microscopy and X-ray Microanalysis, energy dispersive X-ray analysis, confocal Raman microscopy (Alpha300R), and the impedance spectroscopy (ModuLab MTS, Solartron 1260A). The analysis of obtained data made it possible to estimate the presence of three main fractions: chaotic coarse agglomerates with an average size of a few tens of microns, spherical particles of size from hundreds of nanometers to a few microns, and fine grains (of size 5–100 nm), that are observed including on the surface of the spherical particles. The first fraction is fragment particles, residual metal particles that escaped evaporation in the explosion, and graphite. The second and the third fractions are particles formed due to condensation of the evaporated matter and forming a conductive film (of resistivity $\sim 10^7$ Ohm $\cdot$ m). As a result of X-ray mapping of the surface of the samples was estimated that the carbon atoms make up to 33%. To identify carbon forms in the samples and for detection of carbon in a diamond form is necessary to use other techniques, in particular transmission electron microscopy and the ultrasoft X-ray emission spectroscopy which will allow determining the type of hybridization of electron orbitals of carbon atoms in these films [2].
The work was supported by RFBR (project No. 13–02–00633).

---

1. Oreshkin V. I., Chaikovskii S. A., Labetskaya N. A., Ivanov Yu. F., Khishchenko K. V., Levashov P. R., Kuskova N. I., Rud' A. D. // Tech. Phys. 2012.

V. 57. No. 2. P. 198–202.
2. Galakhov V. R., Shamin S. N. // Izv. RAS. Physics. 2009. V. 73. P. 896–898.

MAGNETIC SUSCEPTIBILITY AND ELECTRICAL PROPERTIES OF MULTICOMPONENT COPPER–INDIUM CHALCOGENIDES

Melnikova N.V., Tebenkov A.V., Kandrina Yu.A., Stepanova E.A., Babushkin A.N., Kurochka K.V.*

UrFU, Ekaterinburg, Russia

**kirill.k.v@yandex.ru*

This paper presents the results of a study of the magnetic susceptibility, the electrical properties and magnetoresistance of the compounds $CuInS_2$, $CuInSe_2$, $CuInAsS_3$, $CuInAsSe_3$, $CuInSbS_3$ at atmospheric pressure and at pressures up to 50 GPa.

The compounds were synthesized by melting of elements in evacuated and filled argon silica tubes. The compounds crystallize in the tetragonal crystal system. There is a series of lines of chalcopyrite structure on diffraction pattern. Preferred orientation in the direction $< 112 >$, the degree of orientation is about 65%. The cell parameters of $CuInAsS_3$, $CuInAsSe_3$, $CuInSbS_3$ are close to parameters of $CuInSe_2$ and $CuInS_2$, and vary with atomic radii of composition elements. The temperature dependencies of the conductivity for $CuInSbS_3$ and $CuInAsS_3$ are typical for ionic and mixed electronic-ionic conductors, $CuInAsSe_3$ exhibits ferroelectric properties. The temperature dependencies of the magnetic susceptibility for all investigated compounds in the temperature range from 75 to 300 K are typical for diamagnetics. The magnetic susceptibility decreases in modulus with temperature decrease from 75 to 2 K that can be related to growth of its paramagnetic component. Langevin magnetic susceptibility of the ion cores of the lattice atoms was estimated by Kirkwood equation [1]. The paramagnetic component at low temperatures in the investigated materials was also estimated. The amount of paramagnetic centers was evaluated under condition that Curie-Weiss paramagnetism cause by intrinsic magnetic moments of unpaired electrons in the Cu^{2+} ions, containing an odd number of electrons.

Electric properties at high pressure have been investigated on dc current and by means of impedance measurements. Magnetoresistance has been measured in transverse magnetic field (up to B=1 T). The pressure ranges of noticeable changes in a behavior of magnetoresistance, real and imaginary parts of impedance and admittance are established.

This work was supported in part by the Russian Foundation for Basic Research, project no. 13–02–00633.

1. Dorfman Ya. G. Diamagnetism and chemical bond. // Moscow: Fizmatiz. 1961. 231 p.

STUDY OF ELECTRICAL PROPERTIES OF COPPER CHALCOGENIDES FROM THE SYSTEM OF Cu–Ge–As–Se

Kurochka K.V., Melnikova N.V., Zaikova V.E.*

UrFU, Ekaterinburg, Russia

**vasilisazaykova@gmail.com*

Multicomponent glassy and crystalline materials from the system of Cu-Ge-As-Se are promising objects of investigations because they possess unique physical properties [1].

This work is devoted to the study of the electrical properties of polycrystalline $(CuAsSe_2)_x(GeSe)_{1-x}$ ($x = 0.8$, 0.9). The compounds were synthesized by melting of elements in evacuated and filled argon silica tubes. X-ray diffraction experiments and qualification of materials have been performed by means with diffractometer *Shimadzu XRD* 7000. Electrical properties of materials were analyzed by means of impedance spectroscopy method in the frequency range of AC voltage from 1 Hz to 32 MHz. Measurements of the electrical conductivity at DC in cells with copper and graphite electrodes on the Solartron Analytical Modulab device were performed. The relaxation of conductivity which can be related to the presence of the ion transport in the investigated materials is observed.

This work was supported in part by the Russian Foundation for Basic Research, project no. 13–02–00633.

1. Melnikova N. V., Tebenkov A. V., Kurochka K., Babushkin A. N. Electrical properties of gassy $(GeSe)_{0.05}(CuAsSe_2)_{0.95}$ at the temperature range 10–300 K // Proceedings of the international conference “Phase transitions, critical and nonlinear phenomena in condensed matter” 2009. P. 405–408.

ELECTRICAL RESISTANCE OF MONOMERIC AND ROMBOHEDRAL C_{60} AT HIGH PRESSURE

Petrosyan T.K.,* Tikhomirova G.V., Volkova Ya.Yu.

UrFU, Ekaterinburg, Russia

**aliximik-ptk@rambler.ru*

Comparative studies of monomeric and rombohedral C_{60} resistivity were carry out at pressure up to 29 GPa and room temperature. The time dependence of C_{60} resistivity was studied at different pressures.

High-pressure was generated in a diamond anvil cell (DAC) with electrically conductive anvils of the "rounded cone-plane" type made of synthetic polycrystalline diamonds "carbonado". The samples of C_{60} were placed on the plane anvil after which the cell was closed and load applied. The resistance measurements of C_{60} were carry out at pressure up to 29 GPa during a few loading-unloading cycles.

In this work were found out a new state for the rhombohedral C_{60} at pressures 15 and 26 GPa. As for the monomeric C_{60} we did not observe any new phases, probably due to lack of pressure-treat. It is known that for an source C_{60} the scheme of transformation is: from monomer to dimer, from dimer to two-dimensionally polymerized phase, from 2D polymer to three-dimensionally polymerized phase. While rhombohedral phase C_{60} is already 2D.

This work was supported by the Government of the Sverdlovsk region and RFBR (grant 13–02–96039-r_ural).

PHENOMENOLOGICAL MODELLING OF CRYSTAL LATTICES DYNAMICS WITH PSEUDOATOMS AND NEUTRON INELASTIC SCATTERING EXPERIMENTS

Sedyakina D.V.,*[1] Clementyev E.S.[2]

[1]JIHT RAS, [2]INR RAS, Moscow, Russia

**sedyakina.d@gmail.com*

This work is aimed to study lattice dynamics in YbB_{12} and SmB_6. These rich borides are typical members of the class of materials broadly known as Kondo-insulators. This term denotes compounds which are close to valence instability and become semiconducting with a narrow energy gap at low temperature. We use a Born–von Karman force-constant phenomenological model to describe these materials and compare obtained results with the inelastic neutron scattering experiments.

RESULTS OF NUMERICAL SIMULATION OF TURBULENT FLOWS IN SHEAR LAYER AND THE KHOLMOGOROV'S PROBLEM

Fortova S.V.

ICAD RAS, Moscow, Russia

sfortova@mail.ru

We investigate initial stage of the onset of the turbulence in 3D free shear flow of an ideal compressible gas with (Kholmogorov's problem) and without influence of constant external force. The onset and development of the vortex cascade of hydrodynamic instabilities were traced by the direct simulation of the classical laws of conservation without the influence of viscosity and walls: Euler's equations in case of shear layer and Euler's equations with right side in case of Kholmogorov's problem.Development of the cascade of instabilities is initiated by pre-set harmonic disturbances of initial velocity. For numerical simulation we used monotonic dissipative stable finite-difference scheme with positive operator.

In this work we consider initial stage of the onset of the turbulence for both problems. It is shown that in case of a problem without affecting the constant force of the vortex cascade develops as follows: the evolution of the flow at the beginning demonstrates a quasi-two-dimensional nature (the onset of instability begins with the formation of large-scale vortex). However, evolving further, the large-scale vortex changes its shape with time and finally gets destroyed. Formation of the vortex cascade in Kolmogorov's problem is following. In contrast to the shear layer, the flow loses its stability due to instabilities in the form of a comb across the excited surface. Over time, this comb is stretched due to the formation of new instabilities. Large structure is formed implicitly. This structure finally also gets destroyed. It leads to the collapse into smaller vortexes. Thus, in this case the vortex cascade is also exist. It is shown that as the flow transforms to the turbulent phase there emerge pulsations of velocity of various scale which leads to the formation of a vortex cascade. Decomposition of kinetic energy on wave number reveals correspondence with the energy spectrum of Kolmogorov–Obukhov and $-5/3$ low for both problems.

---

1. Fortova S. V., Belotserkovskii O. M. Investigation of the Cascade Mechanism of Turbulence Development in Free Shear Flow // Doklady Akademii Nauk. 2012. V. 443. No. 1. P. 44–47.

ANALYTICAL MODEL FOR THE TRANSVERSE VIBRATION OF GRAPHENE AND (0001) GRAPHITE SURFACE

Khokonov A.Kh.

KBSU, Nalchik, Russia

azkh@mail.ru

Until now, graphite and graphene lattices vibrations are calculated by numerical methods with dynamic matrix of force constants coming from quantum chemical consideration. In [1], we proposed a simple model describing the transverse oscillation of the atomic monolayer based on on the assumption that the atoms are connected each an other by elastic stretched strings. This approach gives an analitical dispersion equation for graphen transverse oscillation in the form

$$\omega^2 = \omega_0^2(3 \mp \sqrt{3 - 2(\cos(2\pi p_1) + \cos(2\pi p_2) + \cos(2\pi(p_2 - p_1)))}), \quad (1)$$

where upper and lower signs correspond to acoustic and optical modes respectively, $\omega_0 = \sqrt{\frac{T}{M\,d}}$, T is the thread tension, M - atoms mass, d -atoms spacing, $p_{1,2}$ parametrised phonons wave vector $\mathbf{k} = \mathrm{p}_1\,\mathbf{b_1} + \mathrm{p}_2\,\mathbf{b_2}$.

In the long-wavelength approximation for an acoustic mode we have

$$\omega = \pi\omega_0\sqrt{\frac{5}{6}(p_1^2 + p_2^2) - \frac{1}{3}p_1 p_2} \quad (2)$$

This equation allows one to express the thread tension through the acoustic wave velocity. For the directions along $p_1 = p_2$ sound velocity $v_1 = \sqrt{\frac{3}{2}}\,v_0$, where $v_0 = \sqrt{\frac{T\,d}{M}}$.

The same dispersion equation takes place when the potential energy of the lattice is a quadratic form of bending angles of covalent bonds between carbon atoms.

---

1. Khokonov A.Kh., Kokov Z.A., Karamurzov B.S. // Surface Science. 2002. V.496. No.1–2. L13

ON THE METHODS OF MANY-PARTICLE SYSTEM STATE EQUATION EVALUATION BY MEANS OF MOLECULAR DYNAMICS

Khokonov A.Kh., Khokonov M.Kh.*

KBSU, Nalchik, Russia

**khokon6@mail.ru*

Different techniques of state equation calculation have been analyzed by means of molecular dynamics. The following connection of virial force and state equation have been used in our calculations:

$$Pv = k_B T + \frac{1}{3N}\langle W(\mathbf{r}_1, ..., \mathbf{r}_N)\rangle,$$

where

$$W(\mathbf{r}_1, ..., \mathbf{r}_N) = -\sum_{i=1}^{N} \mathbf{r}_i \nabla_i U(\mathbf{r}_1, ..., \mathbf{r}_N),$$

N is the number of particles in system, U is the potential energy of all particle interaction, v is the specific volume, P and T are pressure and temperature. Angular brackets mean the averaging over time.

The trajectories have been calculated by MD method with account of the random force [1]. It has been shown, that a thermostat method gives correct values of state equation parameters for Lennard-Jones systems.

Near the condensation point the results have been verified by high performance hybrid cluster calculation using LAMMPS program. Parameters of Van der Waals approximation are evaluated for Lennard-Jones gas state equation. Calculations using LAMMPS provide the critical temperature with an accuracy of 6 % for xenon and only 17 % for krypton. It means that the pair potential model is adequate enough for xenon but is not acceptable for krypton near the point of phase transition. Calculations show that this conclusion does not depend on the form of the pair potential.

---

1. Norman G. E., Yanilkin A. V., Zhilyaev P. A., Kuskin A. Yu., Pisarev V. V., Stegailov V.V. // Comp. Meth. and Programming. 2010. V. 11. P. 111.

SHEAR-INDUCED HELICAL FLOW IN A MICROCHANNEL WITH SUPER-HYDROPHOBIC WALL

Vagner S.A.,[*1] ***Patlazhan S.A.***[2]

[1]*IPCP RAS, Chernogolovka,* [2]*ICP RAS, Moscow, Russia*

[*]*vagnerserge@gmail.com*

Mixing of fluids in microchannels is of utmost importance in many applications. For instance, homogenization of solutions of reagents in chemical and biological reactions, drug solution dilution and in the control of dispersion of material along the direction of Poiseuille flows. But in microchannels the Reynolds number is so small then hydrodynamic instabilities and turbulence are completely suppressed. In order to enhance mixing, different techniques have been developed.

In this work a super-hydrophobic array of grooves containing trapped gas (stripes) located at an angle TETA to flow direction was considered as mixing technique. The study was carried out by numerical simulation. For simulation CFD code OpenFOAM was used, which based on finite volume method. In a mathematical formulation such surface is a set of strips with stick boundary condition on the liquid-solid interface and slip boundary condition on the liquid-gas interface.

It was shown that such configuration generate transverse secondary flows (helicoidal flow), which cause mixing of flow components. To understand physics of the helicoidal flow, perturbations of velocity on the slip-stick interface was investigated. To reveal how the intensity of the helicoidal flow depends on various parameters of considered system a series of calculations were performed. Also it was made a comparison with similar investigation for microchannel with grooves containing liquid.

UNIVERSALITY OF PHONON–ROTON SPECTRUM IN LIQUIDS AND SUPERFLUIDITY OF He II

Trigger S.A.,[*1] ***Bobrov V.B.,***[1] ***Litinski I.S.***[2]

[1]*JIHT RAS, Moscow, Russia,* [2]*FU, Berlin, Germany*

[*]*satron@mail.ru*

Based on experimental data on inelastic neutron and X-ray scattering in liquids, we assert that the phonon–roton spectrum of elementary excitations, predicted by Landau for superfluid helium, is a universal property of the liquid state. We show that the existence of the roton minimum in the spectrum of collective excitations is caused by the short-range order in liquids. Using the superfluidity criterion, we assume that one more branch

of collective excitations—helons—should exist in He II, whose energy spectrum differs from the phonon–roton spectrum. It was shown in [1–4] the existence of a gap for small momenta in the energetic spectrum of quasiparticles in He II (and in the model of weakly non-ideal Bose gas) is not in contradiction with the Goldstone's theorem for quantum liquids with the Bose-Einstein condensate. The question arises: why this branch of excitations, different from the phonon–roton one, does not manifest itself in the INS and IXS experiments? This can be explained by the assumption that these quasiparticles are related with poles of the single-particle Green function, rather with the poles of the "density-density" Green function. These poles coincide in the classical degenerate Bose gas theory based on anomalous averages, however, the theory of degenerate Bose gas can be constructed without anomalous averages. It is known that the observable phonon–roton excitations are the collective excitations of the dynamical structure factor and there is no necessity to demand their existence and coincidence in the hamiltonian or in single-particle Green function. In the present theory the poles of the single-particle Green function and dynamical structure factor are different as for normal systems. All known experimental data can be explained on the basis of such type theory. The helons, which are the poles the Green function and specific namely for the superfluid state completely determines the energy of the superfluid state. We show in [2],[3] that in the framework of the Landau approach to the thermodynamics of HeII, the existence of the helons gives explanation of the heat capacity singularity at the temperature of the superfluid transition.

---

1. S.A.Trigger and P.P.J.M.Schram, Physica B228, 107 (1996)
2. V.B. Bobrov, S.A. Trigger, and I.M. Yurin, Phys.Lett. A374, 1938 (2010).
3. V.B. Bobrov and S.A. Trigger, J. Low Temp. Phys. 170, 31–42 (2013).
4. V.B. Bobrov and S.A. Trigger, Prog. Theor. Exp. Phys., 043I01–043I10 (2013).

THE ANALYTICAL AND NUMERICAL SOLUTIONS OF THE ELECTROHYDRODYNAMIC EQUATIONS AT A PRE-BREAKDOWN LIQUID INSULATOR

Apfelbaum M.S., Buchko P.V.*

JIHT RAS, Moscow, Russia

**pahomich@tut.by*

The liquid insulator under high voltage reveals well-known features of its behaviour, that is concluded in deviation of the current–field dependence from Ohm's law. In this work we study the pre-breakdown behavior of liquid insulator on the base of our model. According to this model the liquid dielectric is analogous to the weak electrolyte. And the partial dissociation of its molecules takes place. The volume concentrations of the ions $n_\pm$ and the impurities n_p are supposed to satisfy the following conditions:

$$\begin{cases} n_\pm \ll n_a, \\ n_p \ll n_a. \end{cases} \tag{1}$$

n_a — is the concentration of neutral particles (molecules). We also introduce the new variables: $q = (n_+ - n_-)|e|$; $\sigma = (n_- b_- + n_+ b_+)|e|$ and potential ϕ: $E = -\nabla\phi$. Then, we can write the system of macroscopic time dependent equations of ions creating. If we suppose, that ion mobilities are equal for our liquid insulator and its combustion plasma: $b_- = b_+ = b$, witn (1) we will obtain:

$$\begin{cases} \frac{\partial q}{\partial t} + (\overrightarrow{V}, C_q) - \frac{k_B T b}{|e|}\triangle q + (\overrightarrow{E}, C_\sigma) = -\frac{q\sigma}{\varepsilon\varepsilon_0}, \triangle\phi = -\frac{q}{\varepsilon\varepsilon_0}, \\ \frac{\partial \sigma}{\partial t} + (\overrightarrow{V}, C_\sigma) - \frac{k_B T b}{|e|}\triangle\sigma + b^2(\overrightarrow{E}, C_q) + \frac{\sigma^2}{\varepsilon\varepsilon_0} - \\ -\frac{\sigma_0^2}{\varepsilon\varepsilon_0} exp(\beta|\overrightarrow{E}|^{1/2}) exp[\frac{A}{k_B T}(1 - \frac{T}{T_0})] = 0. \end{cases} \tag{2}$$

In (2) t— is time, V — is the hydrodynamic velocity of neutral component and is approximately equal to the velocity of the whole mixture, if (1) is valid, A—is activation energy. The coefficient in first exponent, obtained by Frenkel, at the equations (2) is depended on absolute temperature T, ion charge e and dielectric permittivity of the considered medium. For the case of sphere under constant high voltage U we obtained stationary analytical solution of equations (2) outside non-quasi-neutral boundary layers for the electric potential distribution, consisting to the Frenkel exponential conductivity law for weakly conductive insulators. This law may be obtained from equations (2) in quasi-neutral media under pre-breakdown electric field. For case of partially combustion products for considerable

medium we obtained numerical spherical symmetry solution of equations (2) with emission boundary condition on heat high- voltage cathode.

THERMOPHYSICAL PROPERTIES OF IONIC LIQUIDS: DATA BASES AND CALCULATIONS IN INTERNET

Ustyuzhanin E.E.,* Ochkov V.F., Khusnullin A.Kh., Znamenskiy V.A., Shishakov V.V.

MPEI, Moscow, Russia

**evgust@gmail.com*

Some literature sources and web sites are analyzed in this report. The sources contain information about thermophysical properties of ionic liquids (IL). Our analyses [1, 2] shows that a traditional database is represented by a number of properties, R, including $R = (v, h, s, ...)$ of a substance at given (P, T)—arguments, here v—the specific volume, h—the enthalpy, s—the entropy, (P, T)—the pressure and the temperature. These R properties have a form of tables. There is no Internet resources those are placed in such data base and allow to a client to calculate properties R at input parameters $U = (P, T)$ chosen by a client.

A structure of a data base is considered in the report. The data base is elaborated in frames of the work, includes R properties of ionic liquids and is referred as an "IL catalog". The structure has following components: (1) primary files, every primary file is named as "Compound $(K, R, L, M...)$" and includes some information of a defined IL; (2) a software that consists of several blocks.

Following characteristics are immersed in a primary file: (a) "Compound K", here K—an index of the defined IL; (b) "Property R"; (c) "Algorithm L"; (d) "Mathcad code M" that is used for an analytical description and online calculations of the property, $R(T, P)$; (e) other characteristics.

A special Internet software IRBOC is elaborated to work offline with thermophysical sources data [3]. A program Mathcad is chosen to produce "IL catalog" but not such languages as C, Pascal, BASIC and others. A current variant of "IL catalog" contains approximately 200 compounds and 1000 primary files, its demo-version is located in web sites:

http://www.irboc.com, http://twt.mpei.ac.ru/TTHB/2/IL/index.html.

The work is done as a grant of RFBI.

---

1. Khusnullin A., Ochkov V., Znamenskiy V. // 18th Symposium on Thermophysical Properties, 2012.

2. Ochkov V., Frenkel M., Khusnullin A. // Proceedings of VII Conference of Young Scientists and Specialists "Problems of heat and mass transfer and hydrodynamics in power machinery", September 15–17, 2010, Kazan, Russia. P. 281–284.
3. Ustyuzhanin E. E., Khusnullin A. S., Ochkov V. F. // Book of Abstracts of XXVIII International Conference on Interaction of Intense Energy Fluxes with Matter, Elbrus, 2013.

EXPERIMENTAL RESEARCH OF TECHNOLOGICAL WAVE IMPACT METHOD ON AN ACTIVE RESERVOIR

Maikov I.L.,[1] ***Molchanov D.A.,***[*1] ***Torchinsky V.M.,***[1] ***Ustenko I.G.***[2]

[1]*JIHT RAS,* [2]*NWMTC, Moscow, Russia*

[*]*dmitriy.molchanov13@gmail.com*

Gradual conductivity decreasing takes place in the process of hydrocarbon driving during forced water flooding in the consequence of water film formation on the pore surface and water diaphragm formation between close-range pores.

Experiments were run on the study of the high- and low-frequency wave impact influence for increasing reservoir conductivity ratio and oil-recovery factor.The investigation into revealing geological material-wave-fluid collaborative mechanism and determining the phenomena responsible for reservoir filtration ability increasing was carried out. In the present paper studies concerning the influence of various wave impact parameters and physical hydrocarbon characteristics on filtration process were conducted.

Conditions under which wave impact on holding reservoir may result in inter-pore diaphragm destruction and increasing reservoir conductivity for water-hydrocarbon mixtures were determined. It was demonstrated that resonant modes lead to acceleration of the filtration process on account of the capillary-detained hydrocarbon drive and increasing conductivity ratio.

UNUSUAL BEHAVIOR OF USUAL MATERIALS IN SHOCK WAVES

Kanel G.I.

JIHT RAS, Moscow, Russia

kanel@ficp.ac.ru

The shock-wave techniques provide unique capabilities to study mechanical behavior of materials at extremely high strain rates. Under these conditions, response of solids in some cases is unexpected and exotic. Temperature effects on the flow stress at high strain rate may differ even in sign from that we observe at low and moderate strain rates. Strengthened metals and alloys may demonstrate even lower HEL value than normally less hard ones. At highest strain rates, so-called ideal (ultimate) shear and tensile strength is reached. In the presentation, recent experimental data on the elastic precursor decay and rise times of plastic shock waves in several metals and alloys in various structural states at normal and elevated temperatures are discussed and systematized. The data on precursor decay include measurements at micron and submicron distances where realized shear stresses are comparable with their ideal values. It has been found the precursor decay may occur in several regimes which are characterized by different decay rates. Anomalous growth of the Hugoniot elastic limit with heating correlates with a fast decay regime and is not observed when the decay is relatively slow. Results of measurements have been transformed into dependences of initial plastic strain rate on the shear stress. The strong non-linearity of these dependences is treated as an evidence of nucleation of dislocations under applied stresses. An analysis of the rise times of plastic shock waves shows by order of magnitude faster plastic strain rates at corresponding shear stresses than that at the HEL that is treated as an evidence of intense multiplication of dislocations. Results of measurements of the resistance to high-rate fracture—spall strength show gradual increase of the later with increasing rate of tension and approaching the ideal strength in a picosecond time range. The spall strength not necessary correlates with dynamic yield stress. Although grain boundaries, in general, reduce the resistance to fracture as compared to single crystals, the spall strength of ultra-fine-grained metals usually slightly exceeds that of coarse-grain samples. The spall strength usually decreases with heating although in less degree than the strength at low strain rates does.

The temperature dependences of the spall strength do not correlate with dependences of the yield stress that points on larger contribution of the fracture nucleation processes as compared to the void growth.

THE IMPEDANCE CORRECTION OF THE SAMPLE RECOVERY CAPSULE IN THE SHOCK-WAVE LAB AT THE TU BERGAKADEMIE FREIBERG

Schlothauer T., Heide G., Keller K., Kroke E.*

TUBAF, Freiberg, Germany

**schlotha@mailserver.tu-freiberg.de*

The main goal of the shock wave laboratory at the TU Bergakademie Freiberg (established 2007) is the synthesis of high pressures phases in the gram scale under pressures from 15 to 200 GPa. This requires an effective sample recovery system with increasing stability with increasing pressure. Common sample recovery systems, were container and piston were manufactured of identic materials shows a decreasing stability with increasing pressures [1]. Main reasons for the container breakdown at pressures over 70 GPa are the impedance ratios between container and piston. Under the conditions of weak shock waves with the relation $c_A > Us$ (with c_A as sound velocity in the dense state along the Hugoniot-EoS and Us as shock velocity also along the Hugoniot-EoS) the piston and the container itself shows different properties. Following the impedance equation $Z_H = \rho_H c_A$ after Davison [2] with the impedance Z_H as function of the Hugoniot-EoS also along the release wave fan [3] the impedance of the piston will be higher compared with the container at the density maximum ρ_H and a shock wave will be reflected in direction of the top resulting in complete sample loss. For this reason in Freiberg a combination of austenitic Cr-Ni-Si-steel 1.4828 for the container and black steel St52 for the piston is used for more than 100 experiments without any sample loss. Because the difference between c_A and Us decreases with increasing pressure its stability increases with increasing pressure. The stability limitation of this capsule is a minimum pressure of 15 GPa and not a pressure maximum. The method of impedance correction is also usable for the shock wave treatment of Metals (steel, Ti-alloy) with complete sample recovery without macroscopic fractures.

---

1. Sekine, T. Eur. J. Solid State Inorg. Chem. 1997. V. 34. P. 823–833.

2. Davison, L. W.: Fundamentals of Shock Wave Propagation in Solids. Springer: Heidelberg Berlin, 2008.
3. Antoun, T.: Spall fracture. Springer: New York, 2003.

FORMATION AND STRUCTURE OF SHOCK WAVES IN ELASTIC-PLASTIC MEDIUM

Mayer A.E.,[*1] ***Khishchenko K.V.***[2]

[1]*CSU, Chelyabinsk,* [2]*JIHT RAS, Moscow, Russia*

[*]*mayer@csu.ru*

Plastic properties of substance are traditionally considered as important only at low intensity of shock waves, while the hydrodynamic approximation is used at high intensities most often. Meanwhile, there are experimental and theoretical evidences [1] that elastic-plastic properties reveal themselves in thin metal foils even for intensive compression waves. The reason is the high strain rates realized in these conditions, which leads to increase of the dynamical yield strength [2].

In present report, we numerically investigate an initial stage of shock wave formation after impact and evolution of its structure with time. The dislocation model [3] is used for accounting of dynamic plasticity in aluminum and copper. After impact, the elastic precursor runs away from the plastic front; its velocity is initially higher than the longitudinal wave speed and the shock wave velocity. Amplitude of elastic precursor and its velocity decrease with distance from the impact surface; two scenarios of further evolution exist. If the shock wave velocity is higher than the longitudinal wave speed, then the precursor velocity decreases down to the longitudinal speed and its amplitude decreases down to the static yield strength. In the opposite case, the plastic wave overtakes the precursor with the lapse of time, in this moment amplitude of precursor increases so that its velocity becomes equal to the shock wave velocity; further, the precursor and the plastic front travels together as a unit structure.

A numerical scheme without artificial viscosity but with accounting of physical viscosity is developed for exclusion of artificial heating error. Meanwhile, the heating error is an inherent and physically based feature for any medium with dissipation, viscous or plastic. It has the form of temperature perturbation near the impact surface and can cause melting of metal here even if it is solid behind the steady shock wave front.

This work is supported by grants of the President of Russian Federation MD-286.2014.1 and NSh-6614.2014.2.

---

1. Inogamov N. A., Zhakhovsky V. V., Petrov Yu. V., et al. // Contrib. Plasma Phys. 2013. V. 53. P. 796.
2. Armstrong R. W., Zerilli F. J. // J. Phys. D: Appl. Phys. 2010. V. 43. P. 492002.
3. Mayer A. E., Khishchenko K. V., Levashov P. R., Mayer P. N. // J. Appl. Phys. 2013. V. 113. P. 193508.

THE EFFECT OF SHOCK-WAVE COMPRESSION ON CARBON NANOTUBES

Anan'ev S. Yu.,[*1] ***Dolgoborodov A. Yu.,***[1] ***Mases M.,***[2] ***Soldatov A. V.,***[2] ***Lee J.,***[2] ***Waldbock J.,***[3] ***Milyavskiy V. V.***[1]

[1] *JIHT RAS, Moscow, Russia,* [2] *LTU, Lulea, Sweden,*
[3] *CNRS–University of Lorraine, Villers-les-Nancy, France*

[*] *serg.ananev@gmail.com*

Stability of carbon nanotubes at static compression depends on their diameter and number of walls. The purpose of this study was to probe the structural stability of double wall (DWCNTs) and single wall (SWCNTs) carbon nanotubes under extreme pressure and to determine the threshold above which significant structural damage is induced whereas only minor damage can be detected below. Earlier, experiments were performed to study the stability of nanotubes under exposure of static pressure [1] and under shock wave loading [2].

A three types of carbon nanotubes were exposed to a shock-wave loading: the DWCNTs containing approximately 60% of CNTs, the DWCNTs containing 95% of CNTs, and the HiPco SWCNTs containing > 95% of CNTs. Peak shock pressures in the specimens were achieved by several reverberations of waves between the walls of the recovery ampoules and were 14–98 GPa for DWCNTs (60%), 19–67 GPa for DWCNTs (95%) and 19, 36 GPa for SWCNTs. The carbon nanotube destruction due to high temperature during the shock appears to be minor compared to that of the effect of the pressure influence for the short exposure time in the experiment. The recovered samples were characterized by Raman and HRTEM revealing outer wall disruption along with unzipping and shortening of the CNTs. In all cases, structural damage of the CNTs increases with the shock pressure, and the Raman data exhibit a steep increase of D/G-band intensity ratio. DWCNTs demonstrated higher susceptibility to structural damage at dynamic pressure in comparison to static pressure [1]. The study results for samples of the DWCNTs (60%) after the shock wave

loading were published in [3]. The work was supported by RFBR (project no. 12–08–01284-a).

1. S. You et al. Probing structural stability of double-walled carbon nanotubes at high non-hydrostatic pressure by Raman spectroscopy. // High Pressure Research, 31, 186 (2011).
2. Y.Q. Zhu et al. Collapsing carbon nanotubes and diamond formation under shock waves. // Chemical Physics Letters, 287, 689 (1998).
3. Mases M. et al. The effect of shock wave compression on double walled carbon nanotubes. // Phys. Status Solidi, 12, 2378 (2012).

FRAGMENTATION OF THE ZrO CERAMICS WITH DIFFERENT POROSITY UNDER DYNAMIC LOADING

Uvarov S.V.,* Chudinov V.V., Davydova M.M., Bannikova I.A.

ICMM UB RAS, Perm, Russia

**usv@icmm.ru*

An extensive experimental investigation on zirconia ceramic specimens with different porosity was carried out to evaluate the influence of porosity on fractoluminescence pulse distribution and energy dissipation. Experiments were carried out using Split Hopkinson Pressure Bar (SPHB) setup with strain rate from 500 to $5000s^{-}1$. Porosity of the specimens was varied from 10% to 60% volume fraction. Energy dissipation was calculated from the SPHB data. Acoustic emission is widely used to detect and investigate multiple fracture processes of rocks and concrete. But due to high strain rate it is impossible to use it on the dynamic fragmentation. It was found that the fractoluminescence [1] can provide valuable information about evolution of fragmentation at high strain rates . Despite that the zirconia is not as transparent as fused quartz it was possible to detect fractoluminescence from the surface and sub-surface layers of the specimen. Fractoluminescence was detected by a fast PMT. Signal from the PMT was recorded by oscilloscope with 1 GHz sample rate. Record length was 100M points which is equal to 0.1 s

Analysis of the fragment size distribution shows that it can be approximated by power law where power (slope in log-log coordinates) depends on the porosity.

Fractoluminescence consists of pulses with sharp front and exponential decay with different amplitudes. Pulses were recorded even 10 ms after the loading pulse whit is order of magnitude higher than load pulse duration.

Amplitude of the pulse depends on energy released during single fracture event and position of the fracture (depth and orientation to the PMT) which makes hard to measure energy release alone. We decided to measure intervals between subsequent pulses [2] (or the rate of the pulses as in the Omori law). It was found, that interval complementary cumulative distribution is bimodal power law distribution. Knee position depends on the porosity of the specimen

It was found, that porous ceramic does not fail completely when first failure occurs. The residual strength is about ∼40% of initial strength

This work was supported by projects of RFBR No 11–01–96010-r-ural-a 14–01–00842, 14–01–00370.

---

1. Vettegren V. I., Kuksenko V.. S., Shcherbakov I. P. // Technical Physics. 2011. V. 56. No. 4. P. 577.
2. Davydova M. M., et al. // Frattura ed IntegritÃ Strutturale. 2013. V. 24. P. 60.

SELF-SIMILARITY OF THE WAVE PROFILES IN WATER UNDER DYNAMIC LOADING

Bannikova I.A.,* Uvarov S.V., Naimark O.B.

ICMM UB RAS, Perm, Russia

**malgacheva@icmm.ru*

Distilled water was loaded by electrical explosion of copper wire by discharge of energy stored in capacitors [1]. Free surface velocity was measured by fiber-optical VISAR system [2]. In order to provide free surface conditions a special probe was developed. It consists of plastic tube with a plastic condensing lens inside. Optical fiber was inserted on the one side of the tube and a thin metallized PTFE film was placed on another. Wave profiles were recorded for different energy stored in the capacitors ($W_C = 11 \div 56$ J) and for different distance X from the wire. Analysis of the profiles obtained by processing VISAR data shows us that the first burst in the signal is related to the electromagnetic processes in the loading device. The second part of the signal is associated with the compression wave. Time interval Δt between these two parts depends linearly on the distance X. The velocity of the compression wave obtained from the linear fit is close to the speed of sound in the water $c^* \sim 1470$ m/s with relative error 9%. The typical free surface velocity profiles are similar to the profiles obtained in [3] for the plate-impact experiment. The spall strength P_S was calculated from the velocity profiles. We found that the

spall strength P_S depends on the strain rate $\dot{\varepsilon}$ at unloading part of pulse as $\dot{\varepsilon} \sim P_S^{0.3}$. Calculating the compression pulse amplitude P_0 from the velocity profile and strain rate on the compression wave front we have obtained self-similar relation $\dot{\varepsilon}^* \sim P_0^{3.2}$. The same power law was found for solids in [4, 5].

The work is supported by RFBR projects 12–01–92002-NNS_a, 11–01–96010 r_ural_a and project 14–1-NP-332.

1. Bannikova I. A., Naimark O. B., Uvarov S. V. // Proceeding of the International Conference XX Kharitonov reading, Sarov. 2013. P. 745.
2. Bannikov M. V., Bayandin Yu. V., Lyapunova E. A, Uvarov S. V, Naimark O. B. // Tambov University Reports: Natural and technical Sciences, V. 10, No. 3, 2010. P. 1014. (in Russian)
3. Utkin A. V. // App. Mech. and T. Ph., 2011, V. 52, No. 1. P. 185. (in Russian)
4. Bayandin Yu. V., Naimark O. B. // Phys. Mes., Tomsk, 2004, V. 7, Sp.Iss.,Part 1. P. 305. (in Russian)
5. Swegle J. W., Grady D. E. // J.Apple.Phys, 1985, V. 58, No. 2. P. 692.

STUDY THE DEFORMATION BEHAVIOR OF ALUMINUM ALLOY 6063T6 UNDER SHOCK COMPRESSION

Garkushin G. V.,* Savinykh A. S., Razorenov S. V.

IPCP RAS, Chernogolovka, Russia

**garkushin@ficp.ac.ru*

With aim to search correlation between spectrum defect in material and resistance to deformation and fracture under submicrosecond duration of loading, measurements of dynamic elastic limits and spall fracture of aluminum alloy 6063T6 [1] with different initial inner structure under shock wave loading have been done, that has allowed to estimate the influence of structural factors on strength at high strain rate and spall fracture of all types of samples. Studies were carried out of aluminum alloy with a grain size of 100 microns, 1.2 microns and 1.5 microns. To change the size of grain used equal–channel angular pressing [2]. The number of passes was 2 and 8. The plane shock waves in the samples were generated by impacts of aluminium flyer plates with the velocity of 630 +/-30 m/s. The flyers were launched using explosive facilities [3]. In experiments, the free surface velocity histories were recorded with the VISAR [4]. The study samples aluminum alloy 6063T6 of thickness 8 mm showed that after two passages marked increase in dynamic elastic limit 240 MPa to 400 MPa.

Further increase the number of ECAP passes allowed to increase the elastic limit of 400 MPa to 520 MPa. Dynamic strength of the materials studied with increasing strain rate increases, regardless of the original structure. The change in the structure and texture of the samples has little effect on the strength characteristics at high-speed deformation. Obtain data on the delay of the elastic precursor and the spall strength for samples with coarse-grained and fine-grained structure . Thus, the results in this study clearly showed that the formation of fine-grained internal structure in polycrystalline metals and alloys by severe plastic deformation has not so significant effect on their strain rate deformation and fracture compared with the corresponding behavior of similar materials under static and quasi-static load [1]. This work was supported by the Russian Foundation for Basic Research (grant No. 12–02–31682).

1. Hockauf M., Meyer L., Halle T., Kuprin C., Hietschold M., Schulze S., Kruger L. // International Journal of Material Research 2006. V. 97. No. 10. P. 1392.
2. Valiev R.Z., Islamgaliev R.K., Alexandrov I.V. // Prog. Mater. Sci. 2000, V. 45, P. 103.
3. Kanel G.I., Razorenov S.V. and Fortov V.E. Shock-Wave Phenomena and the Properties of Condensed Matter (Springer New York) 2004. 320 p.
4. Barker L.M. and Hollenbach R.E. 1972 // J. Appl. Phys. 1972 V. 43. P. 4669

MECANICAL PROPERTIES AND FEATURES OF THE ENERGY DISSIPATION PROCESS IN THE ULTRAFINE-GRAINED ALUMINIUM ALLOY AlMn AND Al–Zn–Mg–Cu UNDER DYNAMIC COMPRESSION

Vshivkov A.N.,[*1] ***Prokhorov A.E.,***[1] ***Petrova A.N.,***[2] ***Brodova I.G.,***[2] ***Plekhov O.A.***[1]

[1]*ICMM UB RAS, Perm,* [2]*IMP UB RAS, Ekaterinburg, Russia*

[*]*aleksey.1992@mail.ru*

The paper is devoted the investigation of the features of the energy dissipation in with ultrafine grain metals during dynamic compression. At this time, the grain refinement is considered as one of the perspective ways to improve the mechanical properties of materials. Experimental study is carried out with the specimens of aluminum alloy Al-Mn and Al-Zn-Mg-Cu with the ultrafine-grained (UFG) structure manufactured by the method of dynamic channel-angular pressing (DCAP). The main feature of this work is complex approach which includes detail analysis of the material

before and after deformation and comparison of the structural investigation results with the results of mechanical and thermodynamic tests.

The split-Hopkinson (Kolsky) bar with diameter of 25 mm was applied to implement the dynamic compression test. Experimental setup consisted of a gas gun with caliber of 18 mm which accelerates the projectile with 200 mm length. Cylindrical specimens with diameter of 7.6 mm and with length of 3–4 mm were used. Dynamic characteristics of the material were determined by analyzing of the reflected and transmitted waves taking into account the finite deformation of the specimen. To study the deformation process the set of the specimens with different characteristics such as size of structural fragments (200–600 nm), formation mechanism, stress level, state of the grains boundaries and ratio of fragmented structure to the structure of dynamic recrystallization were used. The infrared camera (4000 fps) recorded the temperature distribution on the specimen surface during dynamic compression. The parts of the dissipated energy and stored energy can be determined on the base of the value of the temperature change on the specimen surface during deformation.

The ration of stored and dissipated energy can be estimated by data of infrared thermography. The structurally sensitive dependence of dissipative ability of the materials has been established Calculation of the energy converted into heat and the energy expended in deformation, allows us to assert that the dissipation ability of UFG material is greatly increases with increasing of degree of previously accumulated strain.

SUPERCONDUCTIVITY OF Cu & CuO_x INTERFACE FORMED IN SHOCK-WAVE CONDITIONS

Shakhray D.V.,[*1] ***Avdonin V.V.,***[1] ***Sidorov N.S.,***[2] ***Palnichenko A.V.***[2]

[1]*IPCP RAS,* [2]*ISSP RAS, Chernogolovka, Russia*

[*]*shakhray@icp.ac.ru*

Since the discovery of superconductivity above 30 K in lanthanum barium copper oxide [1] many similar high-criticaltemperature superconductors (HTSs) have been found. Superconductivity in all of these multilayered oxides is believed to originate in the planes of copper and oxygen atoms, common to these compounds. Therefore, fabrication of synthetic multilayers on the basis of the copper oxide layers is promising for realization of new HTSs. For example, a HTS-like phenomenon was observed by means of electric conductivity measurements in the samples consisting of Cu film deposited onto natural faces of CuO single crystal under special

conditions [2]. A strong indication to superconductivity at 20–90 K has been revealed by dynamic magnetic susceptibility measurements in Cu & CuOx samples prepared by surface oxidation of powdered copper followed by thermal treatment in vacuum. A success in stabilization of the superconducting Cu &CuOx interfaces by the low temperature quenching has motivated our attempts to apply a shock-wave pressure to the Cu &CuOx mixture for their preparation. The energy of the shock-waves leads to local, non-equilibrium overheat of the samples regions at the shock-wave front, followed by their rapid cooling (quenching) as the shock-wave is passed, thus fixing the sample in the metastable state. Furthermore, highly non-equilibrium conditions caused by propagation of the high-pressure shock-waves in the sample can stimulate phase transitions or mechanochemical reactions inaccessible by any equilibrium processes. In this work we report on metastable superconductivity at Tc $\approx$ 19.5 K revealed by the *ac* magnetic susceptibility measurements of the powdered mixture of Cu and CuO subjected to shock-wave pressure of 350 kbar.

The work has been supported by RFBR grant No. 13-02-01217.

1. J. G. Bednorz, K. A. Muller Possible high Tc superconductivity in the Ba-La-Cu-O system // Zeitschrift fur Physik B Condensed Matter V. 64. P. 189–193
2. V. V. Osipov, I. V. Kochev, S. V. Naumov, Giant electric conductivity at the CuO-Cu interface: HTSC-like temperature variations // Journal of Experimental and Theoretical Physics V. 93. P. 1082–1090.

STRUCTURAL MODEL FOR MECHANICAL TWINNING IN FCC AND BCC METALS

Borodin E.N.,[*1] ***Mayer A.E.***[2]

[1]*IPME RAS, Saint Petersburg,* [2]*CSU, Chelyabinsk, Russia*

[*]*elbor7@gmail.com*

A large volume fraction of mechanical twins can be found in FCC and BCC metals after propagation of the shock wave with amplitude above several tens of GPa. It is also supposed that the twinning plays a significant role at Taylor rod test [1]. For correct numerical simulation of such processes one need to have theoretical models for dislocation plasticity and twinning. A model for dislocation plasticity were proposed in [2, 3]. Here we propose a model for twinning which takes into account kinetics, dynamics of twins and detwinning processes [4]. This model is an addition to the dislocation plasticity model [2], and there is only one additional

parameter, which is the stacking fault energy which determines the twin ability of the material.

On the basis of these models we investigate a distribution of dislocations and twins in the volume of the deformed copper and steel samples after the Teylor rod test and the shock wave loading. Different regimes of twins formation at different shock wave amplitudes and the role of twins at Taylor rod deformation are discussed.

This work was supported by the Russian Foundation for Basic Research (Grant Nos. 12–02–31375, 14–01–31454) and by the Grant of the President of Russian Federation (MD-286.2014.1).

---

1. Zerilli F. J., Armstrong R. W. //J. Appl. Phys. 1987. V. 61. No. 5. P. 1816.
2. Krasnikov V. S., Mayer A. E., Yalovets A. P. //Int. J. Plast. 2011. V. 27. No. 8. P. 1294.
3. Mayer A. E., Khishchenko K. V., Levashov P. R., Mayer P. N. //J. Appl. Phys. 2013. V. 113. No. 19. P. 193508.
4. Borodin E. N., Atroshenko S. A., Mayer A. E. Distribution of dislocation and twins in copper and 18Cr-10Ni-Ti steel samples after shock wave loading. //Technical physics. 2014.

EXPERIMENTAL SIMULATION OF SPACECRAFT PROTECTION FROM SPACE DEBRIS AND MICROMETEORITES

Kotov A. V.,* Kozlov A. V., Polistchook V. P., Shurupov A. V.

JIHT RAS, Moscow, Russia

**daleco-m@mail.ru*

Space debris and micrometeorites pose a real threat to the spacecraft (SC). The main requirement to protection system of SC from these factors is a small weight. Sufficiently effective protection of SC can be achieved using the system of few screens. Collision with the first screen destroys the striking element (SE–micrometeorite or space debris) that significantly decreases damage of the next screens. In this paper we present the experimental results of testing such protection system using high speed shooting (200000 frames per second with exposure time of 1 microsecond). The collision conditions were next: SE was lexan cylinder with 15 mm in diameter and mass of 2.1 g. In railgun SE was accelerated up to 3.3 km/s. Mockup of SC protection system consisted of two duralumin screens with 150 mm in diameter and width of 5 mm. SC cover was simulated by the third screen (duralumin disk) with width of 10 mm. Distance between

neighboring screens was 50 mm. The flat circular hole with diameter of 25 mm was burnt through the first screen as a result of SE collision. The hole in the second screen had ragged bent on about 15 mm edges. Multiple craters 3–5 mm in size and 1–2 mm in depth were registered on the surface of this screen. These craters were formed as a result of its collision with destructed fragments of the first screen. No damage was caused to the third screen (SC cover). On its surface, there was a thin condensation film of the first two screens materials. Usage of high speed shooting allowed exploring destruction dynamics specifics of the SC protection mockup such as determination of screen deformation speed and fragments dispersion speed and so on. Initial deformation speed value was 1.2 km/s for the first screen and 0.6 km/s for the second screen respectively. Experimental data confirms effectiveness of spaced screens usage as a protection from aftereffects of SC collisions with high-speed SE. Total thickness of duralumin plates was 20 mm, damaged were only the first two plates. Under the same parameters of collision solid duralumin screen with thickness of 20 mm would have been pierced through.

THE THEORETICAL-EXPERIMENTAL BEHAVIOR OF NATURAL MATERIALS UNDER EXPLOSIVE LOADS

Orlov M.Yu.,[*1] ***Orlova Yu.N.***[2]

[1] *TSU,* [2] *TPU, Tomsk, Russia*

[*] *orloff_m@mail.ru*

Now, there is a need for understanding the processes of deformation and fracture of ice and same natural materials under shockwave loading. Investigations are necessary for the development of transport links in the permafrost, as well as for increased oil and gas production and design of icebreakers and for a new generation of space technology. The investigations are needed for the development of the armed forces in the Far North.

Model behavior environment corresponds to the modern physical notions of deformation and destruction of homogeneous and heterogeneous environments with shock-wave and explosive loads. It is compressibility, elastic-plastic, porous environment that takes into account properties of durability, shock-wave phenomenon. The model uses the concept of joint formation spall and sheared destructions. Equation of State is selected in the form of Walsh.

The objects of study in this paper are polycrystalline ice and limestone. The subject of research are the stress-strain and thermodynamic state with

explosive loads. The work ranged explosive mass. The experiments were obtained jointly with KuzbassSpetsVzryv in late 2013 [1].

As the tool of research used the numerical of the lagrangian method, which is complemented by the mechanisms of splitting nodes and destruction of finite-elements. The originality of technique is a new way of allocating surfaces breaking the continuity of material that does not impose serious restrictions on the modern dynamic contact problems of mechanics of deformable solids. This method is already more than 20 years in the Department of Mechanics of Deformable Solids in the Research Institute of applied mathematics and mechanics at Tomsk State University. Last updated on method was a new mechanism of splitting nodes, applies to both volume and forces criteria of destruction of materials. This innovation allows getting picture closest to real destruction under shock wave loading [2].

The new scientific data was obtained in the forms of graphs, tables and configurations bodies.

The work is supported by RFBR 13–08–00509a.

---

1. http://infored.ru/company/212396/
2. Glazyrin V. P., Orlov M. Yu., Orlov Yu. N. The destruction of the ice under the detonation products // Physics. 2008. V. 51. No. 8/2. P. 136–142.

NUMERICAL SIMULATIONS OF DYNAMIC FRACTURE

Bratov V.A.

IPME RAS, Saint Petersburg, Russia

vladimir@bratov.com

On the basis of the incubation time approach in dynamic fracture embedded into the finite element method different classes of dynamic fracture problems are simulated and analysed. It will be shown that a big variety of phenomena experimentally observed in this class of problems can be obtained numerically utilizing the incubation time fracture criterion as a fracture criterion for FEM. The presented examples will include dynamic crack propagation initiated as the result of dynamic impact loading, dynamic crack propagation initiated as the result of quasistatic loading, impact crater formation problems, penetration problems, problems of rock fragmentation, etc. It will be shown that the proposed approach can be successfully used in order to simulate all the variety of experimentally observed phenomena typical for dynamic fracture. At the same time the approach can be used for practical problems in order to provide engineer-

ing analysis for materials and structures that can undergo dynamic-range loads. This can include crash-test simulations, aerospace applications, problems of fragmentation of natural materials, mining problems, energy cost optimisation problems, etc.

NUMERICAL SIMULATIONS OF CERAMIC PLATES PENETRATION

Kazarinov N.A.,[*1] ***Bratov V.A.,***[2] ***Petrov Y.V.***[2]

[1]*SPbSU, Saint-Petersburg,* [2]*IPME RAS, Saint Petersburg, Russia*

[*]*nkazarinov@gmail.com*

Normal impact of a steel cylinder into ceramic plate is simulated utilizing the finite element method. Incubation time fracture criterion is implemented numerically in order to predict fracture initiation and propagation in ceramic samples. Fracture criterion execution is controlled by an independent C++ code to provide fast and robust calculations and flexibility in output of results. Area of damage (new surface created as a result of fracture process) is considered to be the central parameter characterizing the penetration fracture process. The dependences of damage area on impacter velocity and material properties are studied. The analysis is also providing a possibility to assess energy consumed by creation of a new surface at fracture initiation (value analogous to Griffith energy for quasistatic fracture).

MODELING OF BEHAVIOR OF HETEROGENEOUS FERROCONCRETE DESIGNS AT DYNAMIC LOADING

Radchenko P.A., [*] ***Batuev S.P., Radchenko A.V., Sarkisov D.Y., Goncharov M.E., Tigay O.Y., Plevkov V.S.***

TSUAB, Tomsk, Russia

[*]*radchenko@live.ru*

In work results of numerical and pilot studies of behavior of various ferroconcrete elements are considered at direct, and also slanting non-central short-term dynamic loading. Numerical researches are executed and the dynamic calculation considering nonlinear work of concrete and fittings, wave processes is realized. Results of tests of ferroconcrete elements of dvutavrovy and rectangular sections are presented at short-term pulse non-central compression, a direct and slanting bend. The analysis

and comparison of the received results of numerical and pilot studies is carried out.

NUMERICAL AND EXPERIMENTAL STUDY OF FRACTURE OF THE BEAM FROM GLUED WOOD AT LOW-VELOCITY IMPACT

Radchenko A.V.,* Radchenko P.A., Batuev S.P., Loskutova D.V., Lebedev I.A., Kopanitsa D.G.

TSUAB, Tomsk, Russia

**andrey-radchenko@live.ru*

In work the behavior of a beam from glued wood is experimentally and numericaly investigated at low-velocity impact. Experiments were made on koprovy installation. On a beam of 330 x 110 in size x 3000 mm freight by weight 385 kg was dumped. Height from which freight was dumped, varied from 0.25 to 1.4 m. At tests of samples for increase in duration of action of loading snubbers were used. In the course of experiment measurements of deformations, acselerations and velocities were carried out. For this purpose on a surface of a beam tensoresistors with base 20 mm, the acceleration pickups working in two planes were installed. Numerical modeling was carried out by a method of final elements in three-dimensional statement within phenomenological approach of mechanics of the continuous environment with use of an original numerical technique. The behavior of a material of a beam was described by the anisotropic environment with ortotropny symmetry of elastic and strength properties. At the description of collapse distinctions in strength of wood were considered at compression and a tension. As criteria of collapse tensor and polynomial criteria of the fourth and second order are used. Influence of kinematic and geometrical parameters on dynamics of fracture of a beam is investigated.

MULTISCALE SIMULATION OF MECHANICAL RESPONSE OF NANOSTRUCTURED MATERIALS TO INTENSE IMPULSIVE LOADING

Skripnyak E.G.,* Vaganova I.K., Skripnyak V.A., Skripnyak V.V.

TSU, Tomsk, Russia

**skrp@ftf.tsu.ru*

The approach, in which properties of a representative volume element (RVE) undergo homogenization, is widely applying in computational mechanics for estimating of a constitutive equation.

This approach allows using the mathematical apparatus of continual mechanics for describing the deformation of solid bodies which are structured on micro-, meso-, macroscale levels. Thus the amount of parameters representing the structure of material on each level is reduced. As a result, relations for the macroscale level become simpler. Representative volume element is equal to volume of material particle of continual media and has certain geometric parameters. Estimating the size of RVE two contrary conditions must be met: averaged mechanical properties should be equal for all possible structures taking place on the level under consideration, so the size of RVE has tendency to be smaller, but on the other hand the size should be big enough to provide boundary conditions to not affect on averaged properties. The question of existence of the RVE for structured solid bodies is not trivial. According to the well known principle of micro-, meso-, macro- the size of RVE has to be smaller than body size but include amounts of interacting structured elements from lower levels, which can provide mechanical properties to be stable. However, in case when inelastic deformation, nucleation and growth of damages occur, the structure modifications are taking place in solid bodies.

These modifications result in the appearance of local oriented stresses and instantaneous spatial heterogeneity of the specific internal energy in the RVE. It should be noted, that solid structured bodies are related to the opened thermodynamic system, in which self-organization processes of structural transformation may be triggered and then cause the collective effect. Thus, new substuctures (e.g. block-structure) will appear during the deformation process [1]. The occurrence of these substructures has to be included into consideration when defining the size of RVE. Thereby, in the case of dynamic loadings, such assumptions may lead the RVE size to be increased.

1. Skripnyak E. G., Skripnyak V. A., and Skripnyak V. V. // AIP Conf. Proc. 2012. V. 1426. P. 1157.

DYNAMIC FRACTURE OF LIGHT ALLOYS WITH A BIMODAL GRAIN SIZE DISTRIBUTION

Skripnyak N.V.,* Skripnyak V.V., Skripnyak E.G., Skripnyak V.A.

TSU, Tomsk, Russia

**skrp@ftf.tsu.ru*

It's known, that bulk ultrafine-grained light alloys demonstrated increased the fatigue life in com-parison with coarse grained counterparts. To investigate the physical mechanisms providing an im-provement in the cyclic life of specimens with bimodal grain size distribution , fractal analyses studies on the fracture surfaces obtained by cyclic axial tension-compression loadings were carried out. Tests in low fatigue region were carried out on samples of 4 types: AMg6 and Ma8-1 alloys as-received and AMg6 and Ma2-1 modified by the surface severe plastic deformation treatment. A grain size distributions in the specimens were formed by using of a multi passes Bc ECAP (Equal Channel Angular Pressing) method. Dynamic tension tests were carried out by the Instron VHS 40-50/20. high rate mashine. To execute a comprehensive description of multifractal a number of fractal dimensions should be obtained. The Multifractal approach allows us to separate out the subset fragments for which self-organization properties are observed. To evaluate the Hausdorff fractal dimension fracture surface images were analyzed. Fractal dimensions were determined by triangular method. Grain structure in studied specimens result in increasing the Hausdorff fractal dimension of fatigue fracture surface for Ma8-1 from 2.29 to 2.60 and for AMg6 from 2.39 to 2.57. This confirms an assumption that the fracture surfaces owing to stochastic changing in direction of the crack at mesoscale level. Local changing in propagation direction of crack occurs as affected the residual compression stresses induced in specimen volume by preliminary severe plastic deformation. Thereby, the formation of grain size distribution and the formation of gradient structure of internal stresses field are influencing on the cracks initiation and growth in the light alloys on the base of aluminium and magnesium. The presented results can be used for development of techniques for improving a dynamic strength of aluminium and magnesium alloys.

STRUCTURE OF THERMAL EFFECTS IN A GASEOUS FLOW DUE TO CONDENSED PARTICLES AT DIFFERENT SHOCK-WAVE CONDITIONS

Obruchkova L.R.,* Baldina E.G., Efremov V.P.

JIHT RAS, Moscow, Russia

**o_liliya@ihed.ras.ru*

Many processes in the nature and in the industry occur with contamination of atmosphere. Information on local characteristics of a flow field, such as particles drag coefficient, its heat exchange with environment, ignition time and so on is necessary for safety of supersonic flights by air with small particles.

Thermal influence connected with single stationary condensed particle in a shock-wave gas flow was calculated in present study by means of a two-dimensional hydrodynamic code. Applicability of the used code was checked with stimulatings of passage and reflection of the shock waves in a shock tube and by comparison of the results with the analytical decision [1]. The ideal gas equation was chosen as equation of state for air. The tube and the particle were considered as adiabatic. The tube diameter was much greater than the particle one.

A numerical study of an interaction of passing shock wave with system of stationary bodies was carried out in the recent work [2]. However in [2] calculations of influence of single particle on a flow are not systematized, influence of the body diameter and of Much number change on its streamlining is not determined. Moreover, there are no data on temperature increase and released thermal energy in the compressed gas before the particle.

Our calculations showed that the calculated temperature and the ratio of total released thermal energy to a difference of mass of compressed before a particle gas and mass in the same volume of the flow do not depend on diameter of the particle and are defined only by intensity of the shock wave. Change of all computed parameters of the flow at slowdowning before the particle occurs principally in a subsonic flow region. These data are visualized. The subsonic flow region before the particle joins the particle and has volume of the order of the particles volume. Apart from that the flow is supersonic.

---

1. Gaydon A.G., Hurle I.R. The shock tube in high-temperature chemical physics. / London: Chapman and Hall Ltd, 1963
2. Bedarev I.A., Fedorov A.V. Analiz techeniya okolo sistemy sfericheskix chas-

tic za proxodyashhej udarnoj volnoj // III Minskij mezhdunarodnyj kollokvium po fizike udarnyx voln (MMK-2013) 11–14 noyabrya 2013

NUMERICAL SIMULATION OF THE STRONG SHOCK WAVE EXIT ON A ROUGH SURFACE FOR VARIOUS METALS

Dudin S.V., Shutov A.V.*

IPCP RAS, Chernogolovka, Russia

**shutov@ficp.ac.ru*

The emission of particles from the metal surface at the exit of a strong shock wave was described in detail in [1–5, 9]. IWorks [6–8] shows that the emitted particles move together with a clot of plasma with approximately two times higher velocity than the velocity of the basic mass of the material surface. This paper presents the comparative results of calculation of the strong shock waves exit on the profiled target surface for metals: copper, iron, tungsten, and tantalum. The equations of state [10, 11] were used.

---

1. D.S.Sorenson, R.W.Minich et all. Ejecta particle size distributions for shock loaded Sn and Al metals // Journal of Applied Physics 2002. 92., 10
2. W. S. Vogan, . W. Anderson et all, Piezoelectric characterization of ejecta from shocked tin surfaces // Journal of Applied Physics 2005. 98. 113508
3. A. Ogorodnikov etc. // FGV. 1998. The so-34. No. 6. P. 103.
4. A. G. Ivanov, Yu. D. Lavrovsky et all PMTF. 1992. No. 5. P. 116.
5. A. L. Mikhailov and others // Chem. Phys. 2001. No. 8. P. 73.
6. Kulish M.I., Ushnurtsev A.E. et all Peculiarities of strong shock wave emerging free surface of a metal // XXV Int. Conf. on EOS, 2010, 1–6 March, P. 74.
7. M. I. Kulish, V. B. Mintsev. et all Measurement of the temperature of the copper plasma generated in the process of release of a shock-compressed target // JETP LETT, 2011, 94, 2, c. 101–105
8. S.V.Dudin, M.I. Kulish, et all Investigation of Exit of Strong Shock Wave at the Free Surface of Metal //, Int. Conf. Shock Waves in Condensed Matter, Kiev, Ukraine, 2012, P. 231–238.
9. Dudin S.V., Shutov A.V. calculation of a strong shock wave exit on the metal surface with microdefects, XXV Int. Conf. on EOS, 2010, 1–6 March, Russia, Elbrus, P. 73.
10. V.E.Fortov, K.V.Khishchenko et all, Wide-Range Multi-Phase Equations of State for Metals. Nuclear Instrum.and Methods in Phys.Res., Sec.A, 415(3) (1998) 604–608
11. SESAME, the LANL Equation of state database // report LA-UR-92–3407, 1992, Los Alamos National Laboratory.SESAME

NUMERICAL SIMULATION OF EXPLOSION WELDING

Sultanov V.G.,* Shutov A.V.

IPCP RAS, Chernogolovka, Russia

**sultan@ficp.ac.ru*

he explosive welding of metals was discovered in experiments on cumulation in 1944–1946's. by a group of Soviet scientists under the guidance of M.A. Lavrentyev. Over the past years, the study of this phenomenon was the subject of many experimental works and theoretical models.The lack of adequate model about the nature of the waves on the boundary of metals naturally hinders the development of explosion welding technology because of parameters of welding seam (amplitude and wave lengths) are practically unpredictable.

This paper presents the first results of researching the process of wave formation by the direct numerical simulation of high-speed oblique collision of explosively accelerated plates. The elastic-plastic model of media motion [1], wide-range equations of state for metals [2], the equation of state of explosives, explosion products and kinetics of decomposition of explosive substances [3] were used in two-dimensional numerical simulations.

The data on the size of plasticity zones under glancing collision of plates in conditions of explosion welding with waveformation were obtained. It is shown that in the case of metal plate acceleration by explosives, unlike the collision undisturbed plates, the size of the zone of plasticity significantly increase.

---

1. Abouziarov M., Aiso H., Takahashi T. // Series from research institute of mathematics of Kyoto University. Mathematical analysis in fluid and gas dynamics. 2004, 8470; 1353, P. 192–201.
2. Fortov V. E., Khishchenko K. V. et all, Wide-Range Multi-Phase Equations of State for Metals // Nuclear Instrum.and Methods in Phys.Res., Sec.A, 415(3) (1998) P. 604–608
3. Kanel G. I., Razorenov S. V., Utkin A. V., Fortov V. E. Shock-wave phenomena in condensed matter // 1996. 408 P.

EXPERIMENTAL AND COMPUTING RESEARCH OF SHOCK-WAVE WELDING OF DIVERSE METALS

Yankovskiy B.D.,* Deribas A.A., Anan'ev S.Yu., Andreev A.V.

JIHT RAS, Moscow, Russia

**yiy2004@mail.ru*

Feature of welding by explosion is rapidity of process together with high density of energy. These parameters define formation of strong connection in a solid phase without development of volumetric diffusion. Experiments and statement of mathematical modeling of radial shock-wave loading of coaxial steel cylinders are described in this report.

Soft and stainless steel cylinders were used in experiments. Thickness of walls of cylinders was equal 4 mm. Diameter of a contact surface was equal 48 mm. On surfaces of both cylinders have been cut a trapezoidal screw threads. Threads had a pitch of 8 mm and depth of cutting of 0.5–1.0 mm. Experiments are devoted to working off of technique and intensity of explosive loading. In the base of technique of loading of cylinders have been used axial positions of a cylindrical HE charge with exterior diameters of 8–44 mm. The volume between HE charge and steel cylinders was filled by damping materials (air, sand or water). In quality of a materials of a bandage of steel cylinders were applied or air or water or sand or steel shell. Intensity of loading was varied by type of a damp material in a range of pressure 0.1–10 GPa. Durations of loading 20–50 mks have been defined by time of the expiration of detonation products from initial volume of a charge. Working off of technique of loading had an object to receive representation about residual deformation of steel cylinders. Mathematical modeling is based on use of a program complex of certainly–element analysis SIMULIA ABAQUS which has module ABAQUS EXPLICIT for calculation of non-stationary dynamics of a deformation of solid body. Modeling has a goal to define plastic deformation of cylinders and distribution of residual pressure onto contact surface depending on conditions of pulse pressure loading and geometrical parameters of a thread. A problem of convergence of the decision is arising owing to geometrical nonlinearity of the contact task which is being solved in thermomechanical (adiabatic) problem statement and of the advanced plastic deformation of materials. The developed computing models allow to receive a qualitative picture of plastic deformation and of stressed state in contact area of cylinders.

The work at the given stage is directed at optimization of geometrical parameters of a contact surface of cylinders from the point of view of residual strength.

HUGONIOT ADIABAT OF A POROUS LOW-SENSITIVE EXPLOSIVE

Smirnov E.B.,* Kostitsyn O.V., Tscherbakov V.N., Prosvirnin K.M., Kiselev A.N., Achlustin I.A.

RFNC–VNIITF, Snezhinsk, Russia

**ewgeny_smirnov@mail.ru*

Shock compressibility of explosive materials (HE) is traditionally studied using the "optical lever" method in experiments with wedge samples or with the help of multi-channel electromagnetic gages of wave and mass velocities. In this work, piezo-resistive and radio-interferometric methods were simultaneously used to register shock-wave parameters in a low-sensitive HE. The test HE having different initial porosity was loaded with the help of the explosive shock wave generator. Piezo resistive gages registered pressure of a shock wave entering an HE charge. A radio interferometer registered the x-t diagram of the shock-wave propagation in the test explosive. Detailed tracking of the shock wave trajectory permits one to determine (with an error of several percents) initial velocity of the shock wave entering the test HE and, together with the data on pressure measured using the piezo resistive method, to determine Hugoniot points that correspond to unreacted HE with different initial porosity k. The totality of shock compressibility points is approximated by an analytical expression for the Hugoniot Ph(V). This analytical expression was obtained based on the Mie-Grunheisen equation of state with the potential pressure component in the Tait form. Points on the Hugoniots for different initial porosities are described by a common surface Ph(V/Vo, k) in the "compression-initial porosity" coordinates. The approximating surface gives good description of the data on the shock-wave loading of different-initial-porosity explosives whereas these data were provided by other shock compressibility registration methods.

DETONATION OF ELASTIT DUE TO HIGH-SPEED COLLISION

Kotov A.V.,* Kozlov A.V., Polistchook V.P., Shurupov A.V.

JIHT RAS, Moscow, Russia

**daleco-m@mail.ru*

In this paper we present experimental results of elastit (EL-2) detonation testing under collision with speed of 3–3.5 km/s. Elastit discs of 1 mm in height were placed on recess in the duralumin target 100 mm in

diameter and 40 mm in height. In each recess 1 or 2 plates of elastit were installed. Two schemes of elastit allocation on the target surface were considered. In the first case one disc 60 mm in diameter or two discs 30 mm in diameter each of elastit were installed in the center of the target. In the second case 4 discs 16 mm in diameter were placed in distance between 15 to 40 mm from the center of the target. All targets were hidden under steel disc 5 mm in depth. Railgun was used in order to accelerate polycarbonate projectile with mass of 2.1 g and diameter of 15 mm. Reaction of elastit on high-speed impact mostly varied with distance between impact axis and location of elastit. With this distance no more than 10–15 mm and strikers speed 3.3 km/s detonation of elastit occurred and caused explosive destruction of the steel screen. With this distance changed within 20–30 mm, elastit disc burnt after impact. Initiation of elastit combustion occurs at a temperature of about 200 C. With the distance between impact axis and location of elastit more than 30 mm the initiation of elastit detonation did not occur.

SIZES OF CARBON PARTICLES IN DETONATION OF CONDENSED HIGH EXPLOSIVES

Ten K.A.,[*1] ***Titov V.M.,***[1] ***Pruuel E.R.,***[1] ***Kashkarov A.O.,***[1] ***Shekhtman L.I.,***[2] ***Zhulanov V.V.,***[2] ***Tolochko B.P.***[3]

[1]*LIH SB RAS,* [2]*BINP SB RAS,* [3]*ISSCM SB RAS, Novosibirsk, Russia*

[*]*ten@hydro.nsc.ru*

The investigation into the condensation of carbon in detonation of oxygen-deficient high explosives got off to a good start at Lavrentiev Institute of Hydrodynamics in 1983, when works on the synthesis of detonation nanodiamonds were begun. In the mid 90s, these works were supplemented by the study of TATB at nuclear centers in the U.S. and Russia. Experimental recording of the changing sizes of condensed carbon nanoparticles in detonation of high explosives is currently possible only with diffraction techniques with synchrotron radiation (SR) application. This paper presents experimental data on dynamic registration of small-angle X-ray scattering (SAXS) in detonation of high explosives. Computations show that measured SAXS distributions allow getting information on the size of carbon nanoparticles that condense in the chemical reaction zone, as well as outside it. The works were carried out on the VEPP-3 complex (BINP). SAXS (pulse duration of 1 ns) was recorded with the DIMEX-3 detector with an angular resolution of 0.1 mrad. Investigated were identical samples of high explosives on the basis of 1,3,5-triamino-2,4,6- trinitrobenzene

(TATB) and its mixtures with octogene and ultrafine diamond, as well as trinitrotoluene (TNT) and its mixtures with hexogen and benzotrifuroxane (C6N6O6, BTF). It is seen from the SAXS distributions processed that the condensed carbon nanoparticles in the chemical reaction zone have sizes of *sim*2 nm (TATB) to 3.5 nm (BTF). The dynamics of the sizes of carbon nanoparticles behind the front of detonation of the above high explosives has been shown for the first time. The maximum sizes of carbon nanoparticles are ∼3 nm for the TATB+octogen mixtures and ∼70 nm for BTF. Some experiments were also carried out for analysis of retained products of detonation of the same high explosive charges. The charges were exploded in an ice shell in an explosion chamber made of stainless steel. The resulting products were subjected to microscopic and diffraction studies. Nanodiamonds were isolated via treatment of the products in acid and gas. The resultant distributions of the nanodiamond sizes in the above high explosives coincide with the distributions obtained in dynamic experiments (from SAXS measurement).

ELECTRIC CONDUCTIVITY OF DETONATING TROTYL AT DIFFERENT INITIAL CONDITIONS

Satonkina N.P.,* Ershov A.P., Pruuel E.R., Karpov D.I.

LIH SB RAS, Novosibirsk, Russia

**snp@hydro.nsc.ru*

The investigation method based on the measurements of the conductivity of the detonation products is very efficient for the study of the detonation waves in high explosives such as hexogen, octogen, PETN, trotyl, and for heterogeneous explosives. It was shown in this work that the magnitude of the conductivity for the cast trotyl is three times lower than those for the compressed one at the maximal density. The quantity of the cavities in the cast trotyl is not enough in order to provide the combustion-detonation transition. Therefore, we added hollow glass microspheres to the cast trotyl that ensures the cavities of the known concentration serving possibly as the sources of hot points.

The high-resolution conductivity method developed earlier was applied to study the detonation of the trotyl of the different densities, the mixtures of the trotyl with water, and the trotyl with the addition of hollow glass microspheres with the diameters of 60 mkm.

The conductivity profiles were measured for the cast trotyl placed in a massive metallic shell of the diameter of 8 mm that is smaller then a critical diameter. The conductivity profile is wide (¿ 1 mks) and decreases

gradually. It reaches the value of 28 $Ohm^{-1}cm^{-1}$ that confirms previous result obtained with the method with the worse resolution. The conductivity profiles were obtained for the trotyl of a bulk density. The extra-wide peak with the width of about one millimeter was obtained due to the low trotyl density. We consider this peak corresponds to the zone of chemical reaction.

The cast trotyl with the microspheres is similar to the porous media. We did not registered any influence of the microspheres on the conductivity profiles. The conductivity in this case is lower than for a pure trotyl despite the fact that the microspheres can be additional sources of hot points in explosive. The same result was obtained for the trotyl of low density with microspheres. The micrspheres reduced a mean density of explosive and the conductivity displacing a conductive substance.

The experiments with the mixture of trityl with water were carried out. The trotyl was of a bulk density and water filled the pores. We registered a significant increase of the conductivity that can not be explained by water conductivity.

The work is supported by the Russian Foundation for Basic Researches (grants No 12–01–00177 and 12–03–00077).

ON THE ROLE OF PLASMA JET IN EXPLOSIVE WELDING

Alymov M.I.,* Deribas A.A., Gordopolova I.S.

ISMAN, Chernogolovka, Russia

**alymov@ism.ac.ru*

Discussed is the role of a plasma jet that can be formed in the weld gap during explosive welding of metallic sheets.

There is a serious controversy in the literature concerning the mechanism of explosive welding, especially the issues related to activation of the surfaces to be joined and their self-purification from oxides and dirt. In this communication, we are going to critically revise the concept of gas ionization assumingly taking place within a stand-off gap (weld gap), according to which thus formed plasma jet was declared [1, 2] to play a key role in the activation and self-purification of weld surfaces. Here there are three questions that have to be answered. (i) Are the temperatures developed within the weld gap sufficiently high for plasma formation? (ii) Are these temperatures sufficient for formation of the so-called cold plasma? (iii) Even if such plasma is formed in reality, how significant is its action? As is known, the detonation velocities (D) used in explosive welding never exceed 2500

m/s. At higher D, a weld seam does not form altogether. Therefore, required for gas ionization temperatures, within the range 6000–12,000 K, can hardly can expected to develop in typical conditions of explosive welding. We have demonstrated that, in typical conditions of explosive welding, the ionization within the gap is impossible by energy-balance considerations. We also show that the role of minor amounts of ionized species that may form in the process cannot be significant and distinguished from that of just hot gas. In the presentation, we will suggest the mechanism of explosive welding, including the stages of activation and self-purification, alternative to that reported in [1, 2].

1. Bondarenko S. Yu., Pevukhina O. L., Rikhter D. V., Pervukhin L. B. // Avtomatich. Svarka. 2009. no. 11. P. 46–48.
2. Pervukhin L. B., Rikhter D. V., Pervukhina O. L., Bondarenko S. Yu. // Svarochn. Pr-vo. 2009. no. 7. P. 32–37.

THE INFLUENCE OF ADDITIONS OF DIETHYLENETRIAMINE ON THE REACTION TIME OF NITROMETHANE IN DETONATION WAVES

Lapin S.M.,* Mochalova V.M., Utkin A. V.

IPCP RAS, Chernogolovka, Russia

**lms.lapin12011@yandex.ru*

It is known that small additions of amine can influence the detonation properties of nitromethane. In particular the additions of amines to nitromethane could result in the sharp decrease of the initiation pressure, drop of the failure diameter of liquid nitromethane and etc. [1], [2] In work [3] it is shown that small additions of diethylenetriamine (DETA) increase the initial rate of reaction of nitromethane. At 0.02% of DETA the significant difference from the velocity profile for neat nitromethane is observed—after shock jump the velocity continues to increase, in the vicinity of 10 ns it reaches the maximum and then it drops. The increase of initial reaction rate caused by DETA additions must influence on the reaction time of nitromethane in detonation waves too.

For this purpose the experiments for investigation of DETA influence on the reaction time in nitromethane were conducted. The DETA concentration was change from 0 to 2 weight percentages. The method of definition of the reaction time is well known. It is necessary to carry out the wave profiles measurements at different diameter of charges. If the diameter significantly exceeds failure one, the flow in reaction zone remains

invariable whereas velocity decrease in unloading wave depends on diameter. The diameters of shells were 20.0 and 30.0 mm for solution with weight percentage of DETA 0.5% and 36.4 and 30.5 mm for solution with weight percentage of DETA 2%. The registration of particle velocity profiles on the boundary with the water window was carried out by the laser interferometer VISAR.

The evaluation of the velocity profiles shows that the reaction time decreases from 50 ns for neat nitromethane up to 37 ns and 30 ns for the nitromethane with DETA solutions with the weight percentages 0.5% and 2%, respectively. However this change is not significant in comparison with the decrease of the failure diameter, which drops in 7 times at the increase of DETA concentration in the solution from 0 to 2%.

1. Engelke R. // Phys.Fluids. 1980. V. 23. P. 785–880.
2. Sheffield S. A., et al // 13-th Int. Det. Symp., Norfolk, USA. 2006. P. 401–407.
3. Mochalova V. M., Utkin A. V. // Int. Conference "Shock waves in condensed matter", Kiev, Ukraine. 2012. P. 60–63.

COMBUSTION RATE OF DENSE GASES

Assovskiy I.G.

ICP RAS, Moscow, Russia

assov@chyph.ras.ru

The goal of paper is to study influence of the equation of state of dense premixed gas on dependence of its combustion rate on pressure and initial temperature. Ability to operate by gas pressure not only to control the rate of chemical reactions but their direction was first proved in the early 20th century by Prof. of Artillery Academy, Academician V.N. Ipatyev. However, systematic studies of chemical processes in dense gases began shortly before World War II on the initiative of Yu.B. Khariton. These works were associated primarily with the problem of transition from combustion to detonation, as well as with combustion application in technical devices of high pressure. After the war, work was resumed in the USSR Academy of Sciences in ICP by Yu.N. Ryabinin and A.M. Markevich. In the interior ballistics, calculations of the temperature, pressure and composition of the combustion products typically take into account the equation of real gas state. However, in the theory of combustion of gasifiable systems influence of the real state of the gas phase on the burning rate was not analyzed. The present theoretical analysis has been conducted in the framework of

assumptions of the classical theory of thermal mechanism of combustion of premixed gases by N.N. Semenov, Ya.B. Zeldovich , and D.A. Frank-Kamenetsky, but taking into account the equation of state of a real dense gas. It is shown that the pressure effect on the combustion rate is due to changing of the concentrations of the reactants, changing of macro-kinetics of chemical reactions, and kinetics of molecular transport. It is also shown that the characteristic scale of "high-pressure", under which it is necessary to take into account the deviation of gas state from the ideal state, essentially depends on the temperature, and can vary widely . A formula for the high-pressure scale has been set, as a function of the parameters of the critical state of the gas. It is also shown that knowledge of the experimental dependence of the combustion rate on the pressure together with knowledge of the equation of gas state can provide information on changing of the reaction mechanism with pressure increasing. A method has been proposed for extrapolation to higher pressures of experimental data on the combustion rate obtained for moderate pressures. The analysis on the combustion rate of dense premixed gases is applicable in some cases to combustion of gasifiable condensed systems. It is especially important to compare theory with experiments, since the experimental data available in the literature on combustion at high pressures are mainly obtained for condensed systems.

THE ROLE OF CHEMICALLY NEUTRAL MICRO PARTICLES IN THE PROCESSES OF AEROSOL COMBUSTION: FROM THE DETONATION SUPPRESSION TO THE PARTICLES IMPLANTING INTO THE SUBSTRATE

Ivanov M.F.,* Kiverin A.D., Yakovenko I.S.

JIHT RAS, Moscow, Russia

**ivanov_mf@mail.ru*

The paper presents the study of the combustion and detonation waves propagating within hydrogen-oxygen mixture with chemically neutral micro particles by means of numerical simulation. The dynamics of heterogeneous media was described using the approach of dual-speed dual-temperature continuum model. In most studied cases the particles flow was treated as a continuum and in chosen cases as a set of particles moving under the laws of Stokes dynamics. The typical characteristics of the studied aerosols were chosen as for the practical applications: mass fraction lies in the range 0.01–0.1 and particle size is 100 nm–100μm. First the

process of flame propagation inside channel was studied. In homogeneous case (zero mass fraction of the particles) the chosen combustion regime lead to the detonation formation. For the cases of non-zero mass fraction of the particles the sufficient influence of the dispersed phase on the process was shown. Thus already for 1μm particles and smaller can observe sufficient drop in acceleration rate and even suppression of the transition to detonation. For the large particles of $\sim 100\mu$m there are approximately no influence on the flame evolution and transition to detonation. Such a phenomena can be explained by the difference in relaxation times after which the role of momentum and energy transfer between phases becomes principal. The other aspect of the same phenomena can be observed solving the problem of the particles implanting into the substrate by means of detonation or blast pulse. The larger particles ($\sim 100\mu$m) accelerated by the detonation or blast wave provide better implantation compared with smaller particles ($\sim 10\mu$m and lesser) flown away behind the reflected shock.

ZELDOVICH CONCEPTS FOR TRANSIENT COMBUSTION AND FLAMMABILITY LIMITS DETERMINATION

Kiverin A.D.,* Ivanov M.F., Smygalina A.E.

JIHT RAS, Moscow, Russia

**alexeykiverin@gmail.com*

One of the most constructive methods for analysis of transient ignition and combustion processes was proposed by Ya.B. Zeldovich in 1980 when he solved both problems for non-uniform initial conditions applying the approach elaborated earlier by A.N. Kolmogorov, I.G. Petrovsky and N.S. Piskunov. Such approach allows to describe the combustion wave propagating along the non-uniformly heated or premixed medium as an "intermediate asymptotic" Different physical mechanisms "switch on" and become significant on the different time scales. Therefore the process evolving along the non-uniformity should be determined by different physical mechanisms on the different stages of the process evolution. Thus if one takes the non-uniform distribution of the fuel concentration heated up to the same temperature the ignition will start independently in any part of the distribution. One should observe a so-called spontaneous combustion wave propagating along the non-uniformity so long as the chemical factors play a greater role. In the region of the non-uniformity where the characteristic scales of chemical reaction become much larger then gasdynamical

scales one should observe the switch between spontaneous and gasdynamical mechanisms of process evolution. The part of the non-uniformity where such a switch takes place covers the most rigorous criterion of the combustion initiation—the lower limit of exothermic reaction. Thus such an approach allows to estimate the lower flammability limit knowing the features of the chemical kinetics. In case of the reaction wave propagating along the fuel concentration non-uniformity at normal conditions one should observe clear visualization of the flame propagation criterion—the reaction wave should arise while propagating from the lower flammability limit in the direction of stoichiometric mixture and quench while propagating in the opposite direction. The paper discloses both transient problems using numerical simulations with detailed chemical kinetics mechanisms. It is demonstrated that the reaction starts even if the hydrogen concentration in the mixture is lower than the lean flammability limit. In case of non-uniform stirring the heat wave formed in the lean region may provide conditions for the self-sustaining combustion wave formation in the less lean adjacent region.

THREE-DIMENSIONAL FLOW STRUCTURES INDUCED BY THE ACCELERATING FLAMES IN CHANNELS

Yakovenko I.S.,* Ivanov M.F., Kiverin A.D.

JIHT RAS, Moscow, Russia

**yakovenko.ivan@bk.ru*

Since the first attempts to understand the origins of flame acceleration and transition to detonation (DDT) in channels filled with gaseous combustible mixtures the shadowgraphy and schlieren methods were used in experimental studies as the most informative methods for studying high-speed flows involving shocks where the gradients in the refractive index are large. These methods revealed that one of the leading roles in the DDT phenomena belongs to the shock waves, which are forming and travelling ahead the accelerating flame front before the transition takes place. To capture the features of flame acceleration and the origins of detonation formation one needs accurately resolve both time and space scales and restore three-dimensional pattern of the flow. Unfortunately these issues are beyond the scope of the published experiments. On the contrary one can reproduce the process using the high resolved 3D computations based on detailed models for reacting flows. Nowadays high performance computing allows to reproduce 3D flow pattern with sufficiently high spatial and temporal resolutions which is not available with the existing experimental

techniques. The paper discusses our recent results of 3D simulations of the flame acceleration and DDT within channels filled with hydrogen-oxygen mixture which makes it possible to get the correct interpretation of the experimentally obtained shadow and schlieren images and to resolve many confusions and erroneous conclusions about nature of the phenomena. In particular it is shown that the flow ahead the accelerating flame remains laminar up to the detonation formation. The visible complexity of the flow in the vicinity of the flame front does not connected with flow turbulization which takes place on the time scales sufficiently greater than the duration of the overall process and can be explained by the artifacts of the diagnostics. The interpretation of the Oppenheim's "explosion in the explosion" also can be obtained from the analysis of the 3D flow pattern just before DDT. The results reproduces the mechanism of DDT proposed by the authors earlier using 2D simulations. It should be noted that 2D simulations in general give a correct overall picture of hydrodynamic flow during the flame acceleration and DDT.

VALIDATION OF REDUCED KINETIC MODELS FOR SIMULATIONS OF TRANSIENT COMBUSTION PROCESSES

Smygalina A.E.,* Ivanov M.F., Kiverin A.D.

JIHT RAS, Moscow, Russia

**anna.smygalina@gmail.com*

Transient combustion processes such as flame acceleration, deflagration-to-detonation transition and combustion within IC engines combustors are accompanied by pressure elevation. The key question in numerical modeling of transient combustion processes is the choice of chemical kinetics scheme, which could provide the reliability of numerical results in a wide range of pressures. However, there is no sufficient data in literature for the schemes where their authority in modeling of these processes is discussed. The present work summarizes the analysis of four most widely used kinetic schemes reproducing hydrogen combustion for the perspective of their application in simulation of transient combustion processes. The analysis covers data on induction periods obtained by means of 0D calculations and laminar flame characteristics obtained with the use of 1D calculations. The hydrogen-oxygen and hydrogen-air mixtures are studied. The mathematical model of 1D combustion represents the full system of gasdynamical equations. The general aspect of the work is the performance of the calculations at normal and elevated

pressures (up to 10 atm). All the obtained results are compared with the corresponding experimental data taken from literature. On the basis of the performed comparison the conclusions for each scheme are made. The analysis of kinetic schemes presented in this paper is recommended to use as a test procedure prior to their adoption in simulation of transient combustion processes.

STUDY OF THE EMISSION OF SMALL ADMIXTURE OF Xe ATOMS IN He IN WEAK SHOCK WAVES

Ziborov V.S.,* Efremov V.P., Fortov V.E., Shumova V.V.

JIHT RAS, Moscow, Russia

**vziborov@rambler.ru*

The emission spectra of Xe as small admixture of especially pure He, were measured in shock waves. Shock wave generator was the high vacuum shock tube "Yashma". The measurements were performed in the range of Mach numbers M = 2.2–3.1, the concentration of Xe was (0.1–1.0)%. The time-resolved emission measurements were carried out from the end of the shock tube using monochromator ACTON-150 and CCD-camera LeGa-3, equipped with light amplifier in the range from infrared to vacuum UV. Simultaneously, the laser schlieren method with spatial resolution of 20 microns was applied. The spectra of radiation in shock waves in the range from 200 to 600 nm depending on the intensity of the shock waves, the measurement time and the concentration of Xe, were obtained. The spectra of the studied compounds in a glow discharge of hollow cathode lamp were measured. Spectral lines were identified, they belong to optical transitions from the emitting states near threshold ionization of xenon of about 12 eV.

The principal possibility to obtain reliable experimental data on the energy exchange processes with the transfer of large quantities of energy in one/several collisions in unsteady supersonic gas flows, was shown.

This work was supported by the Russian Foundation for Basic Research Grant No. 12-08-01266 and by the Program of the Presidium of RAS "The matter at high energy densities".

AN OPTICAL EMISSION STUDY OF THE IGNITION OF DILUTE HYDROCARBON–OXYGEN MIXTURES BEHIND SHOCK WAVES

Tereza A.M.,[*1] ***Vlasov P.A.,***[2] ***Smirnov V.N.,***[1] ***Ziborov V.S.,***[3] ***Shumova V.V.***[1]

[1]*ICP RAS, Moscow,* [2]*ICT SB RAS, Novosibirsk,*
[3]*JIHT RAS, Moscow, Russia*

[*]*atereza@bk.ru*

The optical emission of various species during the ignition of fuel-oxidant mixtures provides valuable information on the kinetic mechanism of this process important for both scientific research and technological applications involving the ignition and combustion of gaseous mixtures. Despite a widespread use of emission techniques in studying combustion processes, there remains a lot of poorly understood features of the mechanism of the excitation of radicals, in particular the reliability of quantitative determination of the concentrations of reactive species. In the present work, the behavior of emissions from electronically excited CH^* ($\lambda = 429$ nm), C_2^* ($\lambda = 516.5$ nm), OH^* ($\lambda = 308$ nm) radicals and CO_2^* ($\lambda = 360$ nm) molecule, as well as from thermally excited H_2O ($\sim$1.0 μm and $\sim$1.8 μm) molecules were monitored during the ignition of mixtures of ethane, propane , ethylene, and acetylene with oxygen highly diluted in argon (97–98% Ar) at temperatures 1100–1800 K and a pressure of $\sim$1 atm. The results obtained were found to be in close agreement with the published data on the temperature dependences of the ignition delay times for the tested hydrocarbons. Numerical simulations of the measured emission profiles within the framework of available kinetic mechanisms, together with experimental data reported by other authors, made it possible to identify the main excitation channels and estimate their characteristics.

This work was supported by the Russian Foundation for Basic Research, project no. 12–08-01266-a.

STUDY OF THE PYROLYSIS AND OXIDATION OF ACETYLENE AND DIACETYLENE IN SHOCK WAVES

Vlasov P.A.,[*1] ***Ziborov V.S.,***[2] ***Smirnov V.N.,***[1] ***Shumova V.V.,***[2] ***Tereza A.M.,***[1] ***Agafonov G.L.,***[1] ***Bilera I.V.,***[3] ***Kolbanovsky Yu.A.***[3]

[1]*ICP RAS,* [2]*JIHT RAS,* [3]*TIPS RAS, Moscow, Russia*

[*]*iz@chph.ras.ru*

Acetylene and diacetylene are key intermediate products in the combustion of various hydrocarbons. In [1], the time histories of the products of the pyrolysis and oxidation of various diacetylene-oxygen mixtures were measured and numerically simulated within the framework of a detailed kinetic scheme; in [2], similar studies were carried out for acetylene-oxidant mixtures. Chromatographic analysis of the products of acetylene pyrolysis behind reflected shock waves performed in the present work showed a full qualitative agreement with the results of [2]. In addition, we developed and tested a kinetic model of the pyrolysis and oxidation of acetylene and diacetylene and compared its predictions with the results of our own experiments and the data from [1, 2]. Simulations showed that at low temperatures (T<1500 K) the new kinetic scheme closely describes the temporal behavior of the main products of the pyrolysis and oxidation of diacetylene C_4H_2 in shock waves [1]. However, in describing similar experiments on the oxidation of acetylene in shock waves [2], we encountered a number of difficulties; in particular, at low temperatures, the acetylene consumption rate turned out to be excessively high. On the one hand, for acetylene pyrolysis, a good agreement between the measured [2] and calculated time histories of the final pyrolysis products was observed. Note, that the oxidation of such a rich mixture results in a significant heating of the reaction mixture within a very short time (500–600 K at $T < 1500$ K), in contrast to the pyrolysis experiments, where the temperature remains practically constant. This factor probably causes significant deviations of the shock wave flow from ideal, which, in turn, leads to a discrepancy between the experimental data and the predictions of the ideal-flow model in the product concentrations and in the soot yield.

This work was supported by the RFBR Grant No. 12–08–01266-a.

1. Hidaka Y., Henmi Y., Ohonishi T., Okuno T., Koike T. // Comb. Flame. 2002. V. 130. P. 62–82.
2. Hidaka Y., Hattori K., Okuno T., Inami K., Abe T., Koike T. // Comb. Flame. 1996. V. 107. P. 401–417.

NUMERICAL STUDY OF SHOCK WAVE IMPACTS ON DYNAMIC OBJECTS

Grakhov Yu.V., Khlybov V.I.*

OAO "Makeyev GRTs", Miass, Russia

**src@makeyev.ru*

The paper presents the results of a numerical method based on the solved Navier–Stokes equations that was applied to study impacts of shock waves in the diffraction phase on dynamic objects moving at velocities from low subsonic to supersonic. The method is founded on setting boundary conditions varying in spacial coordinates and time. A software package on the basis of finite (control) volumes with a suitable set of boundary conditions and an advanced command language was taken for application of the developed numerical method to study impacts of shock waves. To validate the package it was tested for different cases of impacts, including diffraction of the shock waves on a cylindrical side. All test results were positive.

A great volume of control computations within the whole range of the above mentioned velocities were made for the method. The analysis of the results led to implementation of the method in designing of flight vehicles.

The results of several control computations are given in the paper.

MODELING TECHNOLOGY OF HYPERSONIC FLOW AROUND THE AIRCRAFT WITH THE CHANGING SHAPE OF THE SURFACE

***Aksenov A.A.,*[1] *Degtyar V.G.,*[2] *Khlybov V.I.,*[2] *Zhluktov S.V.,*[1] *Savitsky D.V.,**[1] *Son E.E.*[1]

[1] *JIHT RAS, Moscow,* [2] *OAO "Makeyev GRTs", Miass, Russia*

**dmvlsav@yandex.ru*

There are a lot of nonequilibrium physicochemical processes in the shock layer around a hypersonic aircraft. Loss of the mass from the surface of the aircraft complicates the flow picture greatly. Modeling of the thermo-chemically nonequilibrium multicomponent gas mixture requires significant computing resources. Therefore, it is interesting to utilize relatively simple models that take into account the main physical effects.

In this paper the simplified approach of the modeling of mass loss from the surface of the aircraft at altitudes less than 50 km is proposed. Approach assumes that the gas mixture consists of three components: the

product of ablation, the oxidant and the neutral. Each of the three components is in the state of "independent" thermo-chemical equilibrium. Radiation of the gas mixture is not considered. This is correct for the aircraft with a radius of the curvature less than 1 m.

Simulation of the hypersonic flow was performed using the "FlowVision" software. Automatic rebuild of the model surface has been done in a CAD. The "IOSO" combines various programs needed to solve the problem and organizes data exchange between them.

The IRV-2 rocket has been chosen as an object of the modeling. The IRV-2 launch vehicle is has sphere-biconic form with a nose radius of 0.01905 m and total length of 1.386 m. Considered gas mixture consists of O_2, N_2, CO_2. Chemical reactions between the equilibrium mixtures of O_2, N_2, CO_2 has not been taken into account.

The numerical results demonstrate modeling technology of hypersonic flow around the aircraft with the changing shape of the surface using the software package "FlowVision".

APPLICATION OF RIEMANN INVARIANTS TO NON-ADIABATIC 1D FLOWS

Son E.E.

JIHT RAS, Moscow, Russia

son.eduard@gmail.com

The generalization of 1DT (space–time) nonlinear wave theory and Riemann Invariants for nonadiabatic flows with energy and heat release is given. The approach is applied to flows with chemical reactions, explosion of conducting wires and Inertial Confined Fusin. The Zeldovich problem for detonation in chemically reacted gases is considered on the base of proposed approach.

SHOCK WAVE–BOUNDARY LAYER INTERACTION ON THE NON-ADIABATIC RAMP SURFACE

Glushniova A.A.,* Saveliev A.S., Son E.E., Tereshonok D.V.

JIHT RAS, Moscow, Russia

**glushniova.alexandra@gmail.com*

In shock wave-boundary layer interaction pressure disturbance leads to thicken of the boundary layer, that causes the outer flow compression and therefore compression waves emerge. Free-interaction theory describes

the interaction behavior and predicts influence of wall temperature on the boundary layer separation [1]. The influence of the wall temperature on the separation emergence was given in [2]. However, theory does not give satisfactory explanation of the experimentally observed phenomenon, so further investigations of wall temperature influence has to be continued. Current work is devoted to the experimental investigation of the interaction of shock wave with turbulent boundary layer on the heated ramp surface. The shadowgraph pictures obtained by Shlieren method was used for measuring of the separation region length for ramp angles of 15, 20, 23, 30°. The temperature ratio T_w/T_∞ in the experiments was varied in the range from 1.8 (adiabatic conditions) to 3. Comparison of experimental results with theory has shown that despite the trends of both dependences were similar the experimental results were beyond the theoretical predictions. The reason of theoretical underestimation of separation length increase could be due to given theory takes into account surface temperature influence only at the interaction onset and does not account temperature influence in reattachment region. For correlation law [3] to completely encounter wall temperature influence it has to be multiplied by factor $0.6T_w/T_\infty$. Boundary layer profiles measured downstream reattachment point by means of PIV confirm surface temperature influence on the reattachment process. The instability of separation region was also studied by means of POD analysis. Experimentally was shown that increase of temperature ratio leads to energy redistribution, namely, increasing amount of energy stored in first spatial modes responsible for motion of separation region. It was proved that surface heating amplifies pulsations of separation region.

---

1. Chang P., Separation of Flow // Oxford: Pergamon, 1972, V. 1.
2. Zacharov N. N. // Trudy CIAM . 1971. V. 507. P. 70.
3. Zheltovodov A. A., Shilein, E. K., Horstman C. C. // Appl. Mech. Tech. Phys. 1993. V. 5, P. 346.

THE INFLUENCE OF THE ADIABATIC INDEX ON THE GAS FLOWS MIXING IN MACH SHOCK WAVES REFLECTION

Nesterov A.S., Gavrenkov S.A., Gvozdeva L.G.*

JIHT RAS, Moscow, Russia

**nesterovalexey@bk.ru*

A gas flows mixing problem is of a big science and practical importance. A lot of researches consider the different aspects of this problem, such as mixing of incompressible flows, compressible, subsonic and supersonic flows, flows with the chemical energy release etc. Among all of these problems there is the less studied one, a problem of mixing layers passing the stationary three shock waves configuration. It is well known that the reflection of shock waves by the rigid surfaces can occur in two ways: the regular reflection and irregular, Mach reflection, which is followed by the appearance of the slip surface where one of two flows passed through incidental and reflected waves and the other through the Mach wave. Since there is a surface with two different flow velocities, a Kelvin-Helmholtz instability appears and the tangential surface curls into a chain of vortices. This problem is of a great interest for rocketry because the same configuration appears in a gas flow effusing from a rocket engine nozzle and in a flow with separated boundary layer within its interaction with a shock wave inside the nozzle. In this article the influence of adiabatic index of gas on a Kelvin-Helmholtz instability evolution in the tangential surfaces behind the shock waves is investigated. The experiments was carried out in a shock tubes, where the work gas can be of any kind [1]. As it is shown earlier, the variation of an adiabatic index leads to a very appreciable increase of mixing on a tangential surface. In this work a consideration of a mixing process is offered in accordance with Batchelor [2] and Rikanati [3] theories. The problem of shock waves allocation in three shock waves configuration of Mach reflection has been solved analytically. These parameters were calculated under the same conditions as in experiments. It has been shown analytically, that adiabatic index actually affects positively on mixing intensity in accordance to experimental data.

Acknowledgment. The present study is supported in part by the Russian Research Foundation for the Fundamental Sciences grant 12-01-31362.

---

1. Bazhenova T.V., Gvozdeva L.G., Nonstationary interaction of shock waves. M., “Nauka”, 1977, 274
2. An. introduction to fluid dynamics. G. K. Batchelor,. frs,. London (Cam-

bridge University Press), 1967.
3. A. Rikanati, U. Alon, D. Shvarts, Phys. Fluids 15, 3776 (2003)

Ya. B. ZELDOVICH—FATHER OF PULSE DETONATION ENGINE RESEARCH

Golub V. V.

JIHT RAS, Moscow, Russia

victor.v.golub@gmail.com

In 1940 Ya. B. Zeldovich showed that thermodynamic efficiency of fuel combustion at detonation regime is greater than at deflagration regimes. The rates of energy release in detonation modes of gas combustion are three orders of magnitude higher than in deflagration combustion modes. This theoretical result gave rise to numerous studies of possibility of creation and utilization of a detonation engine for aviation needs. The current situation in the PDE research will be discussed.

NUMERICAL STUDY OF INFLUENCE OF EJECTOR ON THE EFFICIENCY OF NOZZLE HEAD OF DETONATION ENGINE

Golovastov S. V.,* Korobov A. E.

JIHT RAS, Moscow, Russia

**golovastov@yandex.ru*

High thermal efficiency of the pulse detonation engine (PDE) attracts researchers to apply it as a new technology for the aerospace propulsion. This is because the thermal efficiency of fuel combustion in the detonation wave exceeds the efficiency of fuel combustion at constant pressure [1].

One way to increase the thrust of the engine is the use of an ejector. The increase in thrust results from the growing mass of the working gas by entraining a secondary flow of the external air induced by a primary flow. This due to two factors:

1. Due to the turbulent mixed flow coming from the combustion chamber and ambient air. This mechanism is also valid for steady ejector.

2. Due to the gas pressure in wave can be smaller than the external air pressure at the phase of the expansion wave.

It was showed that using of the ejector can lead to increase the specific impulse up to 35 % in [2] for the engines at a constant rate of gas flow. The phenomenon of abnormally high thrust boost in gas ejection process

with pulsed active jet was opened in 1951 [3]. Thrust augmentation ratios above a factor of 2 were measured by Wilson at al. [4] for the PDE.

The influence of the ejector on gas flow at PDE was investigated. Axisymmetric model was used in our work. Equations of Navies-Stokes were solved using finite-difference scheme Roe of second order of accuracy. The initial conditions were calculated on the base of experimental data. Mathematical simulation of the first two pulses of the engine for three different ejectors was carried out. The gain of thrust was about 17% for two cases compared with the case, when the gap between the combustion chamber and the ejector was closed. Thrust augmentation ratios above a factor of 2 were obtained.

1. Zeldovich Y. B. About the energy use of the detonation combustion. Technical Physics. 1940. No. 1(17). P. 1453–1461.
2. Abramovich G. Nucl. Applied gasdynamic. M. Science, 1969.
3. Chelomei V. N., Kudrin O. I., Kvasnikov A. V., Anomalous high thrust boost in gas ejection process with pulsed active jet. / / Scientific discovery, 1951
4. Wilson J., Sgondea A., Paxson D., Rosenthal B. // J. Propulsion and Power. 2007. V. 23, No. 1.

EXPERIMENTAL INVESTIGATION OF VORTEX STRUCTURES IN GAS MICROJET UNDER ACOUSTIC INFLUENCE

Krivokorytov M.S.,* Golub V.V.

JIHT RAS, Moscow, Russia

**mikhail.k@phystech.edu*

Theoretically and experimentally proved that the free shear flow having an inflection point in the velocity profile is inviscid instability. Its perturbations grow downstream exponentially, forming vortices that are combined with each other to form large coherent structures. However, during the transition to smaller scales the mechanism of jets development is changing. In [1] it is shown that the microjet with parabolic and top-hat velocity profile remain laminar at distances of about 10 calibers jet diameter. In this case there are no Kelvin-Helmholtz ring vortices, and the loss of stability carried out due to asymmetric (sinusoidal) oscillation mode of the jet as a whole. The importance of these studies is obvious both for science and for many technical applications, for example influencing on the reactive gas jet in the diffusion torch it is possible to control the concentration of soot and nitrogen oxides in the combustion products [2]. In [2],

the authors discovered the effect of bifurcation of the diffusion flame, and observed the resonance decreasing in the concentration of nitrogen oxides in the combustion products. Bifurcation of flame caused by dividing the jet has not yet reacted gas. In [3] it is shown that the asymmetric mode of instability develops in the jet under external acoustic influence, which increase downstream leads to crushing the jet on the alternating field, diverging at a certain angle.

It is shown that under the influence of acoustic waves on a plot of jet the adjoining the open end of the tube inside the jet vortex structure are formed. At the same time jet oscillates as a whole. As the distance downstream these oscillations grows and leads to crushing the jet on the alternating field, diverging at a certain angle. This causes to an intensification of the jet gas mixing with the surrounding air.

Work carried out under the program of the Presidium of RAS "Combustion and Explosion".

1. Kozlov V. V. et al. Round and plane jets in a transverse acoustic field // Journal of Engineering Thermophysics, V. 20, No. 3, P. 272–289, 2011.
2. Krivokorytov M. S. et al. The effect of acoustic oscillations on diffusion combustion of methane//Technical Physics Letters,V. 38,No 5,P. 478–480, 2012.
3. Krivokorytov M. S. et al. The evolution of instabilities in gas microjets under acoustic action //Technical Physics Letters, V. 39, No 9, P. 814–817, 2013.

LARGE SCALE DETONATION EXPERIMENTS WITH MIXTURES OF PROPANE AND PROPANE–ACETYLENE IN AIR

Gavrikov A.I.,* Aleksandrov A.O., Chernenko E.V., Chaivanov B.B., Efimenko A.A., Schepetov N.G., Velmakin S.M., Zaretskiy N.P.

NRC KI, Moscow, Russia

**gavrikov_ai@nrcki.ru*

The paper presents results of large scale detonation experiments with propane-air and propane-acetylene-air mixtures. Experiments were carried out in an open cylindrical volume. Volume was covered with polyethylene film and bottom of the volume was located at a height of 0.5 m above ground. The total volume of the cylinder varied from 23.5 to 25.3 m^3, concentration of propane varied from 4.1% to 4.9%. Additional experiments with acetylene-air and acetylene-propane-air mixtures were performed. Initial temperature in all experiments was 300 K and initial pres-

sure - 1 atm. Registration system consisted of 24 pressure sensors and 9 light sensors which were located on 3 rays at a distance from 0 to 20 meters from central axes of cylinder.

Detonation was observed in all experiments. Detailed experimental diagnostics, including gas component chromatography and fast video recording were used in each experiment. Large scale experimental results obtained in a series can be used for verification of numerical and analytical models and improvement of CFD tools.

INFLUENCE OF REFLECTED SOUND WAVES OF DEFLAGRATION-TO-DETONATION TRANSITION IN PROPANE–BUTANE MIXTURE

Mikushkin A. Yu.,* Bivol G. Yu., Golovastov S. V.

JIHT RAS, Moscow, Russia

**notna17@yandex.ru*

Transition from deflagration to detonation in propane-butane-oxygen mixture in a channel with subcritical diameter was studied experimentally. Under subcritical channel we consider a channel, the diameter of which is less than the width of the detonation cell for investigated mixtures. In our case, the width of the detonation cell was equal to 3–8 mm, and the diameter of the channel was 3 mm. So for initiation of detonation prechamber the next method initiation of detonation was used: one end of the narrow channel was connected with a section of a larger diameter. Design settling chamber allowed to change its length and diameter.

The purpose of the work was experimental investigation of the influence of passed/reflected acoustic disturbances generated by the flame front, on the transition burning in a detonation in a narrow channel.

Dynamics of the flame front velocity along the open and closed channels was measured. The speed of propagation of stationary detonation Chapman-Jouget for propane-butane mixture with oxygen was 1880 m/s. The predetonation distance was 100–160 calibers, depending on the ratio of propane-butane mixture with oxygen. ER varied from 0.6 to 1.8.

The effect of the reflected from the end of the channel acoustic disturbance on the speed of the flame front was detected. One end of the channel can be closed and opened. When closed perturbations created by accelerating the flame front is reflected from the channel and help slow down of the flame front. When the flame velocity exceed a certain critical value, reflected disturbances, on the contrary, boost the flame front and the formation of detonation due to the high power density in the zone

of interaction of the waves and the flame front. Non-monotonic effect of acoustic perturbations on the speed of the flame front was found.

The work was supported by the Russian Academy of Science program Combustion and Explosion and Ministry of Education SP-1782.2012.1.

EVOLUTION OF SPHERICAL HYDROGEN–AIR FLAMES AT DIFFERENT INITIATION ENERGY

Petukhov V.A.,* Gutkin L.D., Naboko I.M., Bublik N.P., Gusev P.A., Solntsev O.I.

JIHT RAS, Moscow, Russia

**petukhov@ihed.ras.ru*

Much research is devoted to investigation of moving of spherical flames. However, experimental studies are very limited. The majority of these works have been made in volumes of tens of liters. If the evolution of spherical flames for such mixtures as acetylene-oxygen and hydrogen-oxygen at early phase can be studied in so size volumes, the study of hydrogen-air mixtures require volumes of tens of cubic meters. Hydrodynamic stability is reduced, Re number and auto-turbulization are increased with increase in flame size. Study of the processes of combustion gas mixtures in large volumes is also important for safety concerns. In this work the evolution of the spherical flame of hydrogen-air mixtures have been studied in reaction volume from 7 to 40 m^3 bounded by a thin rubber film and having a shape close to spherical. Reaction volumes were placed inside 13YA3 explosive spherical chamber 12 m in diameter. Initiation of the combustion process was realized by various sources with energy from 1 to 15.600 J. In experiments movements of pressure waves and flame front were registered, moreover the process was recorded using speed video camera.

ENERGETICS OF PYROLYSIS AND COMBUSTION OF ACETYLENE

Emelianov A.V., Eremin A.V.,* Golub V.V., Gurentsov E.V., Fortov V.E.

JIHT RAS, Moscow, Russia

**eremin@ihed.ras.ru*

Acetylene is an exothermic hydrocarbon compound. At pyrolysis of acetylene a graphitized soot and molecular hydrogen are formed:

$$C_2H_2 \rightarrow 2C(\text{graphite}) + H_2(+227\text{kJ/mol}) \quad (1)$$

Owing to an essential heat release, the self-decomposition of acetylene can proceed as in a combustion mode, with the speeds from 10 to 50 cm/s, and in a detonation mode with speeds more than 2000 m/s [1], [2], [3]. It is essential that energy release at acetylene pyrolysis more than twice exceeds energy release (related to total mixture) at its combustion in air:

$$C_2H_2 + 2.5(O_2 + 3.76N_2) \rightarrow 2CO_2 + H_2O(\text{gas}) + 9.4N_2(+105\text{kJ/mol}) \quad (2)$$

Moreover, as a result of reaction (1) the valuable product—the soot, widely used in the industry, and hydrogen which is the important prospective fuel are formed. At combustion of hydrogen in air an additional energy can be obtained:

$$H_2 + 0.5(O_2 + 3.76N_2) \rightarrow H_2O(\text{gas}) + 1.88N_2(+72\text{kJ/mol}) \quad (3)$$

Thus, the usage of process of detonation pyrolysis of acetylene can bring an energy gain about 94 kJ/mol in comparison with its combustion in air. Additional benefits of this process are lack of an ecologically harmful combustion product CO_2 and a yield of a large amount of soot.

In this work the details of the organization of a power cycle on obtaining energy at detonation pyrolysis of acetylene are considered.

This work has been supported by the Russian Foundation for Basic Research (grant No. 13–08–00454).

---

1. Ivanov B. A. // Physics of acetylene explosion 1969.
2. Babushok V. I., Miziolek A. W. // Combustion and Flame. 2004. V. 136. P. 141–145.
3. Emelianov A. V., Eremin A. V., Fortov V. E. // JETP Lett. 2010. V. 92(2). P. 97–101.

EXPERIMENTAL STUDY OF THE INFLUENCE OF QUANTUM EFFECTS ON THE RATE OF CARBON ATOM FORMATION AT SHOCK WAVE PYROLYSIS OF ACETYLENE

Drakon A. V., Emelianov A. V.,* Eremin A. V.

JIHT RAS, Moscow, Russia

**aemelia@ihed.ras.ru*

In a recent paper [1] it was shown that the deviation from Arrhenius dependency of induction times of initiation of detonation waves of condensation observed in experiments [2] can be described by quantum

corrections caused by the increase in high-energy tails of the distribution functions at high pressures due to manifestation of principle of uncertainty for the energy of the colliding particles at high collision frequency.

In many works the deviation from Arrhenius dependence of the dissociation rate constants of the two- and polyatomic molecules (for example NO, SO_2, CH_4, CH_3, C_2H_2 and others) with decreasing temperature and increasing pressure was observed. This deviation, which still has no unambiguous interpretation, presents a serious problem in chemical kinetics. Analysis of the results shows that increasing of the rate of endothermic dissociation reactions of polyatomic molecules may be due to the influence of quantum effects.

In this work the experimental measurements of the rate constant of carbon atoms formation at acetylene decomposition at different temperatures and in a wide range of varying pressure are presented. Investigations were performed behind reflected shock waves using the precise and sensitive method—Atomic Resonance Absorption Spectroscopy (ARAS) for the measurements of the concentration of carbon atoms at a resonance line 165.6 nm in the mixtures initially containing the small concentrations of C_2H_2 in argon.

The experimental results are compared with a kinetic modeling of the thermal decomposition of acetylene at different temperatures and pressures using Chemkin-4 and with the analytical calculation of a change of the rate of acetylene dissociation reaction with quantum effects taken into account.

This work has been supported by contract with SRC FR TRINITI-ROSATOM (dogovor No D-2170/13(29/13–1106)).

---

1. Drakon A. V., Emelianov A. V., Eremin A. V., Gurentsov E. V., Petrushevich Yu. V., Starostin A. N., Taran M. D., Fortov V. E. // Phys. Rev. Lett. 2012. V. 109, P. 183201.
2. Emelianov A. V., Eremin A. V. and Fortov V. E. // JETP Letters. 2010. V. 92, No. 2. P. 97–101.

INFLUENCE OF HALOGEN–CARBON ADDITIVES ON DETONATION WAVE FORMATION IN METHANE–OXYGEN MIXTURES

Drakon A.V., Emelianov A.V., Eremin A.V., Tsirlina E.A.*

JIHT RAS, Moscow, Russia

**elena2509@yandex.ru*

The problem of detonation of methane is extremely important owing to continuous accidents in mines, dangerous explosions at leakages of methane on gas pipelines, in various productions, and even at explosions of household gas. The introduction of small chemically active inhibiting additives like halogen-carbons is considered one of the most perspective approaches. On the other hand, there are some data that under certain conditions the same species can instead of suppressing of combustion processes, to accelerate detonation of hydrocarbon-air mixtures [1, 2].

The goal of this work was to study the influence of additives of CF_3H and CCl_4 on the development of detonation wave in the methane-oxygen mixtures diluted with argon.

Experiments were carried out behind the reflected shock waves in a high pressure shock tube equipped with 5 calibrated pressure gauges and rectangular sapphire windows through which continuous registration of propagation of a shock wave by means of the intensified CCD-camera was performed.

The results of experiments have shown that at elevated temperatures both investigated species demonstrates significant promoting effect. In this work the detailed analysis of CCD-camera records of the development of detonation wave in methane-oxygen mixtures with CF_3H and CCl_4 additives has been performed. The obtained profiles of the propagation of shock wave and flame fronts represent the valuable information about the process of deflagration-detonation transition in all investigated mixtures and the influence of halogen-carbons on the rate and kinetics of detonation formation.

This work has been supported by the Russian Foundation for Basic Research (grant No. 13–03–00852).

---

1. Baugé J. C., Glaude P. A., Pommier P., Battin Leclerc F, Scacchi G., Côme G. M. // Journal de Chimie Physique et de Physico-Chimie Biologique, 1997. Iss. 3. P. 460–476.
2. Drakon A. V., Emelianov A. V., Eremiv A. V. // Proceedings of 6th European Combustion Meeting 26–28 June 2013 Lund Sweden, 2013. P. 1–45.

INFLUENCE OF QUANTUM EFFECTS ON IGNITION KINETICS OF H_2/O_2 AND CH_4/O_2 MIXTURES DOPED BY FIRE SUPPRESSANTS

Drakon A.V.,[*1] ***Emelianov A.V.,***[1] ***Eremin A.V.,***[1]
Petrushevich Yu.V.,[2] ***Starostin A.N.,***[2] ***Taran M.D.***[2]

[1] *JIHT RAS, Moscow,* [2] *SRC RF TRINITI, Troitsk, Russia*

[*] *drakon.a.v@gmail.com*

The influence of quantum effects and chemical inhibitors pyrolysis on the kinetics of ignition of hydrogen- and methane-oxygen mixtures was analyzed and studied experimentally. Recently discovered quantum corrections [1] to chemical reaction rates, though subtle at common conditions, may have dramatic affect on induction times and ignition limits, as chain mechanisms of combustion development are extremely sensible to active radical concentration, and, thus, require thorough consideration during development of methods of explosions prevention.

Kinetic modeling was performed in ChemKin software package using improved GRI mechanism [2]. It was shown that significant deviations of experimentally observed ignition delay time in hydrogen-oxygen mixtures [3] from the predictions of kinetic calculations are quite well described by the proposed quantum corrections for the rate of $H_2 + O_2 \rightarrow 2OH$ reaction, which was not included in the original mechanism as it had very high activation energy and had no influence on ignition in classic approach.

Experimental investigation has shown that well-known chemical detonation suppressors CCl_4 and CF_3H [4] at concentrations 0.5–10% do not prevent ignition but contrary significantly reduces induction time in methane-oxygen mixture at T = 1100–1700 K and P = 5–7 bar. Suggested kinetic mechanism indicated that the promoting species formed by admixtures pyrolysis are actually CF_2 and atomic chlorine, which produce active radicals in reactions $CF_2+O_2 \rightarrow COF_2+O$ and $Cl+CH_4 \rightarrow CH_3+HCl$, initiating chain combustion reactions. An analysis of quantum corrections for rates of various halogenoalkanes pyrolysis reactions was performed and estimations of their possible influence on induction time depending on precursor molecule thermodynamical properties were given.

This work has been supported by RFBR (project No 13–03–00852-a) and SRC FR TRINITI-ROSATOM (contract No D-2170/13(29/13–1106)).

1. A. N. Starostin, A. G. Leonov, Yu.V. Petrushevich, and Vl. K. Rerikh // Plasma Phys. Rep. 31, 123 (2005)
2. Z. Hong, D. Davidson and R. Hanson // Combust. Flame, 158, 633 (2011)

3. G. Pang, D. Davidson and R. Hanson // Proc. Comb. Inst. 32, 181 (2009)
4. Shebeko Yu.N., Azatyan V.V. et al. // Combust. Flame, 121, 542–547

EXPERIMENTAL AND THEORETICAL STUDY OF PREMIXED METHANE JET FLAME

Krikunova A.I.,* Son E.E.

JIHT RAS, Moscow, Russia

**utro-2007@mail.ru*

Modeling of combustion and particularly turbulent combustion is an important problem. It is widely used in design and test gas engines, combustion chambers and at the same time—is an interesting fundamental problem. For verification and design models it is necessary to obtain turbulent flame data, such as spatial distribution of the instantaneous velocities, mean velocity, second and third turbulent moments of velocity and temperature fluctuations.

The experimental setup consists of a burner, plenum chamber, flow seeding device, premixing chamber and section of the air and fuel flow rate control. As the measuring system is used stereo–PIV: double–cavity 130 mJ Nd:YAG pulsed laser (Twins BSL 140: time of pulses – 9 ns, delay in the pair of pulses – 800 ms, delay in vicinal pulses – 40 μs), two 4 Mpix CCD cameras, and a synchronizing processor. The cameras were equipped with narrow-bandwidth optical filters admitting the emission of the laser (532 nm) and suppressing the radiation of the flame. For to obtain precise image scheimpflug devise was used that turn the image obtained from displaced cameras. The Reair number was 4100, it is estimated by the air flow rate—Qair, as volume flow rate of air was more than methane, to provide such equivalence ratio. Qair and Qmethane were adjusted with system of flow rate controllers. The equivalence ratio of the air–methane mixture was 0.7, 1.4 and 2.5. The burner was used a Vitoshinsky contraction nozzle. It organizes jet flow with top-hat exit velocity profile. Exit diameter was equal to 15 mm. For organization a swirl flow inside nozzle was put swirl generator. Swirl rate was equal to 1, based on it geometry. The experiments were performed under atmospheric pressure and room temperature. The laser sheet, passed through a central plane of the flame, is formed by the system of spherical and cylindrical lenses, it had a minimal thickness about 1 mm. PIV method is based on particles displacement for certain period of time. To provide this the flow was seeded by TiO_2 particles with an average diameter below 5 μm. The system was operated by a computer with "Actual Flow" software. 3000 images were for each

regime obtained and handled. As the result the distribution of the instantaneous velocities, mean velocity, second statistical moments of turbulent velocity fluctuations were obtained.

The experimental data was compared with one, obtained by computer modeling. The results have good agreement.

PHYSICAL BASIS OF PARTICLE ACCELERATION IN DETONATION DEVICES USING MULTI-STEP GAS DETONATION

Bivol G. Yu.,* Mikushkin A. Yu.

JIHT RAS, Moscow, Russia

**grigorij-bivol@yandex.ru*

The aim of this work was to study the process of multi-stage detonation in the cylindrical detonation tube with conic sections. To obtain such regime a new experimental installation was developed. The using of conic sections gives us opportunity to produce the detonation wave with force parameters. The main feature of the setup is that it consisted of expanding and contracting sections that allow to monitor various modes of detonation. The setup operates in the frequency mode and has a water cooling system. Diagnostics allows us to measure the velocity of shock waves and flame fronts within the combustion chamber. The experimental setup can be used to produce coatings of various materials, as it can be easily upgraded for the needs of detonation spraying. A stable detonation with frequencies of 0.5 to 2 Hz was obtained in the chamber when using forced cooling. The speeds of 1000 m/s and 670 m/s were measured in different parts of the chamber. In the chamber decomposition of detonation into the flame front and the shock wave was obtained during the experiments. That fact supports the theory of occurrence of detonation decomposition in chambers with an irregular cross-section . This fact allows the use of detonation with increased parameters.

The work was supported by the Russian Academy of Science program "Combustion and Explosion", RFBR 13–08–01227

SCALE COUPLING IN RICHTMYER–MESHKOV FLOWS

Abarzhi S.I.

CMU, Pittsburgh, United States

snezhana.abarzhi@gmail.com

We systematically study the Richtmyer-Meshkov instability (RMI) induced by strong shocks for fluids with contrasting densities and with small and large amplitude initial perturbations imposed at the fluid interface. The Smoothed particle hydrodynamics code (SPHC) is employed to ensure accurate shock capturing, interface tracking, and accounting for the dissipation processes. Simulations results achieve good agreement with existing experiments and with the theoretical analyses including zero-order theory describing the post-shock background motion of the fluids, linear theory providing RMI growth-rate in a broad range of the Mach and Atwood numbers, weakly nonlinear theory accounting for the effect of the initial perturbation amplitude on RMI growth-rate, and highly nonlinear theory describing evolution of RM bubble front. We find that for strong-shock-driven RMI the background motion is supersonic, and the interfacial mixing can be sub-sonic or supersonic. Significant part of the shock energy goes into compression and background motion of the fluids, and only a small portion remains for interfacial mixing. The initial perturbation amplitude appears a key factor of RMI evolution. It strongly influences the dynamics of the interface, in the fluid bulk, and the transmitted shock. In case of large amplitudes, the vector and scalar fields in the fluid bulk are non-uniform. The flow heterogeneities include cumulative reverse jets, checkerboards velocity pattern, shock-focusing effects, and local hot spots with temperature substantially higher than that in the ambient. The dynamics of the nonlinear flow is shown to have a multi-scale character.

---

1. Phys. Plasmas 19, 082706 (2012).
2. Physics of Fluids 25, 106107 (2013).

NON-CLASSICAL BEHAVIOR OF SHOCK AND RAREFACTION WAVES IN QUARK-HADRONIC PHASE TRANSITION REGION

Konyukhov A.V.,* Likhachev A.P.

JIHT RAS, Moscow, Russia

**konyukhov_av@mail.ru*

The equation of state of subhadronic matter describing the quark-hadronic phase transition has been built using the MIT-bag model variant [1]. The theoretical analysis of the EOS constructed has been carried out to check the fulfillment of the criteria of the instability and neutral stability of relativistic plane shock waves [2, 3]. It has been shown that the Taub adiabats passing through mixed phase have segments with an ambiguous representation of the shock wave discontinuity. The ambiguity is due to the implementation of the shock instability condition $j^2(\partial\tau/\partial p)_H < -1$. The thermodynamic abnormality condition $(\partial^2 p/\partial\tau^2)_s < 0$ can be satisfied in the transition region and the appearance of rarefaction shocks or composite rarefaction waves is expected. Such the behavior of shock and rarefaction waves is typical for the media with the phase transition of the first order. This issue for the subhadronic matter has been discussed before in a number of works (see, for instance, [4]). The hadronic matter EOS constructed was embedded in the previously elaborated relativistic hydrodynamic code based on the third order essentially non-oscillatory scheme. The results of calculations have completely confirmed the predictions of the theoretical analysis. Besides, it has been found that for the EOS used the velocities of the precursor shock in hadronic phase and the shock wave of phase transition differ very slightly. Taking into account extremely short time of the interaction, the shock wave splitting may be masked by viscid and nonequilibrium effects. It makes very difficult to identify this phenomenon in collision events. It has been else found that for the MIT-bag equation of state the neutral stability condition is fulfilled only for shocks with the final state in the mixed phase. However, these shocks are unstable with respect to splitting and are not realized as unique wave. Thus, only the shocks of phase transition being a part of the composite compression wave may be neutrally stable.

1. Cleymans J., et al. // Phys. Rep. 1986. V. 130. N. 4. P. 217.
2. Kontorovich V. M. // Sov. Phys. JETP. 1960. V. 34. N. 7. P. 127.
3. Russo G., Anile A. M. // Phys. Fluids. 1987. V. 30. P. 2406.
4. Bugaev K. A., et al. // Phys. Rev. D. 1989. V. 40. N. 9. P. 2903.

ON SHOCK-VORTEX INTERACTION IN HIGH ENERGY RELATIVISTIC JETS

Konyukhov A.V.

JIHT RAS, Moscow, Russia

konyukhov_av@mail.ru

Results of numerical investigation of relativistic shock wave interaction with jet induced relativistic vortex are presented. The plane nonstationary ultrarelativistic jet is injected into the half-space, which contains a matter being at rest in the coordinate system attached to the boundary. Unlike the calculations of the relativistic jets relevant to astrophysical applications [1], the problem formulation is characterized by high density of the surrounding matter (0.05 in units of the rest mass density of the jet) and high internal energy of both jet and surrounding gas (up to value 10^3 in the units of c^2, where c is the speed of light). The first condition leads to formation of developed relativistic vortex, being the result of the interaction between the jet and the medium. The second one provides the characteristic features of high energy relativistic jet [3]; particularly, very high values of Lorentz factor can be reached in the expanding supersonic part of such jet. The boundary conditions ensure that the injection velocity exceeds the ultrarelativistic limit of speed of sound for the adopted equation of state. Therefore, the flow field includes supersonic regions and a system of shock waves which interact with the jet-induced vortex. The flow field pattern of the interaction is presented and analized.The calculations have been performed on the basis of relativistic hydrodynamics equations [2] in two-dimensional formulation with the equation of state $p = (\gamma - 1)(e - \rho c^2)$, where p and e are the pressure and the energy density in the rest coordinate system, ρ is the rest mass density. High resolution numerical method [3] based on the local characteristic approach and non-oscillatory third order scheme has been used in the calculations.

---

1. Marti J.-.M., Muller E. Numerical hydrodynamics in special relativity// Living Rev. Rel. 2003. 6: 7.
2. Landau L.D., Lifshits E.M. Theoretical physics. VI.Hydrodynamics. M.: Nauka, 1988 [in Russian].
3. Konyukhov A. On shocks in high energy relativistic jets: numerical simulation, In: Physics of Extreme States of Matter-2013, Moscow 2013, 126–129.

PILOT PLANT FOR EXTRACTING HELIUM FROM NATURAL GAS WITH MICROSPHERES

Vereshchagin A.S.,* Fomin V.M.

ITAM SB RAS, Novosibirsk, Russia

**vereshchag@itam.nsc.ru*

Microspheres are small hollow particles which mostly consist of glass with some adds. The material of microsphere walls is selectivly permeable for hellium with huge selectivity coefficient (for example, for gas pairs like He/CH_4, He/Ar, He/N_2), so it can be used to obtain helium concentrate. Up to it using hollow glass microspheres as membranes makes it possible to significantly increase surface area, through which the gas components differentiation process takes place. Microsphere sizes vary from 10 to 300 μm, wall thickness is from 1 to 30 μm.

The scheme of a pilot plant for extracting helium from gas mixture with microspheres has been designed. The plant is considered to work on a natural gas deposit. A four step process of helium extracting from helium containing gas mixture is developed. Specifying pilot plant parameters the simulation of helium extracting from gas mixture is made. Time and helium extraction degree is calculated. At the starting time the gas mixture initial concentration distribution corresponds to Kovykta gas condensate field: He—0.276 %, CH_4—92.3 %, the rest gas—7.424 %. Initial gas pressure is 10 MPa. It is shown that after 4 cycles of the process described above (overall time 4 hours 17 min 7 s) the final concentration in poor mixture (pressure), %: He—0.049, CH_4—92.510, the rest gas—7.441; final concentration of helium concentrate mixture in ballon 5 (pressure), %: He—92.438, CH_4—6.999, the rest gas—0.563. Also it is shown, that increasing the coefficient of helium permeability and the compressor flow on the order of 1 does not change the final gas component distribution but decreases the time of the process significantly.

STUDIES ON THE SYNTHESIS OF ELEMENTS USING THE PHYSICS OF EXPLOSION. HISTORICAL REVIEW

Sevalnikov A.Yu.

IPhRAS, Moscow, Russia

sevalnicov@rambler.ru

That work is devoted to works performed in Germany in 30–40 years of the twentieth century. Usually the beginning of work in the area of initiation of thermonuclear reactions using converging shock waves associated

with the names and Adolf Gottfried Guderley Busemann (1942). However, this work has a rich history. More December 21, 1931 members of the German firm AEG was registered patent application "Verfahren zur Anregung und Durchführung von Kernprozessen" (AEG Patent Nr. 622.036). The proposal dealt with the possibility of using the ultra-high temperatures, more than 10 million degrees using the Ramsauer effect and initiate nuclear reactions in heavy water, lithium and boron. Authors were physics Fritz Lange Brush and Arnaud. In 1935 both emigrated from Germany. Brash moved to America, and Fritz Lange in the Soviet Union. Since 1935 he worked at the Kharkov Physico-Technical Institute, where they, together with Vl. Maslov and Viktor Spinel in 1940 and was filed two patents. The first of these describes the possible construction of nuclear uranium bomb, and the second method was proposed for separation of uranium isotopes using multi-chamber centrifuge.

Important work in the mid 30-ies were performed at the Kiel University Heinrich von Traubenberg and Alfred Ekkardt. They studied nuclear reactions in lithium and magnesium. Breakthrough began work in 1942 by Adolf Busemann and Gottfried Guderley focus on the possibility of converging shock waves and getting into this process m extremely high temperatures and pressures [1]. At the initiative of Carl Ramsauer, head of the research department of AEG, on polygons of the Heereswaffenamt (Kurt Diebner and Walter Trinks) and the Marinewaffenhauptamt (Bureau of Naval Weapons) (Otto Haksel) have conducted experiments with hollow balls filled with deuterium. Officially reported failure of such experiments. However, there is direct evidence of Walter Gerlach and Erich Schumann on further experiments in this area [2].

In March 1945, under the Ohrdruf were tested two nuclear devices. Explosive power of the device is about one kiloton, and damage radius of about 600 m. Two weeks after the Soviet GRU test report received from its agents about this test [3]. Currently the details became known. Device tested under Ohrdruf, bore hybrid nature. Exploded enriched ^{235}U, used in the circuit of ^{6}Li. Device was an implosion type. As the explosive used porous trinitrotoluene, treated first with liquid oxygen. Trinitrotoluene composed of 32 bar, specially selected form. Explosion is initiated by electric detonators.

Calculations by focusing convergent shock waves were performed at Goettingen University [4]. The team was led by Richard Becker, a prominent German physicist. In this same group worked Werner Dörring, one of the authors known model detonation Zel'dovich–Neumann–Dörring.

1. Gottfried Guderley. Starke kugelige und zylindrische Verdichtungsstöße in der Nähe des Kugelmittelpunktes bzw. der Zylinderachse. In: Zeitschrift für Luftfahrtforschung, 1942, Bd. 19, Lfg. 9, S. 302–312; Adolf Busemann: Die achsensymmetrische kugelige Überschallströmung. In: ebd., Bd. 19, Lfg. 4, S. 137–145.
2. Erich Schumann. Die Wahrheit über die deutschen Arbeiten und Vorschläge zum Atomkernenergie-Problem (1939–45). Das Manuskript enthält im Kapitel II Hinweise und Konstruktionsvorschläge zur Zündung von Fusionsreaktionen. Bundesarchiv-Militärarchiv.
3. Archive President RF. Fund 93, Dep. 81 (45), Page 37; Reiner Karlsch. Hitlers Bombe. 2005. S. 338–343.
4. Gerhard Rammer. Die Nazifiezierung und Entnazifiezierung der Physik an der Universität Göttingen. Göttingen, 2004.

EXPERIMENTAL STUDY OF POLY- AND MONOCRYSTALLINE SYNTETIC DIAMOND AT NEGATIVE PRESSURES USING PICOSECOND LASER PULSES

Krasyuk I.K.,[*1] ***Abrosimov S.A.,***[1] ***Bazhulin A.P.,***[1]
Fortov V.E.,[2] ***Khishchenko K.V.,***[2] ***Khomich A.A.,***[1]
Konov V.I.,[1] ***Pashinin P.P.,***[1] ***Ralchenko V.G.,***[1]
Semenov A.Yu.,[1] ***Sovyk D.N.,***[1] ***Stuchebryukhov I.A.***[1]

[1]*GPI RAS,* [2]*JIHT RAS, Moscow, Russia*

[*]*krasyuk99@rambler.ru*

The experimental studies of spallation phenomena and dynamic mechanical strength of poly- and monocrystalline synthetic diamond at the influence on them of laser pulse with duration 70 ps are presented. It was realized the strain rate up to 10^8 1/s. In these experiments, we used the neodymium glass laser Kamerton-T facility. The basic radiation was transformed to the second harmonic with the wavelength of 0.527 μm and the laser pulse energy of 2.5 J. Irradiated spot on a target surface was of 0.3 to 0.8 mm in diameter. Then the maximum energy density of the laser radiation flux in the focal area was 10^{13} W/cm^2; the ablation pressure was about 0.66 TPa. Targets had the form of plates with 140 to 400 mkm thickness. The spall phenomenon was used to estimate the dynamic mechanical strength of the materials under study. This phenomenon arises on the rear (free) side of a target as a result of the reflection of a compression wave caused by laser radiation, which is generated on the front surface of the target. As a result, in some plane of the target the tensile strain can exceed materials strength. This leads to the formation of the spallation layer that leaves the sample. In our experiments, it was reached the spall strength of 20 GPa, that equivalent to 30% of the theoretical maximum dynamic strength of diamond. In some cases spallation was observed not only on the back side of the target, but also on its front surface. Morphology of the spall planes was studied using scanning electron microscope and showed decrease of the size of crystallites in comparison with the original polycrystall graines. The Raman spectroscopy revealed that, in the area of spallation on the back side of the target, some amount of the crystalline diamond goes to the graphite phase.

The work is supported by the Russian Foundation for Basic Research (projects No. 12-02-00625, 12-02-00746, 14-08-00967), the Presidium of the Russian Academy of Sciences (programs No. 13P "Extreme light fields and their applications" and 2P "Matter at high energy densities"), and the President of the Russian Federation for Support of Leading Scientific Schools (grants No. NSh-451.2014.2 and NSh-6614.2014.2).

CONDENSED CARBON PHASE TRANSITIONS ON THE LIQUID CARBON–DIAMOND CONTACT BORDER

Basharin A. Yu,* Lysenko I. Yu, Dozhdikov V.S.

JIHT RAS, Moscow, Russia

**abasharin@bk.ru*

Soon or later practical use of the liquid carbon (LC) will be initiate. Here we investigated a diamond ability to hold LC within the short time. For this purpose solid carbon structure obtained by laser pulse (ca. 1 ms duration) melting of dispersed graphite flakes on a diamond substrate in a helium atmosphere at 25 MPa pressure (slightly above the pressure at the carbon graphite-liquid-vapor triple point) was explored. HOPG was treated with a vibratory mill until flakes, 1–20 mkm in size, were produced. The flakes were located on the (111) surface of a natural diamond substrate in the form of islets. A typical sample consisted of a diamond prism (1 mm thick x 3 mm) with graphite islets (5–100 mkm x 3 mkm thick) dispersed on its surface. After laser treatment the cross sectional samples were prepared by focus ion beam (FIB) milling in the Helios SEM/FIB dual beam electron microscope. A high resolution transmission electron microscope TITAN 80–300 were used to study the section with atomic resolution.

Thus some phenomena within diamond and on the contact border between melt and diamond was established: (1) spherulitic growth of the graphite with a diameter ca. 1 mkm take place on the top of the remelting zone; (2) both the ordinary onions formation and dagger-like graphitization occur in the diamond. Dagger-like graphitization begin with an onions formation and terminate in a graphite-carbine phase transition; (3) as a result of the LC amorphization mixture including sp^3 amorphous carbon are obtained; (4) features of the pre-melting phenomena in not fully melted flakes indicated that graphite-liquid phase transition has diffuse character. First of all interlayer translational disorder arises but graphene layers preserve there shape. It is in disagreement with a current molecular dynamics concepts.

The obtained results show that contact of the diamond with LC is accompanied with a phase transition not only in liquid carbon but in a diamond too. Nevertheless diamond is not destroyed but only graphitized. The obvious role of the diamond substrate in the mechanism of sp^3 amorphous carbon formation is in allowing an extremely high cooling rate for LC; this occurs because of the record high thermal conductivity of natural diamond (usually around 2000 W/mK, five times greater than that of copper). For this reason pre-melting phenomena has been observed too.

This work was supported by the Russian Foundation for Basic Research (Grant 13–08–01–098a).

FROZEN NANOSTRUCTURES PRODUCED BY ULTRASHORT LASER PULSE

Khokhlov V.A.,[*1] ***Inogamov N.A.,***[1] ***Anisimov S.I.,***[1] ***Zhakhovsky V.V.,***[2] ***Emirov Yu.N.,***[3] ***Ashitkov S.I.,***[2] ***Komarov P.S.,***[2] ***Agranat M.B.***[2]

[1]*ITP RAS, Chernogolovka, Russia,* [2]*JIHT RAS, Moscow, Russia,* [3]*AMERI FIU, Miami, United States*

**V_A_Kh@mail.ru*

A thin surface layer with high temperature and pressure can be produced by almost isochoric heating with a short enough laser pulse. The stretched molten material is formed during melting and hydrodynamical expansion of this layer. Bubble nucleation and cavitation are initiated if a sufficiently high tensile stress is generated in the melt. Expansion of the bubble ensemble leads to formation of low-dense foam-like material at later times. However, remarkable elasticity of the foam is retained during long time, leading to slow down of expansion. Meanwhile, very high temperature gradient results in ultrafast cooling of the melt. For the laser intensity below the ablation threshold the foam expansion stops, then starts to shrink and finally freezes into complex solid nanostructures, which are observed experimentally. [1]

A comparison of experimental results and molecular dynamics simulation [1, 2] is presented.

This work was supported by the RAS program “Substance with high energy density” and RFBR grant 13–08–01095-a.

---

1. Ashitkov S. I., Inogamov N. A., Zhakhovsky V. V., Emirov Y. N., Agranat M. B., Oleinik I. I., Anisimov S. I. & Fortov V. E. Formation of

Nanocavities in Surface Layer of Aluminum Target irradiated by Femtosecond Laser Pulse // JETP Lett., 2012 V. 95 P. 176–181
[Pis'ma i ZhETF. 2012. V. 95 P. 192–197]
2. Inogamov N. A., Zhakhovsky V. V., Petrov Y. V., Khokhlov V. A., Ashitkov S. I., Migdal K. P., Ilnitsky D. K., Emirov Y. N., Khishchenko K. V. Komarov P. S., Shepelev V. V., Agranat M. B. Anisimov S. I., Oleynik I. I. & Fortov V. E. Ultrashort laser–matter interaction at moderate intensities: two-temperature relaxation, foaming of stretched melt, and freezing of evolving nanostructures // SPIE Proceedings. 2013. V. 9065. P. 906502,1–14.

ATOMISTIC SIMULATION OF LASER PULSE NANOSTRUCTURING OF METALS: STUDY OF SURFACE MODIFICATION PROFILE

Starikov S. V.

JIHT RAS, Moscow, Russia

starikov@ihed.ras.ru

In this work the laser pulse modification of surface is investigated for aluminum and gold by atomistic simulation. The surface modification after laser irradiation can be caused by ablation and melting. At low energy of laser pulse, the nanoscale ripples on surface may be induced by the melting without laser ablation. The nanoscale changes of the surface are due to the splash of molten metal under fluence gradient of the laser beam. The ablation process occurs at a higher pulse energy when a crater is formed on the surface. It is interesting that the melting is responsible for the size of the modification spot for all range of the energies. The two-temperature atomistic model with explicit account of electron pressure and electron thermal conductivity is used. This two-temperature model describes ionic subsystem by means of molecular dynamics while the electron subsystem is considered in the continuum approach. The simulation is performed for the quasi one-dimensional approach as well as for the full-scale approach. The comparison to the available experimental data is performed.

CONTINUAL-ATOMISTIC MODELLING OF FEMTOSECOND LASER ABLATION OF METALS

Fokin V.B.,* Levashov P.R., Povarnitsyn M.E., Khishchenko K.V.

JIHT RAS, Moscow, Russia

**vladimir.fokin@phystech.edu*

Ultrashort laser ablation of metals is used in many applications such as drilling, nanostructuring, nanoparticle production. To accurately describe effects of laser-matter interaction we use a modification of approach [1]. Our model more precisely takes into account the laser energy absorption, electron-phonon/ion scattering and electron thermal conductivity [2]. Thus, combination of molecular dynamics and model of electron subsystem is a power tool for investigation of a material response on laser irradiation. As a result, we can simulate dynamics of laser ablation, melting, evaporation, nucleation, propagation of shock and rarefaction waves as well as nanoparticle formation. In this work we perform simulation of laser ablation of aluminium by 100 fs pulses with fluence from 0.1 to 20 J/cm^2 and find out the ablation crater depth as a function of laser fluence. Besides, we investigate regimes of nanoparticle formation and their size distribution. Results of modelling are in good agreement with experimental findings.

---

1. Ivanov D. S., Zhigilei L. V. // Phys. Rev. B. 2003. V. 68. P. 064114.
2. Povarnitsyn M. E., [et al] // Appl. Surf. Sci. 2012. V. 258. P. 9480.

LASER FORMING OF COLLOIDAL SYSTEMS AND DEPOSITION OF NANOPARTICLES OF NOBLE METALS

Kucherik A.O.,*[1] Antipov A.A.,[1] Arakelian S.M.,[1] Kutrovskaya S.V.,[1] Khorkov K.S.,[1] Itina T.E.,[2] Povarnitsyn M.E.,[3] Levashov P.R.,[3] Khishchenko K.V.[3]

[1] *VlaSU, Vladimir, Russia,* [2] *LHC, Saint-Etienne, France,* [3] *JIHT RAS, Moscow, Russia*

**kucherik@vlsu.ru*

In this work, an experimental technique for the formation of metallic clusters on the surface of optically transparent materials is proposed. Nanoparticles of gold and silver with the size of 10–100 nm have been obtained thanks to laser ablation in a liquid. For laser ablation we use a Ti:sapphire laser setup with 50 fs pulse duration and 1 J/cm^2 fluence. Sim-

ulation of laser ablation of metals in liquid is performed using a numerical model based on two-temperature hydrodynamics. Results of simulation describe early stages of nanoparticle formation.

HOT-SPOT DEVELOPMENT IN A SHORT LASER PULSE PROPAGATING IN TENUOUS PLASMAS

Andreev N.E.,[*1] ***Gorbunov L.M.,***[2] ***Mora P.,***[3] ***Ramazashvili R.R.***[2]

[1]*JIHT RAS, Moscow, Russia,* [2]*LPI RAS, Moscow, Russia,*
[3]*CPHT EP, Palaiseau, France*

[*]*andreev@ras.ru*

Development of a hot-spot in a quite short laser pulse with duration exceeding plasma oscillation period, propagating in plasmas, is examined analytically and numerically. At initial stage of pulse propagation, a hot-spot generates a few growing filaments with transverse scales in excess of the plasma skin depth. However, after some propagation distance, process of filamentation is overtaken by rapidly growing perturbations with larger transverse wave numbers which form plasma waves propagating out of initial hot-spot position and spreading essentially the domain involved in instability. The analytical theory reveals a good agreement with numerical results.

ELECTRON BUNCHES ACCELERATION IN GUIDING STRUCTURES UNDER NON-SYMMETRICAL COUPLING CONDITIONS

Veysman M.E.,* ***Andreev N.E., Kuznetsov S.V.***

JIHT RAS, Moscow, Russia

[*]*bme@ihed.ras.ru*

Guiding structures like capillary waveguides and plasma channels can be used for effective acceleration of electron bunches in wakefileds generated by laser pulses propagated by means of those structures over many Releigh lengths.

In practice the perfect enough focusing of laser pulses into capillary waveguides appeared to be very important for production of high-quality accelerated electron bunches (with minimum energy and spatial spreads), as long as even small displacements of focusing point and laser axis relatively to capillary axis can lead to non-regular wakefields and strong de-

focusing forces acting on accelerated electrons [1–3]. Therefore focusing conditions should be controlled carefully.

Presented work gives analyses of influence of different factors of asymmetry of laser pulses focusing into guiding structures on the quality of accelerated electron bunches: on the energy and spatial spreads, number of trapped and accelerated particles and also on the rate of acceleration. The influence of non-symmetry of laser pulse shape, the displacements of laser pulse focusing point relatively to capillary axis and the non-zero angle of incidence of laser axis relatively to capillary axis on the above mentioned parameters of accelerated electron bunches is studded and discussed.

The conditions on the maximum adoptable assymetry are formulated. The possible influence of initial energy of electrons, injected in the guiding structure, on the requirements on the accuracy of laser pulse focusing into capillary waveguide or plasma channel is also discussed.

---

1. M. Veysman, N. E. Andreev, K. Cassou, Y. Ayoul, G. Maynard, and B. Cros, "Theoretical and experimental study of laser beam propagation in capillary tubes for non-symmetrical coupling conditions", J. Opt. Soc. Am. B, **27**, 1400 (2010).
2. M. Veysman, N. E. Andreev, G. Maynard, and B. Cros, " Nonsymmetric laser-pulse propagation in capillary tubes with variable radius", Phys. Rev. E, **86**, 066411 (2012).
3. Andreev N.E., Kuznetsov S.V., Veysman M.E., "Laser wakefield electron acceleration in capillary waveguides under non-symmetric coupling conditions", NIMA, in print (2013).

3D PIC MODELING OF ION ACCELERATION FROM THIN FOILS UNDER THE ACTION OF FEMTOSECOND LASER PULSES: CONVERGENCE OF RESULTS AND COMPARISON WITH EXPERIMENT

Pugachev L.P.,* Levashov P.R., Andreev N.E.

JIHT RAS, Moscow, Russia

**pugachev@ihed.ras.ru*

The possibility of describing the process of ion acceleration from thin foils under the action of femtosecond laser pulses using 3D PIC-simulation was investigated. For this, calculations with parameters of the experiments [1–4] for pulses with an intensity in the range $5 \cdot 10^{19}$–$2 \cdot 10^{21}$ W/cm^2, 30–900 fs duration and foils with a thickness of 0.005–0.5 microns were carried out. Within computing capabilities of 4000 processor cores convergence of

the results for the characteristic energy of the accelerated ions depending on spatial cell size and number of particles in the cell was verified. The simulation was performed using the PIC-code VLPL [5].

This work was supported by RFBR (project #12-02-31688).

1. Mackinnon A. et al. // Phys. Rev. Lett. 2002. V. 88. P. 215006.
2. Brantov A. et al. // Contrib. to Plasma Phys. 2013. V. 53. P. 161.
3. Henig A. et al. // Phys. Rev. Lett. 2009. V. 103. P. 245003.
4. Kar S. et al. // Phys. Rev. Lett. 2012. V. 109. P. 185006.
5. Pukhov A. // J. Plasma Phys. 1999. V. 61. P. 425.

THE STRUCTURE OF THE ACCELERATING WAKEFIELD GENERATED BY ION BUNCHES

Koshelev A.A.,* Andreev N.E.

JIHT RAS, Moscow, Russia

**antonak92@mail.ru*

The structure of plasma wave excited by an ion bunch is investigated on the base of cold hydrodynamic model. It is shown that this structure changes with the distance from the trailing edge of the bunch. As a result, at a certain distance behind the bunch, trapping of external injected electrons become possible. The condition of trapping external injected electrons for different energy and angle of injection is investigated by numerical modelling [1] [2]. It is shown that electrons trapping is possible only after a few plasma wave periods.

1. Andreev N. E. , Kuznetsov S. V. , Cros B. , Fortov V. E , Maynard G., Mora P., Plasma Phys. Control. Fusion 53 (2011) 014001
2. Andreev N. E. , Kuznetsov S. V. IEEE Transactions on plasma science, V. 36, No. 4, 2008

GENERATION OF LOW FREQUENCY RADIATION IN THE CONDUCTOR ILLUMINATED BY ULTRA-SHORT LASER PULSE

Frolov A.A.,[*1] ***Uryupin S.A.***[2]

[1] *JIHT RAS,* [2] *LPI RAS, Moscow, Russia*

[*] *frolov@ihed.ras.ru*

Interest in the generation of low-frequency radiation pulses in laser radiation interaction with matter arose relatively long time ago. In particular, the generation of terahertz radiation was observed in the interaction of femtosecond pulses with targets of gold, silver and copper. For an explanation of the generation of low-frequency radiation different physical mechanisms are involved. One of the most natural and easy implemented mechanisms is related to the excitation of low-frequency vortex currents in the material under the ponderomotive action of laser radiation on the free electrons. Inherent to this mechanism patterns of low-frequency radiation generation have been studied by us in the case when conductor illuminated by laser pulse focused by a spherical lens. The spectral, angular and energy characteristics of low-frequency radiation are studied. It is shown that emission spectrum has a broad maximum at frequency close to the inverse duration of the laser pulse. The diagram of low-frequency radiation is found and it is shown that it essentially depends on the degree of the laser pulse focusing. For tightly focused laser pulse the generated low-frequency radiation propagates at a small angle to the surface of the conductor. If the focal spot size significantly exceeds the pulse length, the radiation of low frequency waves occurs along directions close to the direction normal to the surface of the conductor. The total energy of low-frequency radiation is found and its dependencies on the degree of the laser pulse focusing and on the collision frequency of the conduction electrons are established. It is shown that at fixed energy and duration of the pulse the energy of low-frequency radiation has maximum when the laser pulse is sharply focused and the electron collision frequency is low. The space-time structure of the electromagnetic field in the pulse of low-frequency radiation is investigated. It was established that low-frequency pulse has duration comparable with the duration of laser pulse.

RAYLEIGH–TAYLOR AND RICHTMAYER–MESHKOV INSTABILITY OF NON-NEWTONIAN FLUIDS IN THE INTERACTIONS OF HIGH ENERGY PARTICLES AND LASER BEAMS WITH THE CONDENSED MATTER

Doludenko A.N.,*[*1] ***Meshkov E.E.,***[2] ***Son E.E.***[1]

[1] *JIHT RAS, Moscow,* [2] *SSPTI MEPhI, Sarov, Russia*

**son.eduard@gmail.com*

In the present paper the experimental part consist of studies of a shock wave at the free surface of a condensed medium, at which an on-lacquer flying microparticles due to manifestations of complex phenomena such as CHIP-ing destruction, surface instability, media development and cavitation. Despite the long history of the study of this process, many questions remain open. Of particular interest is the formation and distribution of fines size and velocity, which depends on the flow parameters and rheological properties of the medium. Phenomenon releases microparticles from the surface of condensed media when leaving the SW has practical value, and this research is currently carried out in the laboratories of leading nuclear countries. Experiments of this kind tend to existing dangerous explosives and are quite expensive.

Theoretical part consists of a numerical study of the turbulent stage of development of Rayleigh–Taylor instability (RTI) and Richtmayer–Meshkov instability (RMI) for viscous, and viscoelastic media with different material rheology for high density, they exhibit the rheological properties of the medium, investigated in-regularities of the development of RTI and RMI in inertial fusion. The theoretical study is given for mass transport, energy and momentum in the non-equilibrium turbulent processes with regard to their anisotropic statistically unsteady, inhomogeneous and multiscale nature to find patterns in the spectra of turbulent motions generated by RTI and RMI, a quantitative description of large-scale invariance. We performed Direct Numerical Simulation (DNS) of turbulent flows arising from the development of RTI and RMI. DNS of instabilities and turbulent stage are considered for viscoplastic, viscoelastic and media with different rheology. A semiempirical theory of turbulence in the nonlinear stage of instability development of the RTI and RMI is developed based on the results of DNS for classical media and media with different rheology. We explore the development of the Rayleigh-Taylor instability studied patterns of formation and viscous Kolmogorov spectra in thermoviscous liquid and explore patterns of development of RTI and RMI in ICF experiments OMEGA at Rochester University and National

Ignition Facility at the National Center for fusion research in the United States.

MATHEMATICAL MODELING OF RADIATIVE AND GAS-DYNAMIC PROCESSES IN PLASMA FOR EXPERIMENTS, WHERE BOTH INTENSE LASER AND HEAVY ION BEAMS ARE USED

Orlov N.Yu.,[*1] ***Denisov O.B.,***[1] ***Vergunova G.A.,***[2] ***Rosmej O.N.***[3]

[1]*JIHT RAS, Moscow, Russia,* [2]*LPI RAS, Moscow, Russia,*
[3]*GSI, Darmstadt, Germany*

[*]*nyuorlov@mail.ru*

Mathematical modeling of radiative and gas-dynamic processes in plasma is carried out for experiments, where both intense laser and heavy ion beams are used. Brief comparative analysis of theoretical models that are used for the radiative opacity calculations is given. Most important features of the ion model (IM) of plasma, which is used for mathematical modeling at present work, are discussed, and reliability of (IM) results is tested with different experiments. The theoretical approach is used for temperature diagnostics of CHO plasma in combined laser and heavy ion beam experiments, where the plasma targets is created for further interaction with heavy ion beam. Then, joint radiative and gas dynamic calculations are performed for comparison with experiment, where hohlraum radiation transmits through the CHO plasma target, and the theoretical spectrum of transmitted radiation is compared with experimental data. Two different CHO substances are considered, namely, triacetate cellulose (TAC, C12H16O8), and (TAC) with a little admixture of gold, and the Rosseland mean free path is calculated for both substances at different temperatures. Influence of little admixture of gold on the radiative opacity characteristics and gas dynamic processes in plasma is discussed as well.
Keywords: The radiative opacity; Rosseland and Planck mean free paths.

TARGET STRUCTURE INFLUENCE ON HEAVY ION STOPPING IN X-RAY PRODUCED PLASMA

Borisenko L.A.,* Sklizkov G.V.

LPI RAS, Moscow, Russia

**borisenko.lidiya@physics.msu.ru*

In early high-power irradiation experiments on low-density targets the structure was reported to have slight or no influence on the major results. Further the distinct unpredicted effects appeared to be connected with initial solid structure, especially when the diagnostic means achieved high resolution and accuracy.

Polymer aerogels, unlike many other low-density materials (foam, dust, nano-snow) have a net-like structure, consisting of macromolecular fibers and globules. That means they are highly regular as regards their spatial structure, so high repeatability was demonstrated in interaction experiments with polymer aerogel targets. However we yet have definite molecular structure in the polymer before irradiation.

Which structural or non-structural effects should we take into account in plasma and which can be neglected? We consider the initial phase of soft x-rays irradiation of extra low-density aerogel and the structure influence on heavy ion stopping.

The classical way to describe energy losses of heavy ions in matter is single-track interaction with almost free electrons of the outer orbitals. The typical approximation is the Bethe-Bloch formulae for ionization losses:

$$-dE/dx = 4\pi Z^2 e^4 n_e/(v^2 m_e) * (ln(2v^2 m_e/I(1-\beta^2)) - \beta^2),$$

with linear growth of the concentration in the beginning of x-ray irradiation and exponential "decay" of the whole system due to Coulomb explosion later. However this Coulomb scattering on electrons can not explain stopping power behaviour on the early times of low-density aerogel plasma formation.

The indirect irradiation of polymer aerogels by laser beam converted into soft x-rays provides milder conditions for target polymer transition into plasma. Primary atomic physics estimations show that times and energies for such transition are capable to produce the bunch shift. Continuous probing of the target by high-energy bunch-structured ion beam is considered, so on the early times of interaction the complex transient disintegration process is not over.

SPALLS FORMATION IN THE THIN POLYCRYSTALLINE TARGETS UNDER THE ACTION OF THE HIGH-POWER LASER PULSE

Timofeev I.S,* Burdonsky I.N, Goltsov A.Yu, Makarov K.N, Leonov A.G, Yufa V.N

MIPT, Dolgoprudny, Russia

**i.s.timofeev@gmail.com*

Shock waves generation in interaction of laser radiation with targets allows to obtain new data on the dynamic strength of different materials (see e.g. [1]). However, almost all of such experiments were conducted using metal samples. This paper presents the research results of the spalls formation in the thin targets made of polycrystalline rock (andesite), the properties of which are cardinally different from the properties of metals. It is of considerable interest from the point of view of possible technological applications and, in particular, laser modeling of micrometeorite impact.

The series of experiments to study craters, formed by laser radiation with intensity 10^{11}–10^{13} W/cm^2 and pulse duration 30 ns in andesite plates with thickness from 250 to 600 microns, was carried out at the facility "Saturn" [2]. Resulting it was discovered, that the spall crater was formed on the target rear surface. Its dimensions differ significantly from the size of the crater on the front surface. There are two specific types of spall depending on the laser pulse energy and a target thickness: with through bore and without it. Analysis of the materials from the spall crater and from the plasma flame, which were sprayed onto the chemically purified silicon substrates, showed significant differences: from separate drops at front surface to solid fragments at rear surface of the target.

Diagnostics of the glow of the target rear surface allowed to estimate the minimum speed of the shock wave in andesite targets: 10–20km/s. These results are in a good agreement with a simplified model of the shock wave generation by laser pulse, developed in [2]. Note, that in these X-ray experiments time-averaged temperature of the formed plasma was measured with thermocouple calorimeters and the results are also in agreement with the model [2](T∼200 eV with intensity $4 \cdot 10^{11}$ W/cm^2).

1. Vovchenko V. I., Krasyuk I. K., Pashinin P. P., Semenov A. Yu. // Quantum Electron. 2007. V. 37. No. 10. P. 897.
2. Burdonsky I. N., Goltsov A. Yu., Leonov A. G., Makarov K. N., Timofeev I. S., Yufa V. N., // Problems of Atomic Science and Technology. 2013. V. 36. No. 2. P. 8.

ELECTRON-PHONON SCATTERING AND RELATED ELECTRICAL CONDUCTIVITY IN NOBLE AND TRANSITION METALS AT HIGH ELECTRON TEMPERATURE

Petrov Yu.V.,* Inogamov N.A.

ITP RAS, Chernogolovka, Russia

**uvp49@mail.ru*

We have calculated electrical resistivity of noble and transition metals in the situation which is specific for the initial stage of the interaction of femtosecond laser pulses with metals. This situation is characterized by the large difference between the electron and ion temperatures (two-temperature pattern). In noble (copper) and transition (iron) metals under consideration laser irradiation leads to the thermal excitation of s- and d-electrons. In the framework of kinetic equations for s- and d-electrons when they undergo collisions with phonons we have found relaxation times of s- and d-electrons as functions of the electron momentum. When calculating the electrical resistivity within the relaxation time approach we have obtained the resistivity decrease at increasing electron temperature. This resistivity diminishing with the electron temperature growth is especially significant for the transition metals and is opposite to the more usual single temperature situation when resistivity increases with the temperature increase.

This work is supported by the RFBR grant No. 13–02–01078.

TWO-TEMPERATURE EQUATIONS OF STATE FOR D-BAND METALS IRRADIATED BY FEMTOSECOND LASER PULSES

Inogamov N.A.,[1] ***Petrov Yu.V.,***[1] ***Zhakhovsky V.V.,***[2] ***Migdal K.P.****[3]

[1]*ITP RAS, Chernogolovka,* [2]*JIHT RAS, Moscow,*
[3]*VNIIA, Moscow, Russia*

**migdal@vniia.ru*

The cold curves for energy and pressure of Copper, Iron, and Tantalum were obtained using methods of the density functional theory [2] [1]. We consider hydrostatic and uniaxial deformations in the range from double compression of the initial volume per atom to double stretching. The presence of allotropic transformation from α-phase of Iron to the hexaferrum with the growth of pressure is observed. In the case of hydrostatic defor-

mations we also have obtained analogous cold curves, but with non-zero electronic temperatures in the range up to 5 eV. The similar volume and electronic temperature ranges have been considered in recent works [3] [4]. The behaviour of electronic internal energy, pressure, and density of states was investigated in the volume and temperature ranges called above. The maximum hydrostatic strains and the types of lattice instrabilities were theoretically predicted for the considered metals.

The influence of high electronic temperature on the electronic heat conductivity and electric resistivity has been provided for d-band metals by the approach based on the solution of Boltzmann kinetic equation in τ-approximation [5]. This data is compared with the results of quantum molecular dynamics simulations for Gold [6].

This work was supported by RFBR (grant No 13–02–1078).

1. Kresse G., Furthmuller J., //Comput. Mater. Sci. 1996. V. 6. No. 1. P. 15.
2. Kresse G., Furthmuller J., // Phys. Rev. B. 1996. V. 54. P. 11169.
3. Khakshouri S., Alfè D, Duffy D. M., // Phys. Rev. B. 2008. V. 78. P. 224304.
4. Sin'ko G.V, Smirnov N.A., Ovechkin A.A., Levashov P.R., Khishchenko K.V. // HEDP. 2013. V. 9. No. 2. P. 309.
5. Inogamov N.A., Petrov Yu.V. // JETP. V. 110. No. 3. P. 446.
6. Norman G., Saitov I., Stegailov V., Zhilyaev P. // Contrib. Plasma Phys. V. 53. No. 4–5. P. 300.

THE QUESTION OF HIGH-ELECTRONIC ENSEMBLE IN IONIC CRYSTALS

Savintsev A.P.,* Gavasheli Yu.O.

KBSU, Nalchik, Russia

**pnr@kbsu.ru*

Currently, much attention is paid to high-temperature electronic assemblies that may arise as a result of exposure to a particular environment of ultrashort intense laser pulses. For example, such a laser irradiation condition creates metals with two temperatures, so-called $2T$ state where $T_e \gg T_i$, where T_e, T_i - electron and ion temperatures [1]. $2T$ - stage metals are very important, since it is there that occurs $2T$ - relaxation with the transfer of laser energy to ions and mainly formed (sometimes significant) warm layer, which plays an important role in the subsequent dynamics. Question about $2T$ states in dielectric medium previously raised in [2]. Further study of this problem has led us to the following results. In ionic crystals exposed to femtosecond laser pulses, excitation mechanisms and

warming temperatures are much different from those that occur in metals. In the crystals of the free electron concentration is usually very small. If in the case of metals irradiation by laser radiation is excited and warm-up of a large number of free electrons [3] (there is a significant T_e), who later betrayed ions (growth occurs T_i), then the situation in crystalline medium (in this respect) is different. Emergence of a significant concentration of free electrons (electronic band) should be preceded at first quite active (e.g., impact) ionization [4] of the dielectric medium with fairly large amounts of energy. Energy transfer arises from the electron beam, and the ions of the crystal lattice due to the growth of T_i is such a mechanism rather locally because of the lower thermal conductivity of these fluids compared with metals [5]. Thus, ionic crystals should not expect a $2T$ distinct states and significant influence on the heating mechanism of such a significant amount of material.

This work was supported within the state task base portion of the KBSU Russian Ministry for 2014–2016 years (project 2014/54–2228).

1. Inogamov N. A., Ashitkov S. I., Zhakhovskii V. V., et al. // Physics of Extreme States of Matter—2009, 2009. P. 7.
2. Savintsev A. P., Gavasheli Yu. O., Gavasheli D. Sh. // Abs. 27 Int. Conf. "Interaction of Intense Energy Fluxes with Matter", 2011. P. 38.
3. Laser radiation / edited by V. J. Grankin. M., 1977.
4. Savintsev A. P., Gavasheli Yu. O. // DAN. 2012. V. 445. No. 4. P. 396.
5. Vorobev A. A. Mechanical and thermal properties of alkali halide crystals. M., 1968.

DETERMINATION OF SURFACE PRESSURE IN SODIUM CHLORIDE UNDER LASER IRRADIATION

Gavasheli Yu.O.,* Savintsev A.P.

KBSU, Nalchik, Russia

**yu-pakhunova@mail.ru*

Since the inception of lasers was a large amount of experimental and theoretical studies of the process of destruction of transparent solids by laser radiation. However, to address the issue of the laser-induced damage mechanism in the short laser pulses area, further research on the role of its own laser radiation absorption mechanisms, shock and multiphoton ionization, as well as the study of the laser ablation physical mechanisms, which are dominant on the surface when exposed to femtosecond laser pulses [1]. In our paper [2] studied the critical electric field dependence of the laser

pulse duration in the radiation damage case of sodium chloride. Approximation was used depending on the desired three curves with different angular coefficient. For further work in this direction, we selected two experimental points [2] (nanosecond laser pulses) and one design point to plot the surface ablation destruction (femtosecond laser pulses). In assessing the ablation pressure p_a used the formula in [3]: $p_a(\text{kbar}) = 4.8 \cdot 10^{-4} I^{1/2}$ (W/cm^2), where I—intensity of the laser radiation. At selected points calculations give : $p_a = 56.2$ kbar at $I = 1.4 \cdot 10^{10}$ W/cm^2, $p_a = 62.4$ kbar at $I = 1.7 \cdot 10^{10}$ W/cm^2, $p_a = 1$ Mbar at $I = 4 \cdot 10^{12}$ W/cm^2. The latter result is of great interest, since the pressures $p_a \sim 1$ Mbar such an effect, as a transition to a metallized state [4, 5], may take place on the surface of a sodium chloride crystal [6]. This area is reflected in the sodium chloride phase diagram, in the case of exposure to the crystal short dynamic loads [2] corresponds to a particularly rapid the surface destruction of an ionic crystal.

This work was supported within the state task base portion of the KBSU Russian Ministry for 2014–2016 years (project 2014/54–2228).

---

1. Manenkov A. A. // Quantum Electronics. 2003. V. 33. No 7. P. 639.
2. Savintsev A. P., Gavasheli Yu. O. // Physics of Extreme States of Matter-2012. Chernogolovka, 2012. P. 104.
3. Karpenko S. V., Savintsev A. P. Temrokov A. I. // DAN. 2008. V. 419. No 2. P. 179.
4. Solids under high pressure / Ed. B. Paul, D. Warschauer. M.: Mir, 1984.
5. Glebov L. B., Efimov O. M., Libenson M. N. etc. // DAN. 1986. V. 287. No 5. P. 1114.
6. Karpenko S. V., Savintsev A. P. Temrokov A. I. // Surface. 2004. No 2. P. 53.
7. Savintsev A. P., Gavasheli Yu. O. // DAN. 2012. V. 445. No 4. P. 396.

THE GLASS NANO-COMPOSITES LASER ABLATION DESTRUCTION STUDIES

Shemanin V.G.,[*1] ***Atkarskaya A.B.,***[1] ***Mkrtychev O.V.,***[2] ***Privalov V.E.***[3]

[1]*KubSTU NPI, Novorossiysk,* [2]*BelgSTU, NB, Novorossiysk,*
[3]*SPbSPU, Saint-Petersburg, Russia*

[*]*svhemanin@nbkstu.org.ru*

The laser ablation [1, 2] is the basics of the laser materials processing and can be applied in the hi-tech manufacturing for the micro processing and modification of the nanophotonics devices [3, 4]. The major problems of the laser ablation studies are the stochastic character of the ablation process and spatial effect [5]. This work purpose is the glass nanocomposites of the various structure laser ablation threshold energy density values experimental studies. The glass nanocomposite samples [3] were the colorless float-glass plates covering with the oxide nanofilms—single-layer film of silicium oxide or titanium oxide and two-layer films silicium oxide and titanium oxide. They have been studied at the laboratory laser ablation station with the YAG-Nd laser in the milliseconds and nanoseconds pulse regimes [4] and the ablation breakdown presence was recorded by the plasma plume light emission. The breakdown probability curve versus the laser energy density dependence were studied for all the samples. It have been derived that the laser destruction threshold energy density value decreases with the samples light transmittance growth for the silicon dioxide films in the 0.3 ms laser pulse time duration regime but the threshold energy density Fb value is nearly constant with our experimental error of 0.12 in 20 ns laser pulse time duration regime. The samples of the titanium dioxide give the such a results in millisecond and nanosecond ranges too. The laser ablation destruction was resulted in the craters or cracks formation on the sample surface [4] that can be explained by the thermoelastic mechanism [5].

1. Voronina E. I., Efremov V. P., Privalov V. E., Charty P. V., Shemanin V. G. // Tech. Phys. 2009. V. 79. N. 5. P. 143.
2. Voronina E. I., Efremov V. P., Privalov V. E., Shemanin V. G. // Tech. Phys. Lett. 2008. V. 34. N. 23. P. 59.
3. Atkarskaya A. B., Mkrtychev O. V., Shemanin V. G. // Izvestiya Vuzov. Physics. 2012. V. 55. N. 8–2. P. 238.
4. Efremov V. P., Privalov V. E., Skripov P. V., Charty P. V., Shemanin V. G. // Proc. SPIE. 2004. V. 5447. P. 234.

5. Koldunov M. F., Manenkov A. A., Pokotilo I. L. // Quantum Electronics. 1998. V. 25. N. 9. P. 833.

EXPERIMENTAL STUDY OF NANOSECOND LASER HEATING OF Mo NANOPARTICLES

Gurentsov E. V.,* Yurischev M. V.

JIHT RAS, Moscow, Russia

**gurentsov@ihed.ras.ru*

The investigation of the process of interaction of intense electromagnetic field with condensed particles is regarded to many applications, such as ignition of heterogeneous fuels [1], laser based diagnostics [2] and laser assisted material synthesis [3]. In this study the measured experimentally temperature time profiles of Mo nanoparticles, heated by a nanosecond laser pulse, are analyzed in dependence on laser fluence. Mo nanoparticles were synthesized using excimer Kr-F laser pulse photolysis [4] of $Mo(CO)_6$ in a 0.5 cm^3 quartz reactor filled with an inert gas at room temperature. The samples of Mo nanoparticles obtained were analyzed by transmission electron microscopy and the mean nanoparticle sizes were found to be in a range of 10–20 nm. The pulse Nd:Yag laser (1064 nm, 12 ns HWHM) was used for nanoparticle heating. The temperature time behavior of laser heated nanoparticles was observed by two color pyrometry at the wavelengths 488 and 760 nm [5]. At low Nd:Yag laser fluencies (< 0.2 J/cm^2) the nanoparticles attained the peak temperature of 2500–3200 K (in dependence on their size) during the time of laser pulse and then cold down to the ambient conditions. At higher fluencies (> 0.2 J/cm^2) the unusual temperature behavior was found (the moment of peak of thermal emission did not coincide with the moment of peak particle temperature). The possible absorption of thermal emission at shorter wavelength by the vapor formed during the laser induced evaporation of Mo nanoparticles is discussed.

This work has been supported by the Russian Foundation for Basic Research (grant No. 14–08–00505).

---

1. Beyrau F., Hadjipanayis M. A., Lindstedt R. P. // Proc. Comb. Inst. 2013. V. 34. P. 2065.
2. Gurentsov E., Eremin A. // High temperature. 2011. V. 49. No. 5. P. 667.
3. Sendova M., Sendova-Vassileva M., Pivin J. C., Hofmeister H., Coffey K., Warren A. // J. Nanosci. Nanotechnol. 2006. V. 6. P. 748.
4. Gurentsov E. V., Eremin A. V. // Nanotechnologies in Russia. 2009. V. 4.

No. 5–6. P. 319.
5. Eremin A., Gurentsov E., Popova E., Priemchenko K. // Appl. Phys. B. 2011. V. 104. P. 285.

INVESTIGATION OF THE PROPERTIES OF CARBON NANOPARTICLES BY PULSE LASER HEATING

Eremin A. V., Gurentsov E. V., Mikheyeva E. Yu.*

JIHT RAS, Moscow, Russia

**mikheyeva@ihed.ras.ru*

This study is of interest in terms of synthesis of new carbon nanomaterials with specific properties. The condensation of carbon in pyrolysis and combustion of hydrocarbons is one of the principal techniques to produce carbon nanoparticles. This study is devoted to the investigation of properties of carbon nanoparticles by pulse laser heating. The nanoparticles were synthesized in pyrolysis of 1% of benzene behind the reflected shock waves in temperature range of 1750–2350 K and pressure of 3–4 bar. The temperature of gas-particle environment during pyrolysis process was observed by emission-absorption spectroscopy technique. The size of nanoparticles was measured by laser-induced incandescence and was in the range of 3–15 nm. The heating of nanoparticles was generated by Nd:YAG laser pulse at the wavelength of 1064 nm and fluence of 0.1–0.5 J/cm^2. The sublimation of carbon nanoparticles induced by a pulse laser heating was observed by reduction of volume fraction of condensed phase, measured by laser light extinction at the wavelength of 633 nm. The peak temperature during laser heating of nanoparticles measured by two-color pyrometry was regarded to the particle sublimating temperature. This temperature was found to be in the range of 3200–4400 K in dependence on nanoparticles size and temperature regime of their formation. The analysis of measured gas-particle environment temperature behavior and chemical kinetic calculation yielded the estimation of the heat of condensation per carbon atom in nanoparticles. According to manifold measurements the increase of temperature of formation of carbon nanoparticles results in the increase of sublimating temperature and in the increase of heat of carbon condensation per one atom in nanoparticle. These results are the evidence of different structure of carbon particles formed at different temperature conditions.

This work has been supported by the Russian Foundation for Basic Research (grant No. 14–08–00505).

INTENSE IRRADIATION BY X- AND γ-RAYS AS A VERSATILE TOOL TO PROBE TRANSPORT PROPERTIES OF ORGANIC SUPERCONDUCTORS

Bardin A.A.,[*1] ***Zverev V.N.,***[2] ***Kotov A.I.,***[1] ***Tolstikova A.O.,***[3] ***Shilov G.V.***[1]

[1]*IPCP RAS, Chernogolovka,* [2]*ISSP RAS, Chernogolovka,*
[3]*MIPT, Dolgoprudny, Russia*

[*]*dr.abardin@gmail.com*

Despite their chemical complexity electronic structure of organic superconductors (OS) is rather simple and may be regarded as a model framework for more complicated systems like high temperature superconductors (HTS) or pnictides. It has been recently proved that *d*-wave pairing symmetry, currently accepted for most of HTS, is realized in OS as well [1]. Conductive state of OS is very sensitive for chemical or physical disturbance and is altered by various means, even by mechanical stress [2]. It is needless to emphasize an importance to unveil the pairing type in the so-called *unconventional* (non-BCS) superconductors as all novel classes of superconductors of particular interest belong to this class.

One of distinct properties of unconventional superconductors that is markedly different from conventional ones is a high sensitivity to *nonmagnetic* scattering centers introduced into the crystal lattice. Lowering of T_c imposed by *magnetic* impurities in *conventional* superconductors is well described by Abrikosov-Gor'kov (AG) formula:

$$\ln\left(\frac{T_{c0}}{T_c^{AG}}\right) = \psi\left(\frac{1}{2} + \frac{\hbar}{4\pi\tau k_B T_c^{AG}}\right) - \psi\left(\frac{1}{2}\right).$$

Surprisingly, the same formula is applicable to describe T_c affected by *nonmagnetic* impurities/disorder in *unconventional* superconductors. One of the tools to introduce disorder into a crystal structure is an irradiation by intense beams of hard X and γ rays. We discuss systematic deviation of T_c suppression from the AG formula in the crystals heavily irradiated by X and γ rays, speculate about possible mechanisms of defect formation and carefully investigate real structure of the crystals in the tight connection with transport measurements proposing further improvements of experimental techniques.

1. Milbradt S., Bardin A. A., Truncik C. J. S., et. al. // Phys. Rev. B. 2013. V. 88. No. 6. P. 064501.
2. Bardin A. A., Burn P. L., Lo S.-C., and Powell B. J. // Phys. Stat. Sol. B. 2012. V. 249. No. 5. P. 979.

X-RAY AND GAMMA-EMISSION FROM SEALED-OFF PLASMA FOCUS CHAMBERS WITH D–D AND D–T FILLINGS

Dulatov A.K., Lemeshko B.D.,* Mikhailov J.V., Prokuratov I.A., Selifanov A.N., Yurkov D.I.

VNIIA, Moscow, Russia

**bogolubov@vniia.ru*

Production of the neutron generators with nanosecond pulse durations based on the plasma focus (PF) chambers is one of the lines of activities of the VNIIA. Lineup of neutron generators on PF chambers with D-D and D-T fillings that provides neutron yield from 10^7 to 10^{12} neutrons per pulse was developed in VNIIA. PF devices could be also used as intensive sources of X-Ray with quanta energy from a few keV to several hundred keV. The X-ray parameters for PF chambers with D-D and D-T fillings were measured in this work. The analysis of the X-ray emission spectra showed that D-D filling provides the hard X-ray emission with the energy of quanta restricted to 250–300 keV. During the experiments with D-T filling two components of the hard electromagnetic emission was founded bremsstrahlung emission with energy up to 250–300 keV and γ-emission with the quanta energy 2–3 MeV. The duration of the hard X-ray pulse is 2–9 ns, the duration of the γ-radiation pulse is 8–50 ns that depends on the neutron yield. γ-radiation appears due the inelastic interactions between neutrons (14 MeV) and nuclei of the chamber material Cu(n,n',γ) and due the subsequent removing energy of the γ-quant from the excited nuclei levels.

MEASUREMENTS ON ABSOLUTE REFLECTIVITY OF SPHERICALLY BENT QUARTZ CRYSTALS FOR X-RAY RADIOGRAPHY APPLICATIONS

Pikuz Jr. S.A.,[*1] ***Volpe L.,***[2] ***Antonelli L.,***[2] ***Folpini G.,***[3] ***Forestier-Colleoni P.,***[2] ***Santos J.J.,***[2] ***Faenov A.Ya.,***[1] ***Fedeli L.,***[3] ***Barbato F.,***[4] ***Giuffrida L.,***[2] ***Fourment C.,***[2] ***Hulin S.,***[2] ***Batani D.***[2]

[1]*JIHT RAS, Moscow, Russia,* [2]*CELIA, Talence, France,* [3]*UMB, Milano, Italy,* [4]*URTV, Rome, Italy*

[*]*spikuz@gmail.com*

Spherically bent Bragg crystals are widely used in various self-emission and backlighting x-ray imaging diagnostics for high energy density investigations. Particularly, they are applied in fast electron transport experiments to get a spatial information about a fast electron beam passing through a fluorescence tracer. It is also interesting to quantify the absolute number of photons imaged to deduce the number of fast electrons. For that, a characterization of the crystal efficiency is needed.

Here we present experimental results on absolute reflectivity of several spherically bent quartz crystals to be applied in the forthcoming experimental studies of relativistic laser plasmas. The experiment, supported by LASERLAB and ESF, has been performed in the Eclipse laser facility at CELIA laboratory in Bordeaux. The facility provided 40 fs laser pulses focused in a 8 um FWHM focal spot reaching peak laser intensity on target of 1e18 W/cm^2.

Different crystals have been used to collect K/*alpha* radiation coming from the interaction between a laser-generated relativistic electron beam with thin (10 um) copper foils. The collected radiation has been reflected into a CCD camera placed at the image plane of the crystal. The same detector has been used to collect photons in the range of 5 to 20 keV coming from the same target in single hit mode. The comparison between the two acquisitions permit us to perform an absolute estimation of the crystal reflectivity. The data were obtained for 3 crystal samples in order to compare the performance of the crystals from 2 different suppliers, as well as to study the ageing of the crystals under numerous expositions to intense ionizing radiation of relativistic laser plasmas. Obtained results are compared with numerical simulations. The measured values will be used to quantitatively interpret the data of X-ray radiography diagnostics in various HEDP experiments.

PHASE-MATCHED COHERENT RADIATION IN TWO-STAGE TRANSIENT-COLLISIONAL EXCITATION PLASMA-MEDIA X-RAY LASER

Nagorskiy N.M.,[*1] ***Magnitskiy S.A.,***[2] ***Faenov A.Ya.,***[1] ***Pikuz T.A.***[1]

[1] *JIHT RAS,* [2] *MSU, Moscow, Russia*

[*] *nikolaynag@gmail.com*

Table-top transient-collisional excitation lasers are promising soft-X-ray sources for wide range of applications from medicine to microelectronics. However, the spatial coherence of such lasers is far from perfection and many efforts are aimed at improving it. One of the effective solutions is to use two-stage mode, when one laser is used as generator and second as amplifier [1]. Recently, an unexpected interference pattern was observed in such two-stage plasma-media laser [2]. It was shown, that observed interference rings have relatively large contrast and do not move from shot to shot.

In this presentation we give simple physical explanation of the observed phenomenon, supported by numerical simulation of generator beam propagation through plasma with given electron density and gain distribution. It is shown, that the interference pattern raises from two phase-matched spherical waves. The center of first one is located in generator and the second one in amplifier. The formation of second virtual point source is accompanied by many optical effects, such as diffraction, laser gain, refraction and gain saturation. Our theoretical model is based on parabolic diffraction equation for inhomogeneous amplifying medium and naturally takes into account all listed effects.

The obtained results provide new approach for theory of amplification of soft-X-ray laser beams and open new opportunities for X-ray plasma diagnostics and two-stage X-ray lasers development.

---

1. Nishikino M., Hasegawa N., Kawachi T., Yamatani H., Sukegawa K., Nagashima K. // Appl. Opt. 2008. V. 47. P. 1129–1134.
2. Magnitskiy S.A., Nagorskiy N.M., Faenov A.Ya., Pikuz T.A., Tanaka M., Ishino M., Nishikino M., Fukuda Y., Kando M., Kawachi T., Kato Y. // Nature communications. 2013. V. 4. No. 1936. doi:10.1038/ncomms2923.

HYBRID 3D-METHOD FOR CALCULATIONS OF ENERGY ABSORPTION OF IONIZING RADIATION IN ELEMENTARY CELLS OF THE HETEROGENEOUS MATERIAL HAVING THE SET OF CHARACTERISTIC STRUCTURAL IRREGULARITIES

Bakulin V.N.,[*1] ***Ostrik A.V.***[2]

[1]*IAM RAS, Moscow,* [2]*IPCP RAS, Chernogolovka, Russia*

[*]*vbak@yandex.ru*

Forecasting of parameters of thermal and mechanical actions of the ionizing radiation (IR) for the heterogeneous coverings (HC) having structure represents considerable practical interest [1]. In many respects correct calculation of energy absorption realized in HC structure components determines also the accuracy of calculation of these parameters. Earlier hybrid numerical code was developed for calculation of IR energy absorption taking place in heterogeneous materials. [2–4]. The regular structure of a material was assumed in this code. The inserts method [2] was used. Transfer of photons was modeled by the Monte-Carlo method. Energy redistribution by secondary electronic radiation paid off analytically [2–4]. Such method allowed considering energy redistribution between the HC components by secondary electronic radiation in not one-dimensional geometry. But the real HC structure is much more difficult. This structure represents a set of the clusters having uneven distribution and various compositions of filler particles. Filler particles differ by the sizes and structure (in particular to be dilapidated or to have form distortions).

In the present work the method [2–4] is applied to a case of the elementary cells containing sets of clusters with irregular determined structure. The numerical code is realized for several most probable sets of clusters and their distributions.

As a result essential changes of energy absorption distributions are received in the HC components when structure and distributions of filler particles clusters are varied. Amplitudes of these changes rise when we increase effective temperatures of Planck's IR spectrum.

---

1. Ostrik A.V. //J. Questions of defensive engineering. Series 15. 2013. Num. 1 (168). P. 8–17.
2. Ostrik A.V. Thermomechanical action of x-ray radiation on multilayered heterogeneous barriers into air. M.: "Informtekhnik", 2003.
3. Gribanov V.M., Ostrik A.V., Romadinova E.A. //J. Constructions from com-

posite materials, 2009. Num. 1. P. 40–47.
4. Bakulin V.N., Ostrik A.V. //Book of Abstracts of the All-Russian conference "Mechanics of Nanomaterials and System", IPRIM RAS, M.: 2012. P. 15–16.

TRANSITIONAL ELEMENTARY CELL OF HETEROGENEOUS COVERINGS WITH COLLAPSING DISPERSE FILLER HAVING IRREGULAR DISTRIBUTION

Bugay I.V.,[*1] ***Ostrik A.V.***[2]

[1]*BMSTU, Moscow,* [2]*IPCP RAS, Chernogolovka, Russia*

[*]*ibug@mail.ru*

Now the method of elementary cell [1, 2] is widely used for calculation of parameters of mechanical action of the ionizing radiation (IR). Usually uniform filler distribution is supposed at creation of elementary cells of heterogeneous materials. This assumption significantly simplifies a task. But the real heterogeneous coverings (HC) have no periodic structure as a result of technological errors. Besides filler distribution uniformity doesn't take place in perspective gradient coverings.

In the present work the non-stationary model of an elementary cell is offered. Phase transitions and irregular structures interaction in a cell are considered. It is supposed that tension establishment in a cell is quasistationary. Then heat exchange between the HC components appears the reason of transitional processes being realized in a cell.

Calculation of tension establishment within an elementary cell is based on the solution of system of the two-dimensional equations of balance for the elastic-plastic environment. This system is solved together with the heat transfer equation in cylindrical coordinates. The equations system is supplemented with wide-range equations of a state and heat-physical characteristics of HC components.

The special attention is paid to the accounting of structural features of the multilayered microspherical fillers used in HC for protection against IR. Stability loss, destruction and irreversible microspheres collapse when IR energy is absorbed by a heterogeneous material are considered.

Settlement tensions profiles are given in heterogeneous coverings with disperse fillers from glass and carbon microspheres (microspheres are covered with tungsten or nickel). These data are submitted at the time of radiation completion depending on the dimensionless relation of radiation impulse time to characteristic time of heat exchange realized in a cell.

1. Ostrik A.V. Thermomechanical action of x-ray radiation on multilayered heterogeneous barriers into air. M.: Scientific and technological Center "Informtekhnik", 2003.
2. Gribanov V.M., Ostrik A.V., Romadinova E.A. Numerical code for calculation of multiple complex action of radiations and particles on multilayer multifunctional heterogeneous plane packet. Chernogolovka: IPCP RAS, 2006.

SET OF DEVICES FOR SIMULATION OF MECHANICAL ACTION OF RADIATIONS AND PARTICLES FLUXES

***Cheprunov A.A.,*[1] *Ostrik A.V.*[2]**

[1]*12CSRI MOD RF, Sergiev Posad,* [2]*IPCP RAS, Chernogolovka, Russia*

**cheprunov@yandex.ru*

The assessment of consequences of mechanical action of radiations and particles fluxes (RPF) on composite designs represents considerable practical interest [1, 2]. Carrying out experimental studies on direct RFP impact realized on designs is impossible or expensive in many cases. Usually settlement and experimental approach [2] is used. Parameters of mechanical RPF action are defined by means of numerical modeling [3]. These parameters are simulated by devices [4] at designs tests. Chemical energy of explosive or electric energy reserved in condenser batteries is used in these devices. A certain interest submits the accounting of thermal RPF action. Preliminary heating reduces designs strength to mechanical RPF action.

In present work the set of devices for simulation of mechanical RPF action realized in the wide range of change of pressure impulses (0.01...1 kPa×s) and durations (0.1...10μs) is offered. Various means of generation of non-stationary loadings are applied. They are explosive detonation and electroexplosion of metal foils and a throwing of plates. Thermal RPF action is reproduced heating by means of highest frequency radiation (with frequency 34 GHz).

Results of research of pulse loads action on composite three-layer samples are represented. Two external layers carry out protective functions (in particular it's damping function). The third protected layer is carrier part of a studied design. The received results allow us to draw important conclusions about efficiency of various variants of constructional protection.

---

1. Ostrik A.V., Gribanov V.M., Cheprunov A.A., and et al. Mechanical X-ray action on thin-walled composite designs. M.: FIZMATLIT. 2008.

2. Ostrik A.V. //J. Questions of defensive engineering. Scientific and technical digest. Series 15. 2013. Num. 1 (168). P. 8–17.
3. Gribanov V.M., Ostrik A.V., Romadinova E.A. Numerical Code for Calculation of Multiple Complex Action of Radiations and particles on multilayer multifunctional heterogeneous plane packet. Chernogolovka: IPCP RAS. 2006.
4. Ostrik A.V., Cheprunov A.A., Bakulin V.N. //Strength and plasticity problems. Inter-higher education institution collection. Nizhny Novgorod. 2000. P. 117–121.

MOTION AND FRACTURE OF CHELYABINSK METEOROID IN ATMOSPHERE

Dudorov A.E.,* Mayer A.E.

CSU, Chelyabinsk, Russia

**dudorov@csu.ru*

The asteroid impact near Chelyabinsk is an example of intensive energy release of natural origin. Total energy of the impact is of about 500 kT of TNT [1]. It initiates bright flash and shock wave in air, which cause glass damage even on distance of several tens of km away from meteoroid trajectory. Investigation of meteoroid is interesting from viewpoint of influence of asteroid impacts as well as structure of cosmic bodies.

Present research is dedicated to explanation of an explosion-like energy release of the Chelyabinsk meteoroid at altitudes above 20 km from the ground surface. Numerical modeling of motion, ablation and fracture of the meteoroid in atmosphere has been done on basis of standard approaches used in the meteoritic astronomy [2–4]. A sharp increase of the meteoroid energy release at altitudes between 45 and 25 km (a kinetic explosion) is a consequence of its mechanical fracture, but not vise versa. The fracture is caused by mechanical stresses in meteoroid created by air pressure on its front surface. An analysis of the observed data (the total mass of fallen fragments and the light curve) can be used for estimation of physical properties of the initial object. Chelyabinsk meteoroid initially was highly inhomogeneous with respect to its mechanical properties—it contained friable areas with low mechanical strength. It led to presence of two fracture cascades—at altitudes 55–50 km and 40–35 km respectively. An intensive ablation of the meteoroid substance took place at altitudes from 50 km down to 25 km; the ablation was mainly in the form of vaporization; the total ablated mass is 99.5 % of the initial mass.

1. Popova O. P., Jenniskens P., Emelyanenko V., et al. // Science. 2013. V. 342. No. 6162, P. 1069.
2. Baldwin B., Sheaffer Y. // J. Geophys. Research. 1971. V. 76. No. 19. P. 4653.
3. Svetsov V. V., Nemtchinov I. V., Teterev A. V. // Icarus. 1995. V. 116. P. 131.
4. Popova O // Earth Moon Planets. 2004. V. 95. P. 303.

DEVELOPMENT OF POSITION-SENSITIVE D–T NEUTRON MONITOR

Ignatiev N.G.,* Krapiva P.S., Lemeshko B.D., Dulatov A.K.

VNIIA, Moscow, Russia

**n_ignatev@list.ru*

This provides information on new experimental development of position-sensitive neutron radiation monitor (SMNI3) designed to image region of fusion D–T neutrons generation for electro-physics and laser facilities in single-image mode. Position-sensitive registration is achieved by converting the energy of the neutron radiation into visible light through the screen assembled from separate scintillation fibers ($\sim$ 90000 pieces). Optical system transfers scintillation flashes to the photocathode intensifier (SFER16), which is also serves as gate and allows the separation of neutron and gamma radiation by time of flight. Image recording is carried out by CCD camera (SPM20). Management and transmission is carried out via fiber optic link. For imaging the region of generation of neutron radiation on the surface of the screen the scintillation neutron penumbral aperture is used. Image registration becomes possible if outputs $\sim 10^{10}$ neutrons per pulse and above. Image recorded in coded form, requiring further treatment. Image reconstruction is performed by deconvolution of the resulting image with the point spread function for the neutron aperture. Here is described the construction of the position-sensitive monitor of D–T neutrons, also here is given the characteristics of the elements included in its composition, shown the results of image registration generation region 14 MeV neutrons in the chamber installation of the plasma focus facility.

DEVELOPMENT OF SCINTILLATION AND CHERENKOV DETECTORS FOR DIAGNOSTICS OF FAST PROCESSES

Ignatiev N.G., Ivanov M.I.,* Moskvichev V.A., Nesterenko A.O.

VNIIA, Moscow, Russia

**ivanov3575@yandex.ru*

This provides information about the new development of scintillation and Cherenkov detectors for dynamic measurements of pulsed neutron, braking and gamma radiation with a pulse duration of a few ns to 100 ms. This is primarily based detectors of high-speed photomultiplier (type SNFT) and photocells (SDF) own design. Their temporal resolution (~ 0.5) ranges from 10 ns for the most sensitive (SSDI8M-02) to 0.5 ns for the least sensitive (SCHDI3). Several highly sensitive scintillation detectors are based on industrial FEU-97 and FEU-139 (SSDI34, 36 and 37) and large plastic scintillators (up to 7 liters), which provide maximum sensitivity over 10^{-9}A·s·cm^2/photon (for gamma-rays with energy 1.25 MeV) with a temporal resolution better than 35 ns. Collectively, given the range of sensitivity adjustment (at least 100) and maximum line current (less than 0.5 A) detectors in combination with modern DVRs allow you to block the dynamic range of measurements of the flux densities of gamma and neutron radiation more than 10 orders of magnitude. The lower limit ($\sim 10^9\gamma(n)/\mathrm{cm}^2 \cdot \mathrm{s}$) limited the allowable level of statistical fluctuations of the amplitude of the signal from the detector (usually no more than $\pm 30\%$) and upper ($\sim 10^{19}\gamma(n)/\mathrm{cm}^2 \cdot \mathrm{s}$). Radiation resistance used scintillator or Cherenkov radiator ($10^2 - 10^3 P$/pulse) . Also considered metrological provision detectors in their production and operation. All developed detectors are certified as special-purpose measurements tool and outperforms earlier counterparts.

PULSED X-RAY SPECTROMETERS FOR DIAGNOSTICS OF FAST PROCESSES

Ignatiev N.G., Krapiva P.S.,* Nesterenko A.O., Svetlov E.V.

VNIIA, Moscow, Russia

**forautoru@land.ru*

Here is the results of development of three types of X-ray spectrometers SMIR11, T20-L16 and SPRK4 designed to study processes in the target of laser fusion facilities, installations of Z-pinch plasma-focus devices and other pulsed sources. The first two types are multichannel X-ray spec-

trometer, which provide dynamic measurements of photon energies in the range from 0.05 to 10 keV (SMIR11) and from 5 to 100 keV (T20-L16) with high temporal resolution. To select and register X-ray radiation in narrow spectral bands there is in the channels of SMIR11 spectrometer (with a total of up to 11 pcs) multilayer mirrors, edge filters and Ross filters (for energies above 1.5 keV) in combination with high-speed semiconductor and vacuum X-ray detectors of different types are used.

Spectrometer T20-L16 is designed to record spectra of hard x ray using the fluorescent converters. Vacuum channels provided with optional filters, converters, collimators and detectors of various types. In particular, the spectrometer is designed for using with sensitive semiconductor detector made of Si, CdTe, and detectors based on layouts compact photomultiplier H10721 and "fast" plastic scintillators. The results of investigation of their characteristics also presented.

SPRK4 spectrometer built under the Cauchois scheme using transmissive crystal and CCD registrator and provides registration of X-ray spectra with energies from 4 to 40 keV in the integrating mode. Quartz crystals of $2d = 2.36$Åand $2d = 8.5$Å, curved cylinder and sphere are located on a goniometer device within the vacuum chamber. Register radiation reflected from the crystal is carried out using a CCD matrix sensor based CCD42–10. The results of the registration of characteristic spectra plasma at variety of facilities are presented.

COMPARISON BETWEEN PULSED CATHODOLUMINESCENCE SPECTRA OF SCINTILLATORS AND SPECTRA OF LUMINESCENCE OF THE SAME CRYSTALS UNDER THE ACTION OF GAMMA-IRRADIATION

Kozlov V.A.,[1] ***Ochkin V.N.,***[1] ***Pestovskiy N.V.,****[1] ***Petrov A.A.,***[1] ***Savinov S.Yu.,***[1] ***Zagumenniy A.I.,***[2] ***Zavertyaev M.V.***[1]

[1]*LPI RAS,* [2]*GPI RAS, Moscow, Russia*

**samosval@mail15.com*

The Pulsed Cathodoluminescence spectra of scintillators CsI:Tl, YAG:Ce^{3+},Tb^{3+} and LFS-3 under the action of powerfull (about 10 MW) and fast (about 2 ns) electron pulse with average energy of electrons about 150 keV, produced by RADAN-EXPERT electron beam accelerator, and spectra of the stationary luminescence of the same crystals under the action of gamma-irradiation with energy 511 keV, which had been emitted by the ^{22}Na source, were investigated. It is found the obtained spectra

are identical. The explanation is given based on the analysis of processes occuring in crystals under the influence of particles with energy less then 1 MeV. This result enables the Pulsed Cathodoluminescence method to be used for scintillator analysys.

THz SENSORS BASED ON TRANSISTOR STRUCTURE WITH PLASMON RESONANCE

Ermolaev D.M.,[1] ***Polushkin E.A.,***[1] ***Zemlyakov V.E.,***[2] ***Egorkin V.I.,***[2] ***Shapoval S.Yu.****[1]

[1]*IMT RAS, Chernogolovka,* [2]*MIEE, Moscow, Russia*

**shapoval@iptm.ru*

Terahertz (THz) detection by a one-dimensional array of series connected field-effect transistors (FETs) is studied experimentally. Such terahertz detector demonstrates greatly enhanced voltaic responsivity up to 2 kV/W. Asymmetrical position of the gate contact in each FET in the array enables strong photovoltaic response.

REACTIVITY OF NANOSELENIUM POLYMERIC COMPOSITES IN THE MICROWAVE FIELD

Savintsev Yu.P.,*[1] ***Savintseva S.A.,***[2] ***Shevchenko V.S.,***[1] ***Urakaev F.Kh.***[1]

[1]*IGM SB RAS,* [2]*IIC SB RAS, Novosibirsk, Russia*

**savincev1940@mail.ru*

Nanoselenium remains the promising substance of the beginning of 21 century. Its numerous modifications are the subjects of a study in many laboratories of the word because of potential applications of selenium in nanoscale state. So red amorphous modification (a-Se) can be used in medicine for orthopedic treatments and anticancer therapy. Crystalline trigonal selenium (t-Se) is the old semiconductor and photoconductor of 20 century. But nanodimensional Se has a new better quality. It can be applied not only in traditional regions as electronics and photonics. So composite of nano-t-Se and graphene can be used as cathode material for Li accumulators. Nanosensors also can be made from trigonal nanoselenium. It is very interesting to make transformations of a-Se into t-Se in nanocomposite polymeric film. But we should know in details its properties, especially chemical reactivity, for going in a proper way. Films of polymeric composites were produced after drying of mixture of water solu-

tions of selenite, surfactant, polyvinyl alcohol, hydrazine hydrate treated with ultrasound. These films were studied as targets for microwave irradiation. They have been placed in microwave oven with controllable gaseous atmosphere. Our nanocomposites were investigated with chemical and X-ray analyses, uv-vis spectrometry, optical, laser confocal and electron scanning microscopies.

NUMERICAL INVESTIGATION OF TENSILE STRENGTH OF METAL MELT

Mayer P.N.,* Mayer A.E.

CSU, Chelyabinsk, Russia

**polina.nik@mail.ru*

Tensile fracture of metal melt takes place under the action of intensive ultra-short electron or laser irradiation [1, 2]. An almost isochoric heating can be realized if the pulse duration is much less than the mechanical relaxation time. A metal layer under irradiated surface is rapidly heated and melted by irradiation and becomes the melt at high temperature (of about several thousands of K) and high pressure (of about several GPa). Consequent expansion of this metal melt creates tensile stresses and makes this melted layer metastable—it can suffer a phase transition from liquid to vapor through the formation of vapor cavities in it. Growth and coalescence of vapor cavities lead to fracture of the melt and to the material ablation in the form of mixture of liquid drops and vapor [3, 4].

In report we numerically investigate the tensile strength of metal melts and its dependence on temperature and strain rate. For simulations we use our previously developed computational model of cavitation and tensile fracture of metal melt. This model treats the metal as a two-phase medium which can be a singly connected liquid with (or without) vapor cavities—on the first stage of evolution; and a singly connected vapor with liquid drops—on the last stage. Thermo-fluctuation nucleation and viscous growth of cavities are considered, as well as the energy and the mass exchange between phases. Cavities can be nucleated in uniform liquid as a result of thermal fluctuations, than the tensile strength is determined by surface tension, first of all. Meanwhile, the target material often has initial pores, and if they remain after melting, they can be the cavitation centers at tension and can considerably decrease the tensile strength. In present investigation influence of initial porosity on the tensile strength is analyzed.

This work was supported by the Russian Foundation for Basic Research (Grant No. 14–01–31454) and the Grant of the President of Russian Federation (MD-286.2014.1).

1. Inogamov N. A., Zhakhovsky V. V., Petrov Yu. V., et al. // Contrib. Plasma Phys. 2013. V. 53. P. 796.
2. Markov A. B., Kitsanov S. A., Rotshtein V. P., et al. // Rus. Phys. J. 2006. V. 49. No 7. P. 758.
3. Mayer P. N., Khishchenko K. V., Levashov P. R., Mayer A. E. // Physics of Extreme States of Matter - 2012. IPCP RAS, Chernogolovka, 2012. P. 113.
4. Mayer P. N., Mayer A. E. // Techn. Phys. Lett. 2012. V. 38. P. 559.

STABILITY OF DEFECTS IN NUCLEAR MATERIALS CLOSE TO PHASE TRANSITIONS

Kuksin A. Yu.

JIHT RAS, Moscow, Russia

alexey.kuksin@gmail.com

Stability, as well as mobility, of point defects and clusters are important factors influencing the behavior of nuclear materials under irradiation. Difference in clustering of interstitials and vacancies provide a driving force for swelling of the material. Diffusivity of stable clusters of interstitials limits the rate of many diffusion-controlled reactions. Moreover, clusters of interstitials possess 1D character of diffusion and are supposed to play a role in formation of superlattices of voids or fission product bubbles.

This work is devoted to study the mechanism, providing the stability of point defects and dislocation loops: both produced during irradiation and shear plastic deformation. The comparison of energies of the defects with different crystallographic orientations is based on the molecular dynamics calculations for temperatures up to a melting point. Several interatomic potentials for γ-U (including new potentials suggested by Beeler et al. and by Smirnova et al. for description of gamma and alpha phases of U), U-Mo alloy and Fe are used in calculations. Both γ-U and α-Fe (at high temperature, close to $\alpha - \gamma$ phase transition) are metals with base centered cubic (BCC) lattice, however the mechanical stability, determined by the shear stiffness constant $(C_{11} - C_{12})/2$, is close to the limit. The corresponding anisotropy of the elastic moduli may lead to the preferential stability of the defects, unusual for most BCC metals.

It is shown for γ-U that the formation energy of self-interstitial atoms is lower, than vacancies. It implies the anomalous self-diffusion controlled

mostly by interstitials. The other effect is that 1D diffusion of interstitials takes place mostly along ⟨100⟩ crystallographic direction instead of ⟨111⟩typical for other BCC metals. This difference may result in an unusual FCC structure of superlattices of voids or bubbles formed in U-Mo alloy during irradiation, while in most BCC metals (including pure Mo) voids arrange themselves into a BCC superlattice. The latter peculiarity has been observed recently in the experiments. The effect of the elastic anisotropy on the structure of shear dislocation loops formed during plastic deformation is also considered.

RESONANT RAYLEIGH SCATTERING BY 2DES IN HIGH MAGNETIC FIELD

Bisti V.E.,* Zhuravlev A.S., Kulik L.V.

ISSP RAS, Chernogolovka, Russia

**bisti@issp.ac.ru*

The resonant Rayleigh scattering (RRS) in two-dimensional electron system (2DES) has been studied in the ultraquantum limit of magnetic fields. The processes including two spin subbands of the zero Landau levels have been considered. It is shown that the main contribution to the resonant Rayleigh scattering is due to localized electrons. This localization is caused by the fluctuations of random impurity potential. A scattering process of the considered type is possible for electron-hole pairs localized in space on a length much shorter than the light wavelength. It is proportional to the number of free localized states multiplied by the squared matrix element for the corresponding RRS transition. Another channel for the resonant Rayleigh scattering is connected with delocalised two-dimensional electrons. This process is considered theoretically in [1], where it is stated that only the partially filled Landau levels are active in this channel of RRS. The new differential technique for obtaining high quality RRS spectra is developed in the previous work [2]. In this work the temperature dependence of the RRS intensity for two allowed optical transitions with different polarizations from the zero heavy hole Landau level to the zero electron Landau level is presented. If low-energy localized states of the lower electron Landau level are filled, the RRS line on this level does not observed. With the rise of the temperature the part of localized electrons transfer to the next higher energy Landau level, and the intensity of RRS line on the lower energy level give rise with the temperature. There is no expected signal from RRS on delocalized electrons, even if the corresponding electron states are partially filled. The obtained

results give the possibility to conclude, that RRS in the 2DES in high magnetic field is connected with excitations of localized electrons from the low-energy side of Landau levels ([3].

1. Vitlina R.Z., Magarill L.I., Chaplik A.V. // ZhETP. 2013. V. 144. No 6. P.1282.
2. Kulik L. V., Ovchinnikov K., Zhuravlev A. S., Bisti V. E., Kukushkin I. V., Schmult S., and Dietsche W. //Phys. Rev. B. 2012. V. 85. P. 113403.
3. Bisti V. E., Kulik L. V., Zhuravlev A. S., Shablya A.O., Kukushkin I. V. //Pis'ma v ZhETP. 2013. V. 98. No 12. P. 877.

STRUCTURE AND PHOTOLUMINESCENCE OF SiGeC IN THE 3C–SiC/SiGeC/Si(100) HETEROSYSTEM

Steinman E.A.,[*1] ***Orlov L.K.***[2]

[1]*ISSP RAS, Chernogolovka,* [2]*IPM RAS, Nizhny Novgorod, Russia*

[*]*steinman@issp.ac.ru*

Increased interest to SiC semiconductor is related to its particular properties, such as high electron mobility, high breikdown electric field, very good thermal characteristics. These properties make it the foremost semiconductor material for the short wavelength optoelectronics, high temperature, radiation resistant, high power abd high frequency electronic devices. On the other hand, taking into account the dominating position of Si in electronics, it is very important to find ways for combining these two materials in one device. Therefore, growing high quality epitaxial layers on Si substrates is an important task for modern microelectronics. The main obstacle for solving this problem is a considerable discrepancy of the crystal structure parameters of SiC and Si. In the present work one of possible ways for solving this problem is discussed. It is based on the use of intermediate solid solution of Si-Ge-C and Si-C. The overwhelming results achieved in the formation, band structure and corresponding properties of Si-Ge-C compounds enabled to create various devices, that ensure advancement of millimeter wave Si devices. The Si-Ge-C system can realize larger and smaller lattice constants compared to Si. This allows lowering the elastic stress at the heterojunction. Addition of 1% of C compensates deformation conditioned by addition of 8% of Ge. The problems are related to the formation of a thin SiGeC base region on the 3C-SiC/Si(100) heterojunction, which is formed during low temperature carbonization of Si surface by molecular beam hydrides and hydrocarbons. X-ray diffraction, secondary ion mass spectroscopy, IR photoluminescence were used to

investigate the properties of the structures. It is shown that a higher Ge content under the SiC film was present even than addition of germanate into the reactor was carried out after creation of a SiC film on Si surface. It is also shown that the structures obtained had well pronounced diode characteristics even at room temperature. The part of the luminescence observed in these layers is likely to be due to recombination via the defect centers in the base region of SiGeC. This is suggested by behavior of the corresponding PL bands.

1. A.R.Powell, K.Eberl, B.A.Ek and S.S.Lyer, Journal of Crystal Growth 127 (1993) 425–429 North-Holland
2. L.K.Orlov, Steinman E.A.,Ivina N.L., Vdovin V.I., Fizika tverdogo tela 2011, 53, 9, P. 1706.

INVESTIGATION OF NOVEL SUPECAPACITOR ELECTRODE MATERIALS FOR RENEWABLE ENERGY SYSTEMS APPLICATION

Vervikishko D.E.,* Yanilkin I.V., Sametov A.A., Atamanyk I.N., Grigorenko A.V., Shkolnikov E.I.

JIHT RAS, Moscow, Russia

**vitkina-darya@yandex.ru*

The study is devoted to the activated carbons structure produced by different techniques and different raw materials and their behavior in model supercapacitor cell. Experiments were carried out to estimate the specific power and specific energy consumption for model cells with different composition of the specimen—aqueous and organic electrolytes, activated carbons based on peat, petroleum pitch, wood of different origins. The results obtained showed that activated carbons obtained from a petroleum pitch and rice husk to be promising candidates for supercapacitor applications. Maximum obtained specific capacitance of the electric double layer was 360 F / g. This result is obtained for T-3 activated carbon, synthesized from wood using sodium hydroxide as catalyst. sulfuric acid with density of 1.2 g/cm^3 was used as electrolyte. For this type of carbon lifetime tests were also conducted, which showed preservation of cell parameters on after 160,000 cycles and the number of studies aimed at reducing the rate of self-discharge. It is shown that the self-discharge of the cell from 1000 to 500 V occurs within 92 hours, which is important from the point of view of possible applications of supercapacitors in systems with renewable energy sources.

The possible applications of supercapacitors in systems with renewable energy sources will be discussed. It is shown that it is expedient in case of a short high peak power, if the energy used in the standard battery is not high enough and does not allow for the discharge currents to cover characteristic peak. There are also a number of applications related to the presence of the consumer powerful electric motors with high starting currents, in which the competitiveness of ultracapacitors over batteries is significantly increased.

UV CURED POLYMERS AS A WORKING MEDIA FOR PULSED PLASMA GENERATORS

Loktionov E. Yu.

BMSTU, Moscow, Russia

stcpe@bmstu.ru

Pulsed plasma generators and thrusters use mainly solid active media in spite of sophisticated transportation and dosing system need. This can be partially resolved in laser plasma generators, where energy is delivered to the source of ablating matter. Liquid media could be much preferable since their transportation and dosing (down to 10^{-12} l) is well developed, but plasma generation results in intensive droplet formation and kinetic energy losses. Combination of liquids transportation advantages and solids plasma generation efficiency is preferable. Liquid-to-solid transition can be induced by cooling down to phase transition temperature, thermo-, photo- or electron induced polymerization. Light cured polymers seem to be very useful as active media for plasma generators, since they can be solidified very fast (ca. 30 ms) just before impact. For the first time we have investigated mass flow rates, momentum coupling coefficient, specific impulse and energy efficiency of both solid and liquid phase of UV curing polymers under 266 and 355 nm nanosecond (12 ns) laser irradiation at ambient conditions. For 266 nm irradiation solid (polymerized with 405 nm laser diode) and liquid phases of investigated UV-inks have demonstrated about similar characteristics relation known for water and ice: liquid phase had greater plasma formation threshold (4.67 vs. 1.02 J/cm^2), mass flow rate (6.77 vs. 0.35 mg/J) and momentum coupling coefficient (0.933 vs. 0.167 mN/W), solid phase had greater specific impulse (476 vs. 138 s), and energy efficiency was about equal (0.064 for liquid and 0.04 for solid). The results of 355 nm irradiation (365 nm is optimal for used medium polymerization) make us to suppose polymerization induced by pulsed laser radiation (plasma formation thresholds were 6.3 J/cm^2 for liquid and 2.69 J/cm^2

for solid), since mass flow rate of initially liquid phase (0.268 mg/J) reduced almost down to solid one (0.21 mg/J) and specific impulse was even greater (1357 s, and 909 s for solid), this resulted in 0.226 energy efficiency of liquid as compared to 0.088 for solid (momentum coupling 0.333 and 0.175 mN/W respectively). The obtained results demonstrate that light cured polymers can be used as working media for pulsed plasma generators. In case of high-power irradiation with a wavelength close to an optimal one for photopolymerization, no preliminary curing is needed, and lenergy efficiency can be even greater than for initially polymerized matter. Use of light curing polymers makes special active media (incl. heterogeneous mixes) preparation, transportation and dosing much easier.

TEMPERATURE DEPENDENCE OF THE EFFECTIVE HEAT CAPACITY OF LIGNOCELLULOSIC MATERIALS

Director L.B., Sinelshchikov V.A.,* Sytchev G.A.

JIHT RAS, Moscow, Russia

**sinelshchikov@mail.ru*

As a result of the heating of lignocellulosic materials, which first of all include various types of vegetal biomass, their decomposition occurs, leading to a change in the aggregate state of the initial material (the final products: solid, liquid and gas phases). In this case complex physical and chemical processes follow, some of which is exothermic. Investigations, aimed at the determination of the temperature dependence of effective heat capacity of lignocellulosic materials and the influence of heating conditions on it, are of interest both from a fundamental point of view and from the point of view of practical application of pyrolytic methods of biomass processing for energy purposes. Data in the literature on this subject are often contradictory and their comparison is difficult because of differences in experimental conditions in which they were received. In the paper there are presented results of experimental investigations of the process of thermal decomposition of wood in the temperature range of 50–500°C. The methods of thermogravimetric analysis (TGA) and differential scanning calorimetry (DSC) were used. Experiments were carried out in an inert gas atmosphere (nitrogen). Comparison of the thermogravimetric curves with the curves, described the temperature dependence of effective heat capacity of an investigated material and obtained in the process of heating (heating rate 10°C/min), has demonstrated the correspondence between the processes of thermal decomposition of main organic components (hemicellulose, cellulose and lignin) and the characteristic endo-and

exothermic peaks in the curve of effective heat capacity. It was shown experimentally that the change of the characteristic size of the investigated sample, as well as its pre- heat treatment in an inert gas atmosphere (so called torrefaction) lead to changes in the temperature dependence of the effective heat capacity in the temperature range corresponding to the thermal decomposition of hemicellulose. The presence of the temperature regions in which the heat, generated as a result of the exothermic reactions, leads to a change in sign of the effective heat capacity was experimentally demonstrated.

BIOMASS PYROLYSIS KINETICS RESEARCHING

Bessmertnykh A.V., Sytchev G.A.,* Zaitchenko V.M.

JIHT RAS, Moscow, Russia

**george.sytchev@gmail.com*

The pyrolysis technology (carried out at the temperatures up to 1000°C without oxygen access) allows improving the energy efficiency and workability of biomass utilization. In the pyrolysis process organic compounds of the initial biomass is decomposed with forming of a non-condensable gases (CO, CO_2 , H_2, CH_4 , etc.), the solid residue and vapors.

The pyrolysis process is controlled (with desired composition of products) by changing the process parameters (temperature, pressure, heating rate, the gas environment composition, the hold up time in pyrolysis reactor). Availability of kinetic equations linking technological parameters and vent of the pyrolysis products with biomass hold up time at preset temperature range is the necessary condition for pyrolysis process controlling. Obtaining of the pyrolysis kinetic parameters based on experimental data of the thermogravimetric analysis was the purpose of this study. The authors studied many types of biomass (not only well-known (i.e. wood) but also those data which is under-explored: crop wastes and chicken litter).

Next kinetic constants were received: the order of the pyrolysis process, the activation energy and pre-exponential factor—for various types of plant biomass: wood, corn straw, rice husk, chicken litter. Obtained constants allow to calculate the reactor characteristics for fixed products of pyrolysis process receiving.

Some further research directions:

-the kinetics constants for different heating rates determination;

-the pyrolysis kinetics in various gas atmospheres exploration;

-study the effect of internal thermal effects (exothermic) on the kinetics of pyrolysis.

BIOMASS-TO-ENERGY COMPLEX THERMAL CONVERSION

Kosov V.F., Lavrenov V.A.,* Zaitchenko V.M.

JIHT RAS, Moscow, Russia

**v.a.lavrenov@gmail.com*

Biomass is a renewable energy source with a great potential. Biomass-to-energy conversion technologies are intensively developed today. Many different processes for converting chemical energy of solid fuels (including biomass) into electricity and heat have been invented. Thermal conversion processes are very efficient for producing energy from biomass. Pyrolysis and gasification are well known and widely spread technologies for the gaseous fuels production from solid biomass. Gaseous fuel has several advantages over solid fuel. The gaseous fuel use in the gas turbines and gas-engine power plants allows efficiently produce electricity and heat. However, conventional processes such as pyrolysis and gasification have several disadvantages. Among them, low calorific value and high levels of dust and tars in the product gas from gasification or low degree of solid fuel energy conversion during pyrolysis process.

The two-stage thermal conversion method has been developed at the Joint Institute for High Temperatures RAS. The first stage is pyrolysis of biomass into solid, liquid and gaseous products. On the second stage the pyrolysis products is blown through the porous carbon at the temperature of about 1000°C. Here pyrolysis products convert into hydrogen and carbon monoxide. The volume of syngas is about 1.4 Nm^3 per kg of processed biomass and its calorific value is about 11 MJ/Nm^3. The absence of the liquid fraction in the final products is also an advantage of the proposed scheme.

The pilot plant capacity of 50 kg of biomass per hour based on the two-stage thermal conversion of biomass has been designed and tested.

BIOMASS TORREFACTION PLANT

Kosov V.F., Kuzmina J.S.,* Zaitchenko V.M.

JIHT RAS, Moscow, Russia

**juli_kuzmina@mail.ru*

Torrefaction (low temperature pyrolysis) is a relatively new and promising way to upgrade thermotechnical characteristics of biomass solid fuel. This method is the thermal treatment of a pre-pelletizied material (heating up to the temperature near 300°C) in oxygen-free environment. This

process gives rise to formation of hydrophobic product, increment of density and combustion heat of produced fuel in comparison with initial raw materials. Torrefaction and pelletization combination (so-termed TOP-process) obtains up to 30%-decreasing of storage and portage investments. Depending on torrefaction operating parameters combustion heat value of torrefied wood-waste pellets can reach 19–23 MJ/kg.

In JIHT RAS a pilot torrefaction moving bed plant with capacity of 50 kg/h of initial biomass was successfully tested. Researching has shown the possibility of torrified biomass obtaining by using exhaust products of gas-piston engine as a source of a heat. Pilot plant has to prove it is able to continuously produce large volumes of high quality torrefied product.

USE OF THE THERMOCHEMICAL CONVERSION METHOD FOR SEWAGE SLUDGE UTILIZATION FROM WASTEWATER TREATMENT FACILITY

Zaitchenko V.M.,[1] ***Kuftov A.F.,***[2] ***Umnova O.M.****[1]

[1]*JIHT RAS,* [2]*BMSTU, Moscow, Russia*

**umnova.olya@gmail.com*

To date, the problem of sewage sludge utilization is a very urgent and requires new approaches to its solution. The fact that the amount of sewage sludge is great because of its high relative humidity (96–98%), and the area of sludge bed which sludge stored is limited. Overflow of sludge bed leads to an ecological catastrophe of areas and water contiguous to the wastewater treatment facility. One way of utilization of sewage sludge is fermentation of sludge in anaerobic digesters. However, in the process the volume of sewage sludge decreases only 5–6%. Mechanical dehumidification of sludge reduces relative humidity to 80–85%, the use of flocculants—up to 50–60%. Application of thermal drying even after using flocculants is a very costly process in terms of energy. At the same time it is known that the dry residue of sewage sludge contains up to 85% of organic substances. In this paper, we propose to use the heat content of the sludge organic component for providing of drying process. We propose the concept sewage sludge utilization, which consists of four sequential processing steps: dehydration of sludge using flocculants (relative humidity decreases to 50–60%), thermal drying (relative humidity decreases to 15–12%), pelletizing (granulation), thermo-chemical conversion (low temperature pyrolysis) of granular dry residue with the fuel gas yield. The latter can be used to provide the energy needs of the sewage sludge recycling process. In this paper, the results of preliminary experiments in

support of the proposed scheme are presented, in particular the composition and volume of the resulting gaseous fuel. Estimates of material and energy balances that the proposed approach can provide autonomous operation of the sewage sludge utilization complex.

THE CREATION OF AUTONOMOUS POWER COMPLEX USING LOCAL FUEL AND ENERGY RESOURCES

Korostina M.A.,* Maikov I.L., Zaitchenko V.M.

JIHT RAS, Moscow, Russia

**korostina@inbox.ru*

The local fuel and energy resources include wood and agricultural waste, peat and other types of waste. In Russia, there is 47% of world reserve of peat and about 25% of the wood one. The system of distributed power generation using local resources creating is a priority for the development of fuel and energy complex. The solution of this problem is connected with the development of technology for the thermal conversion of biomass to produce energy gas with high thermal performance and the creation of energy equipment using produced gas as a fuel. Well-known pyrolysis and gasification processes of producing energy gas from carbonaceous materials due to a number of restrictions cannot be effectively used in the existing power equipment to generate electricity and heat. For the purposes of distributed power generation of up to 3 MW most feasible from an economic point of view is to use the gas piston power plants and mini-TPP.

The parameters of the new process for the thermal conversion of biomass with gas fuel with high thermal parameters producing is developed in JIHT RAS are shown. The results obtained during the first phase of tests of gas piston stations at work on gasification products are presented. The influence of the gas fuel characteristics on the gas piston station operational efficiency is analyzed. On the basis of the researching complex measures aimed at improving of the efficiency of gas-piston power plants and mini-TPP using biomass conversion products as a fuel was discussed.

CHARGED DUST IN PLASMA UNDER LABORATORY AND MICROGRAVITY CONDITIONS: ORDERED STRUCTURES AND PHASE TRANSITIONS

Petrov O.F.,[*1] ***Fortov V.E.,***[1] ***Vasiliev M.M.,***[1] ***Tun Y.,***[2] ***Stacenko K.B.,***[1] ***Vaulina O.S.,***[1] ***Vasilieva E.V.,***[1] ***Lisin E.M.,***[1] ***Myasnikov M.I.***[1]

[1]*JIHT RAS, Moscow,* [2]*MIPT, Dolgoprudny, Russia*

[*]*ofpetrov@ihed.ras.ru*

The charged dust system represent a non-neutral or quasi-neutral systems (dusty plasmas) containing micron-sized particles of a substance with electrical charges up to 102–105e. As a result of strong interaction, the dust particles may form the ordered structures of liquid and crystal types. The laboratory dusty plasma is the unique object for studying the structures, phase transitions and transport phenomena on the kinetic level. The phase transitions in quasi-two-dimensional dust structures suspended in rf discharge were studied. The experimental results have revealed the existence of hexatic phase as well as solid-to-hexatic phase and hexatic-to-liquid transitions. The spatial distribution of pair interparticle interaction forces was recovered by the original method based on solving the inverse problem using Langevin equations. The measured phase-state points with the theoretical phase diagram of two-dimensional Yukawa system have been obtained. The formation of ordered structures from large number ($\sim$104) of charged diamagnetic dust particles in a cusp magnetic trap was studied under microgravity conditions onboard ISS. The magnetic susceptibility and charge of the particles have been estimated. The numerical simulations of the lunar plasma-dust exosphere caused by action of solar ultraviolet radiation and the incoming solar wind on the lunar surface have been carried out. The influence of the solar wind flux on the near-surface photoelectron sheath formation as well as conditions of dust levitation above the lunar surface have been analyzed. This work was partially supported by the Russian Foundation for Basic Research (Projects No. 13–02–01393 and 13–02–12256) and by the Program of the Presidium of RAS 'Matter under High Energy Densities'.

POLARIZED REFLECTIVITY PROPERTIES OF STRONGLY CORRELATED PLASMA

***Zaporozhets Yu.B.,*[1] *Mintsev V.B.,*[1] *Gryaznov V.K.,*[1] *Reinholz H.,*[2] *Röpke G.,*[2] *Fortov V.E.*[3]**

[1] *IPCP RAS, Chernogolovka, Russia,*
[2] *University of Rostock, Rostock, Germany,* [3] *JIHT RAS, Moscow, Russia*

**yubz@icp.ac.ru*

The analysis of the response of dense plasma to electromagnetic waves of moderate intensity can be used as a tool to investigate the validity of the physical models describing the behavior of matter under extreme conditions, high temperatures and pressures. Angular dependence of s- and p-polarized reflectivities at several wavelengths can be used in the integration of Maxwell equations to construct the spatial profile of the density of charge carriers.

Within this work, the new experimental data on oblique incidence of polarized electromagnetic wave, are presented. The study of polarized reflectivity properties of nonideal xenon plasma was accomplished using laser light at ν_{las}=2.83·10^{14} s^{-1}, ν_{las}=4.33·10^{14} s^{-1} and ν_{las}=5.66·10^{14} s^{-1}. The measurements of polarized reflectivity coefficients of explosively driven dense plasmas have been carried out at incident angles up to θ= 75 degrees.

The plasma composition was calculated within a chemical picture [1] and the integration of Maxwell equations are based on an interpolation formula for dc conductivity [2].

---

1. Ebeling W., Förster A., Fortov V., Gryaznov V. and Polishchuk A. Thermophysical Properties of Hot Dense Plasmas. Stuttgart: Teubner, 1991.
2. Esser A. Redmer R. Röpke G. // Contrib. Plasma Phys. 2003. V. 43. P. 33–41.

THERMODYNAMICAL PROPERTIES OF SEMICLASSICAL PARTIALLY IONIZED HYDROGEN AND HELIUM PLASMA

Akhtanova G.B.,* Gabdullin M.T., Ramazanov T.S., Ismagambetova T.N.

KAZNU, Almaty, Kazakhstan

**g.akhtanova@gmail.com*

Non-ideal dense hydrogen and helium plasma has attracted particular attention not only because it is a substance that forms such astrophysical

objects as the bowels of the giant planets (Jupiter and Saturn) and white dwarfs, but also because it can be used in terrestrial conditions, for example, in inertial fusion reactors. Dense (non-ideal) plasma is such a physical system where the interactions between particles play a dominant role, when potential energy at an average distance exceeds their thermal energy. This paper considers thermodynamic properties of partially ionized hydrogen and helium plasma consisting of electrons and ions for following parameters:

Interactions between ionized particles were considered on the basis of the micropotential [1], which takes into account quantum-mechanical effects of diffraction and symmetry at small distances, and for interactions between ionized particles with atoms on the basis of effective potential [2]. Composition of partially ionized plasma was calculated using Saha equation taking into account the reduction of the ionization potential derived from the potential [1]. Thermodynamical properties of plasma (internal energy and equation of state) were obtained through radial distribution functions and interaction potentials between particles, where collective effects were taken into account due to use of hyperchain approach (HCA) in solution of integral equation of the Ornstein-Zernike [3]. The obtained results were compared with the data of other authors.

1. Zh. A. Moldabekov, T. S. Ramazanov, and K. N. Dzhumagulova // Contrib. Plasma Phys. 2012. V. 52. P. 207–210.
2. T.S.Ramazanov, K.N. Dzhumagulova, Yu.A. Omarbakiyeva // Phys. Plasm. 2005. V. 12.
3. L. David, Dover publications, Inc.,P. 500 P. 207–210.

ION RECOMBINATION IN DENSE PLASMA

Lankin A.V.

JIHT RAS, Moscow, Russia

Alex198508@yandex.ru

The results for the rate of recombination in the ion plasma are studied in the work. It is obtained by processing the data of experimental studies of the afterglow of the gas discharge in the environment of sulfur hexafluoride. Slowing the rate of recombination in such media is more as compared to the standard formula for ideal plasma. Deceleration increases with growth the parameter coupling. In the analysis of the mechanism of this phenomenon is set a number of features of ion recombination in strongly coupled plasmas.

The molecular dynamics model that effectively takes into account the collision of charged particles with the neutral component of the system is built. Its use is allowed to confirm the applicability of the model (Lankin, 2008) suppression of recombination in strongly coupled plasma due to the formation of zones of many fluctuations, separating the area of free charged particles and pairs of states to describe a plasma formed in the afterglow of the discharge in media of SF_6. In this case, the recombination rate constant can be described as:

$$k`(P,T,\Gamma) = \begin{cases} k_0(T) \quad for \quad \Gamma < \Gamma_0 \\ \beta \cdot k_0(T) exp[-A/2(2\Gamma + \Delta/T)] \quad for \quad \Gamma > \Gamma_0 \end{cases} \tag{1}$$

where k_0 - recombination rate constant in the limit of an ideal plasma, Δ - an additional contribution of ion-molecule interactions in the width of zone of many-width fluctuations, Γ_0 - point change in the mechanism of recombination, A - model parameter, β - is determined from the continuity of function.

In this case, the coupling parameter Γ_0 at which the change in the mechanism of recombination in the ion plasma is less than the electron-ion plasma, because of the increased width of zone of the fluctuations as a result of many-particle interactions of ions and neutral molecules. In addition, parameter A is reduced several because of the higher probability of large-angle scattering of ion-molecule collisions, compared with the electron-electron.

SPECTRUM OF PRESSURE FLUCTUATIONS IN NON-IDEAL PLASMA

Bystryi R.G.

JIHT RAS, Moscow, Russia

broman.meld@gmail.com

Not Gaussian fluctuations of pressure equilibrium none ideal plasma are presented in article [1]. It directly contradicts [2]. General purpose of this work was to give some explanation of this discrepancy.

The classical molecular dynamics method (MD) is used. Instantaneous values of pressure are calculated at the each step using formula based on virial theorem. Spectrum fluctuations of pressure of singly ionized non ideal plasma are studied. $1/f$-like spectrum behavior are observed. In other words flicker noise is observed in fluctuations of pressure equilibrium non ideal plasma.

For Coulomb systems pressure and potential energy are strongly correlated values [3]. There are articles [4, 5] which reported flicker noise in potential energy of their system. In both cases it is biophysical MD system with a strong coulomb interaction. This demonstrates that the flicker noise is observed for a fairly wide range of different Coulomb systems.

The relationship between the obtained results and conventional theories of pressure fluctuations [3] is discussed.

1. Lankin A., Norman G., Saitov I. Pressure Fluctuations in Nonideal Plasma //Contributions to Plasma Physics. – 2010. – V. 50. – P. 99–103.
2. Landau L. D., Lifshitz E. M. Statistical Physics, Part 1: V. 5 (Course of Theoretical Physics, Volume 5). – 1980.
3. Rudoi Yu.G., Suhanov A.D // UFN. – 2000. – V. 170. – N .12. – P. 1265–1296.
4. Bizzarri A. R., Cannistraro S. Flickering noise in the potential energy fluctuations of proteins as investigated by MD simulation //Physics Letters A. – 1997. – V. 236. – N. 5. – P. 596–601.
5. Sasai M., Ohmine I., Ramaswamy R. Long time fluctuation of liquid water: 1/f spectrum of energy fluctuation in hydrogen bond network rearrangement dynamics //The Journal of chemical physics. – 1992. – V. 96. – P. 3045.

THE ELECTRONIC TRANSPORT COEFFICIENTS AND PRESSURE CALCULATIONS IN PLASMA OF Ti AND Zn

Apfelbaum E.M.

JIHT RAS, Moscow, Russia

apfel_e@mail.ru

The thermophysical properties of various substances are very important in different fundamental tasks and applications. (Here we will consider the electrical conductivity, thermal conductivity, thermal power and pressure). So the corresponding studies have started more than a century ago. But the region of plasma (i. e. the temperatures $T \geq 5$ kK) was of especial difficulty in this researches up to now. The measurements of conductivity, internal energy and pressure in this area have appeared only recently [1–4]. But the temperature can not be measured directly in these experiments. So the development of corresponding theoretical models is still necessary.

In our previous works [5–7], we have developed the model to calculate the ionic composition, electronic transport coefficients, pressure, internal energy for the plasma under study. The ionic composition was calculated on the basis of so-called generalized chemical model (GCM), which originates from well-known Saha or action mass law approach. The pressure

and internal energy can also be obtained by means of this technique. The coefficients were calculated within the relaxation time approach (RTA). The range of applicability of both techniques (GCM and RTA) is limited by the density from above (see corresponding estimates in [6, 7]). But the experimental data [1–4] are located in the area where the application of our approach is still correct. Our model has been successfully applied for plasmas of noble gases, noble metals, silicon and boron [5–7]. Here we use it for two more metals—titanium and zinc. The measurements of the properties under study for titanium are presented in [1, 2], while for zinc—in [4] (at $T \geq 10$ kK). Our calculations have also been carried out under these conditions. The obtained results are in good agreement with the results of measurements and calculations of other authors.

1. Clerouin J., Noiret P. et. al. // Phys. Plasmas. 2012. V. 19. 082702.
2. DeSilva A. W., Vunni G. B. // Phys. Rev. E. 2011. V. 83. 037402.
3. Korobenko V. N., Rakhel A. D. // Phys. Rev. B. 2013. V. 88. 134203.
4. Haun J. et. al. // Phys. Rev. E. 2002. V. 65. 046407.
5. Apfelbaum E. M. // Contr. Plasma Phys. 2011. V. 51. P. 395.
6. Apfelbaum E. M. // Phys. Rev. E. 2011, V. 84. 066403.
7. Apfelbaum E. M. // Contr. Plasma Phys. 2013. V. 53. P. 317.

MD STUDY OF MICROSCOPIC DIFFUSIVE PROCESSES LEADING TO ANOMALY IN IONIC LIQUID

Ivanovskis G.

JIHT RAS, Moscow, Russia

ivanovakis@mail.ru

Room temperature ionic liquids are organic salts with melting temperatures below 100°C. Common features of this chemical compound class includes high charge carrier density, chemical stability, non-flammability and non-volatility which makes them promising candidates for a series of electrochemical applications ranging from reaction media and cellulose dissolution to solar batteries and supercapacitors. Their organic nature makes it possible to adjust smoothly properties of the ionic liquid for a specific application.

Transport properties of the ionic liquids are as important as their thermodynamic characteristics for their usage as supercapacitor electrolyte. While thermodynamics define specific energy density of the device, specific power and charging/discharging time is mostly dependent on dynamic properties of electrolyte. This work is focused on study of diffusion process

in bulk 1-buthyl-3-methylimidazolium tetrafluoroborate ($[bmim]^+[BF_4]^-$) ionic liquid at room temperature.

It was previously shown [1] that in this system a time dependence of mean square displacement of ion centers of mass undergoes a long subdiffusive transition from ballistic to diffusive regime taking place on timescales from 1 ps to 1 ns. Therefore longer simulations are needed to carefully calculate diffusion coefficients of ions. In the same time investigation of ion dynamics during subdiffusion provides better understanding of diffusion mechanisms and factors leading to subdiffusive anomaly. Both approaches give valuable information for ionic liquid supercapacitor technology and enhance our fundamental vision of diffusion in electrolytes.

---

1. Ivanovskis G., Norman G. E., Usmanova D. R. // Doklady Physics. 2012. V. 57. No. 11. P. 150.

STUDY OF ULTRACOLD PLASMA AND RYDBERG ATOMS IN A MAGNETIC FIELD

Zelener B.B.,[*1,2] ***Bobrov A.A.,***[1] ***Saakyan S.A.,***[1]
Butlitsky M.A.,[1] ***Khikhlukha D.R.,***[1] ***Sautenkov V.A.,***[1,3]
Zelener B.V.,[1] ***Fortov V.E.***[1]

[1]*JIHT RAS,* [2]*MEPhI,* [3]*LPI RAS, Moscow, Russia*

**bobozel@mail.ru*

In our simulations we use Monte-Carlo and molecular dynamics methods [1–3]. Our simulations of molecular dynamics show that magnetic field can strongly reduce of the recombination plasma rate. The variation of recombination rate can be change by several orders to compare with magnitude of the recombination rate at B = 0. We assembled setup for preparation and study of ultracold lithium plasma by using tunable lasers [4]. Behavior of laser cooled plasma in external magnetic fields will be investigated. Our studies of ultracold plasma in magnetic field were initiated by opportunity to control laser cooled plasma and possibility to increase a production of anti-hydrogen atoms from cold antiprotons and positrons also for quantum computers. This work was supported by the MK—4092.2014.2, the RFBR 14–02–00828, the Presidium of the RAS (Basic Research Program “ Investigation of Matter in Extreme States ” headed by V.E. Fortov), and the Ministry of Education and Science of the Russian Federation federal program No: 8679, 8513, and 8364.

---

1. Bobrov A. A., Bronin S. Ya., Zelener B. B, Zelener B. V, Manykin E. A., and Khikhlukha D. R. // J. Exp. Theor. Phys. 112, 2011, P. 527.
2. Bronin S. Ya., Zelener B. B, Zelener B. V, Manykin E. A. and Khikhlukha D. R. // J. Exp. Theor. Phys., 2011, 112, 717.
3. Zelener B. B, Zelener B. V and Manykin E. A. // JETP Lett., 2011, 94, 525.
4. Zelener B. B., Saakyan S. A., Sautenkov V. A., Akul'shin A. M., Manykin E. A., Zelener B. V., Fortova V. E. // JETP Letters, 2013, V. 98, No. 11, P. 670–674.

PROTON ENERGY RELAXATION IN ELECTRON GAS IN UNIFORM MAGNETIC FIELD

Bobrov A.A.,[*1] ***Bronin S.Y.,***[1] ***Zelener B.B.,***[1,2] ***Zelener B.V.,***[1] ***Manykin E.A.,***[2] ***Khikhlukha D.R.***[1]

[1] *JIHT RAS,* [2] *MEPhI,* [3] *NRC KI, Moscow, Russia*

[*] *abobrov@inbox.ru*

In experiments on antihydorgen antiprotons are injected into a cloud of ultracold electron gas in magnetic field forming a non-neutral plasma (density of the positrons is about 10^8 cm^{-3} and density of the antiprotons is about 50 times less than that). Antihydrogen is formed during collision recombination process. Great energy difference is one of the problems, the energy of antiprotons is about 100 K that is much higher than positron temperature ($\sim$ 10 K). Because of this it is important to know relaxation rate of the antiproton energy. In this work the relaxation process is studied in analogous convenient system of protons and electrons with the same energies and densities taking into account the presence of magnetic field and non-neutrality. Analytical expression for relaxation rate of proton energy is proposed. Molecular dynamics simulations of the relaxation were also conducted. Results of the simulations agree with analytical expression.

This work was supported by the MK—4092.2014.2, the RFBR 14–02–00828, the Presidium of the RAS (Basic Research Program " Investigation of Matter in Extreme States " headed by V.E. Fortov), and the Ministry of Education and Science of the Russian Federation federal program No. 8679, 8513, and 8364.

MAGNETO-OPTICAL TRAP FOR LASER COOLED LITHIUM ATOMS

Saakyan S.A.,[*1] ***Sautenkov V.A.,***[1,2] ***Akulshine A.M.,***[3] ***Vilshanskaya E.V.,***[1,4] ***Zelener B.B.,***[1,5] ***Zelener B.V.***[1]

[1]*JIHT RAS,* [2]*LPI RAS, Moscow, Russia,*
[3]*SUTMA, Melbourne, Australia,* [4]*MPEI,* [5]*MEPhI, Moscow, Russia*

[*]*saasear@gmail.com*

The goal of this work is to obtain a high density of ultracold atoms ^{7}Li in order to create Rydberg matter and ultra-cold plasma [1–3]. A setup for laser cooling and confining of ^{7}Li atoms in a magnet-optical trap has been built. The possibility of cooling and trapping of ^{7}Li atoms in a wide range of frequency detuning of the cooling laser has been proved experimentally [4]. Density and number of ultracold ^{7}Li atoms on various ground-state sublevels have been measured by using a probe tunable laser. Also the temperature of atoms has been evaluated. This work was supported by the MK-4092.2014.2, the RFBR 14-02-00828, the Presidium of the RAS (Basic Research Program "Investigation of Matter in Extreme States" headed by V. E. Fortov), and the Ministry of Education and Science of the Russian Federation federal program No. 8679, 8513, and 8364.

---

1. Bobrov A. A., Bronin S. Ya., Zelener B. B, Zelener B. V, Manykin E. A., and Khikhlukha D. R. // J. Exp. Theor. Phys. 112, 2011, P. 527.
2. Bronin S. Ya., Zelener B. B, Zelener B. V, Manykin E. A. and Khikhlukha D. R. // J. Exp. Theor. Phys., 2011, 112, 717.
3. Zelener B. B, Zelener B. V and Manykin E. A. // JETP Lett., 2011, 94, 525.
4. Zelener B. B., Saakyan S. A., Sautenkov V. A., Akul'shin A. M., Manykin E. A., Zelener B. V., Fortov V. E. // JETP Letters, 2013, V. 98, No. 11, P. 670–674.

MEASURING THE TEMPERATURE OF THE LITHIUM ATOMS IN MOT

Vilshanskaya E.V.,[*1,2] ***Saakyan S.A.,***[1] ***Bronin S.Y.,***[1] ***Sautenkov V.A.,***[1,3] ***Zelener B.B.,***[1,4] ***Zelener B.V.***[1]

[1]*JIHT RAS,* [2]*MPEI,* [3]*LPI RAS,* [4]*MEPhI, Moscow, Russia*

[*]*eva.villi@gmail.com*

Different techniques for measuring the temperature of cold atoms is discussed [1]. One of the methods [2] has been used for the experimental evaluation of the atomic temperature in our experimental setup [3],

which was designed for optical cooling of atoms and creation ultra-cold Rydberg matter. We have measured the ballistic expansion of cold atoms in the MOT—magneto-optical trap. Obtained temperature corresponds to Doppler limit of optical cooling. The next goals are to get sub-Doppler temperature of atoms and increase accuracy. This work was supported by the MK—4092.2014.2, the RFBR 14–02–00828, the Presidium of the RAS (Basic Research Program " Investigation of Matter in Extreme States " headed by V.E. Fortov), and the Ministry of Education and Science of the Russian Federation federal program No. 8679, 8513, and 8364.

1. William D. Phillips // Nobel Lectures, Physics 1996–2000, Editor Gosta Ekspong, World Scientific Publishing Co., Singapore, 2002. P. 199–237.
2. Entin V. M., Ryabtsev I. I. // JETP Letters, V. 80, No. 3, 2004, P. 161–166.
3. Zelener B. B., Saakyan S. A., Sautenkov V. A., Akul'shin A. M., Manykin E. A., Zelener B. V., Fortova V. E. // JETP Letters, 2013, V. 98. No. 11. P. 670–674.

THE ELECTROSTATIC INTERACTION POTENTIAL OF TWO CHARGED SPHERICAL CONDUCTOR PARTICLES IN A UNIFORM ELECTRIC FIELD

Filippov A. V.

SRC RF TRINITI, Troitsk, Russia

fav@triniti.ru

The paper is devoted to the study of electrostatic interaction of two charged conductor spheres immersed in a uniform dielectric medium in the presence of an external uniform constant electric field. The problem is solved by using the bispherical coordinate system in which the surfaces of two spherical particles are coordinate surfaces and the Laplace equation is separable [1–3]. The exact solution for the electrostatic potential in the whole space is analytically obtained for both constant charges and constant electrostatic surface potentials of the particles. The dependence of the electrostatic interaction potential on the angle between the electric strength vector and a vector directed along the line connecting the centers of the particles is studied. Effects of the uniform external electric field on coagulation rate of dust particles levitating in the cathode sheath of a non-self-sustained discharge are thoroughly considered. The coagulation rate constants are determined for both the diffuse regime and the ballistic one of approach of colliding particles.

1. Filippov A. V. // JETP. 2009. V. 109. No. 3. P. 516.
2. Filippov A. V. // Contributions to Plasma Physics. 2009. V. 49. No. 7–8. P. 433.
3. Munirov V. R., Filippov A. V., // JETP. 2013. V. 109. No. 3. P. 516. V. 117. No. 5. P. 809.

2D AND 3D COULOMB CLUSTERS OF DUST PARTICLES IN ANISOTROPIC PARABOLIC TRAPS

Myasnikov M.I.,* Dyachkov L.G., Petrov O.F.

JIHT RAS, Moscow, Russia

**miasnikovmi@mail.ru*

Dusty plasma is of interest both for technological applications and as an object of basic research [1]. In recent years, a lot of attention is given to the investigations of dust clusters containing from several to thousands particles as a model of strongly coupled Coulomb systems and non-neutral plasmas. Restructuring of the clusters can be considered as an analogue of the phase transition. In many experimental and theoretical works, two-dimensional (2D) clusters which are formed in the sheath of rf discharges have been studied. Three-dimensional (3D) clusters, especially spherically symmetrical, also examined. Most frequently clusters are considered in axially symmetric parabolic traps, in which particles are confined by the potential

$$U_c(\rho, z) = \frac{1}{2} m\omega^2(\rho^2 + \alpha z^2),$$

where m is the mass of the particle, ω is the oscillation frequency in the $x-y$ plain ($\rho^2 = x^2 + y^2$), and α is the anisotropic parameter. In the case of spherical symmetry $\alpha = 1$, while the 2D case corresponds to $\alpha \gg 1$. In this work using MD simulation we consider the shell structure of small clusters in the cusp magnetic trap ($\alpha = 4$) and the transition of two-dimensional (2D) clusters to three-dimensional (3D) ones as the number N of particles in the cluster increases. For sufficiently large N the cluster shape approaches the shape of a uniformly charged fluid (oblate ellipsoid of revolution) [2]. We have considered small Coulomb clusters confined in axially symmetric parabolic traps and the transformation of 2D cluster configuration to 3D as the number of particles N in the cluster increases or the anisotropic parameter α decreases. This study was supported in part by the Program "Thermophysics and Mechanics of Extreme Energy Actions" of the Presidium of the Russian Academy of Sciences and by the RFBR project No. 11–02–01051, 13–02–01393-a and No. 12–02–33166.

1. Fortov V. E., Morfill G. E., Complex and Dusty Plasmas (CRC Press, London), 2010.
2. Petrov O. F., Myasnikov M. I., D'yachkov L. G., Vasiliev M. M., Fortov V. E., Savin S. F., Kaleri A. Yu., Borisenko A. I., Morfill G. E. // Phys. Rev. E. 2012. V. 86. P. 036404.

POTENTIAL ENERGY AND SHAPE OF CLASSICAL COULOMB CLUSTERS IN AXIALLY SYMMETRIC PARABOLIC TRAPS

Dyachkov L.G.

JIHT RAS, Moscow, Russia

dyachk@mail.ru

Configuration of classical Coulomb clusters in potential traps is studied in many theoretical and experimental works. However, either flat or spherically symmetrical clusters are usually considered. At the same time, one of the interesting problems is the restructuring of the cluster configuration when the trap anisotropy is changed (the relation between the confining forces in the axial and radial directions is varied). So, a theory, which allows making simple evaluations of the cluster energy, size and shape depending of the trap anisotropy in general case, would be useful.

In this communication we present a simple analytical model of classical Coulomb clusters giving such a possibility. The cluster is assumed uniformly charged. The latter means that the number of particles N should be sufficiently large ($N \sim 10^3$). Particle motion is not considered; thus, the temperature is assumed zero. Analytical dependences of the cluster size, form and potential energy on the number of particles N and trap anisotropy have been obtained. Effect of possible nonuniformity of charge distribution in the cluster is evaluated. It is shown that the nonuniformity leads to some increase in the cluster size, but almost no effect on its potential energy. The limiting transition to a flat cluster is considered, and in this case our result for the potential energy is compared with the extrapolation (at $1/N \to 0$) of the data of exact numerical calculations. The difference is about 2%, which is obviously due to that our model does not take into account the cluster shell structure. On the basis of the approximation of the data of numerical calculations for flat clusters, we introduce an additional factor into the formula for the potential energy of three-dementional clusters, allowing to apply it for relatively small clusters. Comparison with numerical calculations for clusters containing

23 and 13 particles has shown that even in these cases the model gives acceptable results.

STOCHASTIC HEATING OF DUST PARTICLES IN SYSTEMS WITH ANISOTROPIC INTERACTION

Lisina I.I.,* Vaulina O.S.

JIHT RAS, Moscow, Russia

**irina.lisina@mail.ru*

Dust particles in plasma under certain conditions (e.g. pressure changes or increasing the number of particles) can acquire stochastic kinetic energy up to several eV, which is much higher than the temperature of the surrounding gas. A basic mechanism of the anomalous dust particles heating is usually associated with the temporal and spatial fluctuation of charges [1]. However, these theoretical models do not always allow us to explain an increase (grater than 0.5 eV) in kinetic energy [2]. The other reason for dust particles to acquire stochastic kinetic energy could be ion streaming motion in a sheath region of RF capacitive discharges, where ion clouds in the wake below the dust particles are formed. The behavior of dust particles with anisotropic interaction could significantly differ from the isotropic case. For example in multilayer dust crystals, anisotropic interaction of dust particles could cause vertical string-like alignment of adjacent layers.

Here we present the results of our study of layered and quasi one-dimensional chain-like structures formation in systems of particles with anisotropic interaction via a 3D Langevin molecular-dynamics simulation. We use "dipoles" to simulate the anisotropic interaction. This model easily allows us to simulate various anisotropic distributions of the pair forces between interacting particles by varying the parameters of the anisotropic potential. A similar approach has been previously considered for horizontal motion of particles in [3].

During the numerical simulation of particle systems with the anisotropic energy of interaction we observed an "anomalous heating" of dust particles. The source of additional stochastic kinetic energy of particles in the simulated systems is the existence of non-potential forces that occur due to the anisotropic interparticle interaction. Such non-potential forces are capable to perform positive work which compensates energy dissipation. The simulation results showed good agreement with the proposed theoretical predictions. The growth rate of the dust mean energy is found proportional to the inverse square of friction coefficient.

We acknowledge financial support by the RFBR (Grant Nos. 13–08-00263, 14–08–31633) and the Ministry of Education and Science.

1. Vaulina O. S., Khrapak S. A., Petrov O. F. et al., PRE, 60 (1999) 5959.
2. Fortov V. E. and Morfill G. E. (Editors), Complex and Dusty Plasmas 2010.
3. Schweigert V.A., Schweigert I.V., et al., PRL. 80 (1998) 5345.

MASS TRANSFER PROCESSES IN TWO DIMENSIONAL SYSTEMS

Vaulina O.S., Vasilieva E.V.*

JIHT RAS, Moscow, Russia

**elen_vasilieva@mail.ru*

Investigations of structural properties of non-ideal systems are of great interest from a fundamental point of view. Special focus is on two-dimensional systems, where phase transitions may qualitatively differ from those in three dimensional systems. One of the reasons for this fact is the possibility of direct experimental verification of existing analytical and numerical results, for example, in experiments with monolayer dust structures in plasma of radio frequency capacitive discharge. In addition to the fundamental aspects, these studies are of particular interest for applications related with nano- and micro-technologies, as well as for the development of coatings and materials with specified properties.

In this work we present the results of numerical studies of influence of topological defects on processes of mass transfer in two-dimensional systems. Calculations have been performed in a wide range of parameters, corresponding to the experimental conditions in the laboratory dusty plasmas. A relation between a number of topological defects, a coupling parameter of the system and a diffusion coefficient for particles in two-dimensional non-ideal systems with various isotropic potentials was found for the first time. We revealed that the coefficient of diffusion of particles in the systems under study is completely determined by the number of topological defects in an intermediate, so called hexatic phase. This fact may be regarded as a confirmation of a scenario of two-stage melting of two-dimensional systems, predicted in KTHNY-theory.

THE CONDITIONS OF FORMATION OF VARIOUS SPATIAL CONFIGURATIONS OF CYLINDRICAL DUST GRAINS IN AN EXTERNAL ELECTRICAL FIELD

Vaulina O.S., Lisina I.I., Koss X.G.*

JIHT RAS, Moscow, Russia

**Xeniya.Koss@gmail.com*

Most of the works concerning dusty plasma deal with the spherical dust grains. But not long ago several experimental papers have been published, which describe the dynamics of strongly asymmetrical (cylindrical) grains. In case of strongly asymmetrical grains, dusty plasma systems have considerably wider range of possible conditions. Apart from the "regular" crystal or liquid phase, one can observe different phases with various degree of orientational or positional ordering in these systems. A study of properties of dusty plasma with asymmetrical grains is of a great interest itself; besides, it helps expand opportunities of the contactless diagnostic methods of gas-discharge plasma, for example, to measure the electric fields in gas-discharge chambers.

In this work, we present the results of theoretical and numerical study of the conditions of formation of various positional and orientational configurations in the system of homogeneously charged cylindrical grains. The conditions of formation of various spatial orientation of two homogeneously charged interacting grains are considered, which are located in the external electrical field of the cylindrical trap. We obtained that these conditions are determined by the ratio of the gradients of the trap fields.

The presented results can be useful for the development of the new methods of contactless diagnostics of dusty plasma parameters.

This work was partially supported by the Russian Foundation for Basic Research (13–08–00263, 12–02–33166, 13–02–12256, 14–08–31633), by the Ministry of Education and Science of Russian Federation, and by the Program of the Presidium of RAS.

RELAXATION PROCESSES IN DUST PARTICLES STRUCTURES IN GAS DISCHARGE PLASMA

Timofeev A.V.

JIHT RAS, Moscow, Russia

timofeevalvl@gmail.com

Relaxation processes in rarefied systems, such as ideal plasma and gas have been studied in sufficient detail. At the same time there is no such

good study for the relaxation processes in nonideal plasma, liquids, dusty plasma and the like. Theoretical study of two-temperature relaxation in nonideal plasma [1] offers an extrapolation of the Landau-Spitzer theory. Two stages of relaxation were observed in the study of ultracold plasma, namely the rapid heating of the electron subsystem and the slow exchange of energy between electrons and ions. The results of the MD(molecular dynamics) simulation [2] confirmed that the relaxation in strongly coupled plasma with the stopped electrons or ions occurs in two stages: non-exponential and exponential. The first stage is characterized by short duration and abrupt heating of stopped component. This stage is typical for nonideal systems and its duration increases with increasing of system coupling parameter. The second stage is characterized by an exponential decay of temperature difference $\Delta T =\mid T_1 - T_2 \mid\sim e^{-t/\tau}$, where τ is the characteristic relaxation time. For nonideal systems quantitatively this dependence and the relaxation time are correct only in the exponential relaxation area.

The term "temperature" can be used only after system relaxation to the equilibrium. The time required for relaxation can be determined by using the MD method. However, it appears that the time of maxwellization might exceed the non-exponential relaxation, so one can expect that the partial equilibrium subsystem can be observed in the system.

A method for the relaxation time estimation in nonideal dusty plasma is proposed. Estimations for the characteristic relaxation times of vertical and horizontal motion of dust particles are obtained. These relaxation times appears to be different. The relaxation time of dust particles system moving in all three directions is also estimated. A single hierarchy of relaxation times is proposed. The applicability of the thermodynamic functions for the description of plasma-dust system is discussed.

---

1. Ohde Th., Bonitz M., Bornath Th., et.al. // Phys.Plasmas. 1996. V. 3.P. 1241.
2. Morozov I. V., Norman G. E., Smyslov A. A. // J. Phys. A. Math. Gen. 2003. V. 36. P. 6005.

ABOUT NON-CONGRUENCE AND A PHASE DIAGRAM IN SIMPLIFIED MODELS OF DUSTY PLASMA

Martynova I.A.,* Iosilevskiy I.L.

JIHT RAS, Moscow, Russia

**martina1204@yandex.ru*

Hypothetical non-congruence and a phase diagram in dusty plasma are under discussion. Two simplified variants of a dusty plasma model are considered as a thermodynamically equilibrium combination of classical Coulomb particles: (i) a two -component system of macro- and microions (+ Z, -1), and (ii) a 3- component mixture of macroions (+Z) and two kinds of microions (-1, +1). The base for a consideration is the well-known phase diagram of dusty plasma (Hamaguchi et al. [1,2]) for an equilibrium charged system with the Yukawa potential in its' standard representation in the coordinates: Gamma–Kappa (the Coulomb non-ideality parameter vs. the dimensionless Debye screening parameter). The phase regions for the three states of the system (fluid vs. bcc and fcc crystal) from the Hamaguchi diagram are reconstructed in the standard thermodynamic representation in the coordinates temperature-density. The resulting phase diagram in the logarithmic coordinates lnN-lnT has the form of a linear combination of crystalline and fluid zones separated by the boundaries Gamma = const. Parameters and locations of these zones are analyzed by changing the intrinsic parameter of the model—a charge number of a macroion Z. Also, parameters of a splitting the well-known 1-dimentional fluid-bcc-fcc boundaries of the Hamaguchi diagram (for example, the lines of freezing liquid and melting crystal with a corresponding melting density gap) into two separate boundaries are estimated. The authors compared the so-called non-congruent version with the congruent version of the interphase boundaries in the three -component system (+ Z, -1, +1) and the corresponding further splitting of the phase transition boundary crystal-fluid.

---

1. Hamaguchi S., Farouki R.T. Dubin D. *Phys. Rev. E* **56**, 4671 (1997)
2. Fortov V., Khrapack A., Khrapack S., Molotkov V., Petrov O., *Physics Uspekhi*, **174**, 495–544 (2004)

EFFECT OF DUSTY PARTICLE CHARGE VARIATION ON THE STRUCTURE OF DUSTY PLASMA CRYSTALS

Zolnikov K.P.,* Abdrashitov A.V., Psakhie S.G.

ISPMS SB RAS, Tomsk, Russia

**kost@ispms.tsc.ru*

Effect of dusty plasma particle charge variation versus their location on the structure of dusty plasma crystals was studied by means of molecular dynamics method. A linear change of dusty particle charge along the vertical direction was used. Interparticle interaction was described by Yukawa potential. Dusty particles were confined by parabolic electrostatic potential. Gravity affection was taken into account.

Equilibrium structures of dusty plasma clusters consisting of 120, 360 and 720 particles were obtained. Effect of the particle charge change rate along the vertical direction on the structure of dusty plasma cluster was studied. It was shown that the shape of dusty plasma crystal represents deformed ellipsoid.

The work was supported by RAS Scientific Program "Matter under high density energy".

FORMATION OF THE DUST STRUCTURE BORDERS TAKING INTO ACCOUNT JOULE HEAT RELEASE

Polyakov D.N., Shumova V.V.,* Vasilyak L.M.

JIHT RAS, Moscow, Russia

**shumova@ihed.ras.ru*

We analyze the influence of dust structures on the characteristics of a discharge at higher values of a discharge current considering the heat release in a discharge, and the reverse influence of discharge electric field on the sustenance of dust structures in plasma. The simulation was based on the drift-diffusion model of developed for air [1] and neon [2]. In neon, the possibility of step ionization was considered through the low lying metastable state. The electron temperature, transport coefficients and rate coefficients for electron impact reactions were calculated using the electron Boltzmann equation solver BOLSIG+ combined with the SIGLO Database. For description of dust particle charging the OML (in air) and CEC (in neon) approximations were applied. Using this approach, we have found the radial distributions of ions, metastables and electrons and the electric field for the given dust particle distribution, the total discharge current and gas pressure. To find the radial gas temperature

profile in a discharge tube, we have neglected the convective and electron heat conduction terms and solved the steady-state one-dimensional heat conduction equation. The resulting force acting on the dust particle is a sum of three constituents: electric field force, thermophoretic force and ion drag force. The introduction of dust particles in the positive column of glow discharge in neon leaded to the noticeable increase of the longitudinal electric field strength that results the increase of the Joule heat release in the discharge was received. The arising additional temperature and concentration gradients result in the arising of the resulting force acting on the dust particle in a discharge and leading to the change of the position and shape of dust structures. The arising additional force, leads to the shift of the minimum of potential energy towards the wall of the discharge tube with the increase of the dust particle concentration. The self-consistent electric field and thermophoretic forces play the major role in the formation of voids in dense dust structures, and in the increase of the concentration of dust particles near the outer border of the dust structure.

This work was supported by the RFBR Grant 13–02–00641.

1. Polyakov D. N., Vasilyak L. M., Shumova V. V., Fortov V. E. // Phys.Let.A. 2011. V. 375. No. 37. P. 3300.
2. Vasilyak L., Polyakov D., Shumova V. // Contrib. Plasma Phys. 2013. V. 53. No. 4–5, P. 432.

THE OSCILLATING INSTABILITY OF GLOW DISCHARGE WITH DUST STRUCTURES IN LOW CURRENT MODE

Polyakov D.N.,* Shumova V.V., Vasilyak L.M.

JIHT RAS, Moscow, Russia

**cryolab@ihed.ras.ru*

The plasma losses on a surface of dust particles may exceed diffusion losses and lead to the essential decrease of free electron concentration and compensatory increase of the electric field strength [1]. The increase of a discharge voltage may cause the periodical quenching of glow discharge [2]. In this study, the dynamics of polydisperse hollow glass spheres of 10–120 micrometer in diameter was investigated at low values of the currents of glow discharge in air at pressure of 30 Pa in a discharge tube of 20 mm i.d. After the injection of microspheres in a discharge and quick formation of a dust structure, the discharge current was diminished down to the value of about 0.1 mA and the oscillating instability was observed. The longitudinal electric field strength in the region of the localization of

the dust structure, as well as the total voltage of a discharge, attained the maximum of its value at a moment of stability of dust structure. When the discharge was quenched, the plasma trap was destroyed. The microspheres begun to fall down from the structure and then reach the tube walls, then rose up and went to the surface. In a dust-free space the discharge was able to ignite again (time interval is 0.9 s). After the ignition of a discharge, microspheres were charged and followed from the walls in the discharge volume, skipping the equilibrium position. Then microspheres interacted with the electric field of stratum and were drawn into the strata, being separating by their mass within the stratum. The microspheres with approximately the same size arranged in layers separated by the thin plasma layers from the other layers of microspheres. The organized individual structures accumulated the collective space charge, which interacted with each other and led to their mutual spatial separation. After the completion of the formation of spatially stable dust structure the process was repeated. Such a discharge apparatus may be considered as an analog of multi-vibrator on a base of a triode lamp with a feedback. Dust particles play there the role of a governing electrode blocking the electric current by absorption of electrons.

This work was supported by the RFBR Grant 13–02–00641.

1. Polyakov D.N., Shumova V. V., Vasilyak L. M. // Surf. Eng. Appl. Electrochem. 2013. V. 49. No 2. P. 114.
2. Vasilyak L. M., Vetchinin S.P., Polyakov D.N., Fortov V.E. // JETF 2002. V. 94. No 3. P. 521.

DUST CHAINS AND DIFFUSION IN CRYOGENIC DUSTY PLASMAS

Antipov S.N.,* Vasiliev M.M., Petrov O.F.

JIHT RAS, Moscow, Russia

**antipov@ihed.ras.ru*

Gas discharges at decreased temperature of atoms have many features that may occur in experiments with dusty plasma. For example, at cryogenic temperatures of the discharge tube walls strong anisotropy of ion velocity distribution function takes place, which in turn can cause considerable change of dusty plasma structure properties. In this paper dust structures, which are two-component dust mixtures containing of particles with different dynamical and correlation properties, were obtained for the first time in the dusty plasma experiments. Experiments were conducted

with dc glow discharge at temperatures of 10 and 77 K using micron-sized polydisperse CeO_2 particles. In two-component dust structures observed one of the components consists of dust particles with chain-like ordering, so-called 'dust chains'. The second consists of fast-moving particles diffusing through the dust chain structure of the first component, so-called 'crazy particles'. From the analysis of the observation data particle velocity distribution function for each dust component was obtained. The possible reason of two-component dust structures formation at cryogenic temperatures is discussed.

NUMERICAL SIMULATION OF THE DC DISCHARGE WITH DENSE DUSTY CLOUDS

Zobnin A.V.,* Usachev A.D., Petrov O.F.

JIHT RAS, Moscow, Russia

**zobnin@ihed.ras.ru*

The large and dense dusty cloud can essentially perturb discharge parameters. Recently, the effect of dusty particles on discharge plasma glowing had been observed experimentally under microgravity conditions in frame of the PK-4 project. The direct current discharge with alternating polarity in neon was used in the experiment. A formation of two separated dense dusty clouds and correlation of light emission in neon lines with the clouds positions was observed.

We performed numerical simulation of the positive column with dusty clouds for parameters similar to those in the experiment. The simulation was based on the hybrid model of non-uniform DC discharge positive column with non-local kinetic of electrons. Positions and densities of the dusty clouds were taken from the experiment, but charges of dusty grains were calculated self-consistently.

A local stratification of the discharge under action of the dusty cloud is found. A calculated spatial structure of the discharge glowing is compared with the experimental data. Conditions of the dusty cloud stability are discussed.

THE DUST STRUCTURES CREATED IN INERT GASES BY THE BUNCH OF HEAVY ACCELERATED IONS

Prudnikov P.I.,*[1] ***Rykov V.A.,***[1] ***Zherebtsov V.A.,***[1]
Meshakin V.I.,[1] ***Glotov A.I.,***[1] ***Bazhal S.V.,***[1] ***Romanov V.A.,***[1]
Andryushin I.I.,[1] ***Vladimirov V.I.,***[2] ***Deputatova L.V.***[2]

[1]*SSC RF IPPE, Obninsk,* [2]*JIHT RAS, Moscow, Russia*

**pavel.prudnikov89@gmail.com*

In contrast to the previously performed experiments where dust structures have been obtained in tracks of accelerated protons [1] we made a series of experiments using the accelerator of heavy ions EGP-15 (Elecrostatic Charge-exchangable Generator with energy of accelarated ions up to 15 MeV). The accelerated ions of carbon 12C have been used in the experiments. At first one-charged ions were accelerated (a charge is measured in the units of the electron charge). Then the ions went through the charge-exchange foil acquiring an energy of 12 MeV at a charge of 3 and a value of the accelerating potential of 4 MV. The ions arrived at the target unit going through the ion duct which was pumped up to the high vacuum condition. The experimental cell similar to the cell described in [1] was installed at the target unit.

The rectangular cross-section of the beam at the cell entrance was 6 mm in a height and 4 mm in a width. Since the gas in the cell was under the pressure the beam injected into the cell through the dividing foil which was made of aluminium with a 7 micron width. In the foil the carbon ions lost 9 MeV and changed their charge, on average, up to 3.6. In the experiments argon and helium were used. The particles were made of cerium dioxide.

In the gas the charge-exchange again took place and the charge has changed a little bit. The losses of the ions energes in the gas and a number of ion pairs created at the length unit have been calculated.

For the first time, the dust structures produced under the action of the heavy ions were obtained. The structures obtained are caracterized by the increased sizes and more drawn forms in comparison with the structures obtained at the proton accelerator. The dependence of a form and a structure dispisition upon the gas pressure and the applied voltage has been observed. The specific perculiarity of the structures obtained is the fact that there is a part with the well ordered particles at the structure front.

1. Fortov V.E., Rykov V.A., Budnik A.P., et al. Journal of Physics A. / Math Gen. 39 No 17 (April 28, 2006), 4533–4537

EXPERIMENTAL SETUP FOR INVESTIGATIONS INTO THE SELECTIVE DUST PARTICLES CONFINEMENT FROM THE AIRFLOW

Vladimirov V.I.,* Deputatova L.V., Lapitskiy D.S., Pecherkin V.Ya., Syrovatka R.A.

JIHT RAS, Moscow, Russia

**dlv@ihed.ras.ru*

It has been previously shown that electrodynamic traps are capable to provide confinement of the charged dust particles from an airflow.

The electrodynamic trap with given values of amplitude and frequency of a variable electric field will confinement only those particles which mass lies in a certain gamut of meanings, i.e. the trap possesses selectivity.

For investigations of dust particles selective confinement from an airflow the experimental setup consisting of following devices has been developed and made:

- air filter;
- dust particles handler;
- dust particles charging device;
- multielectrode electrodynamic trap;
- mentilating fan;
- must particles charge control unit.

Diagnostics system includes the high-speed digital camera. For dust particles illumination the green laser with system of the cylindrical lenses formativing a laser knife is used.

DUST PARTICLES CHARGING IN THE AIRFLOW

Syrovatka R.A.,* Pecherkin V.Ya., Lapitskiy D.S., Deputatova L.V., Vladimirov V.I., Vasilyak L.M.

JIHT RAS, Moscow, Russia

**RomanSA_89@mail.ru*

It has been shown that electrodynamic traps are capable to provide confinement of the charged dust particles from an airflow [1, 2].

In this work we developed the dust particles charging device on the basis of a corona discharge. The device provides charging in airflows.

The corona and grounded electrodes are lattices oriented perpendicular to an airflow. The corona electrode is made of a tungsten wire ($d = 70$ microns). The grounded electrode is made of copper plates by section 2×5 mm. Distance between electrodes is 13 mm.

The distribution of the electric field strength between electrodes in the case of one corona electrode and four corona electrodes has been calculated. A voltage between electrodes was equal to 16 kV.

Current-voltage characteristics of the designed device have been measured.

On our estimates the charge of dust particles in the range of sizes 10–20 microns should attain 10^4–10^5 electron charges at an airflow velocity equal to 10–100 cm/s.

1. Filinov V.S., Lapitsky D.S., Deputatova L.V., Vasilyak L.M., Vladimirov V. I., Pecherkin V.Ya. Dust Particles Behavior in an Electrodynamic Trap // Contrib. Plasma Phys. 2013. V.53. No. 4–5. P. 450–456.
2. Vasilyak L.M., Vladimirov V.I., Deputatova L.V., Lapitsky D.S., Molotkov V.I., Pecherkin V.Ya., Filinov V.S.and Fortov V.E. Coulomb stable structures of charged dust particles in a dynamical trap at atmospheric pressure in air // New Journal of Physics. 2013. V.15. P. 43-47.

COMPARISON OF TIME LAGS FOR LIQUIDS WITH AND WITHOUT MICROBUBBLES

Vetchinin S.P.,[*1] ***Son E.E.,***[1] ***Vasilyak L.M.,***[1] ***Pecherkin V.Ya.,***[1] ***Kulikov Y.M.,***[2] ***Panov V.A.***[2]

[1]*JIHT RAS, Moscow,* [2]*MIPT, Dolgoprudny, Russia*

[*]*vpecherkin@yandex.ru*

The difference between electrical breakdown time lags for tap water IPA solution with and without microbubbles was studied experimentally. In our case we determined four stages of the spark channel evolution on the large time scale about 100 microseconds. The first stage begins with the voltage applying and ends with the anode near region glowing. On the next stage propagation of the spark channel occur till the channel bridges the electrode gap. On the third stage a storage capacitor discharges in the electrode gap. After the capacitor is almost discharged we observe the final stage of the spark channel destruction with an afterglow. All these stages have their own durations. A dependence of the total time lag (since the moment the voltage is applied till the channel bridges the gap) on an applied voltage was obtained. It is clear from the results that the total time lag of the microbubble medium spark discharge is three times shorter than for the microbubble-absent medium. It is about 1500 and 4500 microseconds for the microbubble medium with ∼10% volumetric gas content and for the solution without microbubbles respectively. Moreover,

a total time lag decrease with a volumetric gas content increasing. For the liquid without microbubbles, when the applied voltage is just a little above the threshold value the time lag of the initial anode glowing which is due to ionization-overheating instability makes a significant contribution to the total time lag about 1500 microseconds. In contrast, when the applied voltage is 1 kilovolts higher than the threshold one, the first stage time lag becomes just about 50 microseconds. Thus the spark discharge in microbubble medium develops quite faster than in conductive liquids due to early partial discharges in bubbles in the near anode area.

THE FORMATION AND PROPERTIES STUDY OF EXTENDED DUSTY PLASMA STRUCTURES OF NON-SELF-SUSTAINED DISCHARGE

Andryushin I.I.,[*1] ***Zherebtsov V.A.,***[1] ***Meshakin V.I.,***[1] ***Prudnikov P.I.,***[1] ***Rykov V.A.,***[1] ***Vladimirov V.I.,***[2] ***Deputatova L.V.***[2]

[1]*SSC RF IPPE, Obninsk,* [2]*JIHT RAS, Moscow, Russia*

[*]*i.andryushin@gmail.com*

The basic parameters of non-self-sustained discharge in inert gas with dust particles have been evaluated. The discharge is maintained by a beam of protons and is using for simulation of nuclear-induced plasmas and studying of dust plasma structures [1] [2].

The possibilities of extended dust structures formation in the non-self-sustained discharge are considered. That might significantly widen the scope of dusty plasma studies [3].

The stability of extended dust plasma of non-self-sustained discharge at low pressure is investigated. It is shown that in a wide range of wave numbers, so called aperiodic recombination instability may occur, which leads to stratification of the plasma into regions with high and low concentrations of dust particles. Physical mechanism of recombination instability is discussed. The analysis of dependence of the instability growth rate on the discharge parameters is performed.

The studies were conducted with the financial support of the Russian Foundation for Basic Research and the Government of the Kaluga region (grant no. 12–02–97521).

1. Fortov V. E., Rykov V. A., et. al. // Phys.- Doklady, 49 (9) (2004) P. 497.
2. Deputatova L. V., Vladimirov V. I., et. al. // Phys.Rep. 36 (13) (2010) P. 1167–1172

3. Andryushin I. I., Vladimirov V. I., Deputatova L. V., Zherebtsov V. A., Meshakin V. I., Prudnikov P. I., Rykov V. A. // High Temperature 51 (2013) P. 733–741

MAGNETRON DISCHARGE OVER MOSAIC COPPER–GRAPHITE TARGET

Mankelevich Yu.A.,[1] ***Mitin V.S.,***[2] ***Pal A.F.,***[3] ***Ryabinkin A.N.,***[*3] ***Serov A.O.***[3]

[1]*MSU, SINP, Moscow,* [2]*VNIINM, Moscow,*
[3]*SRC RF TRINITI, Troitsk, Russia*

[*]*alex.ryabinkin@gmail.com*

Optical imaging combined with spectral analysis of DC discharge plasma glow over the sputter track during magnetron sputtering of mosaic copper-graphite target was carried out in the range of discharge power density 10–100 W/cm^2 with argon as working gas. Study of the plasma glow patterns shows that in case of higher power density about 100 W/cm^2 the plasma compositions over the adjacent mosaic elements differ from each other. With the discharge current increasing the fraction of copper atoms over the copper surface increases more appreciable than over the graphite one whilst the concentration of argon atoms over the track is more uniform. Influence of the difference on the sputtering rate of the mosaic elements is discussed. The work was supported by RFBR grant #13–02–01161À and Rosatom contract #H.4x.44.90.13.1090

EXPLOSION OF DOUBLE-LAYER CONDUCTORS IN FAST-RISING HIGH MAGNETIC FIELDS

Oreshkin V.I.,[*1] ***Chaikovsky S.A.,***[2] ***Datsko I.M.,***[2] ***Labetskaya N.A.,***[2] ***Ratakhin N.A.***[2]

[1]*TPU,* [2]*IHCE SB RAS, Tomsk, Russia*

[*]*oreshkin@ovpe.hcei.tsc.ru*

An experiment on the electrical explosion of cylindrical conductors of external diameter 3 mm has been performed on the MIG generator at a peak current of 2.5 MA and a current rise time of 100 ns. The parameters of the generator and the dimensions of the conductors provided for a maximum magnetic induction of up to 300 T. The aim of the experiment was to compare the skin explosion of a solid cylindrical conductor with that of a double-layer conductor with the outer layer of lower conductivity. Comparison was performed by recording the surface emission of titanium and

stainless steel conductors using an HSFC Pro four-frame optical camera with a frame exposure time of 3 ns. Double-layer conductors were made so that one half was a solid cylinder and the other was a tube made of titanium or stainless steel of thickness 150–250 mkm with a copper rod inside. This allowed comparison of the behavior of a solid conductor with that of a double-layer conductor in a magnetic field under identical conditions.

It has been shown that the double-layer structure of a conductor with the outer layer of lower conductivity makes it possible to get higher magnetic fields at the conductor surface without its electrical explosion. This can be explained by the decrease in the ratio of the Joule heating density to the energy density of the magnetic field at the surface of a double-layer conductor due to redistribution of the current density over the conductor cross section.

This work was supported in part by the RAS Presidium under the program "Study of matter under high energy densities" and by the Russian Foundation for Basic Research (Grant No. 14–08–00524-a).

MAGNETIC PROBE DIAGNOSTICS IN POWERFUL HIGH PRESSURE DISCHARGE

Pinchuk M.E.,* Budin A.V., Leont'ev V.V., Leks A.G., Bogomaz A.A., Rutberg Ph.G., Pozubenkov A.A.

IEE RAS, Saint-Petersburg, Russia

**pinchme@mail.ru*

Experiments with magnetic probe diagnostics in gas discharge with current amplitude up to 0.5 MA, current rise rate $\sim 10^{10}$ A/s, and at initial pressure up to 30 MPa are carried out. Discharge was initiated by copper wire explosion. Discharge chamber is designed with axisymmetric geometry. The energy source was capacitive storage system with capacity of 1.2 mF. Charging voltage was varied from 1 kV to 15 kV. Energy input was up to 100 kJ. The original construction of magnetic probe, working in condition of high current high pressure discharge with extreme heat and shock load, was designed and created. Operation testing of magnetic probe under this papameters was performed. Measurements of current density distribution were carried out. At time close to maximum current in the circuit the average current density in the discharge channel are rised from ~ 200 kA/cm^2 at initial hydrogen pressure of ~ 5 MPa to ~ 400 kA/cm^2 at initial pressure of ~ 30 MPa. According to the experiments the current channel radius is reduced with increasing initial gas density. The discharge channel is localized around the axis of discharge chamber. The channel

radius is not exceeding 10 mm for investigated pressure range, and most part of the current is bounded in radius of 0.6 cm.

The work is partially supported by Russian Foundation for Basic Research (grant 12–08–01062-a).

FORMATION OF ELECTRICAL DISCHARGES UNDER FREE SURFACE OF CURRENT CARRYING FLUIDS

Klementyeva I.B.,[*1] ***Pinchuk M.E.***[2]

[1]*JIHT RAS, Moscow,* [2]*IEE RAS, Saint-Petersburg, Russia*

[*]*ira.klementyeva@mail.ru*

The work is devoted to investigation of free surface deformation that is a result of interaction of passing through liquid metal electric current with own magnetic field and to investigation of formation of high current discharges emerging under liquid metal at its free surface deformation.

The significance of these investigations is in solving of the fundamental problems of magnetohydrodynamics [1, 2] and also in solving of the application problems related to improving the performance of technical devices for increasing of energy efficiency in power engineering and industry. With the use of magnetohydrodynamics methods it is possible to successfully manage electro-vortex flows, which have a significant impact on heat and mass transfer in many electrometallurgical processes. Another important application of the received results is in nuclear and thermonuclear power engineering. Investigation of influence of electrical and magnetic fields on hydrodynamics and heat-exchange processes in current-carrying fluids with high current discharges under surface is of fundamental interest [3].

The base model of the working area is represented by cilindrical container filled with eutectic alloy In-Ga-Sn and by cylindrical container filled with melted Pb with electric current of 1–30 kA. The container may be surrounded by the conductors creating an external magnetic field of specified configuration. Fiber-optic sensors are capable to get unique experimental data on the turbulent structure of electro-vortex flows created by electromotive body force. High-speed digital cameras Citius C100 provide visualization of objects and processes. High-frequency current and voltage probes are used for measurements of electrical characteristics of the discharge. Experiments are carried out in air and argon media at 1 Atm pressure.

The tasks of the work are to visualize the wave form and the free surface; to determine the mechanism of formation of the discharge over the liquid metal surface and to determine its characteristics and parameters

of ignition; to obtain data on the influence of pinch-effect on the velocity field.

The work was supported by RFBR, 14–08–31078 mol-a.

---

1. Klementyeva I., Moralev I. // IEEE Plasm. Sci., Images. 2011. P. 2144–2145.
2. Klementyeva I. B., et al. // High Temp. 2011. V. 49. No. 6. P. 816–825.
3. Ivochkin Yu. P., et al. // Therm. Proc. Eng. 2012. V. 4. No. 11. P. 487–496.

ON THE SELF-ORGANIZATION OF THE EROSION PATTERN IN THE NEGATIVE CORONA DISCHARGE

Petrov A.A.,[*1] ***Savinov S.Yu.,***[1] ***Pestovskiy N.V.,***[2] ***Korostylev E.V.,***[2] ***Barengolts S.A.,***[3] ***Amirov R.Kh.,***[4] ***Samoylov I.S.***[4]

[1]*LPI RAS, Moscow,* [2]*MIPT, Dolgoprudny,* [3]*GPI RAS, Moscow,* [4]*JIHT RAS, Moscow, Russia*

[*]*petrov@oivtran.ru*

Cathode erosion was studied in the glow mode of the negative corona discharge in air in the point-to-plane configuration. Cathodes made of polycrystalline graphite c-3, pyrographite, graphite fiber and MPG-6 graphite were used. The diameter of the cathode pin was 50–500 μm. The discharge current was 100–200 μA. Reduction of the cathode pin length with typical rate few mkm/min was observed, the specific erosion rate was 10^{-5} - 10^{-4} g/Coul. Formation of hexagon erosion cells with size sim50 μm and depth sim20 μm organized in regular pattern was found at the cathode surface. Each erosion cell was covered with microcraters. According to results of the video registration made with use of microscope, the discharge flame was localized inside a cell jumping from one cell to another with frequency 1–10^3 Hz. The apparent diameter of the negative glow was 20 μm at 760 Torr.

The erosion pattern forms the periodical electric field conditions at the cathode surface. The electric field strength attributed to the cathode geometry was 10^6 V/cm at the edges of a cell and 10^5 V/cm inside a cell. The localization of the discharge flame inside a cell is explained by the formation of the positive space charge in the region of the glow. Hence the magnitude of the electric field produced by the positive space charge of the cathode sheath is on the range of 10^6 V/cm.

The cell structure was not found on metal cathodes because in that case the field conditions and the discharge wandering are governed by oxidation and charging of the surface. In the Trichel pulse mode of the negative

corona the cell erosion pattern cannot be formed because in that case the gap is cleaned from the positive charge after each current pulse. Note that both the temperature and ion sputtering thresholds are not reached in the negative corona discharge. Hence the mechanism of the cathode erosion is unclear and therefore interesting to investigate.

The work has been supported by RBRF, grants 12–08–01223 and 12–08–33031.

THE SPACE-TIME SPECTROSCOPY OF THE PULSED HIGH ENTHALPY PLASMA JET

Pashchina A.S.,* Chinnov V.F., Andriyanova Y.N., Efimov A.V.

JIHT RAS, Moscow, Russia

**fgrach@mail.ru*

Erosive type discharge in pulse mode is one of the techniques for obtaining high enthalpy jets [1]. Cumulative-like plasma jet with sharp boundaries and long propagation range (up to 200...300 capillary calibers) can be created only at a certain range of discharge parameters. Such plasma jets are characterized by high energy capacity (up to 100 $eV/particle$), high electron density (up to $n_e \sim 3 \cdot 10^{17}$ cm^{-3}), high energy of excited molecules ($T_V \sim 8000$°K) and extremely long relaxation time [2].

To investigate this nonstationary object with continuously changing geometry and composition of plasma a complex system is used, which includes a high-speed jet image registration synchronized with Space-Time 2D spectroscopy of high spectral (0.1 nm), spatial (20 microns) and temporal (10 us) resolution.

The features of electron density and temperature distributions inside the capillary and inside the erosion jet at subsonic and supersonic expiration were analyzed. These revealed nonuniform spatial structure and significant difference of plasma parameters (electron temperature and concentration) in the initial and main section of plasma jet, due to the specific distribution of the discharge current and the possible presence of massive charged clusters. Based on the results of quantitative experimental data processing [3] we obtained materials about spatial-temporal changes of plasma jets main parameters. These materials provides a good basis for analyzing the plasma-chemical reactions, mainly the ones where hydrogen and carbon are present.

1. Avramenko R. F. et al, Issledovanie plazmennih obrazovanii, iniciiruemyh erozionnym razrjadom. // Journ. Techn. Phys. (USSR), 1990, V. 600. No. 2. P. 57–64
2. Pashchina A. et al, Study of Dynamics of Enhanced Plasma Formations, Created by Capillary Pulsed Discharge, 50th AIAA , 09–12 January 2012, Nashville, AIAA 2012–1161.
3. Ochkin V. N. Spectroskopiya nizkotemperaturnoi plazmi. Russia, Moscow, Fizmatlit, 2010

SIMULATING PULSED MAGNETIC FIELD OF LIGHTNING FOR FORMING DENSE PLASMA

Vlasov A.N.,* Dubkov M.V., Burobin M.A., Manoshkin A.B., Zhimoloskin S.V., Potashevsky S.S.

RSREU, Ryazan, Russia

**anv@fulcra.ryazan.ru*

In this paper we consider the apparatus to simulate pulsed magnetic field of lightning, based on the using of electrically exploding spirals with copper conductors of large cross section. There were applied two spirals are electrically connected in parallel with the left and right windings, each of which has 8 turns. Total cross section of conductors ranged from 2 to 4 square millimeters. Spirals installed inside the half-open cylindrical chamber on the basis of the dielectric so as to give a common toroidal magnetic field with a ratio of large and small radii equal to 3:1. Twice the sum of large and small radii of the magnetic field ranged from 28 mm to 60 mm. Copper conductors were performed either in the form of round wire of diameter 0.67 mm (parallel to the wires 4 each spiral) or as a multilayer tape (4 to 10 layers) made of foil or 0.1 mm or 0.05 mm, and a width of 2.5 to 5 mm. Spirals connected to the discharge circuit with the capacitor bank 350 thousand microfarads capacitance and maximum voltage of 450 volts. Commutating of the contour was carried out by means of powerful high-speed thyristors providing a current pulse of about 40 kA, which to simulate the current pulse in the lightning channel with the amplitude of order 300 kA. In the experiments we were doing video of processes of electric explosion and were recorded oscillograms of pulse currents, voltages and luminous fluxes when energy input into the plasma. We detected that electrical explosion of the spirals accompanied by the formation of a luminous plasma ring over exploding spirals, and sometimes from the place of electric explosion flying out long-lived luminous object (the maximum lifetime of one of these objects as at Dec. 2013 amounted

to 1.6 seconds). This work was supported by the Ministry of Education and Science of the RF, the contract No 14.518.11.7002 on July 19, 2012.

WORK OF EXPLOSIVE MAGNETIC GENERATORS IN MOBILE TESTING COMPLEX

Zavalova V.E.,[*1] ***Shurupov A.V.,***[1] ***Kozlov A.V.,***[1] ***Gusev A.N.,***[1] ***Shurupova N.P.,***[1] ***Baselyan E.M.,***[2] ***Dudin S.V.,***[3] ***Mintsev V.B.,***[3] ***Chulkov A.N.***[4]

[1]*JIHT RAS, Moscow,* [2]*ENIN, Moscow,* [3]*IPCP RAS, Chernogolovka,* [4]*JSC SET, Shatura, Russia*

[*]*zavalova@fites.ru*

Summarizing of the scientific and practical data obtained during the development and examination of the mobile testing complex on the base of explosive magnetic generator (MTC EMG) was carried out in this paper. This set is designed to simulate the effect of the lightning currents on electrical power engineering objects. For this purpose MTC EMG has to produce the current pulse with amplitude up to 60 kA at the rising time about 20 microseconds on the resistive-inductive load. An analysis of electrical circuits for formation of current and voltage pulses on resistive-inductive load using transformer is represented. The novelty of this scheme is that in comparison with previous model of MTC EMG, the explosive breaker of current in the primary circuit of pulse transformer and contactor in the load circuit have been excluded. The control of the electrical current pulse was realized by use of EMG with special temporal law of inductance output. Required law of inductance output was obtained with help of output cone section of EMG. In this scheme the electrical current pulse duration was defined by the ratio of cone section angle and angle of liner expansion. In this case the function of transformer was not limited by the storage of inductive energy. The influence of the residual resistance in the primary winding of the transformer on the efficiency of energy transfer to the load was examined. As a result, the developed technical solutions able to form the front of the current pulse with parameters close to calculated values. Namely, at the field testing with load impedance of 4 Ohm and 86 mcH inductance circuits—amplitude of about 60 kA and rising time of about 30 microseconds were registered, at a sufficiently high efficiency of the output power to the load.

MEASUREMENT OF ELECTROPHYSICAL PARAMETERS OF ELECTRIC BREAKDOWN ON THE DIELECTRIC SURFACE

Dudin S.V.,* Ushnurtsev A.E., Mintsev V.B.

IPCP RAS, Chernogolovka, Russia

**dudinsv@ficp.ac.ru*

The problem of influence of a powerful electric pulse, in particular the electric discharge of a lightning, on power installations and isolators has a huge practical value. Electric breakdown on a dielectric surface is the phenomenon of a sharp falling of electric resistance at high voltage enclosed to a sample when the spark electric discharge passes on a dielectric surface or in the immediate proximity to it [1–3]. The installation is created, allowing modeling the electric fields similar to the fields from influence of a lightning, on a dielectric surface. Energy which can be allocated at breakdown on a surface of dielectric isolator can be varied in a wide range with the use of different types of pulse generators. Test experiments were carried out and diagnostics of registration was tested. In the work electrophysical parameters at various ratios of tangential and normal components of an electric field are supposed to be investigated. In the experiments, the measurements of a voltage on the sliding electric discharge of a sample with the help of an ohmic divider with dividing capacity C_5 are planned. The current is measured with the help of Rogovsky belt. On the value of current $I(t)$ proceeding through the electric discharge and to a voltage failure on sample $U_X(t)$ the impedance of channels of the electric discharge in function of time $Z_X(t) = U_X(t)/I(t)$ is determined.

1. Grigorjev A. N. et al. Electricheskiy razriad po poverhnosti tverdogo dielektrika, Ch.1. Osobennosti razvitia sushtstvovania poverhnostnogo razriada // Izvestia Tomskogo Politecnicheskogo Universiteta, 2006, V. 309, No. 1, P. 66–69.
2. Bogatenkov I. M., Bocharov J. N., Gumerova N. I. et al. Technica visokih napriazheny, // pod red G. S. Kuchinsky. — SPb.: Energoatomizdat, 2003. — 608 P
3. Mesiyts G. A. Impulsnaia energetika i elektronika. — M.: Nauka, 2004. — 704 P

APPLICATION OF THE ECR PLASMA ETCHING FOR PREPARATION OF THE PATTERNED WAFERS FOR ANALYSIS OF THE BIOLOGICAL LIQUIDS AT THz FREQUENCIES

Mitina A.A.,[*1] ***Polushkin E.A.,***[1] ***Kovalchuk A.V.,***[1] ***Semenenko A.I.,***[2] ***Shapoval S.Yu.***[1]

[1]*IMT RAS, Chernogolovka, Russia,* [2]*IOP NASU, Kyiv, Ukraine*

[*]*alena@iptm.ru*

THz Fourier spectroscopy is a new important analytical technique for analysis of the biological matters. At the same time it is not so easily to develop methods for samples preparation due to strong interference within the wafers with thicknesses about the wavelength value.

In this work we obtain patterned silicon structures using low temperature ECR plasma etching in isotropic or anisotropic modes to eliminate the influence of the interference within silicon wafers. Our samples have the grating system of the capillaries which allows to decries the interference of the THz radiation.

Such samples were used for human plasma blood analysis based on Fourier spectroscopy.

THEORETICAL AND EXPERIMENTAL INVESTIGATION OF PLASMA FORMATION, PROPAGATION OF RADIO SIGNALS AND CHARACTERIZATION OF HEAT-RESISTANT MATERIALS FOR HYPERSONIC VEHICLES

Aksenov A.A.,[1] ***Bityurin V.A.,***[1] ***Bocharov A.N.,***[1] ***Bondar E.A.,***[2] ***Degtyar V.G.,***[3] ***Dyrenkov A.V.,***[4] ***Khlybov V.I.,***[3] ***Isakaev E.H.,***[1] ***Kalashnikov S.T.,***[3] ***Palkin E.A.,***[5] ***Saveliev A.S.,***[1] ***Savitsky D.V.,***[1] ***Son E.E.,***[1] ***Surzhikov S.T.,***[6] ***Tereshonok D.V.,***[*1] ***Tyftyaev A.S.,***[1] ***Zhadjiev M.H.,***[1] ***Zhluktov S.V.***[6]

[1]*JIHT RAS, Moscow,* [2]*ITAM SB RAS, Novosibirsk,* [3]*OAO "Makeyev GRTs", Miass,* [4]*MIPT, Dolgoprudny,* [5]*RNU, Moscow,* [6]*IPMech RAS, Moscow, Russia*

[*]*tereshonokd@gmail.com*

The present work aims to show main results of the experimental and theoretical investigation for plasma formation near the surface of a hypersonic aircraft, propagation of radio signals through this plasma sheath and to understand the mechanism of thermal damaging of the heat-resistant

materials. Numerical simulation for the flying experiment RAMC-II has been performed for altitudes H = 70–150 km by means of the package SMILE. For altitudes less than H = 90 km a numerical simulation has been performed by means of the programs: NERAT ASTEROID, FlowVision and PlasmAero. One of the features of this simulation is the solution of the self conjugate problem—fluid structure interaction. Our computations agree with experimental results for the electron concentration along the surface of the aircraft body for altitudes H = 61, 71 and 81 km. Propagation of the radio signals through a plasma sheath near the surface has been analyzed and calculated in 3D geometry. Characterization testing of heat resistant materials has been performed. Experimental results for the thermal destruction rate of the heat-resistant materials at altitude H = 50 km are in good agreement with the numerical results obtained by means of PlasmAero.

COMPREHENSIVE STUDIES OF THE EFFECTIVENESS OF HEAT-SHIELDING MATERIALS

Son E.E., Isakaev E.H., Chinnov V.F., Gadzhiev M.K., Sargsyan M.A., Kavyrshin D.I.,* Tyftyaev A.S., Senchenko V.N.

JIHT RAS, Moscow, Russia

**dimakav@rambler.ru*

For this study a generator producing laminar high enthalpy plasma streams of air and nitrogen plasma was constructed. It has the following parameters: gas flow rate 1.5–2 g/s, enthalpy at the exit of the plasma torch 40–70 MJ/kg, stream velocity 400–600 m/s. Heat flux measurements were conducted on the plane surface of the cylindrical copper calorimeter with the diameter of 20 mm at normal incidence with slightly divergent plasma jet from the exhaust nozzle with a diameter D = 10 mm with the distance between the nozzle and the surface of 10–30 mm. This technique provided the variance of heat flux from q_{min}=0.1 kW/cm^2 q_{max}= 5 kW/cm^2. The currents applied to plasma torch were in the range of 150–500 A, the arc electrical power was in the range of 15–50 kW.

The emission spectra of nitrogen and air plasma in the incident jet on the isotropic and anisotropic graphite samples were investigated. The spectra are varied depending on the distance of the investigated section of the plasma from the sample surface . When the sample was exposed to 1–2 kW/cm^2 of heat flux the following parameters were determined: sample surface temperature (using the maximum spectral intensity of the

surface according to Wien's displacement law) and its temperature field (using the videograms of the samples glow), plasma electron temperature T_e = 10–12 kK (using the relative intensities of the observed spectral lines N I, O I, Cu I), temperature of heavy particles (T_g), atoms and molecules and ions of nitrogen (using the spectra of the N_2^+ molecular ion and CN radical). Electron concentration was found to be n_e=10^{14}-10^{16} cm^{-3} in the observed zone. Sublimation features of hetero- and homogeneous graphite in air and nitrogen plasma torches were studied. Bulk sublimation of the graphite under the influence of high enthalpy nitrogen jet during the stage of intense warm-up is accompanied by intensive microparticle emission with the size of 10–200μm; the share of expelled micro particles from the total particulate mass loss is significant. This effect is not observed in air plasma presumably due to highly efficient combustion of sublimate (at and near the surface of the sample): C + O →CO. The surface temperatures of the two graphite samples undergoing the intense sublimation during the stage of quasi-stationary heating were determined to be 3000–3500 K by two independent methods (spectroscopic and pyrometric).

VOLUMETRICAL GRAPHITE SUBLIMATION BY HIGH-ENTHALPY PLASMA STREAM

Isakaev E.H., Chinnov V.F., Gadzhiev M.K., Sargsyan M.A.,* Kavyrshin D.I., Ageev A.G.

JIHT RAS, Moscow, Russia

**m.sargsyan86@mail.ru*

This work describes the study of ablation features of hetero- and homogeneous graphite in air and nitrogen plasma torches. Volumetrical ablation of the graphite under the influence of high enthalpy nitrogen jet during the stage of intense heating is accompanied by intensive microparticle emission with the size of 10–200μm; the share of expelled micro particles from the total particulate mass loss is significant. This effect is not observed in air plasma presumably due to highly efficient combustion of sublimate (at and near the surface of the sample): C + O →CO. Computer processing of the high-speed experiment video (experiment length 40–100 s, frame rate 30–50 fps, exposure time 50–150 μs) allows us to estimate the volumetrical ablation rate of carbon and its shares for micro- and nanoparticles. The size of the sample and its mass loss speed are found programmatically and provide information about the changes of its volume and its particulate removal speed. The PML share is found by means of statistical processing of the larger particles observed during the experiment.

High-speed imaging of the graphite sample ablation (typical mass loss rate 0.005–0.03 g/s·cm^2) utilizing absolute calibration of radiation intensity and interference filters allows us to explore the temporal evolution of the temperature field on the sample surface and the dynamics of its heating and sublimation. The surface temperatures of the two graphite samples undergoing the intense ablation during the stage of quasi-stationary heating were determined to be 3000–3500 K by two independent methods (spectroscopic and pyrometric).

THE ENERGY TRANSFER FROM PLASMA DISCHARGE INTO THE GAS FLOW

Golub V.V.,[*1] ***Bocharnikov V.M.,***[1] ***Petrov D.A.,***[2] ***Saveliev A.S.***[1]

[1]*JIHT RAS, Moscow,* [2]*MIPT, Dolgoprudny, Russia*

[*]*golub@ihed.ras.ru*

A dielectric barier discharge (DBD) is notable for its ability to transfer impulse to the surrounding neutral gas [1]. A wall-jet type of flow without the mass flux can be created under certain conditions of the discharge. Of interest is a configuration of the electrodes, when there are two DBD discharges, having shared bottom electrode and pointing at each other.

Problem formulation. We study how the overlap between two plasma regions influences the generation of the flow of two wall-jets, and how they collide and form one wall normal synthetic jet in the middle. It is important to understand the energy flux from the initial energy of the electrodes to the discharge, the flow inertia and the overall heat (both electrodes and convections) for optimization purposes.

Experimental. To answer this questions, we measure the dependence of the thrust, created by the combined wall-normal synthetic jet, as a function of the distance between the electrodes. The results are compared with the doubled input of an isolated wall-jets. Morerover, we undertake flow visualisations with a shadowgraph to estimate the effect of convection on the flow.

Simulations. The usage of the DBD holds much promise for the problems of the active flow control [1]. Experiments suggest that the integral effect one the DBD on the flow comprises two majors factors: impulse and heat transfer to a certain region of the flow. We use this simplified model to study the characteristics of an airfoil numerically. Of interest is the influence of DBD on the lift and drag force .

Installation of plasma actuators based on the DBD of different configurations on the wing of an aircraft can greatly simplify the mechanization of the wing and reduce energy costs for the flight control. This is especially important for unmanned aircraft powered by solar panels, where critical is extra load and where necessary is the simplicity of the design combined with the efficiency of controls.

This work was partially supported by the Program of RAS Presidium #25.

1. Moreau E. // J. Phys. D Appl. Phys. 2007. V. 40. No. 3. P. 605.

DIELECTRIC BARRIER DISCHARGE AS THE SOURCE OF A SYNTHETIC JETS

Bocharnikov V.M.,* Semin N.V., Saveliev A.S., Golub V.V.

JIHT RAS, Moscow, Russia

**vova-bocha@phystech.edu*

There has been a number of studies on the properties of wall jets produced by the dielectric barrier discharge in an asymmetric plasma flow actuator [1]. If two asymmetric actuators are positioned towards each other with a common encapsulated electrode, a symmetrical actuator is created. Each half of the asymmetric actuator acts as a source for the wall jet. Interaction of two wall jets leads to the formation of a synthetic jet. In this context, neither jet velocity distribution nor maximum velocity are relevant, which was previously studied in detail [2], but the momentum transferred to the flow.

Specific thrust of a symmetric actuator's synthetic jet depends on parameters of the dielectric barrier discharge [3], and the distance between the surface electrodes. In present work, we measured the specific thrust of synthetic jets produced by symmetric actuators. An optimal design of a symmetric actuator was determined based on the dependence of the specific thrust on the distance between surface electrodes with different voltages. Visualization of the flow with a shadowgraph allowed us to make a qualitative assessment of the role of convection on the flow for different distances between the surface electrodes.

This work was partially supported by the Program of RAS Presidium #25.

1. Corke T. C., Enloe C. L., Wilkinson S. P., "Dielectric Barrier Discharge

Plasma Actuators for Flow Control", Annual Review of Fluid Mechanics 2010, 42, 505–529.
2. Santhanakrishnan A., Jacob J. D., Suzen Y. B., "Flow control using plasma actuators and linear/annular plasma synthetic jet actuators", In 3rd AIAA Flow Control Conference 2006, V. 3033.
3. Moreau E., "Airflow control by non-thermal plasma actuators", Journal of Physics D: Applied Physics 2007, 40: 605–636.

SPARK CHANNEL PROPAGATION IN TAP WATER IPA SOLUTION

Vasilyak L.M.,[1] ***Kulikov Y.M.,***[2] ***Panov V.A.,***[*2]
Pecherkin V.Ya.,[1] ***Son E.E.***[1]

[1]*JIHT RAS, Moscow,* [2]*MIPT, Dolgoprudny, Russia*

[*]*panovvladislav@gmail.com*

Evolution of the spark channel created by the high voltage pulse generator in tap water 15% Isopropyl alcohol (IPA) solution has been experimentally observed. The experiments were performed in the pin-to-pin geometry. The half amplitude pulse duration was typically 10 ms. The conductivity σ of the solution was about 300 μS/cm. The ballast resistance limits current value less than 3A. Fast camera images show that spark discharge channel propagation starts in (500–600) μs after voltage applying with the anode region glowing which is due to ionization-overheating instability near the surface of anode electrode. Measured propagation velocity is about 4 m/s and points to thermal process of its evolution. The partial discharges in gas bubbles near the spark channel have been observed. Their formation due to vaporization during the Joule heating of highly volatile fraction with conduction currents was observed in subsidiary experiment without electrical breakdown of the electrode gap. When the channel bridges the electrode gap cathode flash of lightning occurs which is much brighter than anode glowing and channel one. The most of energy deposits in the cathode region. The destruction of spark channel takes about 2 ms. Cathode glowing stays for a longer period of time than anode one after the destruction of the channel. After the discharge current drops anode glowing almost disappears opposite to cathode glowing with additional (4–5) ms life-time.

INVESTIGATION OF THE MULTIPIN DISCHARGE IN TWO-PHASE FLOW

Vasilyak L.M.,[1] ***Kulikov Y.M.,***[*2] ***Panov V.A.,***[2]
Pecherkin V.Ya.,[1] ***Son E.E.***[1]

[1]*JIHT RAS, Moscow,* [2]*MIPT, Dolgoprudny, Russia*

[*]*kulikov-yurii@yandex.ru*

Discharge contraction due to the plasma instabilities is one of the major negative factors in the atmospheric discharge implementation. This process leads to a more intense Joule heating and reduces efficiency of plasma water treatment installations. To overcome this problem the special multipin discharge electrode system has been created and tested. A plasma reactor has several 78 pin electrodes, spreading the current across the inner gas-water volume, forms a system of low-current arcs which overlap. This makes possible to create so-called quasi-volume discharge. A special ballast control system has been also designed to stabilize the steady distribution of electric currents . Due to the high density of needle electrodes (pins) discharge region covers 95% of the working area, and adjacent arc interaction leads to substantial decrease of a breakdown voltage.

There are three major mechanisms in plasma cell acting on chemical compounds dissolved in water. The first is an excitation of rotational and vibrational degrees of freedom of the molecule due to Joule heating (the resistive losses) leading ultimately to molecule destruction at a certain temperature. The second agent is the direct impact of high-energy electrons on the interatomic bonds in molecules. The third factor paving the way for effective destruction of the pollutant molecules is plasma produced radiation. These agents enhance the generation of active species and increase the efficiency of oxidation and combustion of organic impurities in the plasma. To ensure efficient oxidation of organic contaminants in the plasma reactor it is necessary to provide a stoichiometric ratio between oxygen and the oxidizable substance changing gas-volume ratio in the flow.

VARIOUS PLASMA SOURCES FOR PLASMA MEDICINE: DIAGNOSTICS AND EFFECT FACTORS

Vasiliev M.M.,[*1] ***Zobnin A.V.,***[1] ***Petrov O.F.,***[1] ***Samoylov I.S.,***[1] ***Lebedev Yu.,***[2] ***Ermolaeva S.,***[3] ***Sysolyatina E.,***[3] ***Naroditsky B.,***[3] ***Shimizu T.,***[4] ***Morfill G.,***[4] ***Grigoriev A.,***[5] ***Fortov V.E.,***[1] ***Gintsburg A.***[3]

[1]*JIHT RAS, Moscow, Russia,* [2]*TIPS RAS, Moscow, Russia,* [3]*GRIEM RAMS, Moscow, Russia,* [4]*MPE, Garching, Germany,* [5]*IBP RAS, Moscow, Russia*

[*]*mixxy@mail.ru*

In this work we present methods and results of diagnostics of cold atmospheric plasma and possible methods of a control and monitoring of its influencing factors, which allow analyzing a contribution of separate components of plasma torch in cumulative effect of CAP. In the experiments we used the argon microwave plasma sources and ferroelectric reactor. The results of probe and optical diagnostics of CAP under various regimes of plasma generation suitable for working with biological objects are presented. By optical diagnostics we obtained experimental data of spectral analysis of plasma flow, including emission and absorption spectra. As a result of spectral measurements we determined plasma components that are corresponded to different spectral line series. Also estimations of metastable argon concentrations in plasma torch, based on analysis of absorption spectra, are made. We obtained integrated absorption coefficient which is equal $1.65 \cdot 10^{11}$ and the concentration of metastable argon, which is equal 19.4 ppm. As for probe diagnostics, we obtained distribution profile of electron concentration for different plasma source. Also a diagnostics of chemical composition of CAP, based on measurements of chemical gas analyzer, was conducted. We measured concentrations of active oxidizing agents in plasma, such as O_2, NO_2 and NO, in dependence on a distance from plasma torch. Also a power of SHF-radiation under various working regimes of generator was measured. We studied a dependence of power flow density of SHF-radiation on power of magnetron in a range from 60 to 150 W. Obtained curve is linear with a good accuracy. A range of flux density is 0.005–0.05 mW/cm^2. These values do not exceed permissible levels of radiation, which is 0.1 mW/cm^2, that is allowed during 2 hours under frequency 2.45 GHz. Finally, in this work we considered problems concerned with a selecting of physical factors that have the most sufficient bactericidal effect.

This work was partially supported by the Ministry of Education and Science and by the Program of the Presidium of RAS.

AN ION SOURCE DEVELOPMENT FOR THE EXECUTION OF MODEL EXPERIMENTS ON SPENT NUCLEAR FUEL PLASMA SEPARATION

Antonov N.N.,*[1] ***Gavrikov A.V.,***[1] ***Smirnov V.P.,***[1]
Timirkhanov R.A.,[1] ***Vorona N.A.,***[1] ***Zhabin S.N.***[2]

[1]*JIHT RAS, Moscow,* [2]*MIPT, Dolgoprudny, Russia*

**antonovnickola@gmail.com*

Plasma separation technology basics are being developed in Joint Institute for High Temperature of RAS nowadays. Constituent elements physical plasma method of separation by mass together with chemical methods could find application in the fuel cycle of fast reactors [1]. Nuclear material with a complicated elemental composition (spent nuclear fuel—SNF) in principle can be divided into groups of elements in a plasma mass separator [2]. The concept under development requires nuclear materials to be converted into a cold plasma flow then injected into space with buffer plasma and with a special configuration of the electric and magnetic field. In crossed electric and magnetic fields plasma flow is separated by mass into "light" and "heavy" groups of ions and then deposited on the collector surface.

To carry out experiments on plasma separation the ion source of the model substance is required. This paper presents a source of lead (Pb) ions. Lead simulates heavy component of SNF. Substance in solid state is placed in the crucible and heated up to 1000°C. In order to inject vapor into zone of the electron-beam ionization Knudsen cell effusion is used. Measurements were carried out at different values of the energy of electrons in the beam at different values of the magnetic field. Ion current measurement was carried out using a Faraday cup. Theoretical estimation of the ion current gives a value close to 40 microamperes. Experimental result is in good agreement with the theoretical estimate.

1. Zhiltsov V. A., KulyginV. M., Semashko N. N., Skovoroda A. A., SmirnovV. P., Timofeev A,V., Kudryavtsev E. G., Rachkov V. I., Orlov V. V. // AtomicEnergy 2006. V. 101. No. 4. P. 755–759.
2. Smirnov V. P., Antonov N. N., Gavrikov A. V., Samokhin A. A., Vorona N. A., Zhabin S. N. // XXVIII International Conference on Interaction of Intense Energy Fluxes with Matter–2013. Elbrus, Russia.

THE STATIONARY VACUUM ARC ON THE MULTI-COMPONENT HOT CATHODES

Amirov R.Kh.,[1] ***Vorona N.A.,***[1] ***Gavrikov A.V.,***[1] ***Zhabin S.N.,***[1]
Lizyakin G.D.,[2] ***Polistchook V.P.,***[1] ***Samoylov I.S.,***[1]
Smirnov V.P.,[1] ***Usmanov R.A.,***[*3] ***Yartsev I.M.***[1]

[1]*JIHT RAS, Moscow,* [2]*MEPhI, Moscow,* [3]*MIPT, Dolgoprudny, Russia*

[*]*ravus46@yandex.ru*

The stationary vacuum arc on hot cathode of spent nuclear fuel (SNF) has great prospects for the plasma technology of ion separation. This discharge generates the high-speed plasma flow of cathode material. Previously we have investigated this discharge on the gadolinium cathode because the characteristics of this discharge must be quite similar to the characteristics of vacuum arc on uranium cathode. However, real SNF has the complex composition of chemical elements with the uranium dioxide as the main component. In this work we present the study of this discharge on the cathodes from pure oxide of refractory metals (niobium and titanium) and their mixes with chromium.

Studied substances were placed in a heat-insulated molybdenum crucible. The crucible had electron beam heater (EBH) that was allowed to change the cathode temperature at fixed arc current. Power of the EBH with maximum voltage of 2 kV reached about 1 kW. The rectifier with output voltage of 0.35 kV and current of 200 A was used as power source. The distance between the electrodes was about 30 mm. Diagnostics system included the crucible temperature, volt-ampere characteristics of discharge, the heat flux from plasma to cathode, and spectrum of plasma radiation.

We have determined the necessary temperature for discharge existence on the cathode with different chemical composition. The minimum temperature of the cathode from pure metal oxides was about 2.4 kK. The minimum cathode temperature was decreased to 1.9 kK when chromium supplement was used. In last case the discharge current and voltage were changed in the range 30–150 A and 10–50 V respectively. We have investigated the influence of discharge conditions on intensity of atomic and ion lines of metals in plasma jet. Quite intensive atomic and ion lines of oxygen were not observed.

This study was partially supported by Rosatom State Atomic Energy Corporation.

AUTHOR INDEX

ORGANIZATION LIST

12CSRI MOD RF — 12 Central Scientific Research Institute of the Ministry of Defense of the Russian Federation, Sergiev Posad 141307, Moscow Region, Russia

AES — A. M. Prokhorov Academy of Engineering Sciences, Presnenskiy Val 19, Moscow 123557, Russia

AGNI-K Ltd. — Limited Company "AGNI-K", Izhorskaya 13 Bldg 2, Moscow 125412, Russia

AMERI FIU — Advanced Materials Engineering Research Institute, Florida International University, Miami, Florida, United States

ANL — Argonne National Laboratory, Argonne, United States

ANL, IPNS — Argonne National Laboratory, Intense Pulsed Neutron Source Division, Argonne, United States

ANO SIC MST — Autonomous Non-commercial Organization "Scientific Innovational Center for Missile and Space Technologies", Moscow, Russia

AO KNU — Astronomical Observatory of Kyiv Taras Shevchenko National University, Kyiv, Ukraine

AQura — AQura GmbH, Hanau, Germany

AstraSU — Astrakhan State University, Tatishcheva 20a, Astrakhan 414056, Astrakhan region, Russia

ASU — Arkansas State University, Jonesboro, Arkansas, United States

AU — Arak University, Arak, Iran

AUTM — Azarbaijan University of Tarbiat Moallem, Tabriz, Iran

BelgSTU, NB — Novorossiysk Branch of the V. G. Shukhov Belgorod State Technological University, Novorossiysk, Russia

BGU — Ben Gurion University, Beer Sheva, Russia

BIC SB RAS — Boreskov Institute of Catalysis of the Siberian Branch of the Russian Academy of Science, Novosibirsk, Russia

BINP SB RAS — G. I. Budker Institute of Nuclear Physics of the Siberian Branch of the Russian Academy of Sciences, Novosibirsk, Russia

BMSTU — Bauman Moscow State Technical University, 2nd Baumanskaya Street 5, Moscow 105005, Russia

BSTU — Belarusian State Technological University, Sverdlova Street 13a, Minsk 220006, Belarus

BSU — Belarusian State University, Nezavisimosti 4, Minsk 220030, Belarus

BSURI — Belarus State University of Radioelectronics and Informatics, Minsk, Belarus

CAI — Central Aerohydrodynamic Institute, Zhukovsky, Russia
CC RAS — A. A. Dorodnitsyn Computing Center of the Russian Academy of Sciences, Vavilova 40, Moscow 119333, Russia
CEA/DIF — Commissariat à l'Energie Atomique, Centre DAM Ile de France, Bruyères le Châtel, France
CELIA — CELIA, University Bordeaux, 351 cours de La Liberation, Talence 33405, France
CFSA — Centre for Fusion, Space and Astrophysics, Department of Physics, University of Warwick, Gibbet Hill Road, Coventry CV47AL, Warwickshire, United Kingdom (Great Britain)
CIAM — P. I. Baranov Central Institute of Aviation Motors Development, Aviamotornaya Street 2, Moscow 111116, Russia
CKC Ltd. — Chugoku Kayaku Company, Limited, Tokyo, Japan
CL — Cavendish Laboratory, Cambridge, United Kingdom (Great Britain)
CLF RAL — Central Laser Facility of Rutherford Appleton Laboratory, Didcot, United Kingdom (Great Britain)
CMTG SSP JU — Condensed Matter Theory Group, School of Studies in Physics, Jiwaji University, Gwalior 474011, Madhya Pradesh, India
CMU — Carnegie Mellon University, Forbes Avenue 5000, Pittsburgh 15213, PA, United States
CNIIMAsh — Central Scientific Research Institute of Machine Building, Korolev, Moscow Region, Russia
CNRS–University of Lorraine — CNRS–University of Lorraine, Villers-les-Nancy, France
Concord — Concord, Pryanishnikova 23a, Moscow 127550, Russia
CPHT EP — Centre de Physique Theorique, CNRS, Ecole Polytechnique, Palaiseau, France
CSRI SE — Central Scientific Research Institute of Special Engineering, Khotkovo, Russia
CSU — Chelyabinsk State University, Bratiev Kashirinykh Street 129, Chelyabinsk 454001, Chelyabinsk Region, Russia
DPLU — Department of Physics, Lund University, Lund, Sweden
EMMI — ExtreMe Matter Institute, Darmstadt, Russia
ENIN — The Krzhizhanovsky Power Engineering Institute, Leninsky Avenue 19, Moscow 117927, Russia
FGUP NIMI — Federal State Unitary Enterprise "Research Institute of Mechanical Engineering", Leningradskoe shosse 58, Moscow 125212, Russia
FIPCE RAS — Frumkin Institute of Physical Chemistry and Electrochemistry of the Russian Academy of Sciences, Moscow, Russia

FORC RAS — Fiber Optics Research Center of the Russian Academy of Sciences, Moscow, Russia

FSUE SRMI — Federal State Unitary Enterprise "Scientific and Research Machinebulding Institute", Leningradskoe Shosse 58, Moscow 125212, Russia

FU — Frei University, Berlin, Germany

GIST — Gwangju Institute of Science and Technology, Gwangju, Korea (South) (Republic)

GPI RAS — A. M. Prokhorov General Physics Institute of the Russian Academy of Sciences, Moscow, Russia

GPL CIW — Geophysical Laboratory, Carnegie Institution of Washington, Washington, DC, United States

GRIEM RAMS — Gamaleya Research Institute of Epidemiology and Microbiology of the Russian Academy of Medical Sciences, Moscow, Russia

GSI — GSI Helmholtzzentrum für Schwerionenforschung GmbH, Darmstadt, Germany

GUN — Goethe Universitat, Frankfurt, Germany

HMTI NASB — Heat and Mass Transfer Institute of the National Academy of Sciences of Belarus, Minsk, Belarus

HSAPS — High School of Applied Professional Studies, Filip Filipovic Street 20, Vranje 17500, Serbia

HUJI — Hebrew University, Jerusalem, Israel

IAI RAS — Institute of Analytical Instrument of the Russian Academy of Science, Saint-Petersburg, Russia

IAM RAS — Institute of Applied Mechanics of the Russian Academy of Sciences, Leninskii Prospekt 32a, Moscow 117334, Russia

IAP NUUz — Institute of Applied Physics of the National University of Uzbekistan, Vuzgorodok 3A, Tashkent 100174, Uzbekistan

IAP RAS — Institute of Applied Physics of the Russian Academy of Sciences, Ulyanova 46, Nizhny Novgorod 603950, Russia

IAPCM — Institute of Applied Physics and Computational Mathematics, Beijing 100088, China

IASDU — Institute for Advanced Studies, Dubna Univeristy, Dubna, Russia

IAU, BB — Bojnourd Branch of the Islamic Azad University, Daneshgah Street, Bojnourd 941769, North Khorasan, Iran

IAU, KB — Khoy Branch of the Islamic Azad University, Khoy Salmas Road 5, Khoy 58135, West Azarbaijan, Iran

IAU, PPRC — Plasma Physics Research Center, Science and Research Branch of the Islamic Azad University, Tehran, Iran

IAU, QB — Qom Branch of the Islamic Azad University, Qom, Iran

IAU, SB — Salmas Branch of the Islamic Azad University, Salmas 67897, Iran

IAU, TB — Tabriz Branch of the Islamic Azad University, Tabriz 653513, Iran

IBP RAS — Institute of Biomedical Problems of the Russian Academy of Sciences, Moscow, Russia

IC RAS — Institute of Crystallography of the Russian Academy of Sciences, Moscow, Russia

ICAD RAS — Institute for Computer-Aided Design of the Russian Academy of Sciences, Vtoraya Brestskaya 19/18, Moscow 123056, Russia

ICCT — Institute of Chemistry and Chemical Technology, Krasnoyarsk, Russia

IChF PAN — Institut Chemii Fizycznej PAN, Warszawa, Poland

ICMM UB RAS — Institute of Continuous Media Mechanics of the Ural Branch of the Russian Academy of Sciences, Academician Korolev Street 1, Perm 614013, Russia

ICP RAS — N. N. Semenov Institute of Chemical Physics of the Russian Academy of Sciences, Moscow, Russia

ICT SB RAS — Institute of Computational Technologies of the Siberian Branch of the Russian Academy of Sciences, Novosibirsk, Russia

IEE RAS — Institute for Electrophysics and Electrical Power of the Russian Academy of Sciences, Dvortsovaya Naberezhnaya 18, Saint-Petersburg 191186, Russia

IEP UB RAS — Institute of Electrophysics of the Ural Branch of the Russian Academy of Sciences, Ekaterinburg, Russia

IETP RAS — Institute of Experimental and Theoretical Physics of the Russian Academy of Sciences, Pushchino, Russia

IFT UWr — Institute for Theoretical Physics of the University of Wroclaw, Max Born Pl. 9, Wroclaw 50-204, Lower Silesia, Poland

IGD RAS — Institute of Geosphere Dynamics of the Russian Academy of Sciences, Moscow, Russia

IGM SB RAS — Sobolev Institute of Geology and Mineralogy of the Siberian Branch of the Russian Academy of Sciences, Akademika Koptyuga 3, Novosibirsk 630090, Russia

IGR DSC RAS — Institute for Geothermal Research of the Daghestan Scientific Center of the Russian Academy of Sciences, Shamil 39A, Makhachkala 367030, Daghestan Republic, Russia

IHCE SB RAS — Institute of High Current Electronics of the Siberian Branch of the Russian Academy of Sciences, Akademichesky Avenue 2/3, Tomsk 634055, Russia

IHPP RAS — Institute for High Pressure Physics of the Russian Academy of Sciences, Kaluzhskoe Shosse 14, Troitsk 142190, Moscow region, Russia

IIC SB RAS — Institute of Inorganic Chemistry of the Siberian Branch of the Russian Academy of Sciences, Novosibirsk, Russia

ILE — Institute of Laser Engineering, Osaka University, Osaka, Japan

ILIT RAS — Institute on Laser and Information Technologies of the Russian Academy of Sciences, Svyatoozerskaya 1, Shatura 140700, Moscow region, Russia

IMACH RAS — Joint Institute for Machine of the Russian Academy of Sciences, Belinskogo 85, Nizhny Novgorod 603024, Russia

IMET RAS — A. A. Baikov Institute of Metallurgy and Materials Science, Moscow, Russia

IMP — Institute of Modern Physics, Lanzhou, China

IMP NASU — G. V. Kurdymov Institute for Metal Physics of the National Academy of Sciences of Ukraine, Vernadsky Street 36, Kyiv 03142, Ukraine

IMP UB RAS — Institute of Metal Physics of the Ural Branch of the Russian Academy of Sciences, Sofya Kovalevskaya Street 18, Ekaterinburg 620219, Russia

IMS NASU — Institute for Material Science of the National Academy of Sciences of Ukraine, Kyiv, Ukraine

IMT RAS — Institute for Microelectronics Technology of the Russian Academy of Sciences, Institutskaya Street 6, Chernogolovka 142432, Moscow Region, Russia

INEPCP RAS — Institute of Energy Problems of Chemical Physics of the Russian Academy of Sciences, Moscow, Russia

INEUM — I. S. Bruk Institute for Electronic Control Machines, Vavilova 24, Moscow 119334, Russia

ING — Institut Neel, Grenoble, France

INR RAS — Institute for Nuclear Research of the Russian Academy of Science, Prospekt 60-letiya Oktyabrya 7a, Moscow 117312, Russia

IOC RAS — N. D. Zelinsky Institute of Organic Chemistry of the Russian Academy of Sciences, Moscow, Russia

IOP NASU — Institute of Physics of the National Academy of Sciences of Ukraine, Kyiv, Ukraine

IP DSC RAS — Institute of Physics of the Daghestan Scientific Center of the Russian Academy of Sciences, Yaragskogo 94, Makhachkala 367003, Daghestan Republic, Russia

IP EMAU — Institute of Physics Ernst-Moritz-Arndt-University, Greifswald, Germany

IP NASB — Institute of Physics of the National Academy of Sciences of Belarus, Logoiskii Trakt 22, Minsk 220090, Belarus

IP UR — Institute of Physics, University of Rostock, Universitatsplatz 3, Rostock D18051, Germany

IPCP RAS — Institute of Problems of Chemical Physics of the Russian Academy of Sciences, Academician Semenov Avenue 1, Chernogolovka 142432, Moscow Region, Russia

IPE RAS — O. Yu. Shmidt Institute of Physics of the Earth of the Russian Academy of Sciences, Bolshaya Gruzinskaya 10, Moscow 123995, Russia

IPhRAS — Institute of Philosophy of the Russian Academy of Sciences, Volkhonka 14 Bldg 5, Moscow 119991, Russia

IPM RAS — Institute for Physics of Microstructures of the Russian Academy of Sciences, Nizhny Novgorod, Russia

IPME RAS — Institute of Problems of Mechanical Engineering of the Russian Academy of Sciences, V.O., Bolshoj pr., 61, Saint Petersburg 199178, Russia

IPMech RAS — Institute for Problems in Mechanics of the Russian Academy of Sciences, Vernadskogo 101-1, Moscow 119526, Russia

IPPT NASU — Institute of Pulse Processes and Technologies of the National Academy of Sciences of Ukraine, Nikolaev, Ukraine

IPRE NASU — Institute of Pulse Research and Engineering of the National Academy of Sciences of Ukraine, Nikolaev, Ukraine

IPTI RAS — A. F. Ioffe Physical Technical Institute of the Russian Academy of Sciences, Polytekhnicheskaya 26, Saint-Petersburg 194021, Russia

IRE RAS, SB — Saratov Branch of the Kotelnikov Institute of Radio Engineering and Electronics of the Russian Academy of Sciences, Saratov, Russia

IS RAS — Institute of Spectroscopy of the Russian Academy of Sciences, Troitsk, Moscow region, Russia

ISMAN — Institute of Structural Macrokinetics and Materials Science of the Russian Academy of Sciences, Academician Osipyan 8, Chernogolovka 142432, Moscow region, Russia

ISP — Institute for Shock Physics, Pullman, United States

ISP NASU — Institute of Semiconductor Physics of the National Academy of Sciences of Ukraine, Kyiv, Ukraine

ISP SB RAS — Institute of Semiconductor Physics of the Siberian Branch of the Russian Academy of Sciences, Novosibirsk, Russia

ISPMS SB RAS — Institute of Strength Physics and Material Science of the Siberian Branch of the Russian Academy of Sciences, Akademicheskii 2/4, Tomsk 634021, Russia

ISSC UB RAS — Institute of Solid State Chemistry of the Ural Branch of the Russian Academy of Sciences, Pervomaiskaya Street 91, Ekaterinburg 620219, Russia

ISSCM SB RAS — Institute of Solid State Chemistry and Mechanochemistry of the Siberian Branch of the Russian Academy of Sciences, Novosibirsk, Russia

ISSP RAS — Institute of Solid State Physics of the Russian Academy of Sciences, Institutskaya Street 2, Chernogolovka 142432, Moscow Region, Russia

ISTC — International Science and Technology Center, Krasnoproletarskaya 32, Moscow 127473, Russia

ISU — Ingush State University, Nazran, Russia

ITAE RAS — Institute for Theoretical and Applied Electromagnetics of the Russian Academy of Sciences, Moscow, Russia

ITAM SB RAS — Institute of Theoretical and Applied Mechanics of the Siberian Branch of the Russian Academy of Sciences, Institutskaya 4/1, Novosibirsk 630090, Russia

ITEB RAS — Institute of Theoretical and Experimental Biophysics of the Russian Academy of Sciences, Puschino, Russia

ITP RAS — L. D. Landau Institute for Theoretical Physics of the Russian Academy of Scienses, Akademika Semenova 1a, Chernogolovka 142432, Moscow Region, Russia

ITP SB RAS — Institute of Thermophysics of the Siberian Branch of the Russian Academy of Sciences, Academician Lavrentyev Avenue 1, Novosibirsk-90 630090, Russia

ITPA — Institut für Theoretische Physik und Astrophysik, Kiel, Germany

JIHT RAS — Joint Institute for High Temperatures of the Russian Academy of Sciences, Izhorskaya 13 Bldg 2, Moscow 125412, Russia

JINR — Joint Institute for Nuclear Research, Dubna, Russia

JKU, ITP — Johannes Kepler University, Institute of Theoretical Physics, Linz, Austria

JSC — Forschzungszentrum Jülich, Supercomputing Centre, Jülich, Germany

JSC SET — Joint Stock Company "Special Energetic Technology", Bolshevik 43a, Shatura 140700, Moscow region, Russia

JU — Jadavpur University, Kolkata, India

KAZNU — Al-Farabi Kazakh National University, Al-farabi 71, Almaty 050040, South Kazakhstan, Kazakhstan

KBSU — Kabardino-Balkarian State University, Chernyshevskogo Street 173, Nalchik 360004, Russia

KIAM RAS — M. V. Keldysh Institute of Applied Mathematics of the Russian Academy of Sciences, Moscow, Russia

KIP SB RAS — Kirensky Institute of Physics of the Siberian Branch of the Russian Academy of Sciences, Akademgorodok 53/38, Krasnoyarsk 660036, Krasnoyarsky Kray, Russia

KNRTU — Kazan National Research Technological University, Karl Marx Street 68, Kazan 420015, Republic of Tatarstan, Russia

KNU — Taras Shevchenko National University of Kiev, Kyiv, Ukraine

KNUT — Khaje Nasir University of Technology, Tehran, Iran

KPSI JAEA — Kansai Photon Science Institute of the Japan Atomic Energy Agency, Kyoto, Japan

KPTI RAS — Kazan Physical-Technical Institute of the Russian Academy of Sciences, Sibirsky Trakt 10/7, Kazan 420029, Tatarstan, Russia

KraSC — Krasnoyarsk Scientific Centre, Kirensky Street 26, Krasnoyarsk 660074, Russia

KrIRT — Krasnoyarsk Institute of Railway Transport – Filial of Irkutsk State University of Railway Engineering, Krasnoyarsk, Russia

KRSCE — S. P. Korolev Rocket-Space Corporation "Energy", Korolev, Russia

KubSTU — Kuban State Technical University, Moskovskaya 2a, Krasnodar 353072, Russia

KubSTU NPI — Novorossiysk Polytechnic Institute of the Kuban State Technical University, Novorossiysk, Russia

LANL — Los Alamos National Laboratory, Los Alamos, United States

LC — Louisiana College, Pineville, United States

LHC — Laboratoire Hubert Curien, Saint-Etienne, France

LIH SB RAS — Lavrentyev Institute of Hydrodynamics of the Siberian Branch of the Russian Academy of Sciences, Lavrentyev Avenue 15, Novosibirsk 630090, Russia

LLNL — Lawrence Livermore National Laboratory, Livermore, United States

LP3 — Laboratory of Lasers, Plasmas and Photonic Processing, Marseille, France

LPD — Laboratoire des Plasmas Denses, Universite P. & M. Curie, Paris, France

LPGP — Laboratoire de Physique des Gaz et des Plasmas, Universite Paris Sud 11, Orsay, France

LPI RAS — P. N. Lebedev Physical Institute of the Russian Academy of Sciences, Leninskii 53, Moscow 119991, Russia

LTU — Lulea University of Technology, Lulea, Sweden

LULI EP — Laboratoire pour l'Utilisation des Lasers Intenses, CNRS-CEA, Ecole Polytechnique, Palaiseau, France

MA SRT — Military Academy of Stratigic Rocket Troops after Peter the Great, Kitaygorodskiy 9, Moscow 109074, Russia

MAI — Moscow Aviation Institute, Volokolamskoe Shosse 4, Moscow 125993, Russia

MEPhI — National Research Nuclear University Moscow Engineering Physics Institute, Moscow, Russia

MIEE — Moscow Institute of Electronic Engineering, Zelenograd, Proezd 4806, Dom 5, Moscow 124498, Russia

MIPT — Moscow Institute of Physics and Technology, Institutskiy Pereulok 9, Dolgoprudny 141700, Moscow Region, Russia

MPE — Max-Planck-Institut für Extraterrestrische Physik, Garching, Germany

MPEI — National Research University Moscow Power Engineering Institute, Krasnokazarmennaya 14, Moscow 111250, Russia

MPK — Max-Planck-Institut für Kernphysik, Heidelberg, Germany

MPS — Max-Planck-Institut für Sonnensystemforschung, Max-Planck-Str. 2, Katlenburg-Lindau 37191, Germany

MPT Ltd. — Limited Company "Modern Plasma Technologies", Izhorskaya 13 Bldg 2, Moscow 125412, Russia

MSU — M. V. Lomonosov Moscow State University, Moscow, Russia

MSU, SAI — Sternberg Astronomical Institute of the Moscow State University, Universitetskii Pr. 13, Moscow 119992, Russia

MSU, SINP — Skobeltsyn Institute for Nuclear Physics of the Moscow State University, Moscow, Russia

MUCTR — D. I. Mendeleev University of Chemical Technology of Russia, Miusskaya 9, Moscow 125047, Russia

MUT, IOE — Military University of Technology, Institute of Optoelectronics, Kaliskiego 2, Warsaw 00-908, Poland

NCSTU — North Caucasus State Technical University, Kulakova Street 2, Stavropol 355029, Stavropolskyi Kray, Russia

NIST — National Institute of Standards and Technology, Boulder, Colorado, United States

NIT — Nanchang Institute of Technology, Yuping East Road 299, Changbei, Nanchang 330013, Jiangxi Province, China

Nordmetall GmbH — Nordmetall GmbH, Adorf/Erzgebirge, Germany

NPL, FSR — Nuclear Physics Laboratory, Faculty of Sciences Rabat, B.P 1014, Rabat R.P, 4 Av. Ibn Battouta, Rabat 10000, Rabat-Sale, Morocco

NPO Saturn, LSTC — A. Lyulka Scienific-and-Technical Center of the Saturn Scientific-Production Association, Kasatkina Street 13, Moscow 129301, Russia

NPO "Komposit" — Scientifically Industrial Association "Komposit", Korolev, Russia

NPTL, FSS — Nuclear Physics and Techniques Laboratory, Faculty of Sciences Semlalia, Marrakech, Morocco

NRC KI — National Research Center "Kurchatov Institute", Kurchatov Square 1, Moscow 123182, Russia

NSTU — Novosibirsk State Technical University, Karl Marx Avenue 20, Novosibirsk 630092, Russia

NSU — Novosibirsk State University, Novosibirsk, Russia

NWMTC — Research Center for Nonlinear Wave Mechanics and Technology, Moscow, Russia

OAO "Makeyev GRTs" — Open Joint Stock Company "Academician V. P. Makeyev State Rocket Centre", Turgoyakskoye Shosse 1, Miass 456300, Chelyabinsk Region, Russia

OGRI RAS — Oil and Gas Research Institute of the Russian Academy of Sciences, Gubkin Street 3, Moscow 119991, Russia

OJSC FGC UES — Open Joint Stock Company Federal Grid Company of the Unified Energy System, Moscow, Russia

OSAF — Odessa State Academy of Freeze, Odessa, Ukraine

PCI PCNU — Physical-Chemical Institute PreCarpathian National University, Ivano-Frankovsk, Ukraine

PGU — Persian Gulf University, Bushehr 75169, Iran

PL KAE — Technical University of Lodz, the Faculty of Electrical, Electronic, Computer and Control Engineering, Department of Electrical Apparatus, Stefanowskiego 18/22, Lodz 90924, Poland

PM & IUSTI — Polytech'Marseille & IUSTI, Marseille, France

PTI NASB — Physical-Technical Institute of the National Academy of Sciences of Belarus, Minsk, Belarus

PULSAR Ltd. — Limited Company "PULSAR", Faran 4, Yavne 81103, Israel

Resonance Ltd. — Limited Company "Resonance", Moscow, Russia

RFNC–VNIIEF — Russian Federal Nuclear Center – All-Russian Research Institute of Experimental Physics, Mira Avenue 37, Sarov 607190, Nizhnii Novgorod region, Russia

RFNC–VNIITF — Russian Federal Nuclear Center – All-Russian Research Institute of Technical Physics, Vasilieva 13, Snezhinsk 456770, Chelyabinsk Region, Russia

RIAMA KBRC RAS — Research Institute of Applied Mathematics and Automation of the Kabardino-Balkarian Research Center of the Russian Academy of Sciences, Scortanova 89, Nalchik 360000, Kabardino-Balkarian Republic, Russia

RIE ShU — Research Institute of Electronics of the Shizuoka University, Hamamatsu, Japan

RIPT — Federal State Unitary Enterprise "Research Institute of Pulse Technique", Luganskaya Street 9, Moscow 115304, Russia

RNU — Russian New University, Moscow, Russia

RRC KI, INS — Institute of Nuclear Synthesis of the Russian Research Center "Kurchatov Institute", Kurchatov Square 1, Moscow 123182, Russia

RSI — Risk and Safety Institute, Moscow, Russia

RSREU — Ryazan State Radio Engineering University, Gagarin Street 59/1, Ryazan 390005, Russia

RUDN — Russian University "Peoples' Friendship", Mikluho-Maklaya 6, Moscow 115569, Russia

SamSTU — Samara State Technical University, Molodogvardeyskaya 244, Samara 443100, Samara region, Russia

SFU — Siberian Federal University, Kirensky street 26, Krasnoyarsk 660074, Krasnoyarsky kray, Russia

SIAS — Scientific Industrial Association "Sintez", Moscow, Russia

SIBGUTI — Siberian State University of Telecommunications and Informatics, Kirova 89, Novosibirsk 630102, Novosibirsk region, Russia

SNL — Sandia National Laboratories, Albuquerque, United States

SOIBC RAS — Shemyakin and Ovchinnikov Institute of Bioorganic Chemistry of the Russian Academy of Sciences, Puschino, Russia

SPbSPU — Saint-Petersburg State Polytechnic University, Saint-Petersburg, Russia

SPbSU — Saint-Petersburg State University, Universitetsky 26, Petrodvorets, Saint-Petersburg 198504, Russia

SPbSU ITMO — Saint-Petersburg State University of Information Technologies, Mechahics and Optics, Kronvergskiy 49, Saint-Petersburg 197101, Russia

SPbSU LTFT — Saint-Petersburg State University of Low Temperature and Food Technology, Saint-Petersburg, Russia

SPhTI SRNU MEPhI — Snezhinsk Physical-Technical Institute of the Scientific Research Nuclear University Moscow Engineering Physics Institute, Komsomolskaya 8, Snezhinsk 456776, Chelyabinsk Region, Russia

SRC AVTEC — Scientific and Research Center AVTEC – Automatics Telemechanics Ecology, Ltd., Kozlova Street 62, Novorossiysk 353920, Krasnodarskiy Kray, Russia

SRC RF TRINITI — State Research Center of the Russian Federation – Troitsk Institute for Innovation and Fusion Research, Pushkovykh Street 12, Troitsk 142190, Moscow Region, Russia

SRI MCS — Scientific Research Institute of Multiprocessor Computing Systems of Southern Federal University, Chekhov Street 2, Taganrog 347928, Russia

SSC RF IPPE — Federal State Unitary Enterprise "State Scientific Centre of the Russian Federation – A. I. Leypunsky Institute for Physics and Power Engineering", Obninsk, Russia

SSC RF ITEP — State Scientific Center of the Russian Federation – Alikhanov Institute for Theoretical and Experimental Physics, Bolshaya Cheremushkinskaya 25, Moscow 117218, Russia

SSPTI MEPhI — Sarov State Physics and Technical Institute of the National Research Nuclear Unuversity Moscow Engineering Physics Institute, Dukhova 6, Sarov 607186, Nizhny Novgorod region, Russia

SSRI ME — State Scientific Research Institute of Mechanical Engineering after V. V. Bakhirev, Dzerzhinsk, Russia

STC "Industrial Safety" — Scientific and Technical Centre "Industrial Safety", Moscow, Russia

SUSU — South-Ural State University, Lenin Avenue 76, Chelyabinsk 454080, Russia

SUT — Sharif University of Technology, Tehran, Iran

SUTMA — Swinburne University of Technology, Melbourne, Australia

SWCMRC KU — Shock Wave and Condensed Matter Research Center, Kumamoto University, Kumamoto, Japan

TAMU — Texas A&M University, College Station, Texas, United States

TC Schlumberger — Technology Company Schlumberger, Moscow, Russia

TIPS RAS — A. V. Topchiev Institute of Petrochemical Synthesis of the

Russian Academy of Sciences, Leninsky Avenue 29, Moscow 119991, Russia

TISNUM — Techonological Institute of Superhard and New Carbon Materials, Troitsk, Russia

TPU — Tomsk Polytechnical University, Lenin Avenue 30, Tomsk 634050, Russia

TSNIISM — The Central Scientific Research Institute of Special Machine Building, Zavodskaya, Khotkovo 141371, Moscow region, Russia

TSU — Tomsk State University, Lenina Avenue 36, Tomsk 634050, Russia

TSU, RIAMM — Research Institute of Applied Mathematics and Mechanics of the Tomsk State University, Lenin Avenue 36, Tomsk 634024, Russia

TSUAB — Tomsk State University of Architecture and Building, Solyanaya 2, Tomsk 634003, Russia

TUBAF — Technical University Bergakademie Freiberg, Freiberg, Germany

TUD — Technical University Darmstadt, Darmstadt, Germany

TUD NL — Technical University of Delft, Delft, Netherlands

TUK — Technical University of Kaiserslautern, Kaiserslautern, Germany

UA — University of Arkansas, Fayetteville, Arkansas, United States

UCAM — University Cadi Ayyad, Marrakech 40000, Morocco

UDE — University of Duisburg-Essen, Duisburg, Germany

UDE, IVG — University of Duisburg-Essen, Institüt für Verbrennung und Gasdynamik, Duisburg, Germany

UEW — University of Education, Winneba, Central Region, Ghana

UFTP — University of Frankfurt am Main, Institute for Theoretical Physics, Max-von-Laue-Str. 1, Frankfurt am Main 60438, Hessen, Germany

UI — University of Ibadan, NW4/260 Akinsanmi Street, Idioro Ekotedo, Ibadan 23402, Oyo state, Nigeria

UMB — Universita di Milano Bicocca, Milano, Italy

UMR CNRS — Laboratoire de Metallurgie Physique CNRS, Poitiers, France

UmU — Umea University, Linnaeus vag, Umea 90187, Sweden

UNICAM — University of Camerino, Via Madonna delle Carceri, Camerino 62032, MC, Italy

University of Bundeswehr — University of Bundeswehr, Munich, Germany

University of Rostock — University of Rostock, Rostock, Germany

University of Ulster — HySAFER Centre, University of Ulster, Newtownabbey, United Kingdom (Great Britain)

Universität Kaiserslautern — Universität Kaiserslautern, Kaiserslautern, Germany
UNSW — University of New South Wales, Sydney 2052, Australia
UOAB — University of Antwerpen, Antwerpen, Belgium
UOBI — University of Baghdad, Baghdad, Iraq
UOCH — University of Chicago, Chicago, United States
UOEB, CSEC — Centre for Science at Extreme Conditions of the University of Edinburgh, Edinburgh, United Kingdom (Great Britain)
UOG — University of Goettingen, Goettingen, Germany
UOG, IPC — University of Goettingen, Institute for Physical Chemistry, Goettingen, Germany
UOIL — University of Illinois, Urbana 61801, Illinois, United States
UOMI — University of Michigan, Ann Arbor, United States
UOT — University of Tokyo, Tokyo, Japan
UOVA — University of Virginia, MSE Department, 395 McCormick Road, P.O. Box 400745, Charlottesville 22904, Virginia, United States
UOY — University of York, York, United Kingdom (Great Britain)
UPB — Universitat Paderborn, Maerchenring 56, Paderborn D33095, Karlsruhe, Germany
UPMC — Universite Pierre et Marie Curie, Paris, France
UrFU — Ural Federal University, Lenina Avenue 51, Ekaterinburg 620000, Russia
URTV — University of Rome "Tor Vergata", Rome, Italy
USF — University of South Florida, Tampa, Florida, United States
UWA — University of Western Australia, Crawley WA6009, Australia
VGI — State Institution "High-Mountain Geophysical Institute", Lenina Avenue 2, Nalchik 360030, Kabardino-Balkarian Republic, Russia
VlaSU — Vladimir State University, Gor'kogo 87, Vladimir 600000, Russia
VNIIA — All-Russia Scientific Research Institute of Automatics, Luganskaya Street 9, Moscow 115304, Russia
VNIIFTRI — All-Russian Scientific Research Institute for Physical-Technical and Radiotechnical Measurements, Mendeleevo, Russia
VNIINM — Bochvar All-Russian Research Institute of Inorganic Materials, Moscow, Russia
WADIS Ltd. — Limited Company "WADIS", 16 Abba Eben, Herzlia 46725, Israel
WCRC — Western-Caucasus Research Center, Tupik Zvezdniy 9, Tuapse 352808, Krasnodar Territory, Russia

PARTICIPANT LIST

1. *Abarzhi Snezhana Ivanovna*, CMU, Pittsburgh, United States, phone: +1(650)8628580, fax: +1(412)2682000, snezhana.abarzhi@gmail.com
2. *Akhtanova Gul'nur Bolatovna*, KAZNU, Almaty, Kazakhstan, phone: +7(705)5608050, fax: +7(727)3773511, g.akhtanova@gmail.com
3. *Aliverdiev Abutrab Alexandrovich*, IGR DSC RAS, Makhachkala, Russia, phone: +7(8722)629357, fax: +7(8722)629357, aliverdi@mail.ru
4. *Alymov Mikhail Ivanovich*, ISMAN, Chernogolovka, Russia, phone: +7(49652)46376, fax: +7(49652)46255, director@ism.ac.ru
5. *Anan'ev Sergei Yurevich*, JIHT RAS, Moscow, Russia, phone: +7(495)9454920, fax: +7(495)9454920, serg.ananev@gmail.com
6. *Andreev Nikolay Evgen'evich*, JIHT RAS, Moscow, Russia, phone: +7(495)4859722, fax: +7(495)4857990, andreev@ras.ru
7. *Andriyanova Yuliya Nikolaevna*, JIHT RAS, Moscow, Russia, phone: +7(915)0079618, fax: +7(915)0079618, andriyanovayn@gmail.com
8. *Andryushin Ivan Igorevich*, SSC RF IPPE, Obninsk, Russia, phone: +7(910)8613699, fax: +7(48439)95772, i.andryushin@gmail.com
9. *Antipov Sergey*, JIHT RAS, Moscow, Russia, phone: +7(495)4842355, fax: +7(495)4857990, antipov@ihed.ras.ru
10. *Antonov Nikolay Nikolaevich*, JIHT RAS, Moscow, Russia, phone: +7(925)2010497, fax: +7(495)4851081, antonovnickola@gmail.com
11. *Apfelbaum Evgeny Mikhailovich*, JIHT RAS, Moscow, Russia, phone: +7(495)4844433, fax: +7(495)4857990, apfel_e@mail.ru
12. *Assovskiy Igor Georgeevich*, ICP RAS, Moscow, Russia, phone: +7(495)9397267, fax: +7(495)6512191, assov@chph.ras.ru
13. *Badretdinova Liaisan Kharisovna*, KNRTU, Kazan, Russia, phone: +7(917)9341899, fax: +7(843)2314091, salamandra_1985@mail.ru
14. *Bakulin Vladimir Nikolaevich*, IAM RAS, Moscow, Russia, phone: +7(499)1584828, fax: +7(499)1584828, vbak@yandex.ru
15. *Bannikova Irina Anatolevna*, ICMM UB RAS, Perm, Russia, phone: +7(342)2378312, fax: +7(342)2378487, malgacheva@icmm.ru
16. *Bardin Andrey Alexandrovich*, IPCP RAS, Chernogolovka, Russia, phone: +7(915)0933198, fax: +7(496)5225636, dr.abardin@gmail.com
17. *Basharin Andrey Yurievich*, JIHT RAS, Moscow, Russia, phone:

+7(495)3625603, fax: +7(495)3625603, ayb@iht.mpei.ac.ru
18. *Batuev Stanislav Pavlovich*, TSUAB, Tomsk, Russia, phone: +7(903)9136107, fax: +7(903)9136107, Antrim@sibmail.com
19. *Bayandin Yuriy Vitalievich*, ICMM UB RAS, Perm, Russia, phone: +7(342)2378312, fax: +7(342)2378487, buv@icmm.ru
20. *Belkheeva Rumiya Katdusovna*, NSU, Novosibirsk, Russia, phone: +7(383)3303244, fax: +7(383)3303255, rumia@post.nsu.ru
21. *Bhat Idris Hamid*, CMTG SSP JU, Gwalior, India, phone: +91(0751)2442777, fax: +91(0751)2442777, idu.idris@gmail.com
22. *Bisti Veronika Evgenyevna*, ISSP RAS, Chernogolovka, Russia, phone: +7(496)5228269, fax: +7(496)5228168, bisti@issp.ac.ru
23. *Bivol Grigory Yurievich*, JIHT RAS, Moscow, Russia, phone: +7(495)4858463, fax: +7(495)4842138, grigorij-bivol@yandex.ru
24. *Bobrov Andrei Alexandrovich*, JIHT RAS, Moscow, Russia, phone: +7(916)8003125, fax: +7(495)3620778, abobrov@inbox.ru
25. *Bocharnikov Vladimir Maksimovich*, JIHT RAS, Moscow, Russia, phone: +7(919)1017468, fax: +7(495)1231212, vova-bocha@phystech.edu
26. *Borisenko Lidia Andreevna*, LPI RAS, Moscow, Russia, phone: +7(916)9293633, fax: +7(499)1358593, borisenko.lidiya@physics.msu.ru
27. *Borodin Elijah Nikolaevich*, IPME RAS, Saint Petersburg, Russia, phone: +7(904)5525717, fax: +7(812)3214771, elbor7@gmail.com
28. *Bratov Vladimir*, IPME RAS, Saint Petersburg, Russia, phone: +7(950)0217203, fax: +7(950)0217203, vladimir@bratov.com
29. *Buchko Pavel Vasilievich*, JIHT RAS, Moscow, Russia, phone: +7(916)4941101, fax: +7(495)4857990, pahomich@tut.by
30. *Bugay Irina Vladimirovna*, BMSTU, Moscow, Russia, phone: +7(499)2636541, fax: +7(499)2636541, ibug@mail.ru
31. *Bukhovich Yevgeny Victorovich*, KubSTU, Krasnodar, Russia, phone: +7(918)0416382, fax: +7(861)2558532, evapo@br.ru
32. *Butlitsky Michael*, JIHT RAS, Moscow, Russia, phone: +7(926)5731035, fax: +7(926)5731035, aristofun@yandex.ru
33. *Bykov Yury Anatol'evich*, JIHT RAS, Moscow, Russia, phone: +7(916)2664168, fax: +7(916)2664168, Yrka.2@mail.ru
34. *Bystryi Roman*, JIHT RAS, Moscow, Russia, phone: +7(985)6474714, fax: +7(495)4858545, broman.meld@gmail.com
35. *Cheprunov Alexander Alexandrovich*, 12CSRI MOD RF, Sergiev Posad, Russia, phone: +7(495)5849962, fax: +7(495)5849962, olga@vnitip.ru

36. *Degtyareva Valentina Feognievna*, ISSP RAS, Chernogolovka, Russia, phone: +7(496)5228176, fax: +7(496)5228160, degtyar@issp.ac.ru
37. *Director Leonid Bentsianovich*, JIHT RAS, Moscow, Russia, phone: +7(495)4859144, fax: +7(495)4841955, director@oivtran.ru
38. *Doludenko Aleksey Nikolaevich*, JIHT RAS, Moscow, Russia, phone: +7(495)4859666, fax: +7(495)4859666, adoludenko@gmail.com
39. *Drakon Alexander Vseslavovich*, JIHT RAS, Moscow, Russia, phone: +7(495)4841966, fax: +7(495)4842222, drakon.a.v@gmail.com
40. *Dudin Sergey Vasilevich*, IPCP RAS, Chernogolovka, Russia, phone: +7(496)5225168, fax: +7(496)5225168, dudinsv@ficp.ac.ru
41. *Dudorov Alexandr Egorovich*, CSU, Chelyabinsk, Russia, phone: +7(351)7997161, fax: +7(351)7420925, dudorov@csu.ru
42. *Dyachkov Lev Gavriilovich*, JIHT RAS, Moscow, Russia, phone: +7(495)3625310, fax: +7(495)4857990, dyachk@mail.ru
43. *Dyachkov Sergey Aleksandrovich*, JIHT RAS, Moscow, Russia, phone: +7(926)2890847, fax: +7(495)4857990, serj.dyachkov@gmail.com
44. *Efremov Vladimir Petrovich*, JIHT RAS, Moscow, Russia, phone: +7(495)4850963, fax: +7(495)4857990, dr.efremov@gmail.com
45. *Egorov Oleg Georgievich*, SRC RF TRINITI, Troitsk, Russia, phone: +7(498)5405058, fax: +7(498)5405058, egorov@triniti.ru
46. *Emelianov Alexander Valentinovich*, JIHT RAS, Moscow, Russia, phone: +7(495)4841966, fax: +7(495)4857990, aemelia@ihed.ras.ru
47. *Emelin Dmitriy Anatol'yevich*, SUSU, Chelyabinsk, Russia, phone: +7(908)5755139, fax: +7(351)2679041, emelin_d_a@mail.ru
48. *Eremin Alexander Victorovich*, JIHT RAS, Moscow, Russia, phone: +7(495)4832314, fax: +7(495)4857990, eremin@ihed.ras.ru
49. *Filinov Vladimir Sergeevich*, JIHT RAS, Moscow, Russia, phone: +7(495)4842429, fax: +7(495)4857990, vladimir_filinov@mail.ru
50. *Filippov Anatoly Vasiljevich*, SRC RF TRINITI, Troitsk, Russia, phone: +7(495)8510446, fax: +7(495)8415776, fav@triniti.ru
51. *Fokin Vladimir Borisovich*, JIHT RAS, Moscow, Russia, phone: +7(495)4842456, fax: +7(495)4859922, Vladimir.fokin@phystech.edu
52. *Fomin Nikita Alexandrovich*, HMTI NASB, Minsk, Belarus, phone: +375(17)2841353, fax: +375(17)2841353, fomin@hmti.ac.by
53. *Fortov Vladimir Evgenievich*, JIHT RAS, Moscow, Russia, phone:

+7(495)4857988, fax: +7(495)4857990, fortov@ihed.ras.ru

54. *Fortova Svetlana Vladimirovna*, ICAD RAS, Moscow, Russia, phone: +7(962)9706136, fax: +7(495)1357919, sfortova@mail.ru
55. *Frolov Alexander Anatol'evich*, JIHT RAS, Moscow, Russia, phone: +7(495)4859722, fax: +7(495)4857990, frolov@ihed.ras.ru
56. *Gadjieva Zaida Rasulovna*, IGR DSC RAS, Makhachkala, Russia, phone: +7(960)4113714, fax: +7(872)2629312, zaida55@mail.ru
57. *Garkushin Gennady Valer'evich*, IPCP RAS, Chernogolovka, Russia, phone: +7(495)49472, fax: +7(495)49472, garkushin@ficp.ac.ru
58. *Gavasheli Yuliya Olegovna*, KBSU, Nalchik, Russia, phone: +7(928)7168367, fax: +7(928)7168367, yu-pakhunova@mail.ru
59. *Gavasheli David Shotaevich*, RIAMA KBRC RAS, Nalchik, Russia, phone: +7(928)7085367, fax: +7(928)7085367, david_gavasheli@yahoo.com
60. *Gavrenkov Sergey Alekseevich*, JIHT RAS, Moscow, Russia, phone: +7(916)6759763, fax: +7(916)6759763, gavrenkov@gmail.com
61. *Gavrikov Andrey Igorevich*, NRC KI, Moscow, Russia, phone: +7(499)1967706, fax: +7(499)1969840, gavrikov_ai@nrcki.ru
62. *Glushniova Alexandra Vladimirovna*, JIHT RAS, Moscow, Russia, phone: +7(916)7878274, fax: +7(495)4857990, Glushniova.alexandra@gmail.com
63. *Goldenko Natalia Alexandrovna*, CNIIMAsh, Korolev, Russia, phone: +7(903)1968198, fax: +7(495)5168198, hatuse4eg@mail.ru
64. *Golovastov Sergey Viktorovich*, JIHT RAS, Moscow, Russia, phone: +7(495)4858463, fax: +7(495)4842138, golovastov@yandex.ru
65. *Golub Victor Vladimirovich*, JIHT RAS, Moscow, Russia, phone: +7(495)4842138, fax: +7(495)4842138, victor.v.golub@gmail.com
66. *Gurentsov Evgeny Valerievich*, JIHT RAS, Moscow, Russia, phone: +7(495)4841966, fax: +7(495)4857990, gurentsov@ihed.ras.ru
67. *Hvatkov Anton Sergeevich*, VNIIA, Moscow, Russia, phone: +7(915)2453520, fax: +7(000)0000000, toshkanu@gmail.com
68. *Ignatiev Nikolaj Georgievich*, VNIIA, Moscow, Russia, phone: +7(499)2715948, fax: +7(495)3214855, n_ignatev@list.ru
69. *Iosilevskiy Igor L'vovich*, JIHT RAS, Moscow, Russia, phone: +7(910)4069314, fax: +7(495)4842300, iosilevskiy@gmail.com
70. *Ivanov Mikhail Ivanovich*, VNIIA, Moscow, Russia, phone: +7(495)3214674, fax: +7(499)9780903, ivanov3575@yandex.ru
71. *Ivanov Michail Fedorovich*, JIHT RAS, Moscow, Russia, phone: +7(495)4844433, fax: +7(495)4841638, ivanov_mf@mail.ru

72. *Ivanovskis Glebs*, JIHT RAS, Moscow, Russia, phone: +7(495)4859263, fax: +7(495)4859922, ivanovakis@mail.ru
73. *Kadatskiy Maksim Alekseevich*, JIHT RAS, Moscow, Russia, phone: +7(965)2412758, fax: +7(965)2412758, makkad@yandex.ru
74. *Kanel Gennady Isaakovich*, JIHT RAS, Moscow, Russia, phone: +7(495)4834374, fax: +7(495)4857990, kanel@ficp.ac.ru
75. *Kavyrshin Dmitriy Igorevich*, JIHT RAS, Moscow, Russia, phone: +7(495)4841855, fax: +7(495)4859163, dimakav@rambler.ru
76. *Kazarinov Nikita Andreevich*, SPbSU, Saint-Petersburg, Russia, phone: +7(964)3666464, fax: +7(964)3666464, nkazarinov@gmail.com
77. *Khishchenko Konstantin Vladimirovich*, JIHT RAS, Moscow, Russia, phone: +7(495)4842483, fax: +7(495)4857990, konst@ihed.ras.ru
78. *Khlybov Vladimir Il'ich*, OAO "Makeyev GRTs", Miass, Russia, phone: +7(3513)286333, fax: +7(3513)566191, src@makeyev.ru
79. *Khokhlov Victor Alexandrovich*, ITP RAS, Chernogolovka, Russia, phone: +7(903)2130112, fax: +7(495)9382077, V_A_Kh@mail.ru
80. *Khokonov Murat Khazretalievich*, KBSU, Nalchik, Russia, phone: +7(928)6910262, fax: +7(495)3379955, khokon6@mail.ru
81. *Khokonov Azamat Khazret-Alievich*, KBSU, Nalchik, Russia, phone: +7(928)0811703, fax: +7(495)3379955, azkh@mail.ru
82. *Khromova Elena Sergeevna*, IPCP RAS, Chernogolovka, Russia, phone: +7(496)5224471, fax: +7(496)5221158, lskh@mail.ru
83. *Kiverin Alexey*, JIHT RAS, Moscow, Russia, phone: +7(495)4844433, fax: +7(495)4859922, alexeykiverin@gmail.com
84. *Klementyeva Irina*, JIHT RAS, Moscow, Russia, phone: +7(495)4858463, fax: +7(495)4842138, ira.klementyeva@mail.ru
85. *Knyazev Dmitry Vladimirovich*, JIHT RAS, Moscow, Russia, phone: +7(495)4857988, fax: +7(495)4857988, d.v.knyazev@yandex.ru
86. *Konyukhov Andrey Victorovich*, JIHT RAS, Moscow, Russia, phone: +7(495)5908620, fax: +7(495)4857990, konyukhov_av@mail.ru
87. *Korostina Marina Aleksandrovna*, JIHT RAS, Moscow, Russia, phone: +7(495)4857981, fax: +7(495)4857981, korostina@inbox.ru
88. *Koshelev Anton*, JIHT RAS, Moscow, Russia, phone: +7(909)6761125, fax: +7(495)4859722, antonak92@mail.ru
89. *Koss Xeniya*, JIHT RAS, Moscow, Russia, phone: +7(495)4842355, fax: +7(495)4857990, Xeniya.Koss@gmail.com

90. *Kotov Andrey Vladimirovich*, JIHT RAS, Moscow, Russia, phone: +7(496)24523714, fax: +7(496)24523714, daleco-m@mail.ru
91. *Krapiva Pavel Sergeevich*, VNIIA, Moscow, Russia, phone: +7(499)2715948, fax: +7(495)3214855, forautoru@land.ru
92. *Krasyuk Igor Kornelievich*, GPI RAS, Moscow, Russia, phone: +7(916)6228254, fax: +7(499)1352055, krasyuk99@rambler.ru
93. *Krikunova Anastasia Igorevna*, JIHT RAS, Moscow, Russia, phone: +7(495)4859666, fax: +7(495)4859666, utro-2007@mail.ru
94. *Krivokorytov Mikhail Sergeevich*, JIHT RAS, Moscow, Russia, phone: +7(495)4858566, fax: +7(495)4858566, mikhail.k@phystech.edu
95. *Kucherik Alexey Olegovich*, VlaSU, Vladimir, Russia, phone: +7(4922)477796, fax: +7(4922)333336, kucherik@vlsu.ru
96. *Kudryavtseva Irina Vladimirovna*, SPbSU ITMO, Saint-Petersburg, Russia, phone: +7(911)9359186, fax: +7(812)3147869, togg1@yandex.ru
97. *Kuksin Alexey Yurievich*, JIHT RAS, Moscow, Russia, phone: +7(926)5362618, fax: +7(495)4857990, alexey.kuksin@gmail.com
98. *Kulikov Yury Matveevich*, JIHT RAS, Moscow, Russia, phone: +7(917)5953822, fax: +7(917)5953822, kulikov-yurii@yandex.ru
99. *Kurakevych Oleksandr Oleksandrovych*, UPMC, Paris, France, phone: +33(0)144274456, fax: +33(0)144273785, oleksandr.kurakevych@impmc.jussieu.fr
100. *Kurochka Kirill Viktorovich*, UrFU, Ekaterinburg, Russia, phone: +7(922)6128069, fax: +7(343)2613124, kirill.k.v@yandex.ru
101. *Kuropatenko Valentin Fedorovich*, RFNC–VNIITF, Snezhinsk, Russia, phone: +7(35146)55153, fax: +7(35146)55118, v.f.kuropatenko@vniitf.ru
102. *Kuzmina Julia Sergeevna*, JIHT RAS, Moscow, Russia, phone: +7(495)4857981, fax: +7(495)4857981, juli_kuzmina@mail.ru
103. *Lankin Alexander*, JIHT RAS, Moscow, Russia, phone: +7(495)4858545, fax: +7(495)4857990, Alex198508@yandex.ru
104. *Lapin Sergey Mikhailovich*, IPCP RAS, Chernogolovka, Russia, phone: +7(49652)24125, fax: +7(49652)49472, lms.lapin12011@yandex.ru
105. *Larkin Alexander Sergeevich*, JIHT RAS, Moscow, Russia, phone: +7(963)6100461, fax: +7(495)4857990, alexanderlarkin@rambler.ru
106. *Lavrenov Vladimir Alexandrovich*, JIHT RAS, Moscow, Russia, phone: +7(495)4857981, fax: +7(495)4857981, v.a.lavrenov@gmail.com

107. *Lemeshko Boris Dmitrievich*, VNIIA, Moscow, Russia, phone: +7(495)3214555, fax: +7(495)7877693, bogolubov@vniia.ru
108. *Lepeshkin Alexander Roaldovich*, CIAM, Moscow, Russia, phone: +7(495)5529634, fax: +7(495)5524611, lepeshkin.ar@gmail.com
109. *Levashov Pavel Remirovich*, JIHT RAS, Moscow, Russia, phone: +7(495)4842456, fax: +7(495)4857990, pasha@ihed.ras.ru
110. *Likhachev Alexandr Pavlovich*, JIHT RAS, Moscow, Russia, phone: +7(495)4842338, fax: +7(495)4857990, apl@ihed.ras.ru
111. *Lisin Evgeny*, JIHT RAS, Moscow, Russia, phone: +7(495)4842355, fax: +7(495)4842355, eaLisin@yandex.ru
112. *Lisina Irina Igorevna*, JIHT RAS, Moscow, Russia, phone: +7(495)4842355, fax: +7(495)4842355, irina.lisina@mail.ru
113. *Loktionov Egor Yuryevitch*, BMSTU, Moscow, Russia, phone: +7(499)2636299, fax: +7(499)2636299, yagor@bmstu.ru
114. *Lomonosov Igor Vladimirovich*, IPCP RAS, Chernogolovka, Russia, phone: +7(+7(495)4842456, fax: +7(495)4857990, ivl143@yahoo.com
115. *Lukin Alexander Nickolayevitch*, WCRC, Tuapse, Russia, phone: +7(918)3080916, fax: +7(861)742975, lukin@wcrc.ru
116. *Majekodunmi Abiodun Yusuf*, UI, Ibadan, Nigeria, phone: +0(818)3849431, fax: +0(818)3842302, vin.nataniel@gmail.com
117. *Maltsev Roman Grigorievich*, KubSTU, Krasnodar, Russia, phone: +7(909)4653323, fax: +7(495)4857990, ooowork@yandex.ru
118. *Mamchuev Mukhtar Osmanovich*, RIAMA KBRC RAS, Nalchik, Russia, phone: +7(928)0754009, fax: +7(662)427006, mamchuevmc@yandex.ru
119. *Martynova Inna Aleksandrovna*, JIHT RAS, Moscow, Russia, phone: +7(965)3790063, fax: +7(495)4842300, martina1204@yandex.ru
120. *Mayer Alexander Evgenievich*, CSU, Chelyabinsk, Russia, phone: +3(351)7997161, fax: +7(351)7420925, mayer@csu.ru
121. *Mayer Polina Nikolaevna*, CSU, Chelyabinsk, Russia, phone: +7(351)7997161, fax: +7(351)7420925, polina.nik@mail.ru
122. *Meilanov Ruslan Pirmetovich*, IGR DSC RAS, Makhachkala, Russia, phone: +7(8722)625715, fax: +7(8722)625715, lanten50@mail.ru
123. *Melnikova Nina Vladimirovna*, UrFU, Ekaterinburg, Russia, phone: +7(343)2617441, fax: +7(343)2616885, nvm.melnikova@gmail.com
124. *Meshkov Evgeny Evgrafovich*, SSPTI MEPhI, Sarov, Russia, phone: +7(83130)76133, fax: +7(83130)76133, eemeshkov@gmail.com

125. *Migdal Kirill Petrovich*, VNIIA, Moscow, Russia, phone: +7(499)9728413, fax: +7(499)9780903, migdal@vniia.ru
126. *Mikheyeva Ekaterina*, JIHT RAS, Moscow, Russia, phone: +7(495)4841966, fax: +7(495)4841966, mikheyeva@ihed.ras.ru
127. *Mikushkin Anton Yuryevich*, JIHT RAS, Moscow, Russia, phone: +7(903)9737520, fax: +7(495)4857990, notna17@yandex.ru
128. *Mintsev Victor Borisovich*, IPCP RAS, Chernogolovka, Russia, phone: +7(496)5224475, fax: +7(496)5224474, minvb@icp.ac.ru
129. *Mitina Aliena Aleksandrovna*, IMT RAS, Chernogolovka, Russia, phone: +7(496)5244141, fax: +7(496)5244141, alena@iptm.ru
130. *Molchanov Dmitry*, JIHT RAS, Moscow, Russia, phone: +7(906)7340796, fax: +7(495)4859922, dmitriy.molchanov13@gmail.com
131. *Myasnikov Maxim Igorevich*, JIHT RAS, Moscow, Russia, phone: +7(903)5760290, fax: +7(495)4842222, miasnikovmi@mail.ru
132. *Nagorskiy Nikolay Mikhailovich*, JIHT RAS, Moscow, Russia, phone: +7(916)8239796, fax: +7(495)4841944, nikolaynag@gmail.com
133. *Nakhushev Adam Maremovich*, RIAMA KBRC RAS, Nalchik, Russia, phone: +7(8662)426661, fax: +7(8662)427006, niipma@mail333.com
134. *Narkevich Ivan Ivanovich*, BSTU, Minsk, Belarus, phone: +3(7517)3271091, fax: +3(7517)3273021, inarkevich@mail.ru
135. *Nesterov Alexey Sergeyevich*, JIHT RAS, Moscow, Russia, phone: +7(495)9733048, fax: +7(495)9733048, nesterovalexey@bk.ru
136. *Obruchkova Liliya Rimovna*, JIHT RAS, Moscow, Russia, phone: +7(495)4842456, fax: +7(495)4857990, o_liliya@ihed.ras.ru
137. *Orekhov Nikita Dmitrievich*, JIHT RAS, Moscow, Russia, phone: +7(985)1886637, fax: +7(495)4858545, nikita.orekhov@gmail.com
138. *Oreshkin Vladimir Ivanovich*, IHCE SB RAS, Tomsk, Russia, phone: +7(3822)492988, fax: +7(3822)492988, oreshkin@ovpe.hcei.tsc.ru
139. *Orlov Nikolay Yurievich*, JIHT RAS, Moscow, Russia, phone: +7(495)4842456, fax: +7(495)4847900, nyuorlov@mail.ru
140. *Orlov Maxim Yurevich*, TSU, Tomsk, Russia, phone: +7(3822)529569, fax: +7(3822)529547, orloff_m@mail.ru
141. *Ostrik Afanasy Victorovich*, IPCP RAS, Chernogolovka, Russia, phone: +7(496)5249472, fax: +7(496)5249472, ostrik@ficp.ac.ru
142. *Panov Vladislav Alexandrovich*, JIHT RAS, Moscow, Russia, phone: +7(926)7558501, fax: +7(495)4842222,

panovvladislav@gmail.com

143. *Pestovskiy Nikolay Valerievich*, LPI RAS, Moscow, Russia, phone: +7(926)8772754, fax: +7(495)1358231, samosval@mail15.com
144. *Petrik Galina Georgievna*, IGR DSC RAS, Makhachkala, Russia, phone: +7(960)4113714, fax: +7(8722)629312, galina_petrik@mail.ru
145. *Petrosyan Tamara Konstantinovna*, UrFU, Ekaterinburg, Russia, phone: +7(912)2705961, fax: +7(343)2616885, alximik-ptk@rambler.ru
146. *Petrov Oleg Fedorovich*, JIHT RAS, Moscow, Russia, phone: +7(495)4842300, fax: +7(495)4857990, ofpetrov@ihed.ras.ru
147. *Petrov Yuri Vasilievich*, ITP RAS, Chernogolovka, Russia, phone: +7(495)7029317, fax: +7(495)7029317, uvp49@mail.ru
148. *Petrov Alexey Alexeevich*, LPI RAS, Moscow, Russia, phone: +7(915)3354976, fax: +7(915)3354976, petrov@oivtran.ru
149. *Petukhov Vyacheslav Alexandrovich*, JIHT RAS, Moscow, Russia, phone: +7(495)4858190, fax: +7(495)4857990, petukhov@ihed.ras.ru
150. *Pikuz Sergey Alexeevich*, JIHT RAS, Moscow, Russia, phone: +7(916)6033489, fax: +7(495)4857990, spikuz@gmail.com
151. *Pinchuk Mikhail Ernestovich*, IEE RAS, Saint-Petersburg, Russia, phone: +7(812)3151757, fax: +7(812)5715056, pinchme@mail.ru
152. *Pobol Igor Leonidovich*, PTI NASB, Minsk, Belarus, phone: +375(17)2635125, fax: +375(17)2635920, i.pobol@gmail.com
153. *Polistchook Vladimir Pavlovich*, JIHT RAS, Moscow, Russia, phone: +7(49645)23714, fax: +7(49645)23714, polistchook@mail.ru
154. *Polyakov Dmitry Nikolaevich*, JIHT RAS, Moscow, Russia, phone: +7(495)4841810, fax: +7(495)4857990, cryolab@ihed.ras.ru
155. *Povarnitsyn Mikhail*, JIHT RAS, Moscow, Russia, phone: +7(495)4842456, fax: +7(495)4857990, povar@ihed.ras.ru
156. *Prokhorov Alexander Evgenievich*, ICMM UB RAS, Perm, Russia, phone: +7(342)2378312, fax: +7(342)2378487, alexproher@gmail.com
157. *Prudnikov Pavel Igorevich*, SSC RF IPPE, Obninsk, Russia, phone: +7(920)6152499, fax: +7(920)6152499, pavel.prudnikov89@gmail.com
158. *Pugachev Leonid Petrovich*, JIHT RAS, Moscow, Russia, phone: +7(495)4842456, fax: +7(495)4857990, pugachev@ihed.ras.ru
159. *Radchenko Andrey*, TSUAB, Tomsk, Russia, phone: +7(3822)472891, fax: +7(3822)472891, andrey-radchenko@live.ru

160. *Radchenko Pavel*, TSUAB, Tomsk, Russia, phone: +7(903)9502064, fax: +7(3822)472891, radchenko@live.ru
161. *Romashevskiy Sergey Andreevich*, JIHT RAS, Moscow, Russia, phone: +7(495)2294241, fax: +7(495)2294241, sa.romashevskiy@gmail.com
162. *Rusin Sergey Petrovich*, JIHT RAS, Moscow, Russia, phone: +7(495)3625333, fax: +7(495)3620778, sprusin@yandex.ru
163. *Ryabinkin Alexey Nikolaevich*, SRC RF TRINITI, Troitsk, Russia, phone: +7(495)9394953, fax: +7(495)9390896, alex.ryabinkin@gmail.com
164. *Rykov Vladimir Alekseevich*, SPbSU ITMO, Saint-Petersburg, Russia, phone: +7(911)8337605, fax: +7(812)3153617, rykov-vladimir@rambler.ru
165. *Rykov Sergey Vladimirovich*, SPbSU ITMO, Saint-Petersburg, Russia, phone: +7(962)3435206, fax: +7(812)3147869, togg1@yandex.ru
166. *Saakyan Sergey Aramovich*, JIHT RAS, Moscow, Russia, phone: +7(903)5728113, fax: +7(495)4851063, saasear@gmail.com
167. *Sargsyan Mikael Armenovich*, JIHT RAS, Moscow, Russia, phone: +7(925)7396219, fax: +7(925)7396219, m.sargsyan86@mail.ru
168. *Satonkina Natalia Petrovna*, LIH SB RAS, Novosibirsk, Russia, phone: +7(913)7400572, fax: +7(383)3331612, snp@hydro.nsc.ru
169. *Sattarova Chulpan Ilgizarovna*, JIHT RAS, Moscow, Russia, phone: +7(495)4859755, fax: +7(495)4832298, cchupa@yandex.ru
170. *Saveliev Andrey*, JIHT RAS, Moscow, Russia, phone: +7(495)4858063, fax: +7(495)4857990, fisteh@mail.ru
171. *Savintsev Alexey Petrovich*, KBSU, Nalchik, Russia, phone: +7(8662)423777, fax: +7(8662)422560, pnr@kbsu.ru
172. *Savintsev Yuriy Petrovich*, IGM SB RAS, Novosibirsk, Russia, phone: +7(383)3332007, fax: +7(383)3332792, savincev1940@mail.ru
173. *Savitsky Dmitry Vladimirovich*, JIHT RAS, Moscow, Russia, phone: +7(926)5215548, fax: +7(495)4859922, dmvlsav@yandex.ru
174. *Schlothauer Thomas*, TUBAF, Freiberg, Germany, phone: +49(3731)393540, fax: +49(3731)393129, schlotha@mailserver.tu-freiberg.de
175. *Sedyakina Daria Valeryevna*, JIHT RAS, Moscow, Russia, phone: +7(915)0352228, fax: +7(495)4859722, sedyakina.d@gmail.com
176. *Semin Nikolay Valentinovich*, JIHT RAS, Moscow, Russia, phone: +7(495)4842138, fax: +7(495)4842138, seminnikolay@gmail.com

177. *Serov Alexander Olegovich*, SRC RF TRINITI, Troitsk, Russia, phone: +7(495)9394953, fax: +7(495)9390896, aserov@mics.msu.su
178. *Sevalnikov Andrey Yurjevich*, IPhRAS, Moscow, Russia, phone: +7(495)6979209, fax: +7(495)6099350, sevalnicov@rambler.ru
179. *Shakhray Denis Vladimirovich*, IPCP RAS, Chernogolovka, Russia, phone: +7(496)5221756, fax: +7(496)5221870, shakhray@icp.ac.ru
180. *Shapoval Sergey Yurievich*, IMT RAS, Chernogolovka, Russia, phone: +7(496)5244141, fax: +7(496)5244141, shapoval@iptm.ru
181. *Shemanin Valery Gennad'evich*, KubSTU NPI, Novorossiysk, Russia, phone: +7(8617)613291, fax: +7(8617)641814, vshemanin@nbkstu.org.ru
182. *Shishkina Nadezhda Anatolevna*, JIHT RAS, Moscow, Russia, phone: +7(495)4857927, fax: +7(495)4832298, shisnadya@yandex.ru
183. *Shpatakovskaya Galina Vasilievna*, KIAM RAS, Moscow, Russia, phone: +7(903)1528974, fax: +7(499)9720737, shpagalya@yandex.ru
184. *Shumikhin Aleksey Sergeevich*, JIHT RAS, Moscow, Russia, phone: +7(495)4842110, fax: +7(495)4859922, shum_ac@mail.ru
185. *Shumova Valeria Valerievna*, JIHT RAS, Moscow, Russia, phone: +7(495)4842610, fax: +7(495)4857990, shumova@ihed.ras.ru
186. *Shurupov Alexey Vasilievich*, JIHT RAS, Moscow, Russia, phone: +7(495)7887460, fax: +7(49645)23714, shurupov@fites.ru
187. *Shutov Alexander Vladimirovich*, IPCP RAS, Chernogolovka, Russia, phone: +7(496)5249472, fax: +7(496)5249472, shutov@ficp.ac.ru
188. *Sinelshchikov Vladimir Alexandrovich*, JIHT RAS, Moscow, Russia, phone: +7(495)4842447, fax: +7(495)4842447, sinelshchikov@mail.ru
189. *Skripnyak Vladimir Albertovich*, TSU, Tomsk, Russia, phone: +7(382)2529845, fax: +7(382)2529829, skrp2006@yandex.ru
190. *Skripnyak Evgeniya Georgievna*, TSU, Tomsk, Russia, phone: +7(382)2529845, fax: +7(382)2529829, skrp2006@yandex.ru
191. *Smirnov Evgeny Borisovich*, RFNC–VNIITF, Snezhinsk, Russia, phone: +7(912)7901161, fax: +7(912)7901161, ewgeny_smirnov@mail.ru
192. *Smygalina Anna Evgenievna*, JIHT RAS, Moscow, Russia, phone: +7(915)0404284, fax: +7(495)4844433, anna.smygalina@gmail.com
193. *Sobko Aleksandr Aleksandrovich*, AES, Moscow, Russia, phone: +7(916)1919120, fax: +7(499)7028379, ainrf@mail.ru

194. *Son Eduard Evgenievich*, JIHT RAS, Moscow, Russia, phone: +7(495)4841655, fax: +7(495)4857990, son.eduard@gmail.com
195. *Sorokin Andrey Arturovich*, NPO Saturn, LSTC, Moscow, Russia, phone: +7(919)7274888, fax: +7(919)7274888, andey.sorokin@okb.umpo.ru
196. *Starikov Sergey*, JIHT RAS, Moscow, Russia, phone: +7(926)8950020, fax: +7(495)4857990, starikov@ihed.ras.ru
197. *Steinman Eduard Alexandrovich*, ISSP RAS, Chernogolovka, Russia, phone: +7(496)5223244, fax: +7(496)5228160, steinman@issp.ac.ru
198. *Stroyev Nikita Eugenyevich*, JIHT RAS, Moscow, Russia, phone: +7(919)0329457, fax: +7(919)0329457, jackal.snenost@gmail.com
199. *Sultanov Valery Gulyamovitch*, IPCP RAS, Chernogolovka, Russia, phone: +7(496)5249472, fax: +7(496)5249472, sultan@ficp.ac.ru
200. *Syrovatka Roman Alexandrovich*, JIHT RAS, Moscow, Russia, phone: +7(915)0688114, fax: +7(495)4857990, romansa_89@mail.ru
201. *Sytchev George Alexandrovich*, JIHT RAS, Moscow, Russia, phone: +7(905)5066014, fax: +7(495)4857981, george.sytchev@gmail.com
202. *Ten Konstantin Alekseevich*, LIH SB RAS, Novosibirsk, Russia, phone: +7(913)9031515, fax: +7(383)333162, ten@hydro.nsc.ru
203. *Tereshonok Dmitry Viktorovich*, JIHT RAS, Moscow, Russia, phone: +7(495)4859666, fax: +7(495)4859666, tereshonokd@gmail.com
204. *Tereza Anatoly Mikhailovich*, ICP RAS, Moscow, Russia, phone: +7(495)9397396, fax: +7(495)9397396, atereza@bk.ru
205. *Timofeev Ivan Sergeyevich*, MIPT, Dolgoprudny, Russia, phone: +7(926)7308971, fax: +7(495)3332166, i.s.timofeev@gmail.com
206. *Timofeev Alexey Vladimirovich*, JIHT RAS, Moscow, Russia, phone: +7(495)4859263, fax: +7(495)4857990, timofeevalvl@gmail.com
207. *Titova Victoriya Borisovna*, RFNC–VNIIEF, Sarov, Russia, phone: +7(83130)90232, fax: +7(83130)90232, titovsarov@gmail.com
208. *Trigger Sergey Alexandrovich*, JIHT RAS, Moscow, Russia, phone: +7(495)3625310, fax: +7(495)4857990, satron@mail.ru
209. *Tsirlina Elena Arkadievna*, JIHT RAS, Moscow, Russia, phone: +7(495)4842456, fax: +7(495)4857990, elena2509@yandex.ru
210. *Umnova Olga Mikhailovna*, JIHT RAS, Moscow, Russia, phone: +7(495)4842447, fax: +7(495)4859009, umnova.olya@gmail.com
211. *Usmanov Ravil Anatolevich*, JIHT RAS, Moscow, Russia, phone: +7(495)4851081, fax: +7(495)4851081, ravus46@yandex.ru

212. *Ustyuzhanin Evgueny Evguenievich*, MPEI, Moscow, Russia, phone: +7(926)2696999, fax: +7(495)4857990, evgust@gmail.com
213. *Uvarov Sergey Vitalievich*, ICMM UB RAS, Perm, Russia, phone: +7(342)2378312, fax: +7(342)2378312, usv@icmm.ru
214. *Vagner Sergey Aleksandrovich*, IPCP RAS, Chernogolovka, Russia, phone: +7(916)0692033, fax: +7(916)0692033, vagnerserge@gmail.com
215. *Vasiliev Mikhail*, JIHT RAS, Moscow, Russia, phone: +7(495)4842355, fax: +7(495)4857990, mixxy@mail.ru
216. *Vasilieva Elena Valerievna*, JIHT RAS, Moscow, Russia, phone: +7(495)4835523, fax: +7(495)4835523, elen_vasilieva@mail.ru
217. *Vereshchagin Anton Sergeevich*, ITAM SB RAS, Novosibirsk, Russia, phone: +7(913)9896591, fax: +7(383)3307268, vereshchag@itam.nsc.ru
218. *Vervikishko Daria*, JIHT RAS, Moscow, Russia, phone: +7(905)7512659, fax: +7(495)4859411, vitkina-darya@yandex.ru
219. *Vetchinin Sergey Petrovich*, JIHT RAS, Moscow, Russia, phone: +7(495)4841810, fax: +7(495)4857990, vpecherkin@yandex.ru
220. *Veysman Mikhail*, JIHT RAS, Moscow, Russia, phone: +7(495)4859722, fax: +7(495)4857990, bme@ihed.ras.ru
221. *Vilshanskaya Evgenya V*, JIHT RAS, Moscow, Russia, phone: +7(903)5585363, fax: +7(495)4851063, eva.villi@gmail.com
222. *Vladimirov Vladimir Ivanovich*, JIHT RAS, Moscow, Russia, phone: +7(495)4842429, fax: +7(495)4857990, dlv@ihed.ras.ru
223. *Vlasov Aleksandr Nikolaevich*, RSREU, Ryazan, Russia, phone: +7(4912)460352, fax: +7(4912)922215, anv@fulcra.ryazan.ru
224. *Vlasov Pavel Aleksandrovich*, ICP RAS, Moscow, Russia, phone: +7(495)9397396, fax: +7(495)9397396, iz@chph.ras.ru
225. *Volkov Grigory Aleksandrovich*, IPME RAS, Saint Petersburg, Russia, phone: +7(812)3214779, fax: +7(812)3214771, volkovgrig@mail.ru
226. *Vorobieva Galina Yurievna*, IPCP RAS, Chernogolovka, Russia, phone: +7(916)1383071, fax: +7(496)5221158, vorobeva@icp.ac.ru
227. *Vshivkov Aleksey Nikolaevich*, ICMM UB RAS, Perm, Russia, phone: +7(342)2378312, fax: +7(342)2378487, aleksey.1992@mail.ru
228. *Yakovenko Ivan Sergeevich*, JIHT RAS, Moscow, Russia, phone: +7(495)4844433, fax: +7(495)4844433, yakovenko.ivan@bk.ru
229. *Yankovskiy Boris Denisovich*, JIHT RAS, Moscow, Russia, phone: +7(495)4832295, fax: +7(495)4857990, yiy2004@mail.ru

230. *Zaikova Vasilisa Evgenevna*, UrFU, Ekaterinburg, Russia, phone: +7(919)3770159, fax: +7(343)2613124, vasilisazaykova@gmail.com
231. *Zaporozhets Yury Borisovich*, IPCP RAS, Chernogolovka, Russia, phone: +7(49652)21474, fax: +7(49652)21474, yubz@icp.ac.ru
232. *Zelener Boris Borisovich*, JIHT RAS, Moscow, Russia, phone: +7(495)3620778, fax: +7(495)4842333, bobozel@mail.ru
233. *Ziborov Vadim Serafimovich*, JIHT RAS, Moscow, Russia, phone: +7(495)4858527, fax: +7(495)4857990, vziborov@rambler.ru
234. *Zobnin Andrey Vjacheslavovich*, JIHT RAS, Moscow, Russia, phone: +7(495)4842492, fax: +7(495)4857990, zobnin@ihed.ras.ru
235. *Zolnikov Konstantin Petrovich*, ISPMS SB RAS, Tomsk, Russia, phone: +7(382)2286972, fax: +7(382)2492576, kost@ispms.tsc.ru

XXIX International Conference on Equations of State for Matter, March 1–6, 2014, Elbrus, Russia. Book of Abstracts

Publishing Group "Granica"
123007 Moscow,
highway Horoshevskoe, building 38
Telephone: +7 (495) 941-26-66, fax: +7 (495) 941-36-46
E-mail: granica_publish@mail.ru
http://granicagroup.ru/

Signed to print on 13.02.14
Print run 180 issues
Customer order No. 607